



**UCGE Reports  
Number 20196**

Department of Geomatics Engineering

**Automated Traffic Incident Detection Using GPS  
Based Transit Probe Vehicles**

(URL: <http://www.geomatics.ucalgary.ca/links/GradTheses.html>)

by

**Chaminda Basnayake**

**June 2004**



UNIVERSITY OF CALGARY

Automated Traffic Incident Detection Using GPS-Based Transit Probe Vehicles

by

Chaminda Basnayake

A THESIS

SUBMITTED TO THE FACULTY OF GRADUATE STUDIES

IN PARTIAL FULFILLMENT OF THE REQUIREMENTS FOR THE

DEGREE OF DOCTOR OF PHILOSOPHY

DEPARTMENT OF GEOMATICS ENGINEERING

CALGARY, ALBERTA

June 2004

© Chaminda Basnayake 2004

## Abstract

The recent advancements in electronics, communication and information processing and the application of such technologies to transportation through Intelligent Transportation Systems (ITS) have resulted in safer, faster and more efficient surface transportation systems. ITS have contributed significantly to the current state of technology in automated traffic monitoring, and probe vehicle-based traffic monitoring is one of these techniques. Although the potential of probe vehicle-based traffic monitoring was well understood, its wider application was severely restricted by the state of vehicle positioning system capabilities and associated cost considerations.

This thesis presents the development and performance analysis of a probe vehicle-based automated traffic incident detection system that uses transit vehicles equipped with GPS as a passive probe vehicle fleet. Since these vehicles serve primary purposes other than providing vehicle-tracking data, such vehicles are more likely to be equipped with systems such as GPS, thus providing multiple benefits. However, passive probe vehicle-based traffic incident detection has its own challenges over dedicated probe vehicles. These challenges are addressed and solutions are developed in two stages in this thesis.

Firstly, the need for a GPS positioning technique that provides better performance in urban environments is addressed with an outline of advantages of High Sensitivity GPS (HSGPS). HSGPS error mitigation techniques are discussed with the emphasis on map-matching augmentations; a major advantage being their independence from vehicle sensors. A discussion of HSGPS map-matching issues, pros and cons of using internally filtered HSGPS positions, and alternative filtering techniques are also presented.

Secondly, probe-based incident detection algorithms and their performances are analyzed. Instead of conducting a complex field data collection for probe and traffic incident data collection, a traffic microsimulation model was developed to simulate

transit probe vehicles with and without simulated incidents. The simulation model is calibrated using actual transit vehicle and non-transit vehicle data collected over several days. Incidents detection performance was analyzed with respect to three indicators: Detection Rate (DR), Time to Detect (TTD) and False Alarm Rate (FAR). Performance under varying incident characteristics and GPS performance levels were investigated and the results show over a 90 % DR and a TTD of under 5 minutes for all simulated scenarios.

## Acknowledgements

I would like to thank my supervisor Dr. Gérard Lachapelle and my co-supervisor Dr. Andrew MacIver for their continuous encouragement, guidance, and support. Their extremely valuable comments and suggestions throughout the years were a major driving force behind the successful completion of this cross-disciplinary research. I am extremely grateful to Dr. Gérard Lachapelle for giving me an opportunity to pursue my graduate studies in a world-class research facility in the Position, Location and Navigation (PLAN) research group. My gratitude also extends to Dr. Elizabeth Cannon and the members of the PLAN research group for making me a part of many interesting research projects and making my three-year stay at the University of Calgary a memorable experience. I would also like to acknowledge the contributions made by Dr. John Morrall who was in my initial supervisory committee.

My sincere appreciation goes to Scott Mackie, Doug Morgan, and Vince Lee of the City of Calgary and Deborah Nikkel and Kathleen Cymbal of Calgary Transit for assisting me in numerous ways during field surveys and tests. My special thanks goes to Travis MacLeod for exhaustively proofreading this thesis. The Informatics Circle of Research Excellence (iCORE), Auto21 Network of Centres of Excellence, and the University of Calgary are gratefully acknowledged for generously funding my graduate studies.

I would also like to thank Drs. Saman Bandara and Amal Kumarage who rooted my fascination of Intelligent Transportation Systems over the years of my studies and research at the University of Moratuwa. I would especially like to thank Dr. Chandana Wirasinghe for leading my way to the University of Calgary.

My heartfelt gratitude goes to my parents for instilling within me the desire to achieve the highest level of education possible and for providing me with the means to do so. Finally, my heartfelt gratitude extends to my loving wife Priyanwada for sharing all the highs and lows of my life in Calgary and for making this work possible through her endless support, encouragement and understanding.

## Dedication

To my Mother and Father,

With gratitude for everything you have done for me ...

## Table of Contents

<b>ABSTRACT</b> .....	<b>II</b>
<b>ACKNOWLEDGEMENTS</b> .....	<b>IV</b>
<b>DEDICATION</b> .....	<b>V</b>
<b>TABLE OF CONTENTS</b> .....	<b>VI</b>
<b>LIST OF TABLES</b> .....	<b>XI</b>
<b>LIST OF FIGURES</b> .....	<b>XII</b>
<b>LIST OF SYMBOLS, ABBREVIATIONS, NOMENCLATURE</b> .....	<b>XV</b>
SYMBOLS .....	XV
ABBREVIATIONS AND ACRONYMS .....	XVI
NOMENCLATURE.....	XVII
<b>CHAPTER ONE: INTRODUCTION</b> .....	<b>1</b>
1.1    BACKGROUND.....	1
1.2    LIMITATION OF PREVIOUS WORK.....	5
1.3    OBJECTIVES AND CONTRIBUTION OF THE THESIS.....	8
1.4    THESIS OUTLINE .....	11
<b>CHAPTER TWO: INTELLIGENT TRANSPORTATION SYSTEMS</b> .....	<b>14</b>
2.1    INTELLIGENT TRANSPORTATION SYSTEMS.....	14
2.1.1    Traveler Information Services .....	14
2.1.2    Traffic Management Services .....	15
2.1.3    Public Transportation Services .....	15
2.1.4    Electronic Payment Services.....	16
2.1.5    Commercial Vehicle Operations.....	16
2.1.6    Emergency Management Services .....	16
2.1.7    Vehicle Safety and Control Systems.....	16
2.1.8    Information Warehousing Services.....	17
2.2    AUTOMATIC VEHICLE LOCATION (AVL) APPLICATIONS IN ITS.....	17
2.2.1    Probe Vehicle Applications .....	18
2.2.2    Instrumented Vehicle Applications.....	18
2.3    TRAFFIC INCIDENTS AND TRAFFIC INCIDENT DETECTION .....	19
2.3.1    The Importance of Traffic Incident Detection .....	19
2.3.2    Freeway, Arterial and Urban Street Classification .....	20
2.3.3    Incident Detection in Freeways .....	20
2.3.4    Challenges in Arterial Incident Detection.....	21
2.3.5    Arterial Incident Detection Algorithms .....	22
2.3.6    Algorithm Performance Evaluation .....	24
2.4    PERFORMANCE MONITORING IN ARTERIALS.....	24
2.4.1    Performance Measures for Arterial Traffic Monitoring .....	25
2.4.2    Data Requirements for Performance Monitoring .....	25

<b>CHAPTER THREE: GLOBAL POSITIONING SYSTEM .....</b>	<b>27</b>
3.1 OVERVIEW OF GPS .....	27
3.1.1 GPS Signal Structure .....	28
3.1.2 GPS Position, Velocity and Time Estimation.....	29
3.1.2.1 Code or Pseudorange Measurement.....	29
3.1.2.2 Carrier Phase Measurement .....	30
3.1.3 GPS Error Sources .....	31
3.1.3.1 Control Segment Errors .....	31
3.1.3.2 Signal Propagation Errors .....	32
3.1.3.3 User End Errors.....	32
3.1.4 GPS Error Budget .....	33
3.2 HIGH SENSITIVITY GPS (HSGPS).....	34
3.3 GPS AUGMENTATIONS .....	34
3.3.1 Differential GPS (DGPS).....	35
3.3.2 Assisted GPS (A-GPS) .....	36
3.3.3 Map-Matching Techniques .....	36
3.4 MAP-MATCHING ALGORITHM FOR PROBE VEHICLE POSITIONING .....	36
3.4.1 Map Estimation Module (MEM) .....	37
3.4.2 Vehicle Dynamic Model (VDM).....	39
3.4.3 Vehicle Dynamic Model Parameter Accuracy Estimation .....	42
3.4.4 Vehicle Dynamic Modeling Techniques .....	43
3.4.4.1 Constant Position Model.....	43
3.4.4.2 Constant Velocity Model .....	44
3.4.4.3 Constant Acceleration Model .....	46
3.4.5 HSGPS Data Filtering Module (DFM).....	46
3.5 HSGPS MEASUREMENTS .....	50
3.5.1 Internal Position and Velocity Measurements .....	50
3.5.2 Raw GPS Measurements.....	50
3.5.3 Application of HSGPS.....	51
3.6 TESTING THE ALGORITHM WITH THE GNSS SIMULATOR .....	52
3.6.1 GNSS Simulator Test Setup.....	52
3.6.2 Simulation Test Scenarios.....	53
3.6.2.1 GPS Outages in Urban Canyons.....	55
3.6.2.2 Map-Matching with Simulated Multipath .....	57
3.6.2.3 Map Matching Under Weak GPS Signal Reception.....	59
3.7 AIDING WITH ODOMETRY AND DIFFERENTIAL ODOMETRY.....	62
3.8 INERTIAL AIDING FOR URBAN VEHICLE NAVIGATION .....	63
3.8.1 Sensor Integration Strategy.....	64
3.8.1.1 Turn Detection Module (TDM) .....	65
3.8.1.2 Stop Detection Module (SDM).....	65
3.8.2 Multi Sensor Navigation Algorithm .....	66
3.8.2.1 Testing the Multi Sensor Navigation Algorithm .....	67
3.8.2.2 Equipment Setup.....	69
3.8.2.3 Sensor Data and Integration Results.....	70

3.9	CONSTRAINED MAP-MATCHING FOR TRANSIT VEHICLE NAVIGATION.....	75
<b>CHAPTER FOUR: TRANSIT PROBE &amp; INCIDENT DETECTION SYSTEM....</b>		<b>76</b>
4.1	TRANSIT VEHICLE POSITIONING .....	76
4.1.1	Overall Vehicle Positioning System .....	76
4.1.2	Constraining Along-Track Error.....	77
4.1.3	Field Testing .....	81
4.1.4	HSGPS Data Characteristics.....	82
4.1.4.1	Availability .....	82
4.1.4.2	Across-Track Correction.....	83
4.1.4.3	Across-Track Correction Distribution .....	85
4.1.5	Conclusions of HSGPS Data Characteristics Analysis.....	86
4.1.6	Algorithm Performance Analysis .....	86
4.1.6.1	HSGPS Vehicle Trajectory.....	87
4.1.6.2	Along-Track Position Correction and Position Fixing .....	88
4.1.6.3	Analysis Summary .....	89
4.2	DATA PROCESSING.....	91
4.2.1	Street Segment Selection .....	91
4.2.2	Transit Vehicle Travel Time Estimation.....	92
4.2.2.1	Transit Data Characteristics.....	93
4.2.2.2	Measurements and Dwelling Time Estimation.....	95
4.2.2.3	Modification Algorithm .....	96
4.2.2.4	Modification Algorithm Testing with Field Data .....	97
4.2.3	Travel Time Modeling Framework.....	97
4.2.4	Outlier Detection.....	101
4.3	TRAFFIC PERFORMANCE INDICATORS & INCIDENT DETECTION .....	103
4.3.1	Variables of Interest.....	104
4.3.2	Acceleration Noise.....	105
4.3.3	Street Segment Travel Time Variation .....	107
4.4	CONTROL CHARTS FOR TRAVEL TIME MONITORING .....	110
4.4.1	SQC Variables .....	111
4.4.2	Control Chart Designing.....	111
4.5	INCIDENT DETECTION ALGORITHM.....	114
4.5.1	Combining Incident Detection Parameters.....	114
4.5.2	Combining Indicators from Multiple Streets for Incident Detection.....	115
4.6	ALGORITHM PERFORMANCE EVALUATION .....	116
<b>CHAPTER FIVE: MICROSCOPIC TRAFFIC SIMULATION.....</b>		<b>117</b>
5.1	OVERVIEW OF TRAFFIC SIMULATION .....	117
5.1.1	Simulation Model Classification Based on Modeling Details.....	117
5.1.2	Other Simulation Model Classes .....	118
5.2	INCIDENT DETECTION ALGORITHM PERFORMANCE EVALUATION .....	119
5.2.1	Ability to Control Environmental Variables.....	119
5.2.2	Traffic Incidents and Incident Characteristics .....	120
5.2.3	Repeatability .....	120

5.2.4	Data Collection Requirements and Limitations .....	120
5.2.5	Complications Associated with Data Collection .....	122
5.3	MICROSIMULATION FOR ALGORITHM PERFORMANCE EVALUATION .....	122
5.3.1	Microsimulator Components .....	123
5.3.1.1	Car-Following Models .....	123
5.3.1.2	Lane Changing Models .....	124
5.3.2	PARAMICS Microsimulator .....	125
5.4	CALIBRATION AND VALIDATION OF MICROSCOPIC TRAFFIC MODELS .....	125
5.4.1	Calibration Parameters .....	126
5.4.2	Calibration and Validation Criteria .....	126
5.4.3	Uncertainty of Inputs and Model Variability .....	127
5.5	INTERPRETATION OF MICROSIMULATOR RESULTS .....	127
5.6	INCIDENT DETECTION ALGORITHM PERFORMANCE EVALUATION .....	128
5.6.1	Validation of Concept Developed in the Thesis .....	128
5.6.2	Analysis of Statistical Properties of Street Segment Travel Time .....	128
5.6.3	Incident Detection Capability of Incident Detection Parameters .....	128
5.6.4	Algorithm Development .....	129
5.6.5	Traffic Incident Scenarios .....	129
5.6.6	Performance Improvements with Dedicated Probe Vehicles .....	129
5.6.7	Analysis of Performance Degradation with GPS Errors .....	129
<b>CHAPTER SIX: FIELD TESTING AND SIMULATIONS .....</b>		<b>131</b>
6.1	TRANSIT AND DEDICATED PROBE VEHICLE SURVEYS .....	131
6.1.1	Field Survey Area .....	132
6.1.2	Test Vehicles and Test Setup .....	133
6.1.2.1	Transit Test Vehicles .....	134
6.1.2.2	Dedicated Test Vehicles .....	135
6.1.3	Data Collection Methodology .....	136
6.1.4	Data Collection Summary .....	137
6.2	LOCATING DESIGNATED TRANSIT STOPS .....	138
6.2.1	Equipment Setup and Methodology .....	138
6.2.2	GPS Data Processing .....	139
6.2.3	Transit Stop Location .....	139
6.3	DATA ANALYSIS .....	140
6.3.1	Acceleration / Deceleration Characteristic Curves .....	141
6.3.2	Calibrating the Transit Travel Time Modification Algorithm .....	141
6.4	DATA COLLECTION FOR SIMULATION MODEL .....	144
6.4.1	Data for Simulation Model Building .....	144
6.4.1.1	Geometrical Data .....	146
6.4.1.2	Traffic Activity Data .....	147
6.4.1.3	Traffic Control System Data .....	147
6.4.2	Transit Operation Data .....	148
6.4.3	Data for Model Validation and Calibration .....	148
6.5	MICROSIMULATION MODEL BUILDING .....	149
6.5.1	Traffic Demand Modeling .....	150

6.6	MODEL CALIBRATION AND VALIDATION .....	151
6.6.1	PARAMICS Model Calibration.....	151
6.6.2	Simulation Model Validation.....	154
6.7	TRAFFIC INCIDENT SIMULATION .....	156
<b>CHAPTER SEVEN: INCIDENT DETECTION PERFORMANCE.....</b>		<b>157</b>
7.1	ANALYSIS SCENARIOS .....	157
7.1.1	Performance of Individual Incident Indicator Parameters .....	158
7.1.2	Performance Degradation with GPS Errors .....	158
7.1.3	Incident Location .....	158
7.1.4	Impact of Downstream Incidents .....	159
7.1.5	Performance of the Incident Detection Parameters and Algorithm .....	159
7.1.6	Performance Improvement with Additional Dedicated Probe Vehicles .....	159
7.2	SELECTION OF INCIDENT SCENARIOS .....	159
7.2.1	Incident Intensity .....	160
7.2.3	Incident Lane Selection.....	160
7.3	ANALYSIS OF INCIDENT DETECTION VARIABLES WITH NO GPS ERRORS .....	161
7.3.1	Incident Detection Variable: Acceleration Noise .....	162
7.3.1.1	Incident Scenario 1 .....	162
7.3.1.2	Incident Scenario 2 .....	167
7.3.2	Incident Detection Variable: Travel Time Variation .....	171
7.3.2.1	Street Segment Travel Time Analysis: Type 1 .....	171
7.3.2.2	Street Segment Travel Time Analysis: Type 2 .....	172
7.3.2.3	Travel Time Based Incident Detection: Type 1 .....	174
7.4	INCIDENT DETECTION PERFORMANCE WITH SIMULATED GPS ERRORS .....	184
7.4.1	Incident Detection Variable: Acceleration Noise .....	184
7.4.1.1	Incident Scenario 1 .....	184
7.4.1.2	Incident Scenario 2 .....	188
7.4.2	Incident Detection Variable: Travel Time Variation .....	189
7.4.2.1	Street Segment Travel Time Analysis: Type 1 .....	189
7.4.2.2	Street Segment Travel Time Analysis: Type 2 .....	190
7.4.2.3	Travel Time Based Incident Detection: Type 1 .....	191
7.4.2.4	Travel Time Based Incident Detection: Type 2 .....	194
7.5	INCIDENT DETECTION WITH TRAVEL TIME AND ACCELERATION NOISE .....	194
<b>CHAPTER EIGHT: CONCLUSIONS &amp; FUTURE DIRECTIONS .....</b>		<b>198</b>
8.1	CONCLUSIONS.....	198
8.1.1	Vehicular Navigation Systems for ITS .....	198
8.1.2	Automated Traffic Incident Detection .....	199
8.2	FUTURE DIRECTIONS.....	202
8.2.1	Vehicular Navigation Systems in ITS.....	203
8.2.2	Automated Traffic Incident Detection .....	203
<b>REFERENCES.....</b>		<b>206</b>

## List of Tables

Table 2.1: Performance measures used in incident detection .....	25
Table 3.1: GPS Signal Structure .....	28
Table 3.2: SPS Performance Specifications for Position and Time .....	31
Table 3.3: Typical GPS Error Budget .....	33
Table 3.4: GNSS 6560 Simulator specifications .....	52
Table 3.5: SiRF XTrack™ HSGPS receiver specifications.....	53
Table 3.6: Summary of map-matched GPS outage simulation.....	56
Table 3.7: Murata ENV-05D specifications .....	69
Table 3.8: VTI SCA 610 accelerometer specifications .....	69
Table 4.1: Availability statistics for HSGPS and HSGPS-SP .....	83
Table 4.2: Across-track correction statistics for HSGPS and HSGPS-SP.....	85
Table 4.3: Traffic incident related performance measures .....	105
Table 6.1: Data collection summary .....	137
Table 6.2: Simulation scenarios .....	156
Table 7.1: Analysis scenarios .....	161
Table 7.2: Total acceleration noise statistics for normal operation .....	166
Table 7.3: Total acceleration noise statistics for Scenario 1.....	166
Table 7.4: Acceleration noise-based detection on Segment A: Scenario 1 .....	167
Table 7.5: Acceleration noise-based detection on Segment B: Scenario 2.....	170
Table 7.6: Average DR, TTD and FAR for all simulations: in-segment.....	178
Table 7.7: Summary of DR, TTD and FAR: downstream segment.....	180
Table 7.8: Summary of DR, TTD and FAR for all simulations .....	183
Table 7.9: Acceleration noise: normal operation/ with GPS errors .....	187
Table 7.10: Acceleration noise-based detection: Segment A/ Scenario 1 .....	188
Table 7.11: Acceleration noise-based detection: Segment B/ Scenario 2 .....	188
Table 7.12: Average DR, TTD and FAR for all simulations: in-segment.....	191
Table 7.13: Summary of DR, TTD and FAR: downstream segment.....	193
Table 7.14: Average DR, TTD and FAR for all simulations: in-segment.....	194

## List of Figures

Figure 3.1: Map-matching algorithm operation.....	37
Figure 3.2: State model for constant position model .....	44
Figure 3.3: State model for constant velocity model .....	44
Figure 3.4: Modified state model with time-correlated acceleration .....	46
Figure 3.5: State Model for Constant Acceleration Model.....	46
Figure 3.6: VDM prediction adjustment in DFM .....	47
Figure 3.7: Illustration of the algorithm operation.....	49
Figure 3.8: Test setup with the simulator.....	53
Figure 3.9: Test trajectory for GNSS simulator testing .....	54
Figure 3.10: Simulated vehicle speed profile .....	54
Figure 3.11: Typical GPS outage simulation .....	55
Figure 3.12: GPS outages and map-matching with accelerations and turns.....	56
Figure 3.13: Typical pseudorange error profile for multipath simulation .....	57
Figure 3.14: Simulated multipath & map-matched vehicle trajectory.....	58
Figure 3.15: Minimizing multipath error with changing vehicle dynamics .....	59
Figure 3.16: Simulated C/N0 degradation .....	60
Figure 3.17: Map-matched vehicle trajectory with weak GPS signals.....	61
Figure 3.18: Algorithm modified as a function of receiver C/N0.....	62
Figure 3.19: Enhanced navigation algorithm.....	66
Figure 3.20: Test trajectory in downtown Calgary .....	67
Figure 3.21: Part of test trajectory with clear view of the sky.....	68
Figure 3.22: Part of test trajectory with urban canyon conditions.....	68
Figure 3.23: HSGPS and integrated trajectories (Test Run 2).....	71
Figure 3.24: Zoomed 1st loop from Test Run 2.....	71
Figure 3.25: Numerical analysis of accuracy in Test Run 2.....	72
Figure 3.26: HSGPS and integrated trajectories (Test Run 3).....	73
Figure 3.27: Zoomed 3rd loop from Test Run 3 .....	74
Figure 3.28: Numerical analysis of accuracy in Test Run 3 .....	74
Figure 3.29: Modified algorithm for transit vehicle positioning .....	75
Figure 4.1: Transit vehicle positioning system .....	77
Figure 4.2: Along-track error constraining algorithm.....	78
Figure 4.3: Test trajectory for transit vehicle position algorithm testing .....	81
Figure 4.4: Across-track position and velocity corrections .....	84
Figure 4.5: Across-track position correction for HSGPS and HSGPS-SP .....	85
Figure 4.6: Across-track velocity correction for HSGPS and HSGPS-SP .....	86
Figure 4.7: Along-track position vs. Northing and Easting .....	87
Figure 4.8: Along-track position vs. heading.....	88
Figure 4.9: Along-track position fixing and during-stop position fixing.....	88
Figure 4.10: Route constrained map-matched solution for Test Run 6 .....	89
Figure 4.11: Northing and Easting results for Test Run 6 .....	90
Figure 4.12: Corrected vehicle heading Test Run 6 .....	90
Figure 4.13: HCM2000 definition of highway segments and systems.....	91

Figure 4.14: Urban street unit of analysis .....	92
Figure 4.15: Speed-acceleration curves (urban-congested) .....	94
Figure 4.16: Speed-acceleration curves (suburban-uncongested) .....	94
Figure 4.17: Travel time modeling framework .....	98
Figure 4.18: Outlier (Left) and incident (Right) influenced $\bar{X}$ and $\bar{R}$ .....	102
Figure 4.19: Time differenced $\bar{X}$ and $\bar{R}$ .....	103
Figure 4.20: Standard deviation of acceleration noise (Winzer, 1980) .....	106
Figure 4.21: Travel time PDF for an unsignalized street segment .....	108
Figure 4.22: Travel time vs. arrival time for a Type 2 Street Segment .....	109
Figure 4.23: Travel time PDF for a Type 2 Street Segment .....	110
Figure 4.24: Travel time central tendency control chart ( $\bar{X}$ chart) .....	113
Figure 4.25: Travel time range control chart ( $\bar{R}$ chart) .....	113
Figure 4.26: Incident detection algorithm .....	114
Figure 4.27: Two-variable incident detection parameter space .....	115
Figure 5.1: Existing traffic sensor network in Calgary .....	121
Figure 6.1: Transit routes in vehicle tracking data collection .....	132
Figure 6.2(a): Calgary Transit test vehicle .....	133
Figure 6.2(b): Dedicated test vehicles: Hyundai Elantra & Dodge Caravan .....	133
Figure 6.3: GPS receiver/ data logger configuration (Setup 2) .....	134
Figure 6.4(a): In-vehicle instrumentation for transit vehicles .....	135
Figure 6.4(b): Transit vehicle instrument setup .....	135
Figure 6.5: Instrument setup for dedicated vehicles (Setup 2) .....	136
Figure 6.6: Transit stop zones for Routes 2 and 3 (Northern section only) .....	140
Figure 6.7: Transit route sections selected for travel time analysis .....	142
Figure 6.8: Transit and dedicated vehicle travel times (coincident trips) .....	143
Figure 6.9: Modified transit and dedicated vehicle travel times .....	143
Figure 6.10: Correlation of transit and probe vehicle travel times .....	144
Figure 6.11: PARAMICS simulation model of Calgary .....	145
Figure 6.12: Aerial view of simulated area: North of downtown .....	146
Figure 6.13: Traffic demand estimation using survey data .....	151
Figure 6.14: Speed-acceleration data: Driver 1/ Vehicle 1 .....	153
Figure 6.15: Speed-acceleration data: Driver 2/ Vehicle 2 .....	153
Figure 6.16: Speed-acceleration data: Driver 3 & 4/ Transit .....	154
Figure 6.17: Simulated & observed mean travel times: 5th and 6th Ave .....	155
Figure 6.18: Simulated & observed mean travel times: Centre Street .....	155
Figure 7.1: Simulation test bed .....	157
Figure 7.2: Incident Scenarios 1 and 2 .....	162
Figure 7.3: Speed contour: incident Scenario 1: Test Run 4 .....	163
Figure 7.4: Acceleration noise contour: incident Scenario 1: Test Run 4 .....	164
Figure 7.5: Acceleration noise: Scenario 1: Test Run 4 .....	165
Figure 7.6: Speed contour plot for incident Scenario 2: Test Run 2 .....	168
Figure 7.7: Acceleration noise contour: incident Scenario 2: Test Run 2 .....	169
Figure 7.8: Acceleration noise: Scenario 2: Test Run 2 .....	169
Figure 7.9: Street segment travel time histogram: Type 1 .....	172

Figure 7.10: Vehicle travel times vs. signal stage at arrival time .....	173
Figure 7.11: Travel time PDF for Cluster 1 and 2 observations .....	174
Figure 7.12: Transit and dedicated probe vehicle travel time observations .....	175
Figure 7.13: Transit and transit & dedicated probe mean control charts .....	176
Figure 7.14: Transit and transit & dedicated probe range control chart .....	177
Figure 7.15: TTD for all simulations in Scenario 1 .....	179
Figure 7.16: Transit and dedicated probe vehicle travel time observations .....	181
Figure 7.17: Transit and transit with dedicated probe mean control chart .....	182
Figure 7.18: Transit and transit with dedicated probe range control chart .....	183
Figure 7.19: Speed contour plots for Simulation 4 of Scenario 1 .....	185
Figure 7.20: Acceleration noise contours for Simulation 4 of Scenario 1 .....	186
Figure 7.21: Acceleration noise: Scenario 1/ Test Run 4 .....	187
Figure 7.22: Travel time distribution in Street Segment A .....	189
Figure 7.23: Travel time distribution with GPS errors .....	190
Figure 7.24: TTD for all simulations in Scenario 1 .....	193
Figure 7.25: Time evolution of mean control and acceleration noise .....	195
Figure 7.26: Central tendency control and acceleration noise .....	196
Figure 7.28: Central tendency and acceleration noise : normal operation .....	197

## List of Symbols, Abbreviations, Nomenclature

### Symbols

$A$	State transition matrix
$c$	Speed of light in vacuum
$DT$	Dwelling time
$dt$	Between epoch time interval
$d$	Along-track vehicle position
$H$	Observation matrix
$I_\rho(t)$	Ionospheric delay
$K$	Kalman gain
$LT$	Lost time
$N$	Integer cyclic ambiguity
$N, E$	Position
$P$	Likelihood estimate
$Q$	Process noise covariance matrix
$R$	Measurement noise covariance matrix
$R_r$	Receiver position vector
$r^s$	Satellite position vector
$T_\rho(t)$	Tropospheric delay
$t$	Time
$u$	Measurement noise
$v_x, v_y$	Velocity
$w$	Process noise
$x, y$	Position
$\bar{X}$	Predicted state vector
$X$	Updated state vector
$Z$	Measurement vector
$\rho(t)$	Geometric range
$d\rho(t)$	Geometric range error (orbital error)
$\tau$	Transit time
$\delta t^s$	Satellite clock bias
$\delta t_u$	User clock bias
$\mathcal{E}_\rho$	Unmodeled errors in pseudorange measurement
$\lambda$	Carrier wavelength
$\sigma_x, \sigma_y$	Position error estimates
$1/\alpha$	Autocorrelation time constant
$\delta d$	Estimated along-track positioning error

## Abbreviations and Acronyms

ADVANCE	Advanced Driver and Vehicle Navigation and Advisory Concept
AID	Automatic Incident Detection
AoD	Age of Data
A-GPS	Assisted GPS
AS	Anti-Spoofing
AVL	Automatic Vehicle Location
C/A	Course Acquisition
CDS	Collaborative Driving System
CCIT	Calgary Center for Innovative Technology
DFM	Data Filtering Module
DGPS	Differential GPS
DR	Detection Rate
EGNOS	European Geostationary Navigation Overlay System
FAA	Federal Aviation Administration
FAR	False Alarm Rate
FHWA	Federal Highway Administration
Galileo	European GNSS
GLONASS	GLOBAL NAVIGATION Satellite System
GPS	Global Positioning Systems
GPST	GPS Time
GNSS	Global Navigation Satellite System
HCM	Highway Capacity Manual
HSGPS	High Sensitivity GPS
iCORE	Informatics Circle of Research Excellence
IMU	Inertial Measurement Unit
INS	Inertial Navigation System
ITS	Intelligent Transportation Systems
LCL	Lower Control Limit
MEM	Map Estimation Model
MAP	Maximum a Posteriori
MSAS	Multifunction Transportation Satellite Based Augmentation System
NCHRP	National Cooperative Highway Research Program
NP	Nearest Point
OCTA	California Orange County Transit Authority
ORNL	Oak Ridge National Laboratory
PARAMICS	PARAllel MICROscopic Traffic Simulator
PPS	Precise Positioning Service
PRN	Pseudorandom Noise
RAIM	Receiver Autonomous Integrity Monitoring
RF	Radio Frequency

rms	Root Mean Square
SA	Selective Availability
SPS	Standard Positioning Service
TEC	Total Electron Content
TRANSMIT	TRANSCOM's System for Managing Incidents and Traffic
TRB	Transportation Research Board
TTD	Time To Detect
UCL	Upper Control Limit
USDOD	US Department of Defense
USDOT	US Department of Transportation
VDM	Vehicle Dynamic Module
WAAS	Wider Area Augmentation System

## **Nomenclature**

The term HSGPS was used to describe a High Sensitivity version of GPS. The HSGPS receiver used in this research provided two measurement options. The term HSGPS measurement was specifically referred to the default option used throughout this work. The second measurement option was also used in parts of this work for comparison purposes. Every effort was made to clearly distinguish between the two types of HSGPS measurements and their application.

# CHAPTER ONE

## INTRODUCTION

### 1.1 Background

The ever-increasing demand for mobility in urban centres has resulted in increased vehicular traffic congestion and a multitude of problems associated with it. Congestion has become a problem for all sectors of land transportation, both freeways and urban streets alike. Urban streets are the focus of this thesis and are defined as streets where traffic flow is controlled by signals with a signal spacing of 3.0 km or less (HCM2000, 2000). In the context of monitoring and managing congestion, freeways and urban streets require different approaches due to their differences in operating characteristics. Freeway traffic monitoring has been the focus of extensive research over the years; however, considerably less knowledge exists on traffic monitoring in urban streets. The lack of proven techniques for urban street traffic monitoring is mainly attributable to their traffic flow characteristics and technological limitations in effectively capturing such characteristics.

Traffic congestion in urban streets can be classified as recurrent or non-recurrent (NCHRP 20-58, 2002; Cambridge Sys Inc et al., 1998). Recurrent congestion refers to congestion that is directly related to daily traffic flow variations in an area and it is more directly associated with morning and evening peak periods. Although recurrent traffic congestion is fairly predictable, provided local traffic demand patterns are known, any unplanned street capacity reductions during these periods can result in unpredictably high congestion in terms of the area affected, duration, and intensity. Some of the common causes for such street capacity reductions are traffic accidents, vehicle breakdowns, and illegally parked vehicles, commonly referred to as “traffic incidents”. Considering the impact traffic incidents have on day-to-day traffic operations in urban areas, it is equally important to minimize the impact from traffic incidents while maintaining measures to

minimize the recurrent congestion in the first place through strategies such as route diversions and increased public transport usage.

The obvious first measure for minimizing the impact of traffic incidents is to detect them quickly and restore the normal operation of the affected street, which in turn requires fast and accurate detection of incidents. Automated traffic incident detection systems monitor traffic activity through a wide variety of sensors either built into roadways such as traffic flow sensors and video monitoring or vehicle based sensors known as probe vehicles. The origins of automated traffic incident detection lie in freeway incident detection mostly using inductive loop detectors (Peeta & Das, 1998). Similar techniques were later on applied for urban street incident detection with varying degrees of success (Bhandari et al., 1995). With further knowledge of arterial incident detection through projects such as ADVANCE (Advanced Driver and Vehicle Navigation and Advisory Concept), it became apparent that multiple sensor techniques and detailed sensor data were needed to achieve comparable incident detection performance with freeways (Seti et al., 1995; Sermons & Koppelman, 1996). This also introduced probe vehicle techniques for detailed traffic information gathering although their commercial application was initially severely limited by vehicle positioning capabilities and the cost of deploying an adequate number of probe vehicles.

With the advent of the Global Positioning System (GPS) and the economic feasibility for mass in-vehicle usage in the near future, knowledge of probe vehicle-based incident detection has grown rapidly over the past few years. Although there are no probe vehicle-based incident detection systems currently operational, there exist conceptually similar systems for driver assistance and route guidance such as the TrafficMaster system, which is considered to be a highly successful commercial implementation of the probe vehicle concept (TrafficMaster, 2004). These systems archive records from thousands of probe vehicles in order to build travel time databases for real-time users. However, these systems are essentially offline and do not reflect real-time information, which may be supplemented by other Intelligent Transportation System (ITS)

components. The main barrier for these systems to becoming real-time systems is the limitation of real-time information sources, a result of the inadequate number of vehicles with in-vehicle positioning and communication capabilities. GPS and such in-vehicle supporting technologies are still limited to a handful of high-end automobiles and issues such as information sharing and privacy need to be addressed when it comes to reporting detailed vehicle tracking information.

Traffic monitoring usually encompasses monitoring traffic volume, speed, density, travel time and many other derivatives of these fundamental measurements such as vehicle emissions. Real-time probe vehicle-based traffic monitoring requires a considerable proportion of vehicles to have an in-vehicle positioning capability, the proportion being a factor of type of facility monitored, level of detail of the information required and driver and vehicle characteristics (Sirinivasan & Jovanis, 1996). In the case of probe-based urban street traffic monitoring, interaction between traffic flow and traffic controlling devices make it even more complicated, thus requiring special techniques to derive unbiased estimates of traffic flow properties using probe vehicle data (Hellinga & Fu, 2002).

However, detecting signs of incident-induced disruptions in traffic flow requires less precise information as impact from majority of incidents is visible over the variations accountable for routine changes of flow such as demand variations. Considering the fact that minimizing the impact of traffic incidents is a priority and only a limited number of probe vehicles are currently available, this thesis investigates the use of a transit vehicle fleet as a probe vehicle system for an automated incident detection system. The concept of using transit vehicles for traffic monitoring or as transit probes has been the topic of several projects in the past, with the California Orange County Transit Authority (OCTA) transit probe project being one of the leading projects (Hall et al., 1999; PBS&J, 2001). Driven by the advantage of using existing vehicle fleets with in-vehicle tracking systems as probes, there has been a similar focus towards using freeway patrol vehicles for traffic monitoring (Metropolitan Transportation Commission, 2001). Although using such in-

operation fleets for traffic incident or performance monitoring has the advantage of a guaranteed information source, fleets do inherit highly biased traffic characteristics that may not be representative of the average characteristics of the traffic flow (HCM2000, 2000). For instance, transit vehicles stop at designated transit stops and may use priority facilities such as transit-only lanes, which are not representative of any other vehicles in the traffic flow. Unless measures are implemented to minimize the influence of such biases on the outcome of the system, information gathered from such systems becomes less reliable and could eventually fail due to lower user confidence of the system.

The work presented in this thesis focuses on all stages of a probe-based incident detection system, starting from the vehicle positioning and tracking component. Several GPS based vehicle-positioning techniques are evaluated with emphasis on their performance in typical urban environments. Results from extensive field experiments are presented and High Sensitivity GPS (HSGPS) receiver technology is adopted for the positioning of transit probes in order to improve availability in urban canyons where standard GPS receiver technology usually fails. Further discussion is presented on map-matching as a tool for augmenting HSGPS and as a data association mechanism between the GPS spatial information domain and street network domain. Results from field experiments and simulation-based vehicle tracking system performance evaluations are also presented.

Traffic flow characteristics for incident detection are derived from transit tracking data and are combined into algorithms for automated incident detection. Testing algorithms entirely based on field experiments involve considerable resources and detailed knowledge of many factors affecting road traffic. Instead, a microscopic traffic simulation model was used for algorithm testing, greatly simplifying testing while retaining the capability to incorporate field data to calibrate the model. A vehicle travel time variation and acceleration noise based traffic incident detection algorithm is developed and extensively analyzed using simulated traffic. The results are analyzed using key incident detection algorithm performance elevators, namely Detection Rate (DR), False Alarm Rate (FAR) and Time to Detect (TTD).

## **1.2 Limitation of Previous Work**

The advances in technologies such as GPS have been used in many branches of traffic and transportation engineering to improve the level of service and safety for road users over the years through the incorporation of intelligence into transportation systems. Traffic monitoring and incident detection have been integral components of this constant drive for improvements and the emergence of GPS has resulted in a range of promising future prospects. However, in the context of this thesis, the following limitations are identified in the current state of knowledge:

### **Capabilities of GPS and Limitations**

GPS can provide an unmatched position and velocity measurement capability ranging from around a 10 metre position accuracy under open sky conditions using pseudorange techniques to centimetre level positioning using precise kinematic positioning techniques. However, this level of accuracy is often not available in many of the urban environments where most of the GPS-based techniques are put into operation. For instance, urban canyon conditions can create position errors of hundreds of metres and even result in losing the GPS positioning capability for short durations (Basnayake & Lachapelle, 2003; Basnayake et al., 2004).

Almost all of the GPS-based traffic monitoring and incident detection applications have neglected this GPS degradation aspect, thus most systems become unusable, if not highly unreliable, in urban environment operations. Although the GPS community has developed a multitude of augmentations and advanced GPS processing techniques for mitigating such performance degradations, they are seldom adopted in traffic engineering applications, thereby greatly reducing user confidence.

### **Using Passive Probe Vehicles for Incident Detection**

Passive probe vehicles provide vehicle-tracking information for traffic management purposes while operating for a primary purpose other than serving as vehicle probes such as transit or freeway patrol vehicles. Although this concept was employed in several previous projects, there exists more unknowns in using them as probes, thus almost all of these projects resulted in failure when it came to real-life operation (Hall et al., 1999; Moore et al., 2001). The success of using passive probe data is highly dependent on making unbiased estimates of traffic flow characteristics by observing only a small proportion of vehicles with highly distinguishable vehicle characteristics, often operating for another primary purpose such as transit vehicles. Therefore, the root cause of many of these failures lies in the accuracy and the information provided by the positioning systems. For instance, the California Orange County Transit Authority (OCTA) transit probe system, which was not capable of measuring the actual time a transit vehicle spends at a designated stop, relied on an explicit model for dwelling time estimation. Thus, it was impossible to distinguish between longer travel times resulting from congestion and longer dwelling times spent in designated transit stops. Therefore, the system was highly unreliable in detecting congestion induced delays (Hall et al., 1999).

### **GPS Augmentation with Map-Matching**

Map-matching is probably the most widely used augmentation and data association tool used in GPS-based traffic monitoring and data collection applications (TRB, 2004). Although map-matching techniques are often referred to as a GPS augmentation only, it is often used for associating GPS spatial data into other information processing domains such as street network for traffic monitoring applications. Most map-matching algorithms minimize the across-track error either on an epoch-by-epoch basis or with some sort of a short-term memory of vehicle location (Greenfeld, 2002; White, 2000). However, very limited research has been done on minimizing the along-track error while

minimizing the across-track error simultaneously. In terms of traffic monitoring applications, the inability to control along track errors poses an enormous draw back, as such applications often make use of along-track measurements while across-track measurements are only required for data association to streets. Furthermore, as it stands at present, pseudorange GPS measurements are not accurate enough to provide any useful street lane level information.

### **Parameters and Algorithms for Incident Detection in Urban Streets**

Traffic incident detection had been almost exclusively concentrated on freeway incident detection until after 1990. First efforts to extend the research scope to arterial streets were made in 1996 through a workshop organized by the US Federal Highway Administration (FHWA) and Oak Ridge National Laboratory (ORNL) (Cambridge Sys Inc. et al., 1998). Since then, projects such as ADVANCE have contributed substantial knowledge to urban street incident detection algorithms and variables of interest for automated incident detection. Although assumptions are being made about the impact of traffic incidents in urban street traffic flow characteristics, especially on travel time variation and acceleration noise characteristics to a lesser extent, little is done to actually quantify such assumptions (Seti et al., 1995).

### **Impact from Incidents in Urban Streets**

Further to identifying the traffic flow characteristics that reflect the onset of traffic incidents, there exists minimal knowledge on related field experiments. The main reason for such lack of knowledge is the limitation of resources for conducting large-scale surveys with individual vehicle level data, required for detailed analysis of impact from incidents. Furthermore, lack of control in actual field experiments, data reporting problems and influences from many more variables (such as weather) increases the

complexity of such attempts. The US Department of Transportation's Intelligent Transportation Systems Field Operational Test (FOT), TRANSMIT (TRANSCOM's Systems For Managing Incidents and Traffic) is one of the few field experiments conducted in probe-based incident detection, and can be regarded as a feasibility study for future technologies that provides limited analysis on the impact of incidents (Booz, Allen & Hamilton, 1998).

### **1.3 Objectives and Contribution of the Thesis**

#### **1. Uninterrupted Vehicle Tracking Using GPS and HSGPS**

The accuracy, reliability and availability of the vehicle positioning system are critical aspects of any probe vehicle application. Although GPS was used for many transportation-related applications, the reliability of GPS-based systems in urban environments, where its performance is vital, is seldom addressed. The work presented in this thesis investigates the performance of conventional GPS and its improved version, namely High Sensitive GPS (HSGPS), which offers better performance, in the context of providing a higher level of system availability and thus uninterrupted vehicle tracking capability for traffic engineering applications.

#### **2. Map-Matching as a HSGPS Augmentation**

GPS-based traffic monitoring and data collection applications often depend on along-track measurements such as travel time rather than across-track measurements, partially due to the accuracy achievable using HSGPS pseudorange measurements, which is not precise enough to monitor lateral movements of the vehicle such as lane changes. However, almost all map-matching algorithms focus on across-track corrections, and little can be done to minimize the along-track errors using conventional map-matching

techniques. The inability to control along-track errors poses an enormous drawback for ITS and traffic engineering applications. Therefore, this thesis investigates methods of controlling along-track errors with map-matching techniques combined with additional low-cost sensors and prior knowledge of vehicle routes, as applicable for transit vehicles.

### **3. Vehicle Tracking Information Processing for Traffic Engineering Application**

Information processing is a vital component of ITS applications. Previous experiences with ITS vehicle tracking have shown that the vast amounts of data gathered by vehicle tracking are often not used effectively due to improper management of information. This thesis forms a framework of information gathering and processing based on well-established guidance provided by the Highway Capacity Manual for urban street performance analysis (HCM2000, 2000).

### **4. Probe-Based Traffic Incident Detection Parameters**

Based on existing knowledge, this thesis approaches the problem of probe-based incident detection with the premise that individual vehicle travel times in street segments and acceleration noise are correlated with the level of traffic congestion and hence show significant variation with incident induced congestion. Although a field experiment to confirm the validity of this premise would be ideal, such experimentation was not possible due to limited resources, limited ability to control the environment variables and other complexities involved in field experiments. Therefore, a traffic microsimulation model was used instead to illustrate the validity of using street segment travel time variation and acceleration noise for traffic incident detection in urban streets. An effort was also made to characterize the response of these measures to incident characteristics.

## **5. Traffic Incident Detection Algorithms**

Algorithms are proposed to monitor vehicle-tracking data from transit probe vehicles and to automatically detect the onset of traffic incidents. The basis for the formulation of such algorithms is the knowledge gained by analyzing parameters derived from probe vehicle tracking data, namely the street segment travel time variation and acceleration noise.

## **6. Performance Evaluation of Incident Detection Algorithms**

Incident Detection algorithm performance may vary in terms of accuracy and reliability under different operating conditions. Therefore, it is of great importance to establish accuracy and reliability measures for incident detection algorithms. Following the wider consensus in traffic incident detection research, three performance indicators were used for analyzing the algorithm performance, namely Time to Detect (TTD), False Alarm Rate (FAR) and Detection Rate (DR). The correlation of these parameters with traffic incident characteristics and characteristics of the streets is also investigated. Furthermore, algorithm performance degradation with travel time measurement errors, which is a considerable factor due to GPS performance in urban areas, was also investigated.

## **7. Recommendations for Future Work**

Although this thesis provides a comprehensive analysis of incident detection parameters and algorithms under selected traffic volume to capacity ratios, driver and vehicle characteristics, and control conditions, it is possible to observe exceptions. For instance, very high traffic volume to capacity ratios could naturally increase the probe vehicle acceleration noise thus making it impossible to provide any useful information for

incident detection. Therefore, the thesis also identifies areas where further work is needed for improvement.

#### **1.4 Thesis Outline**

The thesis begins with an introduction of ITS in Chapter 2. All major areas of ITS are addressed with emphasis on Automatic Vehicle Location (AVL) applications. Incident detection and performance monitoring using AVL data is discussed in detail in the context of both freeways and urban arterial streets. The challenges in arterial incident and performance monitoring in comparison with freeway traffic monitoring is discussed along with a brief literature review on related research. A comparison of data requirements for traffic incident detection and performance monitoring is also presented and the chapter concludes with a lead to Chapter 3 where enabling technologies for the traffic incident monitoring system are discussed.

Chapter 3 summarizes the Global Positioning System and its augmentations. GPS fundamentals are outlined with the emphasis on vehicle navigation in urban areas. Since real-time or near real-time traffic monitoring is especially important in urban areas and the positioning capability of the probe system plays a critical role, a major part of this chapter is devoted to GPS performance issues in urban areas. Error sources such as GPS signal degradation and multipath are outlined and enhanced GPS technologies such as High Sensitivity GPS (HSGPS) are discussed in the urban vehicle navigation context. The main GPS augmentation in the probe system, map-matching, is also introduced in this section. A general introduction to map-matching is presented along with a detailed insight into the algorithms developed for the transit probe system. Several map-matching scenarios are considered including moderate to severe GPS signal degradation with or without prior knowledge of the vehicle route. In addition to improving across-track accuracy, techniques to minimize along-track errors either by using GPS velocity information or by using additional sensors are also investigated. Augmentations with Inertial Measurement Units (IMU) are also discussed and a low-cost integrated

navigation system is developed, incorporating the techniques developed throughout the chapter.

The overall system configuration of the transit probe-based traffic incident monitoring system is presented in Chapter 4. The chapter is subdivided into four sections based on the system functionality. The chapter starts with the most important component of the system, the vehicle positioning system. Techniques presented in Chapter 3 are further developed to build a robust positioning system. HSGPS and map-matching-based positioning system performances are analyzed using data from field surveys conducted in Calgary, Alberta and simulated data from a Sprint Global Navigation Satellite System (GNSS) RF signal simulator in the Department of Geomatics Engineering, University of Calgary. Two further scenarios are considered for the vehicle positioning system. Firstly, vehicle routes are considered known a priori, which is the case for transit vehicles, and secondly, the case of unknown routes, which is applicable for dedicated probe vehicles not restricted to a particular route. The second sub-section in the chapter introduces the data processing algorithms in the system. Transit tracking data processing algorithms that associate GPS vehicle tracking data into street segments and remove transit specific features from tracking data are presented. Emphasis is given to the travel time modeling framework, which combines historical data with real-time data for optimum estimation of system variables. The chapter concludes with a presentation of the incident detection algorithm combining algorithms and models presented in the preceding subsection and a brief outline on extending the travel time modeling framework for multiple variables of interest.

The field performance evaluation of a traffic incident detection system is an enormous undertaking. The resources required and the limited control over environmental variables in real life transportation systems were the main obstacles to overcome. Therefore, field experimentation was considered beyond the scope of this thesis. Alternatively, a microscopic traffic simulation model was used for all algorithm performance evaluation phases in this thesis. Chapter 5 outlines some of the basic aspects of microscopic traffic

simulation and the factors that warranted the use of simulation modeling for this research. A brief introduction is also given to the traffic microsimulator used in this research, PARAMICS. Emphasis is given to model building, calibration and validations as links between data collected in field experiments and the simulated environment.

Chapter 6 outlines the field data collections conducted and simulation model scenarios developed in this thesis. The chapter is divided into two subsections. The first section outlines field data collections conducted for navigation system testing and performance analysis. The second section summarizes field data collections conducted for simulation model building and data analysis procedures for incident monitoring system algorithms, simulation model calibration using field data and finally the simulation scenario building for the incident detection algorithm performance evaluation.

The incident detection system is analyzed in Chapter 7 using the PARAMICS simulator model. This simulation-based analysis includes the algorithm performance evaluation in terms of performance evaluators such as incident Detection Rate (DR), False Alarm Rate (FAR) and Time to Detect (TTD) with different levels of transit probe vehicle populations and with additional dedicated probe vehicles in the system. The degradation of these performance evaluators with deteriorating GPS accuracy is also investigated. Further discussion investigates the possibility of using the transit based traffic incident monitoring system as a traffic performance monitoring system with additional dedicated probe vehicles.

The conclusions of this research are presented in Chapter 8. The contributions to the areas of urban vehicle navigation in the context of transit and probe vehicle positioning are presented. Furthermore, knowledge gained in the areas of real-time or near real-time traffic modeling, traffic incident and performance monitoring variables and incident detection algorithms are summarized. Areas of further research are also identified, and recommendations are made for further future developments.

## CHAPTER TWO

### INTELLIGENT TRANSPORTATION SYSTEMS

This chapter outlines the fundamental concepts of ITS and their benefits to the users. The rest of the chapter is focused on GPS-based ITS applications; particularly traffic monitoring and incident detection using AVL.

#### **2.1 Intelligent Transportation Systems**

The term Intelligent Transportation Systems can be defined as the use of advanced technology in information gathering, processing, telecommunication and many other branches of engineering for providing efficient, safe, and less congested land transportation solutions with less impact on the environment (Transport Canada, 2004). The classification of these technologies is done based on many factors. For the discussion in this thesis, Transport Canada's ITS user services classification based on functionality is used, see Transport Canada (2004). This classification is discussed in detail below.

##### **2.1.1 Traveler Information Services**

Travel information services include four major information categories. The first service category includes providing traveler information through interactive and broadcast media and providing real-time ridesharing information. The second service category includes route guidance and navigation information services, which provide route guidance information, traffic estimation and prediction information and in-vehicle navigation information. Real-time and pre-trip ride matching and traveler services and reservations constitute the other service categories, which include all sub-services relating to ride-matching, traveler yellow pages and managing parking facilities.

### **2.1.2 Traffic Management Services**

Traffic control is a major component of traffic management services in ITS. This includes monitoring all surface streets and highways using fixed sensors, ITS-based monitoring techniques such as probe vehicles, traffic estimation and prediction, dissemination of traffic information to different layers of traffic management and the control network, and controlling all transportation facilities. Traffic incident management is also a service under this category, which includes monitoring and detecting traffic incidents, incident prediction and incident management coordination. The scope of this research also falls into this category. Other user services in this category include travel demand management, environmental conditions management, operations and maintenance, automated dynamic warning and enforcement, non-vehicular road user safety and multi-modal junction safety and control.

### **2.1.3 Public Transportation Services**

Although congestion can be minimized using advanced technologies, controlling the traffic demand often becomes the last resort, as no technology could improve the capacity of transportation facilities for an endless demand. Encouraging travelers to increase the use of public transport is one of the most successful solutions for managing peak period traffic congestion in many cities around the world.

Public transportation services provide passengers with real-time transit vehicle locations through vehicle tracking systems, en-route transit information and multi-modal travel information. This service category also includes demand responsive transit services, route operation management and travel security services. The research presented in this thesis provides a transit fleet tracking system in addition to its primary use as an incident monitoring system thus provides vehicle tracking information for public transport services.

#### **2.1.4 Electronic Payment Services**

This ITS service category includes providing user-friendly payment techniques for electronic toll collection, electronic parking payments, and transit and traveler information service payments.

#### **2.1.5 Commercial Vehicle Operations**

ITS commercial vehicle operations services focus on making commercial vehicle operations safer, faster and efficient through the application of advanced technology. This includes providing electronic clearance services through faster inspection systems such as Weigh-In-Motion (WIM), automated roadside safety inspections, onboard safety monitoring, and fleet management.

#### **2.1.6 Emergency Management Services**

Emergency management services provide services that are oriented for the safety and security of individual users and the safe and efficient operation of transportation infrastructure as a whole. The former includes in-vehicle emergency notification systems and stolen vehicle tracking whereas the latter includes a wider range of services including emergency vehicle management, incident and disaster response management and hazardous material transportation solutions. Emergency management systems integrate with other services for gathering incident or disaster information and subsequently with traffic management services to implement incident response plans.

#### **2.1.7 Vehicle Safety and Control Systems**

Vehicle safety systems encompass a range of technologies that improve the safety of users. Automated vehicle collision avoidance systems are among the more prominent

technologies in this category. Furthermore, infrastructure-based collision avoidance systems also provide the same service, with intersection collision avoidance being one of the more likely systems to appear in the near future. In-vehicle safety and control systems also include vehicle and driver safety monitoring and driving enhancement systems. These include task automation systems ranging from proximity-based vehicle acceleration control to Collaborative Driving Systems (CDS). A Canadian initiative in CDS research and the development of a vehicle positioning system for CDS is discussed in detail in Cannon et al. (2003).

### **2.1.8 Information Warehousing Services**

Information warehousing includes archiving, processing and dissemination of information relating to the operation of transportation infrastructure. The information concerned may include traffic activity data such as travel time of traffic flow, weather information, and incident or disaster information. In the context of this thesis, historical travel time data is archived and used with real-time information to provide optimum estimates about the status of the transportation network.

## **2.2 Automatic Vehicle Location (AVL) Applications in ITS**

Accurate vehicle location and tracking are the basic requirements for many ITS technologies. For instance, commercial vehicle fleet tracking and public transport tracking systems depend on vehicle location capabilities. GPS provides an unmatched vehicle location and tracking capability compared to any other technology available, and thus it is extensively utilized in a variety of ITS applications. GPS technology was first used in ITS applications for data collection and surveys, mainly to gather information such as trip travel times, driving, and route choice patterns (Gallagher, 1996; Roden, 1996; Roden, 1997; Laird, 1996). A brief historical overview of AVL applications is given below.

### **2.2.1 Probe Vehicle Applications**

Although similar in the applied technology, GPS vehicle tracking data is extensively used for studying two levels of traffic and vehicle operations: firstly, to study the behaviour of individual vehicles and their interactions with other vehicles in traffic flow and infrastructure and secondly, for estimating traffic flow conditions using vehicle-tracking data. The former is usually referred to as instrumented vehicles where vehicle or driver specific information is the focus (Brackstone et al., 2000; McDonald et al., 1997; McDonald & Brackstone, 1997). In the latter case, such vehicles are known as probe vehicles, which sample traffic flow behaviour and enable the estimation of flow characteristics (Sanwal & Walrand, 1995; Yim & Cayford, 2001). Probe vehicles equipped with GPS are extensively used in traffic data collection. These include dedicated vehicle probes or a combination of dedicated and non-dedicated vehicles such as transit or freeway patrol and maintenance vehicles. The San Francisco Bay Area traffic information system (TravInfo) is an example of such a combined approach to collect traffic network data using probe vehicles (Metropolitan Transportation Commission, 2001).

### **2.2.2 Instrumented Vehicle Applications**

Tests with instrumented vehicles opened the avenue for testing models such as car-following models with real data instead of simulations or laboratory tests (Wolshon & Hatipkarasulu, 2000; McDonald et al., 1997). The necessity for higher accuracy levels in some applications prompted researchers to use alternative GPS techniques such as Differential GPS (DGPS) (Ibrahim, 2000). With the development of precise GPS carrier phase techniques, research ventured into individual vehicle level, analyzing microscopic traffic behaviour such as headway distributions and platoon behaviours (Woo & Choi, 2001). However, the accuracy of such systems is limited to line-of-sight to the GPS satellites, which is present only in sub-urban areas. Therefore, such systems, as

standalone systems, are of limited use in urban environments due to signal shading by tall buildings.

### **2.3 Traffic Incidents and Traffic Incident Detection**

Traffic incidents can be defined as any event that disrupts the normal operation of a transportation facility. According to the US Department of Transportation (US DOT) ITS documentation, “incident” refers to any event that degrades safety and slows traffic, including disabled vehicles, crashes, maintenance activities, adverse weather conditions, special events, and debris on the roadway. Incident-related traffic congestion (including secondary impacts) has detrimental effects on public safety, the local economy, and the environment (ITS US DOT, 2000). Therefore, faster detection and response (often called incident management) are essential for maintaining high levels of efficiency and safety in roadways. Incident management yields significant benefits through reduced vehicle delays due to incidents and enhanced safety through the reduction of incident frequency and improved response and clearance times. The first operational traffic incident detection and management system was developed in the city of Detroit in 1961, comprising of a CCTV (Closed Circuit TV) and inductance loop detector system for monitoring and a system of variable message signs for informing the road users of any incidents.

#### **2.3.1 The Importance of Traffic Incident Detection**

Traffic incidents either reduce the available capacity of a roadway or degrade the performance, usually measured by lower operating speeds and increased congestion. They may also increase the likelihood of secondary incidents and performance degradation in roadways that are not even directly influenced by the incident through circumstances such as *rubbernecking* (Cambridge Sys Inc. et al., 1998). Although incident detection and management under any roadway condition is essential, the impact

of an incident may be highly correlated with other major factors such as traffic flow or the level of congestion at the time of the incident. For instance, the impact of a traffic incident in non-congested flow conditions is highly localized. However, incidents that occur in time periods with high levels of congestion may have considerably higher impact on the rest of the roadway network. Traffic congestion under normal conditions can be categorized as recurrent and non-recurrent congestion, and recurrent traffic congestions are fairly predictable with the knowledge of local traffic demand conditions (NCHRP 20-58, 2002). Although incidents may have a localized impact on the rest of the roadway network under non-congested normal operation, even minor disruptions to traffic flow in time periods with recurrent congestion could result in unpredictably high congestion affecting a wider area.

### **2.3.2 Freeway, Arterial and Urban Street Classification**

Roadways used for land transportation can be broadly classified into two categories, freeways and urban streets (or arterials). The recommended classifications are given in the Highway Capacity Manual (HCM2000, 2000). Based on HCM2000 guidelines, freeways are defined as multilane, divided highways with a minimum of two lanes for the exclusive use of traffic in each direction with full control of access without any interruption to traffic. HCM2000 also defines arterial streets as signalized streets with signals at a spacing of 3.0 km or less, primarily serving through traffic while providing access to abutting properties. The term urban street is also used for arterials throughout this thesis, which, according to HCM2000, has similar traffic signal control features and a relatively high density of driveway access.

### **2.3.3 Incident Detection in Freeways**

Freeway incident detection, by far, has been the predominant domain for automated incident detection (AID) research. This is primarily due to the fact that fixed detectors

such as inductive loop detectors dominated the traffic flow-monitoring arena until the recent emergence of automatic vehicle location (AVL) technologies, and such technologies are fairly limited in application to urban streets. Stephanedes et al. (1992) provide a comprehensive analysis of many freeway incident detection algorithms used in early stages of incident detection algorithm development. The common approach for fixed detector-based incident detection is to analyze a *fingerprint* of speed, volume or occupancy measurements from a detector for anticipated incident induced features (Corby & Saccomanno, 1997).

Although mostly limited to simulation-based performance evaluations, due to limited availability in AVL-equipped vehicles, AVL-based AID has shown promising success. With AVL, the ability to gather finer details of vehicle characteristics, and their changes with incidents, enable faster and more accurate incident detection. For instance, monitoring the statistical characteristics of travel time and speed of individual vehicles provides an enhanced capability to detect incidents over conventional methods (Hellinga & Knapp, 2000).

#### **2.3.4 Challenges in Arterial Incident Detection**

Incident detection had been almost exclusively concentrated on freeways until 1990. First efforts to extend the research scope to arterial streets were made in 1996 through a workshop organized by the US Federal Highway Administration (FHWA) and Oak Ridge National Laboratory (ORNL) (Cambridge Sys Inc. et al., 1998). The lack of high-density sensor networks in arterial streets is mainly blamed for the limited research on arterial incident detection. However, research has also shown that conventional traffic flow sensors such as inductive loop detectors are of limited use in capturing the impact of traffic incidents in arterial streets. For instance, the traffic flow characteristics revealed by analyzing upstream and downstream vehicle speed and occupancy data in an arterial will differ significantly from that of a freeway scenario primarily due to the filtering effect of traffic signals, which in turn produces platoons of vehicles.

In fact, arterial segment travel times are often dominated by traffic signal delays in non-congested operating conditions and the traffic control induced delay is highly correlated with the time a vehicle approaches the signal (Graves et al., 1998). In one of the few attempts to use transit vehicles as probes, this phenomenon was also confirmed by the California Orange County Transit probe project, which eventually failed to materialize due to limitations in the measurements provided by the transit probe system (Hall & Vyas, 2000).

Although freeway incidents share some similarities with arterial incidents, anecdotal evidence exists that suggest some unique features. Raud & Schofer (1997) conducted a study that recorded over 1,800 traffic incidents over a period of twenty-eight days in suburban Chicago and identified several arterial incident features. In contrast to freeway incidents, where disabled vehicles caused the majority of incidents, many more factors contribute to incidents, such as traffic crashes (35 %), stops due to police activity (30 %) and disabled vehicles (27 %). Raud & Schofer (1997) concluded that up to 15 % of crashes may be classified as secondary incidents due to earlier incidents, and their work remains one of the very few studies done on arterial traffic incidents and their impact.

### **2.3.5 Arterial Incident Detection Algorithms**

Although significantly different in operating characteristics, freeway incident detection algorithms have had a considerable influence on arterial incident detection algorithm development. Analogous to freeway incident detection, Hounsell et al. (1988) proposed the analysis of occupancy data from a series of sensors to characterize incident-induced traffic flow variations; however, he presented no explicit algorithms for incident detection. Han & May (1988) investigated the relationship between the three fundamental traffic flow variables, flow, occupancy and speed under incident and non-incident conditions to characterize the incident induced variations using an artificial intelligence approach. Han & May (1989) further investigated the impact of the incident

location on the traffic flow disturbances. Thancanamootoo & Bell (1988) used a time series analysis of traffic flow variables for arterial incident detection with an exponentially smoothed time series of vehicle speeds and travel time.

One of the first AVL-based arterial incident detection algorithms was presented by Parkany & Bernstine (1993), and the importance of monitoring individual vehicle behaviour changes to detect traffic incidents was first taken into consideration. However, research investigating the correlation between congestion and individual vehicle behaviour had been going on as early as 1980, especially research on the correlation between vehicle acceleration noise and the level of interaction between vehicles and hence with incidents (Winzer, 1980).

With the wider availability of technology to track vehicles in high detail, for instance vehicle location and speed measurements every second, later projects ventured into probe-based incident detection and performance monitoring. The reader is referred to publications on ADVANCE (Advance Driver and Vehicle Advisory Navigation Concept) and TRANSMIT (TRANSCOM's System for Managing Incidents and Traffic) projects (Koppelman et al., 1996; Booz, Allen & Hamilton, 1998). The limitation of the size of available probe vehicle populations has been one of the major obstacles for wider implementation of the probe vehicle-based systems. The alternative of using existing commercial vehicle fleets such as transit vehicles or highway patrol vehicles as probes was also investigated as described by Hall et al. (1999) and Moore et al. (2001). Although field experimentation with these techniques failed to prove successful due to system implementation issues, they have provided considerable knowledge for future system development (Hall & Vyas, 2000; Hall et al., 1999).

Overall, several conclusions can be drawn from all the research conducted so far on arterial incident detection. Firstly, arterial incidents only affect the area in close proximity. For instance, a mid-block incident will only affect the flow patterns in the same street while the upstream impact will be severely altered by the traffic controlling

devices. Furthermore, incidents in intersections could impact both upstream and downstream streets. One of the objectives of this thesis was to investigate such incidents features. Secondly, no generalized rules are established for implementation of automated traffic incident detection that performs satisfactorily in any environment. Moreover, combining multiple data sources was seen as the solution for robust incident detection (Bhandari et al., 1995).

### **2.3.6 Algorithm Performance Evaluation**

The performances of incident detection algorithms are evaluated using three performance indicators, namely, DR, TTD and the FAR. DR is defined as the percentage of successfully detected incidents out of all incidents while TTD is expressed as the time lag between the time of the incident and the time of the incident detection. FAR is the percentage of times in which incidents were indicated by the algorithm when there was no actual incident. An incident detection algorithm with a higher DR, lower FAR and a faster TTD is capable of functioning as a powerful tool for automated traffic monitoring.

## **2.4 Performance Monitoring in Arterials**

Traffic performance monitoring involves investigating the variation of key performance indicator variables for different purposes. For instance, travel time is a key indicator of traffic network performance even in a non-engineering context. Drivers often use alternative routes based on their knowledge of the area or other information available to them to avoid longer travel times and to get to their destination in the shortest possible time. Although this thesis does not intend to investigate traffic performance evaluation, some of the key issues related to incident detection are addressed below. For a detailed description of the current state of practice in highway performance monitoring in the United States, the reader is referred to NCHRP (2003).

### 2.4.1 Performance Measures for Arterial Traffic Monitoring

Arterial performance measures should reflect a broad range of performance characteristics including finer details of performance during normal operations and characteristics of traffic with incidents and congestion, both recurring and non-recurring. The performance measures are used in a variety of applications ranging from real-time public information to archived information for long-term facility management. Furthermore, traffic incident detection could be regarded as a subset of traffic performance monitoring, and some of the key performance measures form a part in traffic incident detection. Some of the key performance measures that are commonly used in incident detection are summarized in Table 2.1 along with typical objectives of monitoring those measures. A detailed discussion on this topic is given in NCHRP (2003).

Table 2.1: Performance measures used in incident detection and their usage

<b>Performance Measure</b>	<b>Definition</b>	<b>Usage</b>
Incident Induced Delay	Travel Time Increases Due to Traffic Incidents	Safety Management, Public Information Systems and Other ITS Applications
Duration of Congestion	Time Period with Congestion	Public Information Systems, Quality Management, Planning, Congestion Management and Other ITS Applications
Incidents	Traffic Interruptions Caused by Accidents and Other Unplanned Events	Safety Management, Public Information Systems, Quality Management, Planning, Congestion Management and Other ITS Applications
Operating Speed	Distance Traveled Over Time	Safety Management, Public Information Systems, Quality Management, Planning, Congestion Management and Other ITS Applications
Travel Time and Travel Rate Index (NCHRP, 2003)	Distance Over Speed and Amount of Extra Travel Time	Safety Management, Public Information Systems, Quality Management, Planning, Congestion Management and Other ITS Applications
Travel Time Reliability	Variability of Travel Time	Similar as Travel Time

### 2.4.2 Data Requirements for Performance Monitoring

Traffic incident detection shares a subset of objectives and technologies in traffic performance monitoring. In terms of the information content required, incident detection

requires only a fraction of information required by traffic performance monitoring. In the context of using probe vehicles, performance monitoring would require a fairly large probe vehicle population, well distributed in the traffic flow for reliable, unbiased and timely performance evaluation. When such conditions are not met, techniques are required to minimize the biases in the information gathered. For instance, Hellinga & Fu (2002) describe a technique to remove travel time measurement biases from probe vehicles using a stratified sampling technique. For further information on performance monitoring data requirements, see NCHRP (2003).

## CHAPTER THREE

### GLOBAL POSITIONING SYSTEM AND AUGMENTATIONS

This chapter outlines the fundamentals of GPS. A further discussion on GPS error sources in the context of urban vehicle navigation and error mitigation and augmentation techniques are discussed.

#### **3.1 Overview of GPS**

GPS consists of a constellation of satellites that continuously broadcast ranging signals on multiple radio frequencies. The baseline constellation consists of 24 satellites orbiting in inclined orbits approximately 20,000 km above the Earth. The system consists of three segments, namely the space, control and the user segment. The space segment consists of the earth orbiting GPS satellites, and the control segment on the earth's surface maintains the space segment. The control segment constantly monitors the health of satellites, predicts their orbits and clock parameters, updates satellite navigation messages and most importantly maintains the GPS time standard. The United States Coast Guard provides users with the current status of the GPS constellation (NAVCEN, 2004). A comprehensive description of GPS is given in Wells et al. (1987), Misra & Enge (2001) and Parkinson et al. (1996).

The user segment consists of all civilian and military users of the system. The developer of the system, the U. S. Department of Defense (USDoD), intended to develop an all-weather, globally available system that could offer precise position, velocity and time for military and civilian users. The system provides two services, namely the Standard Positioning Service (SPS) for civilian users and the Precise Positioning Service (PPS) for authorized (military) users. The PPS is only available to users with special encryption keys through a system called Anti-Spoofing (AS). The SPS was built with a precision

degradation feature called Selective Availability (SA) that can only be removed by the authorized users to obtain the full accuracy of the system. However, SA was deactivated on a Presidential Order on May 2<sup>nd</sup> 2000, thus providing access to non-degraded GPS to the civilian population.

### 3.1.1 GPS Signal Structure

At present, GPS broadcasts two signals in the L-band between 1 GHz and 2 GHz referred to as L1 and L2. Ranging codes or pseudo-random noise (PRN) codes and navigation data are modulated onto the carrier signal and the receivers generate their own versions of PRN codes to correlate and identify the satellite broadcasting the signal and subsequently decode the information for position, velocity and time estimation. GPS satellites transmit two PRN codes, namely the coarse/acquisition (C/A) code and the precision (encrypted) P(Y) code. Only the C/A code is available to civilians. GPS signals also contain a navigation message modulated onto the rest of the signal though a technique called bi-phase modulation. This message contains information on approximate location and velocities of all satellites in the GPS constellation, their clock bias information and health status. The navigation message is transmitted at a rate of 50 bits per second and would take up to 12.5 minutes for a receiver to download the entire message. GPS signals and the information contained in each signal are summarized in Table 3.1.

Table 3.1: GPS Signal Structure

Signal	Ranging Signal	Code		Navigation Message
		Chip Width	Chipping Rate	
L1 1575.42 MHz	C/A	300 m	1.023 MHz	Data Rate 50 bps Chip Width 20 ms Duration 12.5 minutes
	P(Y)	30 m	10.23 MHz	
L2 1227.6 MHz	P(Y)			

GPS is currently going through a modernization program and the plan is to have an additional civilian code on L2 and a new civil signal on the 1176.45 MHz frequency called L5. These modernization plans are outlined in this thesis as an indication of

improved future capabilities, and for further details the reader is referred to Misra & Enge (2001).

### 3.1.2 GPS Position, Velocity and Time Estimation

GPS provides two types of measurements, namely the code and the carrier phase. A brief outline of the two measurements is given below.

#### 3.1.2.1 Code or Pseudorange Measurement

GPS receivers use the autocorrelation properties of PRN codes to identify individual satellites and align the received signal with the receiver clock. Once the signals are aligned, the transmitted time of the signal can be retrieved from the information provided by the GPS signal. The basic pseudorange equation in units of metres is given by:

$$P(t) = \rho(t) + d\rho(t) + I_{\rho}(t) + T_{\rho}(t) + c[\delta t_u(t) - \delta t^s(t - \tau)] + \varepsilon_{\rho}(t) \quad (3.1)$$

where

$t$	time of reception GPS time (GPST)
$\rho(t)$	geometric range
$d\rho(t)$	geometric range error (orbital error)
$I_{\rho}(t)$	ionospheric delay
$T_{\rho}(t)$	tropospheric delay
$\tau$	transit time seconds
$\delta t^s(t - \tau)$	satellite clock bias relative to GPST
$\delta t_u(t)$	user clock bias relative to GPST
$\varepsilon_{\rho}$	unmodeled errors in the pseudorange measurement
$c$	speed of light in a vacuum.

The geometric range measurement in Equation (3.1) can be rewritten as:

$$\rho(t) = \|r^s - R_r\| \quad (3.2)$$

where

$$\begin{array}{ll} r^s & \text{satellite position vector} \\ R_r & \text{receiver position vector.} \end{array}$$

### 3.1.2.2 Carrier Phase Measurement

The carrier phase measurement is the phase difference between the received signal and the receiver-generated signal at the instant of the measurement. Hence, the carrier phase measurement is much more precise compared to the code measurement. However, as there is no time mark on the carrier as in the case of the code, this relation can be made to any of the phases thus making the measurement ambiguous. Analogous to the pseudorange measurement, the carrier phase measurement can be written in the form:

$$\phi(t) = \rho(t) + d\rho(t) + N\lambda - I_\phi(t) + T_\phi(t) + c[\delta t_u(t) - \delta t^s(t - \tau)] + \varepsilon_\phi(t) \quad (3.3)$$

where

$$\begin{array}{ll} N & \text{integer cyclic ambiguity} \\ \lambda & \text{carrier wavelength} \\ \delta t^s(t - \tau) & \text{satellite clock bias relative to GPST} \\ \delta t_u(t) & \text{user clock bias relative to GPST} \\ \varepsilon_\phi & \text{unmodeled errors in pseudorange measurement.} \end{array}$$

Therefore, the precision offered by the carrier phase measurement can only be used if the integer ambiguity is resolved. However, delta pseudoranges obtained by time differenced carrier phase measurements do not contain ambiguity terms, thus enabling the user to

benefit from the carrier phase precision without the need for ambiguity estimation, although continuous carrier tracking is essential for carrier phase time differentiation. Further discussions of these topics are given in Misra & Enge (2001) and Parkinson et al. (1996).

### 3.1.3 GPS Error Sources

GPS error sources and their treatment are of great importance to obtain the best performance of the system. The discussion in this thesis is limited to the dominant error sources in the context of vehicle navigation applications, and other error sources are briefly outlined. The reader is referred to Misra & Enge (2001) and Parkinson et al. (1996) for more details. GPS has standard performance specifications for position, time and velocity estimation for both SPS and PPS. Presented in Table 3.2 are the performance specifications for the SPS. Table 3.2 does not include velocity accuracy, which is estimated to be better than 0.1 m/s in any dimension for PPS users in constant velocity scenarios (Misra & Enge, 2001).

Table 3.2: SPS Performance Specifications for Position and Time (Misra & Enge, 2001)

ERROR (95 %)	SPS
Position (Horizontal)	10 m
Position (Vertical)	15 m
Time	50 ns

GPS error sources can be categorized into three classes as given below, based on the source of the error.

#### 3.1.3.1 Control Segment Errors

Satellite clock and ephemeris errors belong to the category of control segment errors. The current values of these parameters are obtained by filtering techniques in the control

segment and are predicted for the navigation messages broadcast with the GPS signal hence, the errors associated with these parameters grow with the age of the data (AoD). Post-mission GPS applications can use modified clock and ephemeris parameters modified using actual range observations, and are thus able to minimize the control segment error. GPS minimizes the error for real-time applications through a range of techniques including frequent parameter uploads and future modifications such as the Autonav capability (Misra & Enge, 2001).

### 3.1.3.2 Signal Propagation Errors

Propagation errors consist of residual errors from ionospheric and tropospheric delay models. The ionospheric delay is caused by GPS signal propagation through the ionosphere, which extends from a height of about 50 km to 1000 km. The total delay is a function of the total electron content (TEC) in the path of the signal and the frequency of the signal. Therefore, dual frequency users can effectively remove the ionospheric delay from their measurements, whereas single frequency users have to use the broadcast model to remove the delay. The tropospheric delay is caused by the lower part of the earth's atmosphere, and is composed of two components: the dry and the wet tropospheric delay. These delays can be estimated with a high degree of accuracy using several well-established models.

### 3.1.3.3 User End Errors

Minimizing the errors belonging to this category of GPS errors is the focus of several developments presented in this thesis. Measurement errors due to receiver noise and multipath errors are the dominant user end errors. The former is often limited to a maximum of 0.5 m. However, it is impossible to establish a maximum for the multipath error in cases where access to the direct signals is limited, often known as echo-only tracking. Receiver noise is generated by unrelated in-band RF signals, noise induced by

the amplifier, cables and signal processing noise. GPS is a line-of-sight system, and it is often possible to have multiple reflected signals, especially when reflective surfaces are in the vicinity of the GPS antenna. Although complete elimination of multipath errors is almost impossible, it can be limited by antenna design or special receiver technologies. Furthermore, GPS is capable of identifying multipath effects up to 150 m when direct signals are available.

### 3.1.4 GPS Error Budget

As a means of comparison of the relative impact of each of the above error sources on GPS position estimation, Table 3.3 illustrates a typical error budget for a GPS receiver that uses pseudorange measurements for position estimation. One of the important aspects illustrated in Table 3.3 is the multipath error. Although multipath in most environments is on the order of metres, in urban canyon conditions, multipath errors could be as high as several hundred metres in echo-only tracking situations.

Table 3.3: Typical GPS Error Budget (Misra & Enge, 2001)

Error Source	Error Size	Description
Satellite Clock Model	2 m (rms)	
Ephemeris Prediction	2 m (rms)	Along Line-of-Sight
Ionosphere/ Troposphere	5 m (rms)	Satellite Elevation Dependent
Receiver Noise	Code: 0.25-0.5 m Carrier Phase: 0.5-1.0 m	Different for Code and Carrier
	Code: up to tens of metres	At Low Signal Strengths / Urban Canyons
Multipath	Code: 0.5-1.0 m Carrier: 0.5-1.0 cm	Clean Environment
	Code: Up to hundreds of metres	At Low Signal Strengths / Urban Canyons

### **3.2 High Sensitivity GPS (HSGPS)**

Being a line-of-sight system, GPS provides an excellent positioning accuracy under open sky conditions where satellite visibility is not a concern. However, in the context of the application of this thesis, vehicles do encounter areas with limited sky visibility, often created by tall built structures on either side of the road, known as urban canyons. Urban canyons are also characterized by weak GPS signals, which degrade in strength as they travel through or, are reflected by, buildings and tree canopy or become unavailable in extreme conditions. Therefore, the capability to acquire and track weaker GPS signals is especially important in urban canyon conditions.

HSGPS uses longer signal integration times (known as non-coherent integration) in its signal acquisition and tracking, typically as long as several hundred milliseconds during acquisition and tens of milliseconds during tracking (MacGougan et al., 2002). Such long integration times allow the tracking of very weak signals with fading of up to 25 dB with respect to the nominal GPS signal power of  $-160$  dBW. It has been shown that GPS signals as weak as  $-185$  dBW could be tracked using HSGPS (Kuusniemi & Lachapelle, 2004). However, owing to the very nature of GPS signal degradation in urban canyons, high sensitivity to reflected or weakened signals also increases the likelihood of additional error sources: signal cross-correlation, multipath and echo-only signal tracking. Some of these error sources and their mitigation in the context of urban vehicular navigation are discussed later in this thesis.

### **3.3 GPS Augmentations**

GPS augmentation techniques improve the availability and accuracy of unaided GPS. A brief outline of major GPS augmentation techniques is given below and emphasis is on map-matching as an augmentation for HSGPS.

### 3.3.1 Differential GPS (DGPS)

The basic principle behind DGPS is based on the fact the GPS control system and the propagation errors (satellite ephemeris, satellite clock, tropospheric and ionospheric errors) are highly correlated for users separated by even hundreds of kilometres under normal environmental conditions, and the errors only change slowly over time. The correlation is therefore a function of temporal and spatial separation of the users. DGPS operates by using this correlation to correct a user's GPS observations using similar observations made from a known location, referred to as a base station. The base station essentially estimates the GPS errors affecting the area and transmits the corrections to users.

However, due to the spatial decorrelation and the transmit times to far distances, corrections from a single base station may not be effective for a large geographic region and the effective area for a single base station is often defined by atmospheric activity. Application of this correction technique for a local area is known as Local DGPS. However, with a large number of autonomous DGPS stations covering a wide area (such as a continent), it is possible to provide any user in a large geographical area with corrections that are estimated according to the user's location. This version of DGPS is known as Wide Area DGPS, and there are several commercially available wide-area DGPS systems at present, including the US Federal Aviation Administration (FAA)'s Wide Area Augmentation System WAAS, the European version of WAAS named European Geostationary Navigation Overlay System (EGNOS) and the Japanese Multifunction Transportation Satellite (MTSAT) Based Satellite Augmentation System (MSAS). These systems are effective over wide regions covering the boundaries of North America, Europe and Japan respectively.

### **3.3.2 Assisted GPS (A-GPS)**

Assisted GPS (A-GPS) provides GPS-aiding information through alternative means such as wireless links, thus enabling the GPS receivers to function without having uninterrupted reception to download navigation information and other information through GPS signals. Typical data provided through existing systems include receiver timing aiding, ephemeris, clock corrections, ionospheric corrections, almanac, and DGPS corrections. For further information on A-GPS, see Biacs et al. (2002) and Chansarkar & Garin (2000).

### **3.3.3 Map-Matching Techniques**

A vehicle is restricted to move within the boundaries of streets and parking spaces under normal circumstances, and this is especially true for urban areas. The use of this concept to augment vehicle navigation systems with street maps is known as map-matching. These techniques vary from simple point-by-point matching to shape matching and from position-only matching to position and velocity mapping. Basnayake et al. (2003), Greenfeld (2002), Scott and Drane (1994) have discussed some of these techniques in detail. In terms of transportation and traffic engineering applications, map-matching serves as a data association tool between the sensor measurement domain and the data analysis domain, such as a series of streets (TRB, 2004). Therefore, in the context of this thesis, map-matching is addressed in detail as an augmentation tool for GPS based vehicle navigation.

## **3.4 Map-matching Algorithm for Probe Vehicle Positioning**

The map-matching algorithm developed in this thesis is based on an epoch-by-epoch position and velocity mapping procedure and a vehicle dynamic model that combines mapped positions into a vehicle trajectory. The algorithm operation is briefly outlined in Figure 3.1. Three major functional subroutines were developed in this research and were

incorporated into the algorithm. This include a Map Estimation Module (MEM) based on a Maximum a posteriori (MAP) estimator, a Kalman filter-based Vehicle Dynamic Model (VDM) and a MAP Estimation Selector Routine (ESR).

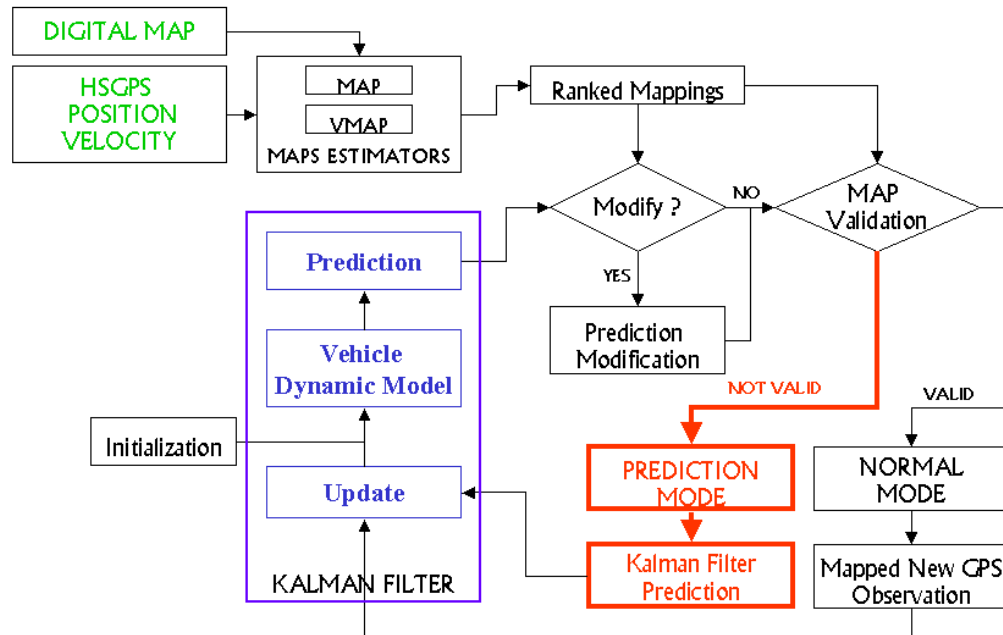


Figure 3.1: Map-matching algorithm operation

### 3.4.1 Map Estimation Module (MEM)

The mapping approach used for the algorithm assumes predominant across-track errors while assuming considerably less along-track errors. These assumptions hold true for HSGPS position measurements used in this research for most of the operating conditions except for severe levels of GPS signal degradation. For such cases, alternative approaches to deal with the along-track error are discussed in the algorithm enhancements later on in the thesis. MEM uses two Maximum a posteriori (MAP) estimators for position and velocity mapping. Two estimators were considered as probable candidates for the estimator function, which also included a more intuitive Nearest Point (NP) estimator. However, an NP estimator assumes no along track error whereas the MAP estimator could take into account the correlated error characteristics in

the measurements. Therefore, the MAP estimators were utilized for the estimator function. MAP estimators and their characteristics are discussed in detail in Bar-Shalom & Fortmann (1988) and Scott & Drane (1994).

The MEM estimates mappings of HSGPS position and velocity measurements to a selected set of streets. The selection of the street set requires a position measurement, which is given by HSGPS, and covariance estimates for the measurements, which are derived using the Kalman filter error estimates. Streets that satisfy a set of predefined across-track and along-track conditions are selected as candidates for mapped position and velocity estimate generation. These conditions are given by:

$$\frac{|a_j x_{i,GPS} + b_j y_{i,GPS} + c_j|}{\sqrt{a_j^2 + b_j^2}} \leq k_y \sigma_{i,y} \quad (3.4)$$

and

$$x_{j,1} - k_x \sigma_{i,x} \leq x_{i,GPS} \leq x_{j,2} + k_x \sigma_{i,x} \quad (3.5)$$

where

$a_j x + b_j y + c_j = 0$	centreline of street $j$
$x_{i,GPS}, y_{i,GPS}$	HSGPS position estimate in local street coordinate system at time $I$
$x_{j,1}, x_{j,2}$	end coordinates of street $j$
$\sigma_{i,x}, \sigma_{i,y}$	HSGPS position error estimates at time $i$
$k_x, k_y$	empirical constants for error region selection.

According to the above formulation, multiple position and velocity mapping could result for a single HSGPS measurement epoch, thus warranting a likelihood estimate for each position and velocity mapping. This will enable the selection of the most likely mapping to update the Vehicle Dynamic Module (VDM). For the MAP position estimator, the

correction applied to map the HSGPS coordinates to the street provides an inversely proportional reliability measure given by

$$D(p_c, p_r) = \frac{1}{1 + \frac{\|p_c - p_r\|^2}{\sigma^2}} \quad (3.6)$$

where

$p_c, p_r$            observed position and MAP estimated position of the vehicle  
 $\sigma$                standard deviation of the position estimate.

Similarly for the MAP velocity estimator, the agreement between the measured vehicle heading and the street heading could be used to calculate a reliability measure given by

$$V(\vec{v}_c, \vec{v}_r) = \frac{(\vec{v}_c \cdot \vec{v}_r)^2}{\|\vec{v}_r\|^2 \|\vec{v}_c\|^2} \quad (3.7)$$

where  $\vec{v}_r, \vec{v}_c$  are the observed and MAP estimated velocities respectively.

Although these two reliability measures provide a relative statistical measurement of likelihood, they do not provide an absolute accuracy measure. For instance, in the case of a single HSGPS position measurement with a blunder, all likely position estimates could jump to an adjacent street as there is no absolute accuracy measure at this stage of estimation. However, with HSGPS technique used in this research, such blunders will be taken care of by the internal filtering, thereby eliminating the possibility of such vehicle position jumps.

### 3.4.2 Vehicle Dynamic Model (VDM)

The Vehicle Dynamic Model (VDM) performs a vital role in the map-matching algorithm. Firstly, VDM position and velocity predictions and their accuracy estimates

are used to estimate the most likely states of the vehicle in the next time epoch thus providing an absolute measure. Secondly, most likely mapped HSGPS estimates are then used to update the VDM creating a continuous vehicle trajectory. The VDM is implemented as a Kalman filter and uses a state vector with four states, namely position and velocity states for orthogonal directions in two-dimensional space denoted by:

$$X = \begin{bmatrix} x \\ y \\ v_x \\ v_y \end{bmatrix} \quad (3.8)$$

where

- $x$  position in x direction
- $y$  position in y direction
- $v_x$  magnitude of velocity in x direction
- $v_y$  magnitude of velocity in y direction.

Following the classical Kalman filter derivation, the VDM contains two models. The process model propagates the vehicle states in time and the observation model updates the filter with new measurements. The process model and the observation models are given by

$$\bar{X}_i = AX_{i-1} + w_{i-1} \quad (3.9)$$

$$Z_i = HX_i + u_i \quad (3.10)$$

where

- $\bar{X}_i$  predicted state vector at time epoch  $i$  based on information up to epoch  $i - 1$
- $X_i$  updated state vector with observations at epoch  $i$
- $A$  state transition matrix
- $H$  observation matrix
- $w$  process noise with the probability distribution  $N(0, Q)$

$u$  measurement noise with the probability distribution  $N(0, R)$ .

The filter is initialized at the beginning of the vehicle tracking process. At each time epoch, HSGPS measurements are mapped using the MEM and then directed to the HSGPS Data Filtering Module (DFM) to determine the most likely mapping and the operating mode for the next epoch. The DFM also uses the predicted state of the VDM for this operation. Provided the DFM validated a mapped estimate for the current epoch, the VDM updates itself with the validated measurement. First, the Kalman gain is calculated, which determines the weights given to the measurement and the predicted state. In the second step, the state vector is updated by blending in new information in the form of the innovation into the filter prediction. Finally, the state covariance is also updated. The three-step measurement update is given by

$$K_i = \bar{P}_i H^T (H \bar{P}_i H^T + R)^{-1} \quad (3.11)$$

$$X_i = \bar{X}_i + K_i (Z_i - H \bar{X}_i) \quad (3.12)$$

$$P_i = (I - K_i H) \bar{P}_i \quad (3.13)$$

where

$K_i$  Kalman gain at epoch  $i$

$P_i, \bar{P}_i$  updated and predicted state covariance matrix at epoch  $i$

$R$  measurement noise covariance matrix

$Z_i$  measurement vector.

The VDM also stores the current street and the estimated distance the vehicle has traveled in that street, using the information in the updated state vector. More specifically using the integration given by

$$d_{k,i} = d_{k,i-1} + \int v_x dt + \int v_y dt \quad (3.14)$$

where

$d_{k,i}, d_{k,i-1}$  distance from street origin of street  $k$  at times  $i$  and  $(i-1)$   
 $dt$  between epoch time interval.

The next step involves predicting the state vector for the next time epoch with the time update model. This involves predicting both the state vector and the state covariance matrix given by

$$\bar{X}_i = AX_{i-1} \quad (3.15)$$

$$\bar{P}_i = AP_{i-1}A^T + Q \quad (3.16)$$

where  $Q$  is the process noise covariance matrix.

Provided the DFM determines that none of the mappings for the current epoch are valid, the VDM operation is switched to prediction mode effectively neglecting the new information gained in the invalid current epoch. This is achieved by setting the Kalman gain to zero in the updating step. Following the same notation adopted so far in this chapter, the prediction mode Kalman filter update is given by

$$K_i = 0 \quad (3.17)$$

$$X_i = \bar{X}_i + K_i(Z_i - HX_i) \quad (3.18)$$

$$P_i = (I - K_iH)\bar{P}_i \quad (3.19)$$

### 3.4.3 Vehicle Dynamic Model Parameter Accuracy Estimation

While the above discussion was solely concentrated on estimating the system parameters, this section discusses the estimation of parameter accuracy. The primary tool for monitoring the parameter accuracy is the state covariance of the Kalman filter. The state covariance matrix provides accuracy measures for all state variables as



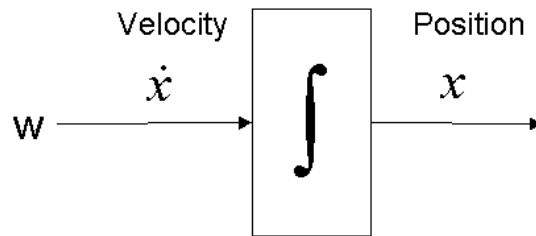


Figure 3.2: State model for constant position model

#### 3.4.4.2 Constant Velocity Model

Constant velocity modeling approach assumes constant velocity and acceleration modeled by a white noise process. Although acceleration may not resemble a white noise process in land vehicle navigation, this model yields acceptable results and is the most widely used model for land vehicle applications. The state representation is illustrated in Figure 3.3.

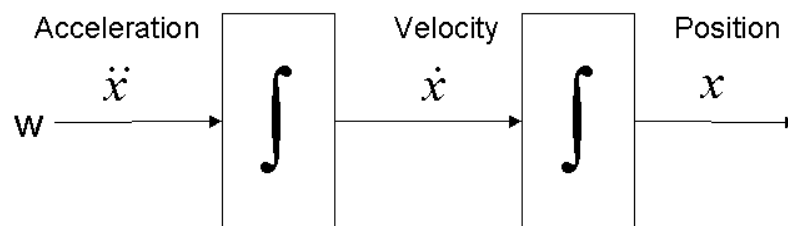


Figure 3.3: State model for constant velocity model

The system transition matrix for the constant velocity model is:

$$A = \begin{bmatrix} 1 & dt \\ 0 & 1 \end{bmatrix} \quad (3.21)$$

where  $dt$  is the between-epoch time interval.

This model was considered to provide the most acceptable results for the VDM due to the relatively slow vehicle dynamics encountered. However, the constant velocity model can be improved considerably by modeling acceleration as a time correlated Gauss-Markov process, which is much more realistic than modeling it as a white noise process (Moore & Wang, 2003). The order of a Gauss-Markov process indicates the number of previous measurements needed to predict the process value in the next measurement epoch. For vehicle navigation application, a first order Gauss-Markov process can be used to model the acceleration. The time-correlated acceleration therefore has an exponential auto-correlation function given by:

$$R(\tau) = \sigma_a^2 e^{-\alpha|\tau|} = E[a(t)a(t+\tau)] \quad (3.22)$$

where

$\sigma_a^2$  acceleration variance

$1/\alpha$  autocorrelation time constant.

With the first order Gauss-Markov acceleration modeling, Equation (3.21) can be rewritten as

$$A = \begin{bmatrix} 1 & (1 - e^{-\alpha dt})/\alpha \\ 0 & e^{-\alpha dt} \end{bmatrix} \quad (3.23)$$

where

$dt$  between-epoch time interval

$1/\alpha$  autocorrelation time constant.

The state space representation of the constant velocity model with time-correlated acceleration can be written symbolically as a modified version of the state diagram in Figure 3.3, with time correlated feedback.

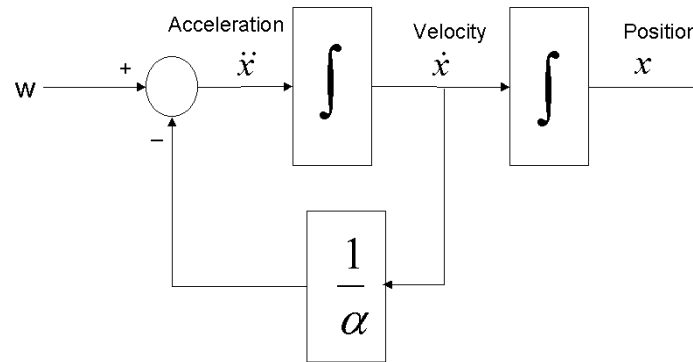


Figure 3.4: Modified state model with time-correlated acceleration

#### 3.4.4.3 Constant Acceleration Model

Following a similar modeling approach as in the above two models, the constant acceleration model assumes a white noise process for the next higher order input, namely the jerk. The corresponding state space model is illustrated in Figure 3.5.

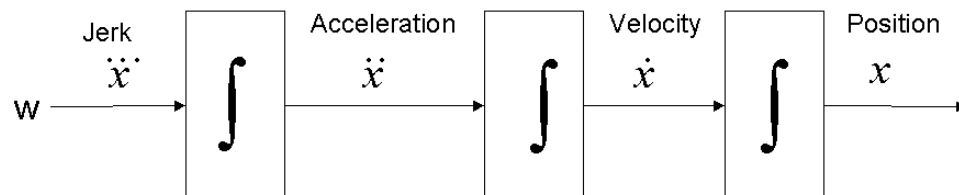


Figure 3.5: State Model for Constant Acceleration Model

For a detailed discussion and the derivation of transition matrices and process noise covariance of these models, see Gelb (1974).

#### 3.4.5 HSGPS Data Filtering Module (DFM)

The DFM validates each HSGPS measurement using corresponding MEM mappings and VDM state prediction. HSGPS performance analysis have shown that integrated Doppler

velocities and pseudorange measurements may degrade differently, especially in weak GPS signal conditions (Mezentsev et al., 2002). Therefore, validation is conducted independently in both position and velocity domains. This ensures that all valid information is taken into account. For instance, some data epochs could have a valid position measurement while the velocity measurement could be invalid and visa versa. The validation starts by evaluating the likelihood of a vehicle passing an intersection and turning into another street at the current time. This step is shown as the prediction modification in Figure 3.1. Using the integrated distance traveled, a turn is predicted if:

$$\bar{d}_{k,i+1} > l_k \quad (3.24)$$

where

$\bar{d}_{k,i+1}$  distance traveled on street  $k$  at time  $(i + 1)$

$l_k$  length of street  $k$ .

If the above condition is met, the DFM refers back to the street network database and retrieves all connecting streets at the end of the current street. However, the VDM assumes a continuation of the vehicle in the current street thus requiring an adjustment be made if a turn is declared. This scenario is illustrated in Figure 3.6 below.

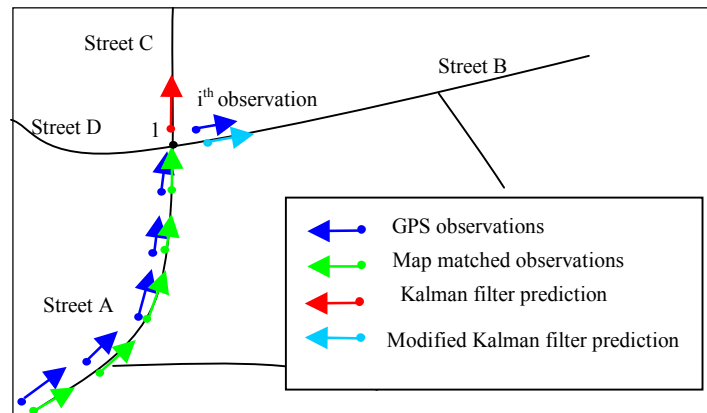


Figure 3.6: VDM prediction adjustment in DFM

Although turn detection using  $\bar{d}_{k,i+1}$  may appear theoretically sound, empirical results show that turn detection is much more complex. Features associated with turns such as lower speeds at turns, deceleration in turn approaches, stops at traffic control devices and associated HSGPS error behaviour makes turn detection much more complex. Therefore, a street likelihood weighting scheme and the state prediction modification are combined for the turn detection. At each time epoch, the most likely MEM mapping is selected on a weighting scheme given as;

$$P_{k,i} = C_{k,1}P_{k,i-1} + C_{k,2}D_{k,i} + C_{k,3}V_{k,i} \quad (3.25)$$

where

- $P_{k,i}$                     likelihood of vehicle in street  $k$  at time  $i$   
 $D_{k,i}$                     MAP position reliability given by equation (3.6) onto street  $k$  at time  $i$   
 $V_{k,i}$                     MAP velocity reliability given by equation (3.7) onto street  $k$  at time  $i$   
 $C_{k,1}, C_{k,2}$  and  $C_{k,3}$     empirical coefficients.

The scheme increases the likelihood of the vehicle continuing in the same street using the first term in the model. In addition, high position and velocity correlation is also required for a validation as specified by the second and third terms respectively. The best MEM mapping is selected using two criteria namely, a minimum innovation in the adjusted VDM dynamics model and a maximum likelihood in the street-weighting scheme, defined as

$$\min((Z_{k,i} - (HX_{i-1})_k)(Z_{k,i} - (HX_{i-1})_k)') \quad (3.26)$$

$$P_{Threshold} < P_{k,i} \text{ and } \max(P_{k,i}) \quad (3.27)$$

where

- $Z_{k,i}$                     observation vector with position and velocity mappings onto street  $k$   
 $(HX_{i-1})_k$             VDM vehicle state prediction with turn adjustment if turn is anticipated  
 $P_{Threshold}$             threshold for street weighting scheme.

Figure 3.7 illustrates the stepwise VDM-DFM measurement selection and updating process. The top left subplot shows the estimated vehicle position and the velocity vector at time  $i$  (Green) and the VDM predicted state of the vehicle in time  $(i+1)$  (Light Blue). The top right subplot shows the HSGPS measurements for the time epoch  $(i+1)$  along with the error region estimated using the VDM Kalman filter error covariance given by Equation 3.20. The error ellipse encompasses a larger across-track error while the along-track error is relatively smaller. In the next step shown in the bottom left subplot, the MEM maps measurement  $(i+1)$  onto all streets within the error region and provides likelihood estimates for each position and velocity mapping using Equation 3.29. In this illustration, MEM has provided five likely position and velocity MAP estimates (Magenta). The bottom right subplot shows the last step in which the DFM selected the most likely mapping. This was used to update the VDM thus providing an estimated vehicle state estimate for the epoch  $(i+1)$ .

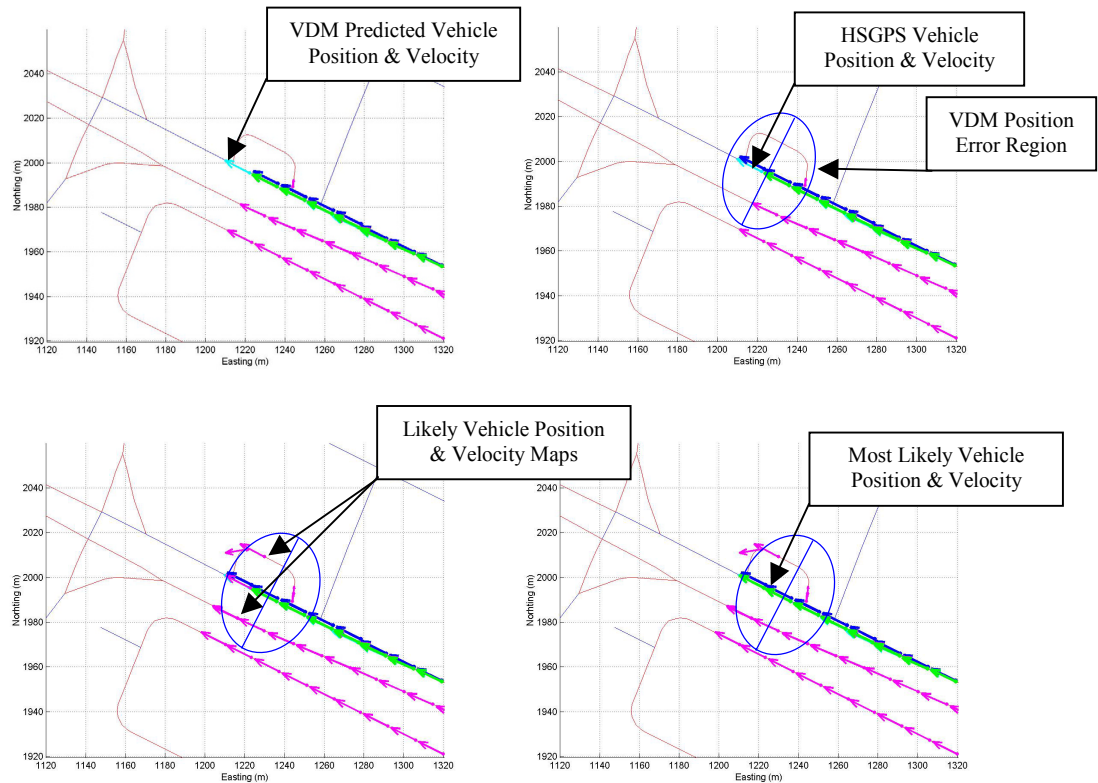


Figure 3.7: Illustration of the algorithm operation

### **3.5 HSGPS Measurements**

A SiRF XTrack™ HSGPS receiver was used for most of the field surveys and GPS simulator-based testing conducted in this research. This receiver uses longer GPS signal integration times in its signal processing, making it capable of tracking GPS signals with up to 20-25 dB of fading. The reader is referred to SiRF Technologies (2004) for a detailed discussion on its overall capabilities and performance. This receiver provides two measurement options as outlined in the following discussion.

#### **3.5.1 Internal Position and Velocity Measurements**

This measurement option uses a filtering technique built-in to the receiver. The user is provided with heavily filtered receiver position and velocity. However, no accuracy or reliability information is provided with the receiver internal estimates. In terms of the measurement quality, field experiments have shown highly improved solution availability and smoothness with internal solutions over position and velocity estimates derived using least-squares techniques on an epoch-by-epoch basis (Mezentsev et al., 2002). This difference can be attributed to the Kalman filter-based internal filter, which combines information from multiple epochs for a smoother solution. However, as discussed in Mezentsev et al. (2002), internal filtering results in considerably high errors and overshooting effects, particularly at turns under extreme urban canyon conditions. The filter appears to have been implemented to increase availability and continuity at the cost of reliability. Furthermore, as no reliability measurements are available with the internal solution, fault detection and correction is difficult to implement.

#### **3.5.2 Raw GPS Measurements**

This option provides the user with raw measurements corresponding to all visible GPS satellites on an epoch-by-epoch basis. Subsequently, receiver position and velocity can be estimated using least-squares techniques. This technique is illustrated later in this

thesis using the C<sup>3</sup>NAVIG<sup>2</sup>™ (Combined Code and Carrier for NAVigation with GPS and GLONASS) software developed by the University of Calgary PLAN research group (Petovello et al., 2000). One of the key advantages in using least-squares techniques is the ability to incorporate user-level reliability monitoring schemes, providing a means of fault detection. These user-level reliability monitoring schemes, commonly referred to as Receiver Autonomous Integrity Monitoring (RAIM) involve statistically testing least-squares residuals of the observations. Included in the raw measurements are the C/N<sub>0</sub> measurements, which provide valuable information on the level of signal attenuation.

RAIM techniques enable the identification of faulty measurements, which has a great importance in rectifying the impact of GPS error sources, particularly multipath. However, RAIM techniques require observation redundancy for successful fault detection, a condition rarely satisfied with GPS as the only GNSS available, especially in urban environments where such techniques could prove highly useful. Although the importance of incorporating these rapidly evolving techniques to systems proposed in this thesis is identified as of high importance, it was considered beyond the scope of this thesis. The reader is referred to Kuusniemi & Lachapelle (2004) for a comprehensive discussion of RAIM techniques and their application to GPS and combined GPS-Galileo.

### **3.5.3 Application of HSGPS**

The decision to choose either the internal solution or the least-squares based epoch-by-epoch HSGPS solutions for this research involved analyzing all of the above aspects. While the advantages of using least-squares-based techniques are clear, especially in detection and rectifying faults, incorporating such techniques to this research was considered beyond its scope. Instead, internally filtered HSGPS measurements were used for all applications. Furthermore, in order to rectify the shortcomings in internally filtered HSGPS solutions, either additional sensors or alternative augmentation techniques were used with it. These techniques are discussed in detail in various stages of the thesis.

### 3.6 Testing the Algorithm with the GNSS Simulator

Although the map-matching algorithm is theoretically capable of providing robust vehicle navigation accuracy and reliability over unaided HSGPS, its operation is entirely dependent on the quality of HSGPS measurements. Therefore, analyzing the algorithm response to GPS signal degradations such as multipath, weak GPS signals and brief signal interruptions, which are typical of urban and suburban streets is important. In order to assess the performance of the algorithm in terms of maximum GPS signal loss and multipath magnitude tolerable under predictable vehicle dynamics, a GNSS simulator was used to simulate the GPS constellation and error sources. The simulator approach provides very precise vehicle dynamics control and eliminates accuracy issues associated with digital maps. A part of the digital street map of Calgary was used to develop the simulated map. The vehicle trajectory was created precisely on the street map, thus eliminating errors from discrepancies between the vehicle trajectory and the digital map.

#### 3.6.1 GNSS Simulator Test Setup

The heart of the simulation setup was a Spirent 6560 GPS simulator. It was used to simulate GPS L1 signals using 12 signal channels. The simulator control and scenario development was done with the Spirent SimGEN software. The radio frequency signals (RF) were preamplified and fed through a DC block to a SiRF HSGPS receiver. The technical specifications of the 6560 simulator and SiRF HSGPS receiver are given in Tables 3.4 and 3.5 respectively. The test setup is shown in Figure 3.8.

Tabel 3.4: GNSS 6560 Simulator specifications

Spirent 6560 Simulator	
Signal Source	12 channels (L1)
Signal Level	-130 dBm
Channel Hardware Update Rate	100 Hz
Signal Dynamics	+/- 15,000 ms <sup>-1</sup> +/- 450 ms <sup>-2</sup>

Table 3.5: SiRF XTrack™ HSGPS receiver specifications

Chipset	SiRF STARIIe
Tracking	L1 C/A Code
Channels	12
Sensitivity <ul style="list-style-type: none"> <li>• Specifications</li> <li>• Emphirical</li> </ul>	-172 dBW -180 dBW
Acquisition <ul style="list-style-type: none"> <li>• Cold Start</li> <li>• Hot Start</li> </ul>	< 50 sec < 8 sec

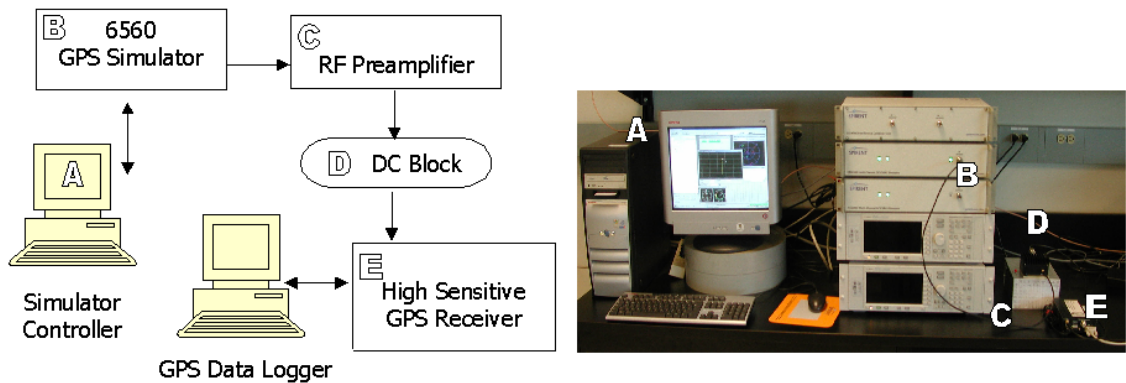


Figure 3.8: Test setup with the simulator

### 3.6.2 Simulation Test Scenarios

The simulations were done using a test trajectory developed with a digital map of the Northwestern part of Calgary. The approximate length of the trajectory was 5.5 km with mostly straight roads and two turns of approximately 90 degrees. Figure 3.9 shows the test trajectory overlapped on the digital street map of the area.

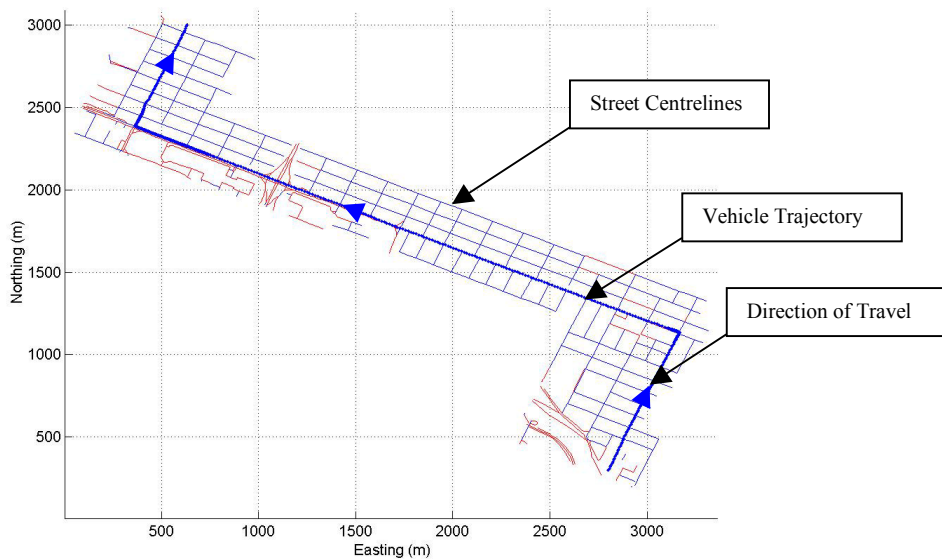


Figure 3.9: Test trajectory for GNSS simulator testing

The simulated speeds were designed to be consistent with the posted speed limits of the actual area. The speed profile of simulated vehicles is shown in Figure 3.10. Average speeds of up to 54 km/h were simulated and during turns, the speed was reduced to about 10 km/h.

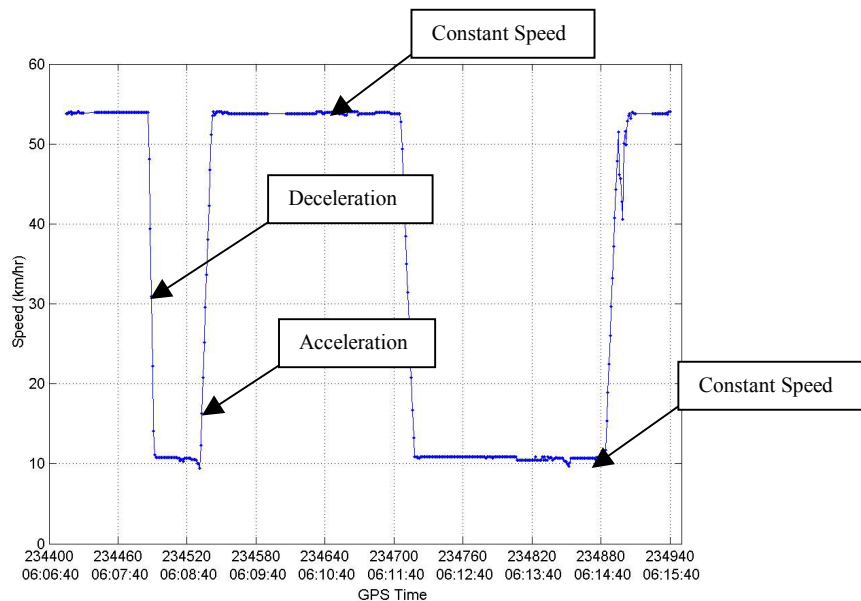


Figure 3.10: Simulated vehicle speed profile

### 3.6.2.1 GPS Outages in Urban Canyons

The first series of simulations was conducted to investigate the capability of the algorithm to bridge short duration GPS signal outages under constant vehicle dynamics. More specifically, outages were simulated while the vehicle was traveling in predominantly straight stretches of road under constant velocity. For the simulation of GPS signal outages, the GPS receiver output corresponding to the appropriate duration was removed. Starting from short durations (5 seconds) of complete data loss, longer outage durations were simulated. A typical scenario simulating three complete GPS outages of 10, 15 and 15 seconds in duration is illustrated in Figure 3.11.

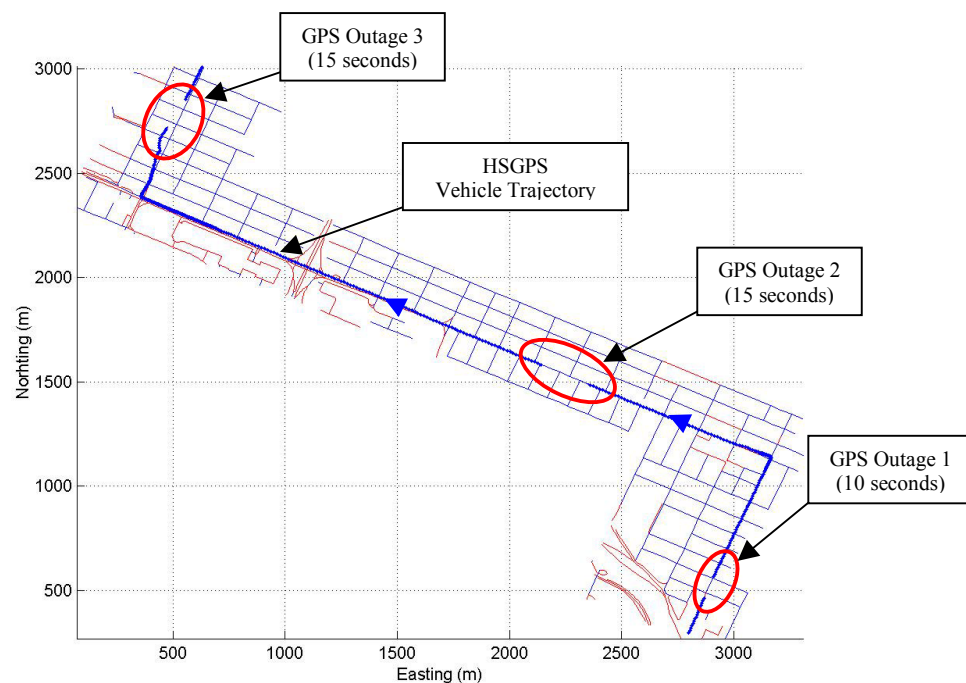


Figure 3.11: Typical GPS outage simulation

Simulations were done for complete GPS outages ranging from 5 seconds to 60 seconds with the objective of estimating the position accuracy degradation. The position errors observed in those tests are summarized in Table 3.6.

Table 3.6: Summary of map-matched GPS outage simulation

Outage Duration (seconds)	RMS Position Error (metres)
5	1.8
10	1.9
15	1.8
20	1.9
25	2.1
30	2.3
60	3.8

Although map-matching and the prediction capability in the algorithm could provide acceptable performance in GPS outages under constant dynamics, variations in the vehicle dynamics severely limit the performance. In order to illustrate this limitation, a simulation was performed with a GPS outage while the vehicle was undergoing acceleration and a turn. The simulation contained three outages of 4, 6 and 4 seconds respectively. The vehicle accelerated during the second outage and reached a constant speed. The results of this simulation shown in Figure 3.12 illustrate the limitations of map matching with GPS as the only sensor available.

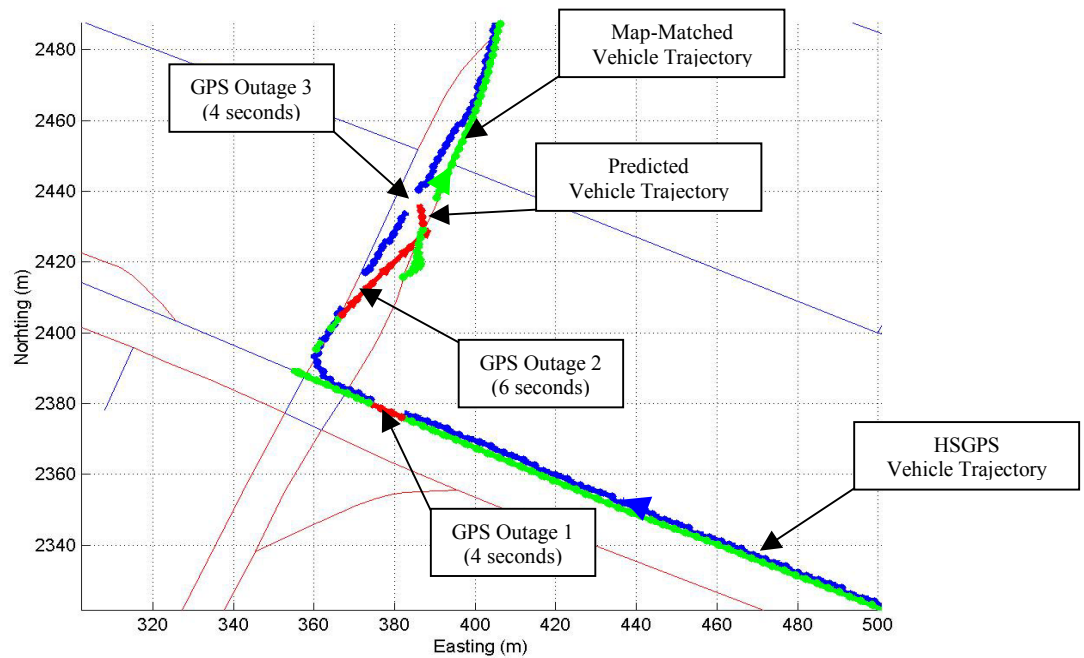


Figure 3.12: GPS outages and map-matching with accelerations and turns

The HSGPS vehicle trajectory is depicted in Blue and the map-matched vehicle trajectory is shown in Green. The predicted vehicle trajectory generated by the VDM during GPS outages is shown in Red. The first outage was successfully predicted as it occurred under constant vehicle dynamics. The second outage occurred after the vehicle started accelerating, and this is reflected in the predicted estimates. However, the filter loses information regarding constant speed as the outage has occurred during the same time. This results in projecting the vehicle position further at the end of the second outage. The third outage reflects the unstable filter states after the second one. However, as soon as good observations become available, the filter regains its stability.

### 3.6.2.2 Map-Matching with Simulated Multipath

In the second series of simulations, controlled levels of multipath was introduced to selected GPS satellite signals. The impact of multipath errors was simulated by simulated pseudorange errors. The magnitude of multipath was varied over the simulation period and a typical pseudorange error profile is illustrated in Figure 3.13.

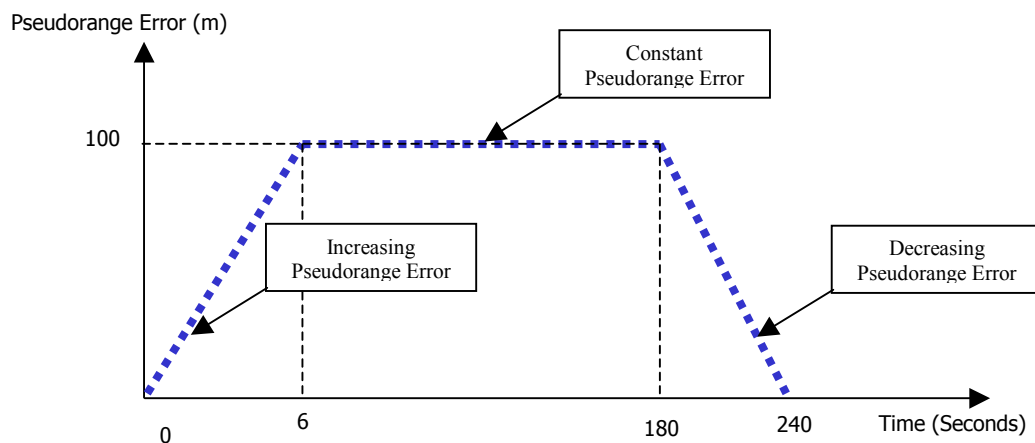


Figure 3.13: Typical pseudorange error profile for multipath simulation

Two vehicle dynamic scenarios were investigated with simulated multipath conditions. The first scenario considered was the impact of multipath error with varying vehicle

dynamics and straight-line heading. The second scenario was under similar conditions with changing vehicle heading. Figure 3.14 illustrates the HSGPS positions and corresponding map-matched estimates under the first scenario, varying dynamics but with constant heading. This clearly illustrates the capability of the algorithm to maintain the location of the vehicle with respect to the actual street it is traveling. However, the along-track position and velocity estimates are directly effected by the multipath errors and cannot be controlled without additional data from sensors other than GPS.

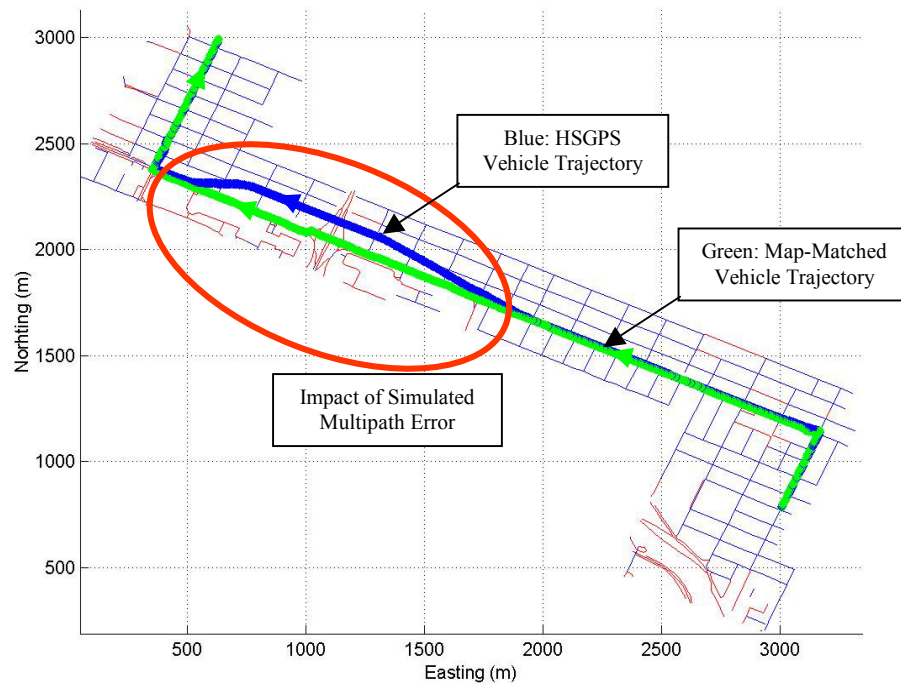


Figure 3.14: Typical multipath simulation and map-matched vehicle trajectory

The second scenario is illustrated in Figure 3.15. In this case, multipath conditions are encountered during the second turn and its approach. In this case, the algorithm was able to keep the map-matched estimates in the correct street until multipath effects made it impossible to detect the correct turn. However, the algorithm follows a most probable path consistent with HSGPS measurements. The continuity factor considered in map-matching, which prevented the estimates from jumping to an adjacent street before the

turn continues to model the vehicle in a wrong street that is parallel to the correct street. However, as soon as reliable HSGPS measurements became available, the map-matched estimate converged to the correct street.

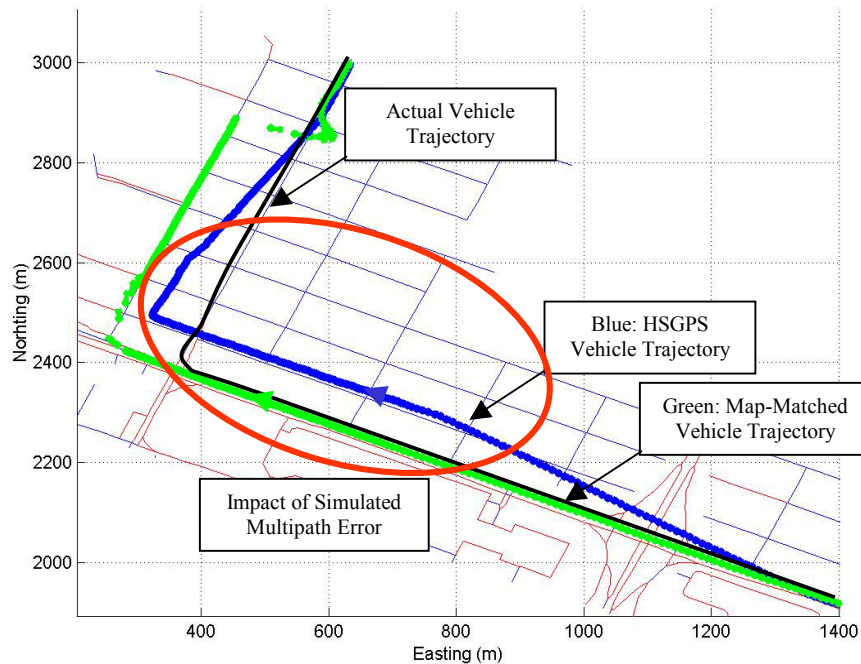


Figure 3.15: Minimizing multipath error with changing vehicle dynamics

### 3.6.2.3 Map Matching Under Weak GPS Signal Reception

HSGPS has a clear advantage over conventional GPS in tracking weak GPS signals. Research has shown that the HSGPS receiver used in this research is capable of tracking signals as weak as  $-185$  dBW whereas the typical GPS signal strength is  $-160$  dBW (Kuusniemi & Lachapelle, 2004). However, signal degradation increases measurement noise and introduces additional error sources. In the position domain, these weak signals translate into noisy position and velocity estimates.

The effect of weak signals in the HSGPS position domain and the performance of the map-matching algorithm in such weak signal environments were also investigated using

simulations. This was done by controlling the simulated GPS signal power in such a manner that reflects entering and leaving a weak signal environment. Illustrated in Figure 3.16 is the simulated and received signal power during the simulation. Initially, the signal power was set to provide a received  $C/N_0$  of 43 dB for all satellites, which is standard for line-of-sight tracking. Then the signal power was lowered until the  $C/N_0$  reached 19 dB, which is considered the threshold for this HSGPS receiver. The power level was left for 40 seconds at the lowest level and then increased back to the original level in 20 seconds.

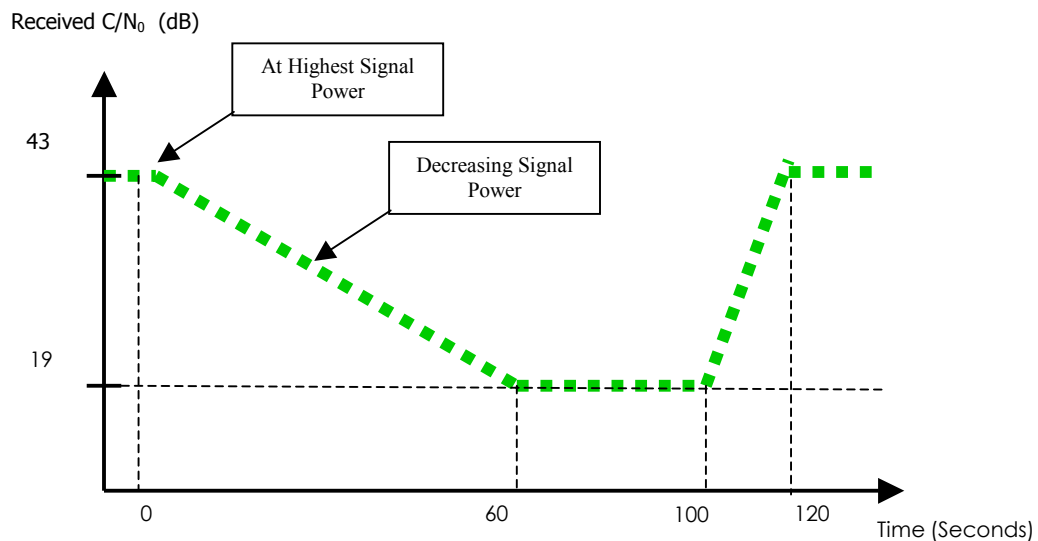


Figure 3.16: Simulated  $C/N_0$  degradation

Weaker GPS signals in the simulation result in larger errors in the position domain as depicted in Figure 3.17. Across-track errors on the order of 10-20 metres were observed before the turn. The turn is distorted towards east of the actual intersection. As the signal strength is increased, the position error decreases, and HSGPS position measurements return to the actual vehicle trajectory. The map-matched estimates were able to remain in the correct street before the turn. However, an observed shift in the HSGPS measurements around the turn prevents the identification of a turn at the intersection. This has been identified as a result of the internal filter overshooting effect (Mezentsev et al., 2002). Therefore, map-matched estimates continue to match the

HSGPS data onto a wrong street assuming the vehicle continued straight through the intersection. This goes on until sufficient evidence is found to switch mappings to the correct street and to declare previous mappings as invalid. This switching of streets results in noise in the map-matched estimates, and the filter reaches stability half way to the third street block.

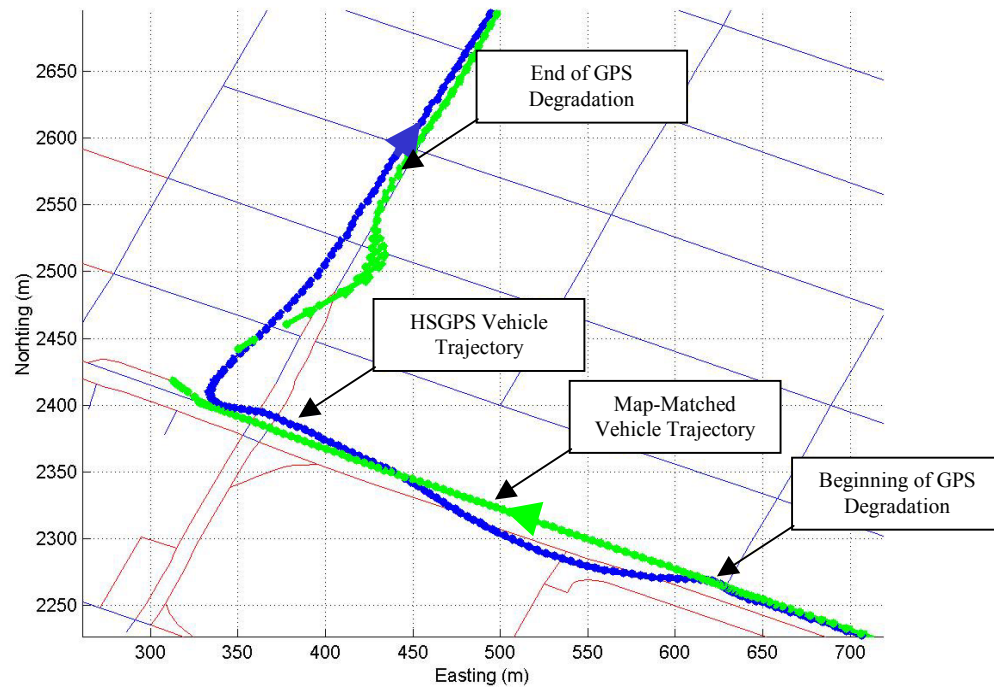


Figure 3.17: Map-matched vehicle trajectory with weak GPS signals

In order to illustrate the potential of the algorithm, the same HSGPS data set was processed with a modified version of the algorithm. The algorithm was modified to consider received  $C/N_0$  in selecting the most probable mapping. This results in a faster recovery in the map matching as shown in Figure 3.18. Since HSGPS signals around the turn are weak, lower weight is given to the position estimates around the turn. As the signal power increases, more weight is given to HSGPS position estimates derived from GPS signals with higher signal strengths. This results in a faster identification of a fault and hence identifying the correct street mapping. The modified algorithm converges to

the correct street halfway to the second street block. In the time domain, the correct street was identified 6 seconds earlier. Although the receiver  $C/N_0$  provides limited information for identifying multipath errors without the aid of techniques such as RAIM, the above modification illustrates the adaptability of the map-matching algorithm with additional information sources.

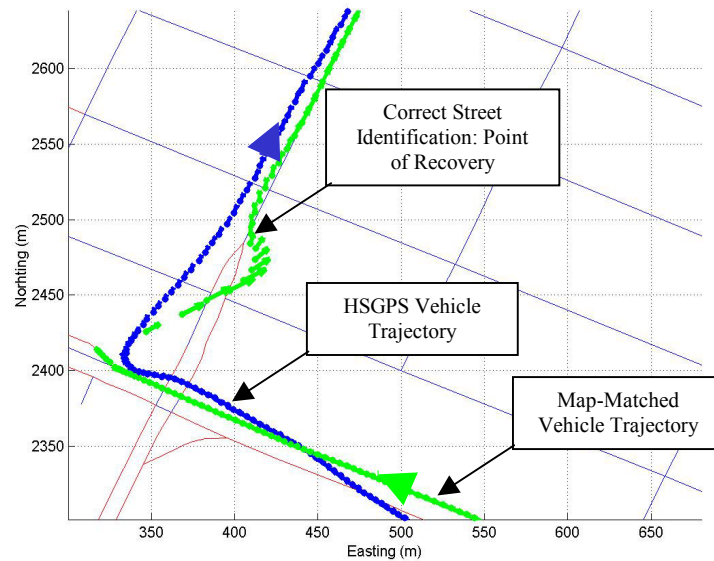


Figure 3.18: Algorithm modified as a function of receiver  $C/N_0$

### 3.7 Aiding With Odometry and Differential Odometry

A vehicle odometer is a device that measures the distance traveled by the vehicle. This often involves measurements from all wheels of a vehicle, making it possible to measure distances traveled by each individual tire. This leads to differential odometry, where differences in distance traveled by each wheel could be used to estimate the vehicle heading, a technique known as differential odometry. One of the attractive features of odometry is the low-cost of an in-vehicle odometer. Almost all vehicles come with a transmission-based odometer for distance measurement and most of the new vehicles have additional wheel rotation sensors for Anti-lock Breaking Systems (ABS) and

traction control systems. Therefore, the system is available at almost no additional cost on sensors. Several odometer sensor types are employed for distance measurement. This includes variable reluctance sensors, Hall effect sensors, optical sensors and radar sensors. A detailed discussion of these sensor types is given in Stephen (2000).

The primary error source in odometry sensors is directly linked with the estimation of the distance traveled based on the wheel rotation observations. There are two possible sources of errors. Firstly, the wheel circumference may slightly change due to several factors, requiring a scaling factor for distance estimation. Secondly, wheel slippage has to be considered. These error sources and their treatment are discussed in detail in Stephen (2000) who has also shown that in a GPS augmented system, odometry can help maintain a navigation solution that is accurate at the 20 metre level. However, this involved the calibration of odometry measurements using GPS, thus the error could be as high as 100 metres in urban canyons where conventional GPS may not provide calibration data.

Although odometry offers an attractive sensor for augmenting with HSGPS and map-matching, odometry sensors are often custom made for an individual vehicle type. Hence, the sensor augmentation has to be vehicle specific, which restricts the portability of the navigation system. Therefore, odometry augmentation was not considered an option in this research. However, the possibility of incorporating it to the integrated positioning system is discussed later on in this thesis.

### **3.8 Inertial Aiding for Urban Vehicle Navigation**

Although aiding HSGPS with map-matching improves the availability and accuracy of vehicle navigation data under limited vehicle dynamics and environmental conditions effecting GPS reception, urban vehicle navigation involves many situations where such conditions are not met. For instance, losing GPS reception or high levels of multipath signals while negotiating a turn could easily mislead the map matching algorithms during

real-time operation. However in the case where GPS is the only sensor used for navigation and is degraded in accuracy, a map-matching algorithm could only predict the current state of the vehicle. In the case of a turn or a sudden dynamics change such as acceleration, capturing such changes is only possible through the sensors.

There exist many augmentation techniques for GPS, with an Inertial Navigation System (INS) being one of the preferred options owing to its complementary integration capability with GPS. An INS does not suffer from outages that are characteristic of GPS for urban environments and errors such as multipath. However, INS sensors accumulate biases over time and could lead to tens of metres of bias after a short duration depending on the grade of the INS used. Typically, GPS/INS navigation systems use GPS to initialize INS at points where accurate GPS measurements are available and use INS to bridge GPS outages, thus using them as complementary sensors (Petovello, 2003). However, the cost of INS sensors with good bias characteristics and stringent initialization requirements have limited the wider commercial application of low-cost INS/GPS vehicle navigation systems (Basnayake et al., 2004; Mezentsev et al., 2002; Petovello, 2003).

### **3.8.1 Sensor Integration Strategy**

The GNSS simulator based algorithm analysis clearly shows the need for additional sensors to aid GPS. Further field performance analysis showed two major weaknesses of HSGPS for urban vehicle navigation. Firstly, detecting vehicle turns under GPS signal-masking conditions was highly sensitive to GPS errors and biases in the case of HSGPS. Secondly, position measurement errors tend to create virtual movement of the vehicle even when the vehicle is at a complete stop. Comprehensive analyses of these phenomena are given in Basnayake & Lachapelle (2003). Based on these findings, two add-on modules were developed using low-cost sensors to enhance the positioning capability of the map matching/ HSGPS positioning algorithm.

### 3.8.1.1 Turn Detection Module (TDM)

The TDM is based on a low-cost rate gyro that aids the vehicle navigation system in detecting turns taken by the vehicle. Stephen (2000) has shown that low-cost gyros provide an excellent sensor for detecting turns with intermittent bias corrections from GPS. Rate gyro performance is primarily characterized by their drift characteristics, and the gyro used in this application has a drift rate of 100 degrees/ second. Therefore, if used as a sensor for heading measurement, it would require a mechanism to minimize the drift. For this application, gyro data was only used for detecting sharp turns (usually, around 90 degrees). Under average vehicle dynamics, a sharp turn is made in 2 or 3 seconds. The gyro drift in such a short time will be considerably smaller than the actual turn angle, for instance, 90 degrees (projections of vehicular roll and pitch angular velocities on the gyro sensitivity axis are negligible comparing to the gyro bias). Therefore, once a significant change in the gyro output is detected in a time window of 2 to 3 seconds, a left or right turn can reliably be detected. In all other situations, such as changing lanes or mild turns, a turn is not reliably detected, and the TDM output aiding is not considered in the map-matching routine. Such a gyro setup and gyro data processing algorithm does not require any initialization, as the objective of the gyro is solely the detection of turns. Upon detection of turns based on gyro response, the module retrieves appropriate turning streets from the digital street database.

### 3.8.1.2 Stop Detection Module (SDM)

The second sensor module integrates an accelerometer through the SDM. The map-matching algorithm relies on both HSGPS estimates and VDM estimates to warrant SDM requests for detecting the vehicle stops. The vehicle must be in a state of deceleration and the velocity should be less than a predefined minimum in order to request an SDM lookup. Upon detection of these minimum requirements for a stop, the SDM triggers an accelerometer data reference to look for stops. If a stop is detected, the best-known vehicle position is maintained until the vehicle movement is resumed based on the

accelerometer data. Accelerometer based vehicle stop detection is entirely based on analyzing the variance of the accelerometer measurements. During a complete vehicle stop, the variance of the accelerometer data should be very small, while during motion, the accelerometer outputs consist of substantial spikes and variations mostly due to the nature of driving in congested areas. Based on empirical results from Basnayake et al (2004), a time window of 15 seconds was selected for the acceleration variance analysis.

### 3.8.2 Multi Sensor Navigation Algorithm

The enhanced navigation algorithm is illustrated in Figure 3.19. The enhancements are integrated into the initial map matching/ HSGPS algorithm through two functionalities. Firstly, turn detection is entirely conducted by the TDM. The TDM provides a street reference after each turn to the MEM for initializing a new street. Therefore, the TDM is linked to the VDM, MEM and the rate gyro. Secondly, the SDM is invoked each time where VDM-estimated vehicle speed fall below a predefined threshold. If a stop is detected, a MEM routine is called to fix the current vehicle position until vehicle movement is detected. Therefore, the SDM links with VDM, MEM and the accelerometer.

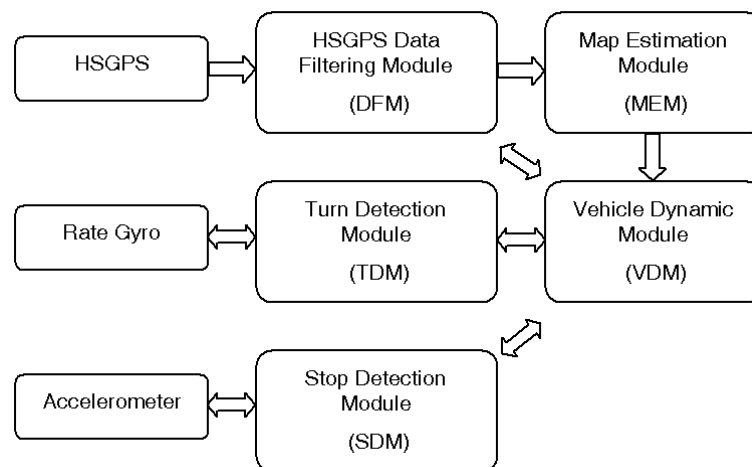


Figure 3.19: Enhanced navigation algorithm

### 3.8.2.1 Testing the Multi Sensor Navigation Algorithm

A test was conducted in and around downtown Calgary. The test trajectory was designed to travel through the downtown core and suburban areas. The start and end of the trajectory were in areas with clear reception of GPS signals while some sections experienced extreme urban canyon conditions. Figure 3.20 shows the full test trajectory, which was close to 8 km long and which included three loops around street blocks where tall buildings restricted views of the sky creating urban canyon conditions. Figures 3.21 and 3.22 show parts of the trajectory with good view of the sky and parts with severe urban canyon conditions, respectively.

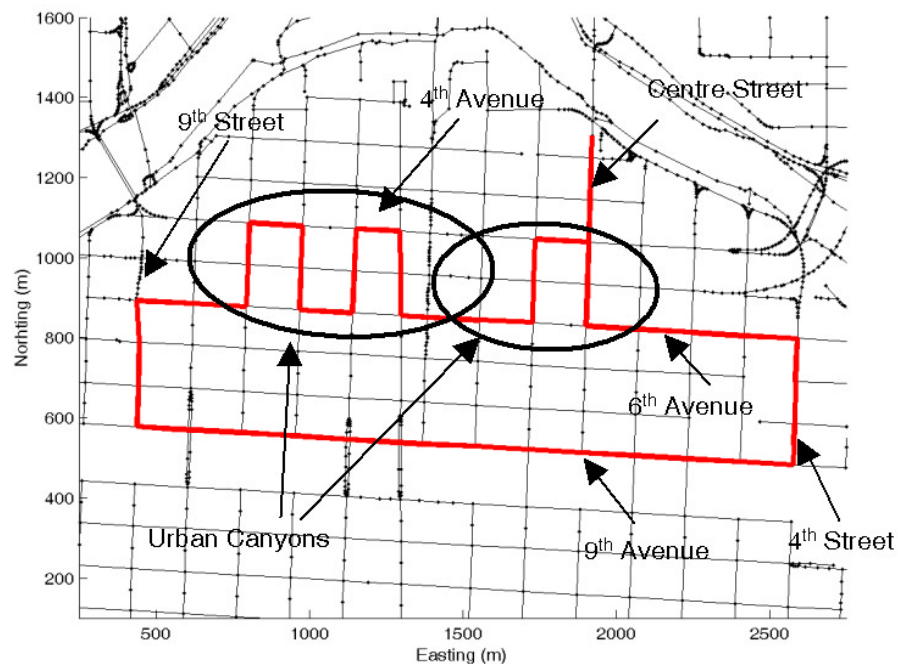


Figure 3.20: Test trajectory in downtown Calgary



Figure 3.21: Part of test trajectory with clear view of the sky



Figure 3.22: Part of test trajectory with urban canyon conditions

### 3.8.2.2 Equipment Setup

A SiRF XTrack™ HSGPS receiver was used as the primary sensor in the test setup. In addition, a NovAtel OEM4 geodetic grade receiver was also used for time tagging sensor data with GPS time. A Murata ENV-05D vehicular grade gyro was installed such that its sensitivity axis approximately coincided with the vehicle vertical. The specifications for the Murata gyro are given in Table 3.7. A detailed discussion and an assessment of its performance in the context of GPS augmentation are discussed in Stephen (2000).

Table 3.7: Murata ENV-05D specifications

Angular Velocity Range	-80 to 80 deg/second
Scale Factor	22.2 mV/deg/sec
Dimensions	18 x 30 x 41 mm
Weight	50 g

Two VTI SCA 610 series accelerometers were installed in an approximately horizontal plane in the vehicle with its sensitivity axes perpendicular to each other, which comprised the sensor test setup. The accelerometer specifications are given in Table 3.8. A detailed discussion on its performance is given in Collin et al. (2001).

Table 3.8: VTI SCA 610 accelerometer specifications

Acceleration Range (max.)	1.7 g (1.7 x 9.81 m/s <sup>2</sup> )
Output	Analog Voltage
Size	11.3 x 10.5 mm

Time matching pluses were generated throughout the test and after decoding the GPS data and time of the pulses, sensor data was matched to the GPS marks with interpolation when appropriate. The accuracy of such a time alignment of the sensors data essentially

depends on the stability of the Data Acquisition card (DAQ) oscillator and is expected to be at the millisecond level. For the purpose of using the sensor's data to aid the map-matching routine, such a timing accuracy was considered sufficient.

The digital maps used in the integration provided centrelines of all major and minor streets within Calgary city limits. These maps were provided by the City of Calgary and were generated using aerial photographs. The stated accuracy of the maps is 10 metres rms.

### 3.8.2.3 Sensor Data and Integration Results

The performance of the navigation system is analyzed and presented in this section. Out of a total of five test runs, two representative runs were selected based on poor HSGPS availability and accuracy. This enables an analysis of system accuracy, availability and reliability when the primary positioning system (HSGPS) is performing poorly, but the navigation system is still required to maintain a certain minimum level of performance. It should be noted that only the across-track errors are analyzed since it is the only accuracy that can be assessed, thanks to the available digital map reference.

Shown in Figure 3.23 is the HSGPS and integrated vehicle trajectories for Test Run 2. Figure 3.24 shows a zoomed view of Figure 3.23 at the first of the three loops. The weaknesses of HSGPS are clearly improved by the integration algorithm as shown in Figure 3.23. These improvements include correct detection of turns and stops, constraining position error while the vehicle is stopped, minimizing the effects of multipath errors and bridging short HSGPS gaps using map-matched predictions.

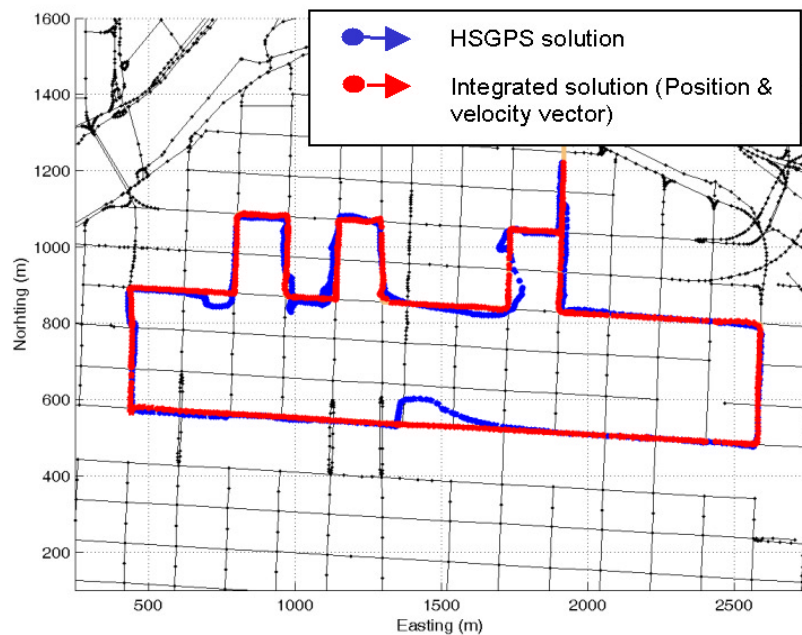


Figure 3.23: HSGPS and integrated trajectories (Test Run 2)

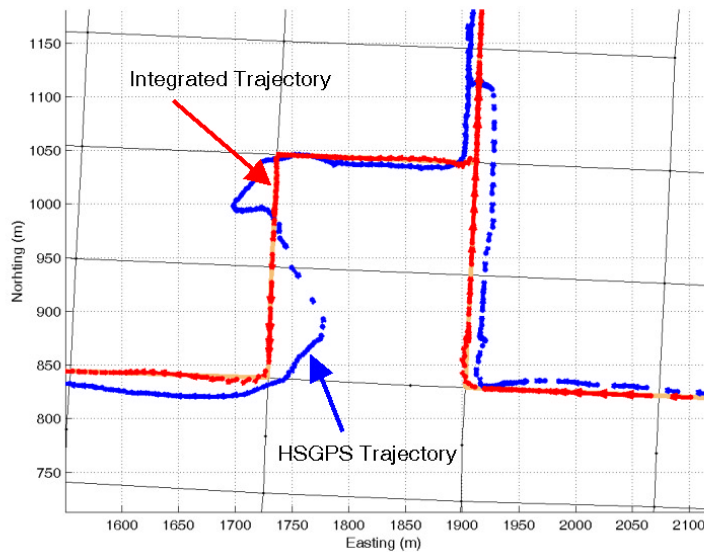


Figure 3.24: Zoomed 1<sup>st</sup> loop from Test Run 2

The navigation system accuracy is numerically analyzed in Figure 3.25. The top plot shows the position error calculated as the minimum distance from the street centreline to the HSGPS position estimate for the entire test run. The HSGPS position estimate errors

of 50 metres or above are shown as 50 metres in Figure 3.25. The bottom plot in Figure 3.25 further analyses the distribution of the HSGPS position errors. Position errors at each epoch were put into 1 m wide error bins (the first bin contains the number of epochs where the position error was between 0 and 1 m). Errors of up to 45 m were considered and the number of epochs in each error bin is shown in the bottom plot in Figure 3.25.

The total driving time for Test Run 2 was around 24 minutes (1442 seconds), which means 1442 GPS epochs should be included in the position solution for the test run as the data rate was set to 1 Hz. During this test run, there were 69 GPS epochs where no valid HSGPS position estimate was available. If one includes HSGPS position estimates with errors of more than 50 metres, 5.4 % of the HSGPS position estimates were more than 50 metres in error (including no position estimates). For the estimation of accuracy, the Table 3.2 GPS SPS positioning specification of 10 metres (95 %) was used as the threshold. From all HSGPS data epochs, 26.8 % of the HSGPS position estimates were beyond this threshold. However, the integrated navigation system was able to provide a position solution 93 % of the time with reference to the actual street.

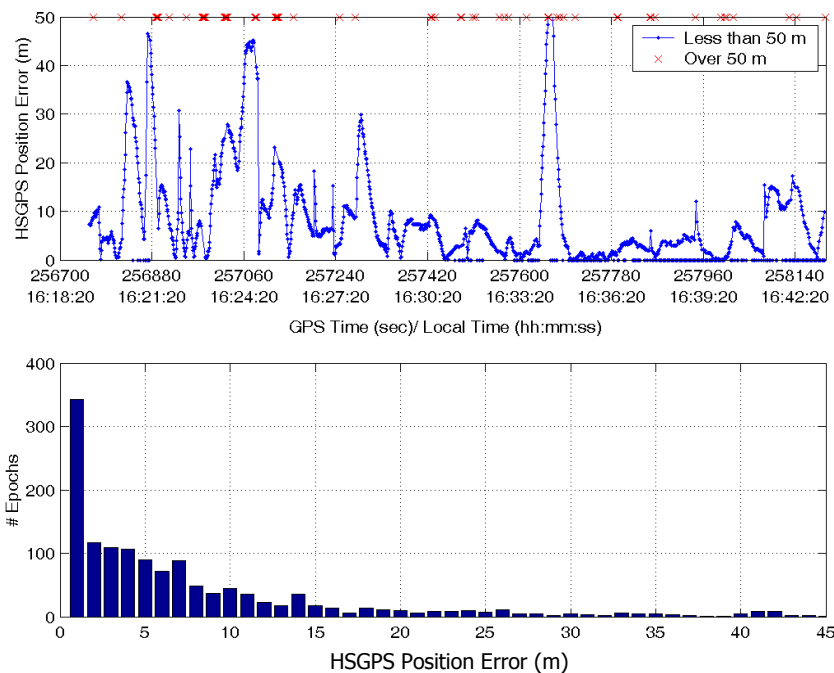


Figure 3.25: Numerical analysis of accuracy in Test Run 2



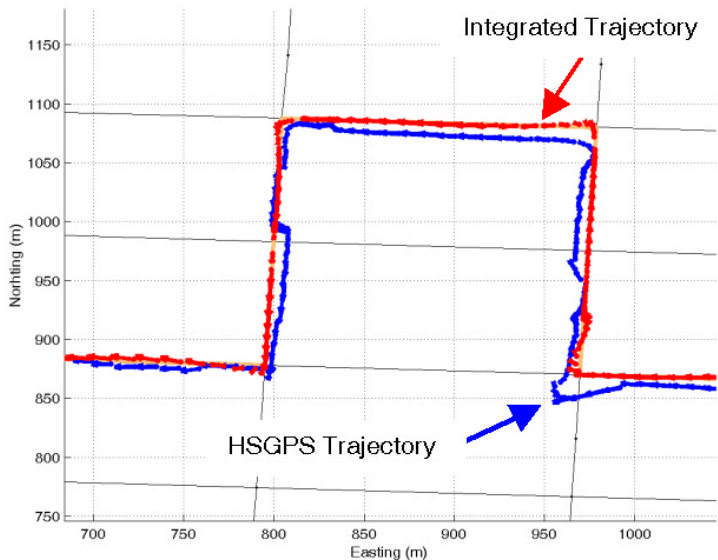


Figure 3.27: Zoomed 3<sup>rd</sup> loop from Test Run 3

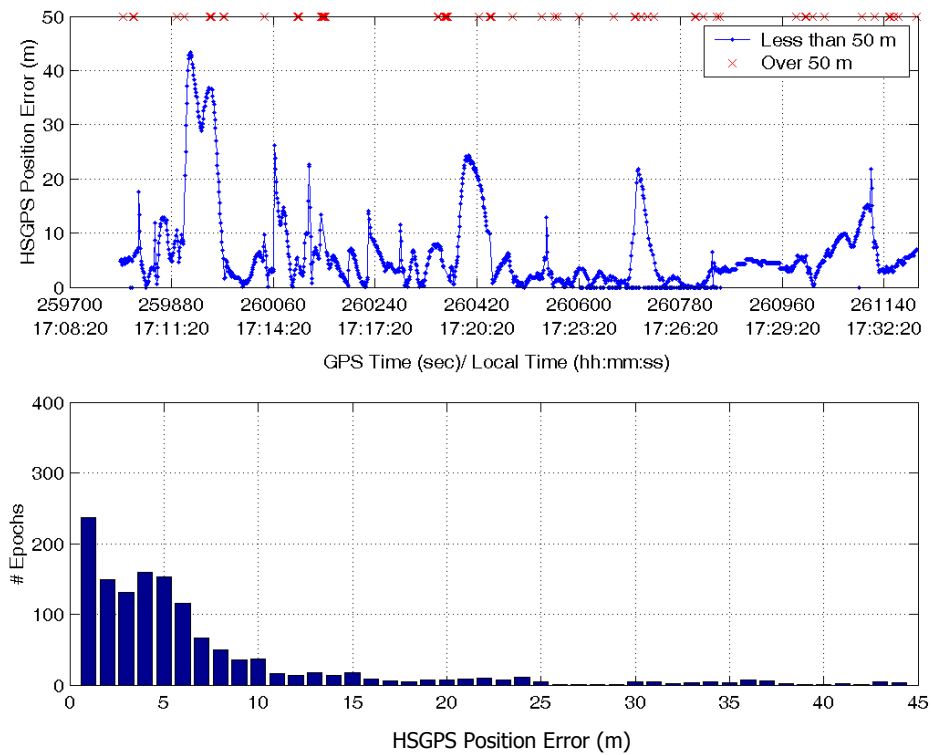


Figure 3.28: Numerical analysis of accuracy in Test Run 3



## CHAPTER FOUR

### OVERVIEW OF TRANSIT PROBE SYSTEM AND INCIDENT DETECTION SYSTEM

This chapter outlines the transit probe based incident detection system development. The chapter is presented in two sections, first section on the vehicle-positioning component of the system and the second section on data processing aspects.

#### **4.1 Transit Vehicle Positioning**

Transit vehicle positioning has the advantage of prior knowledge of vehicle routes as transit vehicles are assigned to predefined routes. This additional vehicle route information was used to further improve the performance of map-matching/ HSGPS combined vehicle-positioning system developed in Section 3.4. This section outlines the concepts involved and the results from field tests.

##### **4.1.1 Overall Vehicle Positioning System**

This section outlines the modifications made to the HSGPS/ map-matching vehicle positioning algorithms presented in Section 3.4, for positioning transit vehicles. Emphasis was given to two aspects in developing the transit vehicle positioning system. Firstly, the unit cost of an in-vehicle system had to be low and secondly, the system operation had to be highly automated to minimize operator intervention required. In order to achieve both of these objectives, an HSGPS receiver was used as the only onboard sensor in the transit vehicles. Although no real-time operation was conducted for the work presented in this thesis, data collected in transit vehicles were analyzed sequentially in post-mission to simulate real-time conditions. Thus there is no theoretical

reason why this system could not be implemented in real-time. Figure 4.1 illustrates the proposed system configuration for transit vehicle positioning.

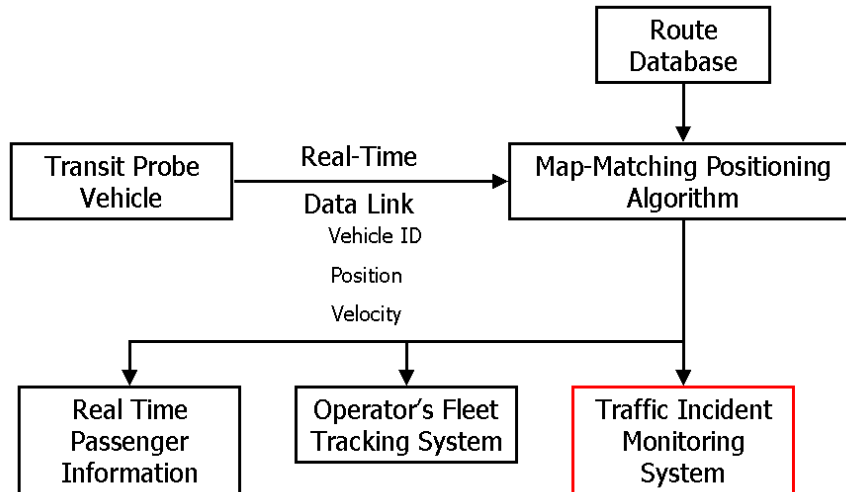


Figure 4.1: Transit vehicle positioning system

As illustrated in Figure 4.1, transit vehicle positioning is actually conducted in a control center server with the aid of a route constrained map-matching algorithm and a digital street map database containing transit route information. Typical route information database includes transit routes as a collection of streets and the location of all transit stops as an along-track feature of streets.

#### 4.1.2 Constraining Along-Track Error

The modifications made to the basic HSGPS/ map-matching vehicle positioning algorithms developed in Chapter 3 focus on minimizing the along-track error of the transit vehicles. The modification involved matching route features such as turns and transit stops with the observations from vehicle tracking data and fixing the vehicle position at such locations. For instance, an approximate 90-degree turn in the route can be identified using heading changes in vehicle tracking data. Furthermore, longer stops (i.e. stops longer than 2-3 minutes are unlikely at traffic signals) are more likely at transit stops and could be identified with speed and position observations in vehicle tracking

data. A simplified algorithm outline is presented in Figure 4.2, which is a detailed version of Figure 3.29. The validity of using these two position-fixing approaches is proven using field data later in the chapter.

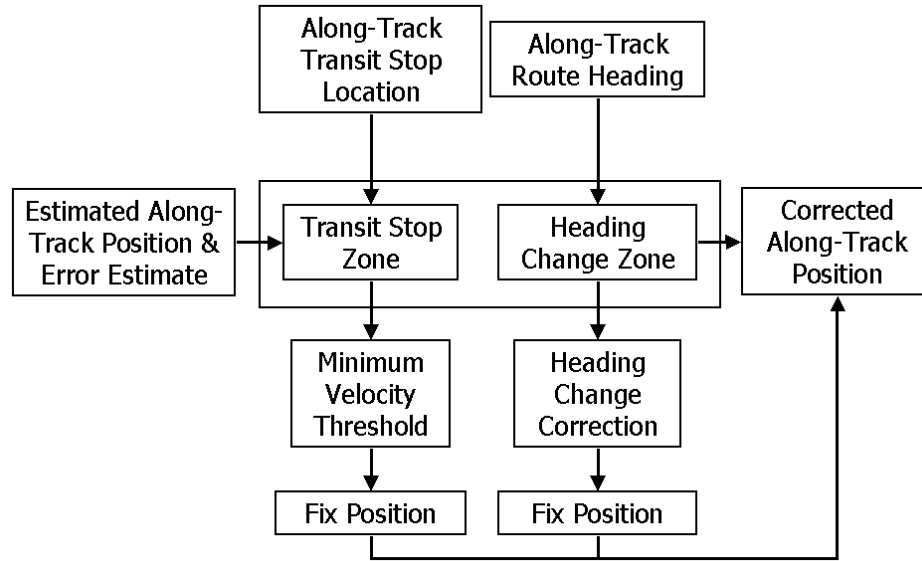


Figure 4.2: Along-track error constraining algorithm

In the first position fixing approach, the estimated along-track position of the vehicle was used to search for known along-route attribute changes, such as heading changes and latitude and longitude limits. If a heading change that matches along-route heading variation was found and either Northing or Easting limit corresponding to the feature was reached, the vehicle position was fixed to the along-track position of the route feature. The estimated along-track location of the vehicle, associated error estimate from the VDM and the along-track location of route attributes were used to find the along-track position fixing locations using the following equation

$$d_{r,j} - \delta d < d_{v,i} < d_{r,j} + \delta d \quad (4.1)$$

where

$d_{r,j}$  along-track position of route feature  $j$  in route  $r$

$\delta d$  estimated along-track positioning error using VDM

$d_{v,i}$  estimated along-track position of vehicle  $v$  at time  $i$ .

Upon reaching such regions, vehicle heading changes were compared with the route-heading attribute changes as given by

$$H_{r,j} - H_{j,r-\delta d} = (H_{v,i} - H_{v,i-\delta t})k_h \quad (4.2)$$

where

$H_{r,j} - H_{j,r-\delta d}$  route heading change over distance  $j - (j - \delta d)$

$(H_{v,i} - H_{v,i-\delta t})$  observed vehicle heading change over time  $i - (i - \delta t)$

$k_h$  empirical scale factor for heading error.

If the observed heading change satisfies the condition given in Equation (4.2) and the vehicle is within a predefined distance from the expected heading change, it is possible to declare a turn. The predefined distance assessment is defined by

$$|N_{r,j} - N_{v,i}| < \delta_N \quad (4.3)$$

$$|E_{r,j} - E_{v,i}| < \delta_E \quad (4.4)$$

where

$N_{r,j}, E_{r,j}$  position of the route feature  $j$  on route  $r$

$N_{v,i}, E_{v,i}$  position of vehicle  $i$  at time  $i$

$|N_{r,j} - N_{v,i}|$  Northing proximity to route feature  $j$

$\delta_N$  empirical Northing threshold

$|E_{r,j} - E_{v,i}|$  easting proximity to route feature  $j$

$\delta_E$  empirical Easting threshold.

Following the same notation, position fixing at the turn is given by

$$N_{v,j} = N_{r,i} \quad \text{and} \quad E_{v,j} = E_{r,i} \quad (4.5)$$

In the second position fixing approach, the estimated along-track vehicle location was used for detecting the vehicle entering into designated transit stop zones. With a slightly modified model of Equation (4.1), the entry to a transit stop zone was identified using the model

$$d_{r,j} - \delta d - 0.5l_{zone} < d_{v,i} < d_{r,j} + \delta d + 0.5l_{zone} \quad (4.6)$$

where

- $d_{r,j}$  along-track distance to transit stop  $j$  in route  $r$
- $\delta d$  estimated along-track error
- $l_{zone}$  length of transit stop zone

Furthermore, an entry to a transit stop can be confirmed by using Equations (4.3), (4.4) and (4.6). Upon confirming the entry, the vehicle speed was observed for detecting stops. This was conducted by checking for speed reductions below a speed threshold given by

$$|v_{v,i}| < \delta v \quad (4.7)$$

where

- $v_{v,i}$  speed of vehicle  $v$  at time  $i$
- $\delta v$  minimum speed threshold.

Based on empirical findings, the vehicle position was often found to show virtual movement during stops due to HSGPS position errors. Therefore, maintaining the vehicle position fixed during the stop and distinguishing between the virtual movement and the vehicle actually moving out of the transit stop zone were important. This was achieved by detecting vehicle speeds over the minimum threshold set in Equation (4.7) while the heading during such speeds agreed with the current street heading as given by

$$|v_{v,i}| > \delta_v \quad (4.8)$$

and

$$|H_{r,j} - H_{v,i}| < \delta_h \quad (4.9)$$

where

$|H_{r,j} - H_{v,i}|$  street and vehicle heading difference

$\delta_h$  heading threshold.

### 4.1.3 Field Testing

The field experiments outlined in Chapter 6 recorded over forty vehicle trajectories through downtown Calgary, thus providing data for illustrating the performance of the constrained map-matching algorithm. Six representative vehicle trajectories were selected for the analysis in this section. The route chosen for this analysis is depicted in Figure 4.3, which includes a part of the downtown core of Calgary, the test field used for this thesis. As in the case of most of the vehicle test trajectories used in this thesis, the area shown in Figure 4.3 included streets with severe urban canyons conditions and partly open-skies.

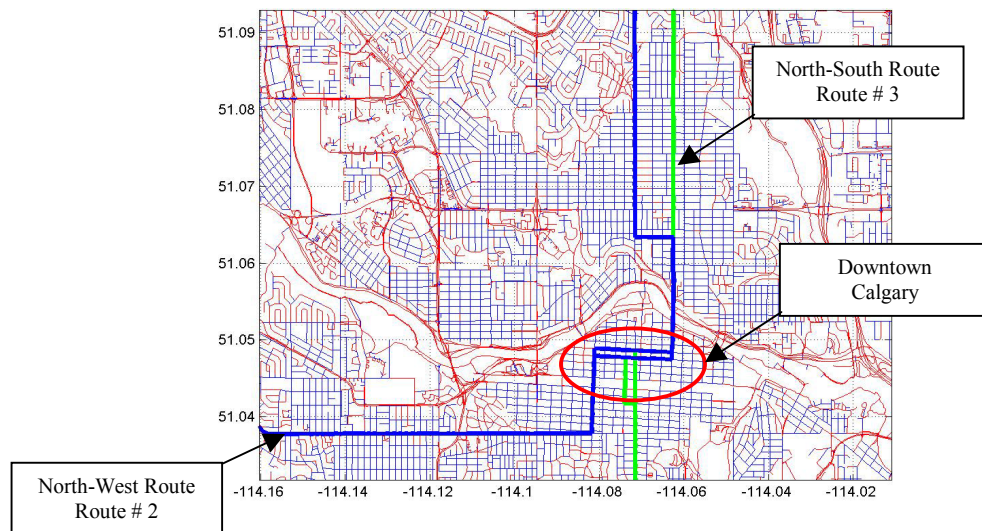


Figure 4.3: Test trajectory for transit vehicle position algorithm testing

#### 4.1.4 HSGPS Data Characteristics

The HSGPS receiver used in this field survey was a SiRF XTrack™. This receiver offers both internally filtered vehicle position and velocity measurements and measured pseudorange and Doppler observations, thus enabling least-squares-based position and velocity estimation by the user. These aspects were discussed in Chapter 3 and a quantitative comparison is made in this section. The internally filtered HSGPS measurements, which is referred to as HSGPS measurements in this thesis, provides far better availability and smoother vehicle position and velocity estimates compared to epoch-by-epoch estimates. However, these measurements provide no error estimation parameters and are the result of heavy internal filtering that is not accessible by the user. This significantly limits the research applications of the HSGPS measurements. Alternatively, the least-squares based single point solutions, which are referred to as single point HSGPS measurements (HSGPS-SP) in the thesis, provide access to least-squares estimate residuals and within the control of the user. However, the availability and the smoothness of HSGPS-SP measurements both in the position and velocity domains are considerably poorer than HSGPS measurements. This is due to the fact that single point least-squares based estimation uses information from a single data epoch, whereas the HSGPS measurements have the advantage of additional information from previous data epochs.

This analysis investigated the characteristics of both HSGPS measurements and HSGPS-SP measurements with the objective of selecting one of the measurements as the sensor data for the transit vehicle-positioning algorithm. Several characteristics are analyzed and discussed in considerable detail below.

##### 4.1.4.1 Availability

Availability was defined as the number of epochs when a valid measurement from either HSGPS or HSGPS-SP technique was available as a percentage of the total duration of the

test. The availability was calculated for all four-test runs for position and velocity in local two-dimensional coordinate system, giving four availability statistics for each test run. For position measurements, any measurement beyond 200 metres from the test trajectory was regarded as an invalid estimate. For velocity, a range from  $-5 \text{ ms}^{-1}$  to  $15 \text{ ms}^{-1}$  was set as the valid limit, and was estimated based on the maximum vehicle speed allowed in the route streets and the orientation of the streets. The results are given in Table 4.1.

Table 4.1: Availability statistics for HSGPS and HSGPS-SP

TEST RUN	POSITION AVAILABILITY (%)				VELOCITY AVAILABILITY (%)			
	HSGPS		HSGPS-SP		HSGPS		HSGPS-SP	
	X	Y	X	Y	V <sub>x</sub>	V <sub>y</sub>	V <sub>x</sub>	V <sub>y</sub>
1	55	55	53	42	55	55	54	53
2	47	42	35	38	48	48	48	47
3	58	52	38	38	60	60	42	41
4	41	38	39	38	41	41	40	39

#### 4.1.4.2 Across-Track Correction

The lack of a technique that is superior to GPS in performance to establish the precise reference positions and velocities of the vehicle during the test was a major drawback for analyzing the accuracy of either HSGPS or HSGPS-SP measurements. Therefore, an assumption was made to simplify the analysis. It was assumed that the position measurements only contain across-track errors, and these could be calculated as the distance to the Nearest Point (NP) mapping of the HSGPS or HSGPS-SP position estimate onto the route. Furthermore, instead of comparing the accuracy of HSGPS and HSGPS-SP, the across-track correction at each epoch was compared. The definition of the across-track correction is illustrated in Figure 4.4.

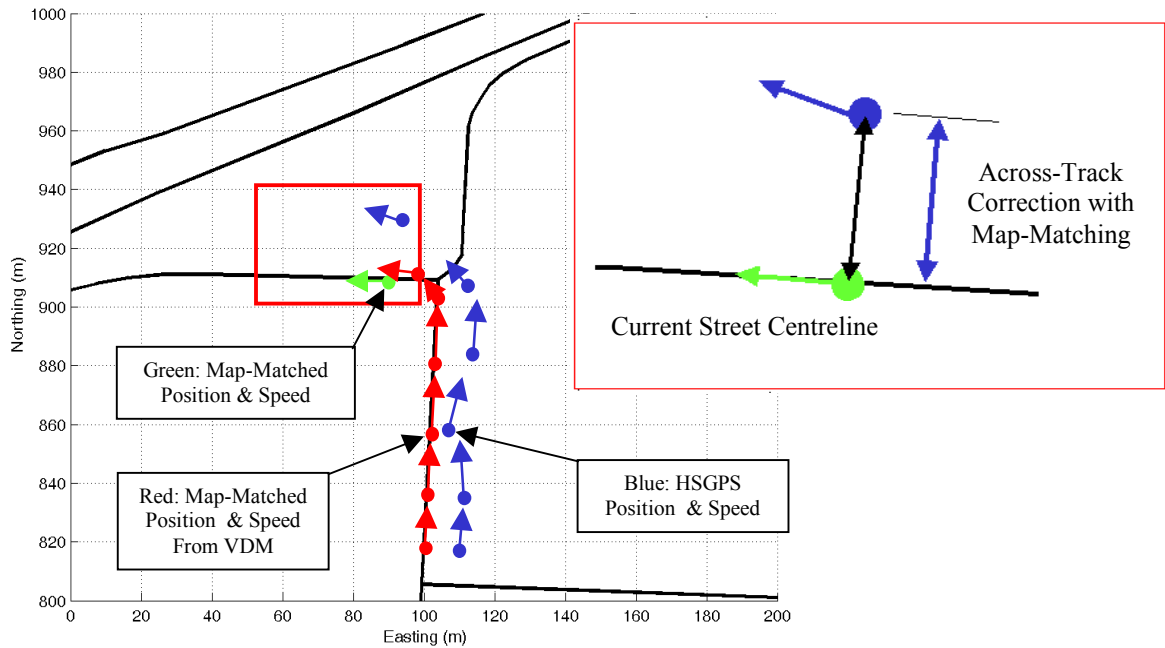


Figure 4.4: Across-track position and velocity corrections

Due to the presence of considerably large along-track errors, especially in the case of HSGPS-SP, some of the position and velocity measurements made during the test had no NP mappings. As HSGPS and HSGPS-SP measurements of even the same test run had different error characteristics, this made it possible to have different numbers of data epochs available for comparison from two estimate sets, thus making the result biased. In order to avoid using a different number of epochs from HSGPS and HSGPS-SP of the same test, only the epochs that have NP mappings for both HSGPS and HSGPS-SP measurements were used in the analysis.

According to the above criterion, each test run produced two time series of across-track position and velocity corrections for each HSGPS estimate set. The means of these time series are presented in Table 4.2. See Appendix B for time series figures and additional statistics.

Table 4.2: Across-track correction statistics for HSGPS and HSGPS-SP

TEST RUN	ACROSS-TRACK POSITION MEAN CORRECTION (m)				ACROSS-TRACK VELOCITY MEAN CORRECTION (m/s)			
	HSGPS		HSGPS-SP		HSGPS		HSGPS-SP	
	X	Y	X	Y	V <sub>x</sub>	V <sub>y</sub>	V <sub>x</sub>	V <sub>y</sub>
1	4.0	7.8	7.8	10.9	0.1	0.5	0.4	0.8
2	5.1	4.3	9.5	7.7	0.1	0.3	0.9	0.8
3	7.6	6.0	8.1	9.6	0.2	0.4	0.5	1.0
4	6.2	10.5	8.4	11.2	0.1	0.3	0.3	0.7

#### 4.1.4.3 Across-Track Correction Distribution

Both HSGPS and HSGPS-SP measurements are contaminated by random noise as well as coloured noise. Previous research has also shown that HSGPS measurement may be highly biased and may contain a considerable amount of coloured noise, especially under severe urban canyon conditions (Mezentsev et al., 2002). Across-track corrections for position and velocity measurements calculated in Section 4.1.4.2 for all four test runs were combined into across-track correction histograms as illustrated in Figures 4.5 and 4.6.

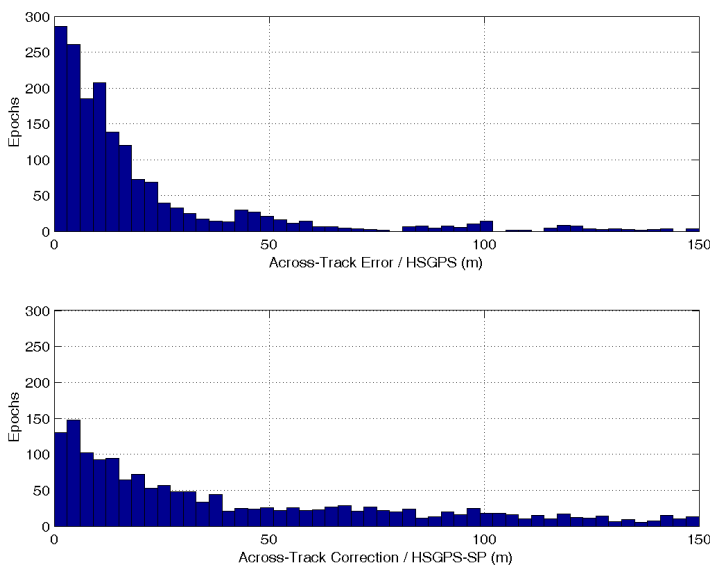


Figure 4.5: Across-track position correction for HSGPS and HSGPS-SP

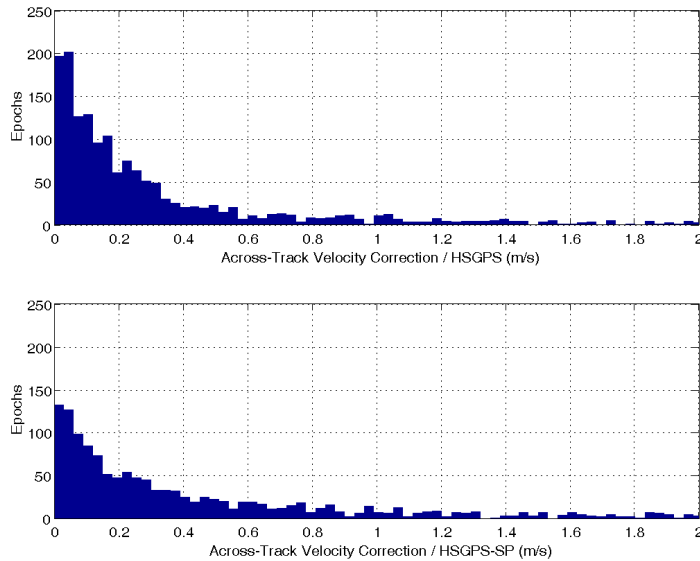


Figure 4.6: Across-track velocity correction for HSGPS and HSGPS-SP

#### 4.1.5 Conclusions of HSGPS Data Characteristics Analysis

The following conclusions were reached based on the data analysis:

- HSGPS-SP measurements were far below the availability and data smoothness requirements for the application considered in this thesis
- However, HSGPS-SP could be improved with the aid of additional sensors
- HSGPS measurements provide the required level of availability as well as highly smoothed data although they are biased, particularly at vehicle stops and turns
- HSGPS measurements can be used for this application, provided techniques are used to minimize the relatively large errors occurring in urban canyons.

#### 4.1.6 Algorithm Performance Analysis

The performance of the modified HSGPS/ map-matching algorithm is analyzed in this section. From nearly forty tracking data sets collected by transit vehicles, four

representative test runs were selected for the analysis. One of the vehicle trajectories is analyzed in detail in this section while Appendix B provides the results from all test runs.

#### 4.1.6.1 HSGPS Vehicle Trajectory

This section presents an analysis of HSGPS vehicle position and velocity characteristics of the 4<sup>th</sup> Test Run. Since there was no superior vehicle position and velocity measurement technique to compare with, HSGPS measurements were analyzed using the estimated along-track positions of the vehicle, thus providing a means of comparison with along-track features of the vehicle route. Three along-track route properties were used for this comparison, namely, the Northing, Easting and the heading. Figures 4.7 and 4.8 depict the HSGPS based vehicle Northing, Easting and heading as a function of the estimated along-track position of the vehicle. The corresponding function of the known vehicle route is also illustrated in Figures 4.7 and 4.8.

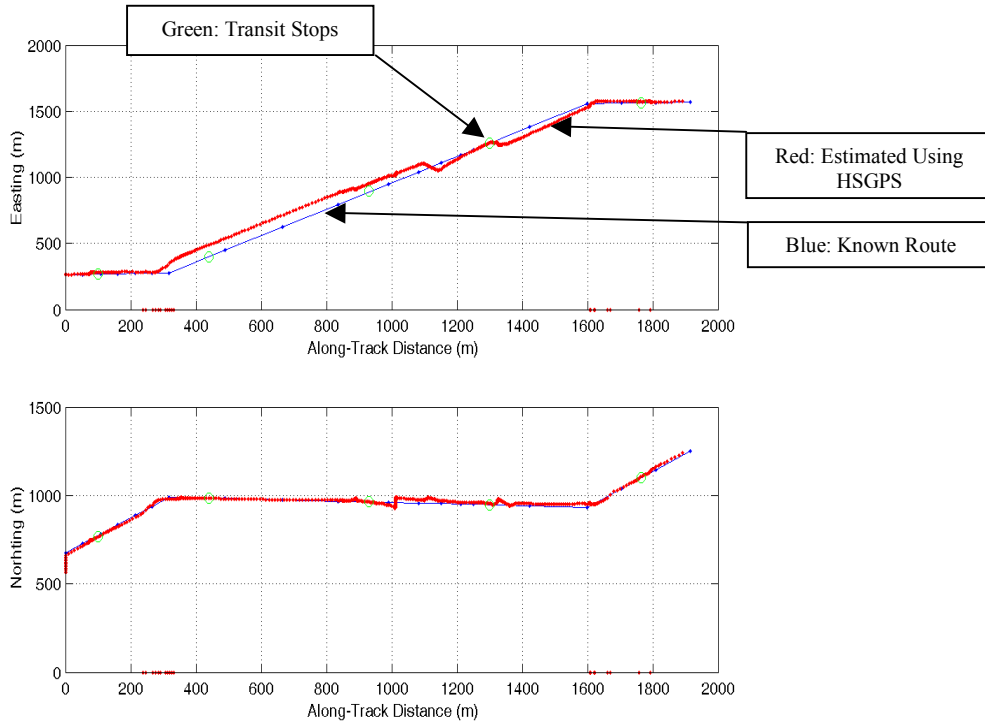


Figure 4.7: Along-track position vs. Northing and Easting

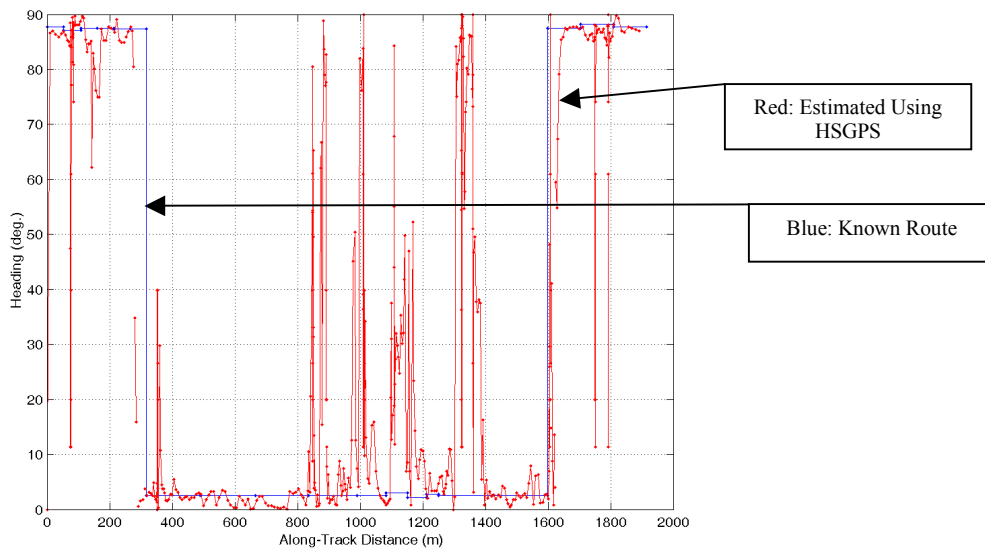


Figure 4.8: Along-track position vs. heading

#### 4.1.6.2 Along-Track Position Correction and Position Fixing

Figure 4.9 shows two along-track position correction locations identified using route heading information and three position-fixing locations identified at transit stops.

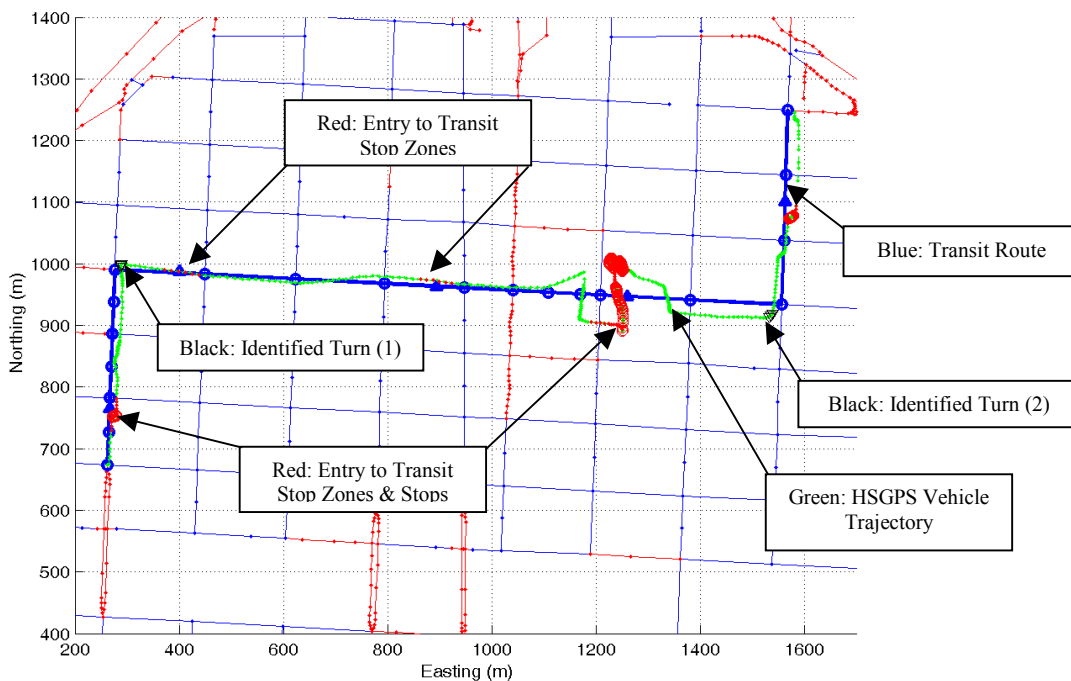


Figure 4.9: Along-track position fixing and during-stop position fixing

#### 4.1.6.3 Analysis Summary

Since no absolute vehicle position and velocity data exists to measure the absolute accuracy of the route constrained map-matched/ HSGPS transit vehicle-positioning system, the agreement of the along-track route features with vehicle position and velocity estimates was considered as the system performance measure. Depicted in Figure 4.10 is the constrained map-matched solution of the HSGPS vehicle trajectory of test run 6. Figures 4.11 and 4.12 illustrate the corrected Northing and Easting solutions and the corrected along-track distance vs. vehicle heading.

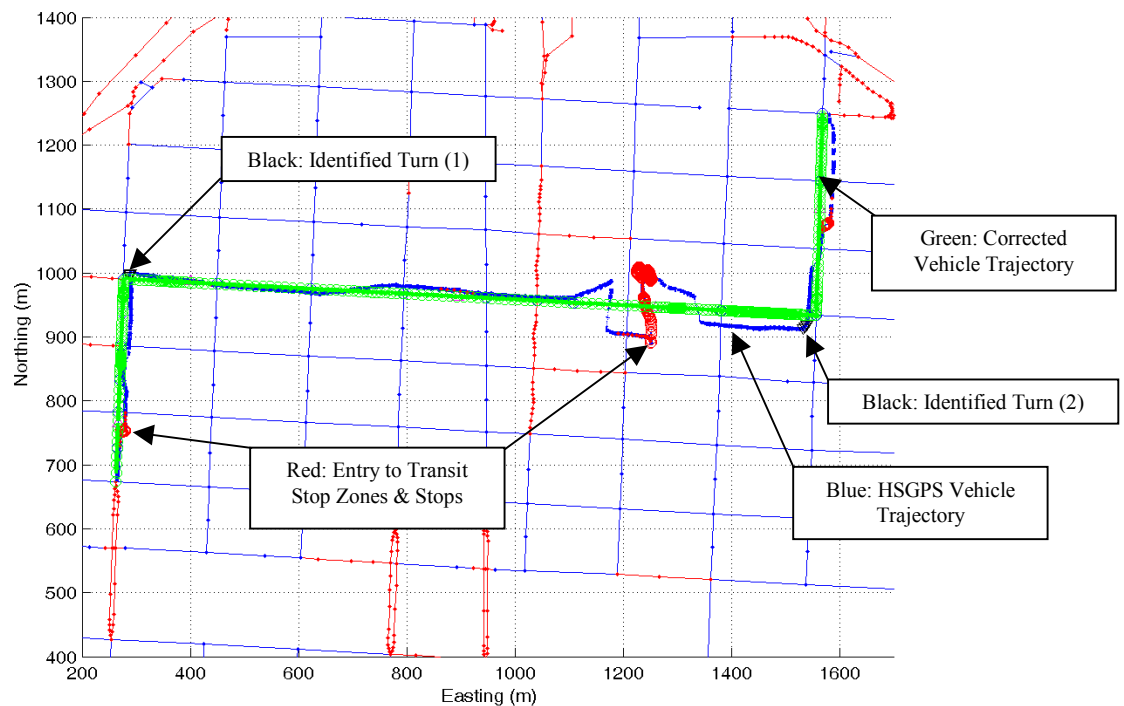


Figure 4.10: Route constrained map-matched solution for Test Run 6

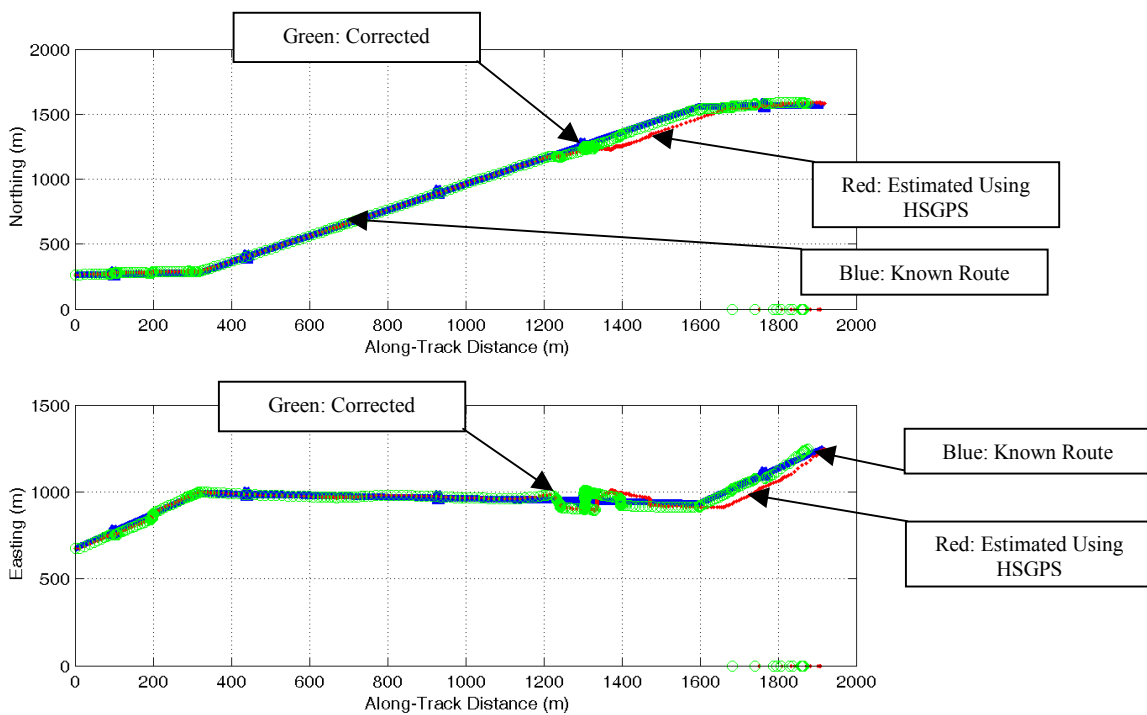


Figure 4.11: Northing and Easting results for Test Run 6

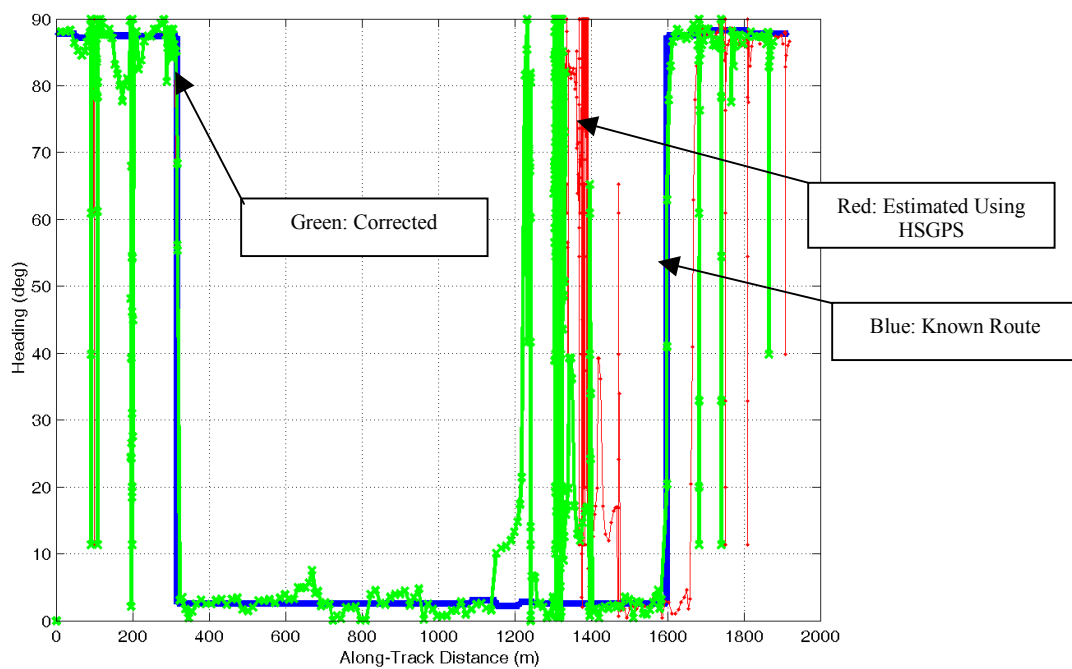


Figure 4.12: Corrected vehicle heading Test Run 6

## 4.2 Data Processing

This section outlines the transit vehicle travel time data collection, association with streets, outlier detection, and transit travel time modifications for incident detection.

### 4.2.1 Street Segment Selection

Transportation networks include a variety of elements ranging from segments of streets connecting two intersections, which are few hundred metres long, to freeways that may run for thousands of metres. Therefore, it is extremely important to have a standard method of classifying different facilities according to their functionality or characteristics in monitoring and analyzing their performance. The highway capacity manual provides such a classification system and provides the basis for defining the scope of this thesis (HCM2000, 2000). HCM2000 defines highway systems using collections of points known as nodes and collections of links between nodes. The former could be either a signalized or unsignalized intersection while the latter is referred to street segments. It also classifies highway systems into three types as illustrated in Figure 4.13.

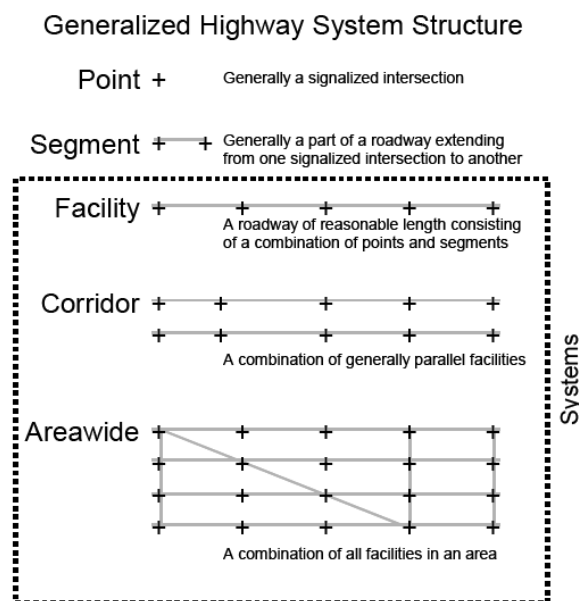


Figure 4.13: HCM2000 definition of highway segments and systems

The scope of this thesis is limited to monitoring traffic activity in individual road segments and adjacent segments with the objective of detecting traffic incidents. The overall layout of the segments is not of critical importance; however, a collection of urban street segments, classified as a facility according to the above definition is used for analysis throughout the thesis. The Highway Capacity Manual further defines a unit of analysis for such urban streets. Figure 4.14 illustrates the street segments selected for analysis in this research, a part of the street network in downtown Calgary. A segment is defined as the roadway connecting two intersections and each segment contains an intersection. For instance, the facility shown in Figure 4.14 has two segments, segment A and B with each including one intersection. However, only the segment B has a signalized intersection, and segment A has a priority controlled intersection where through traffic had the priority.

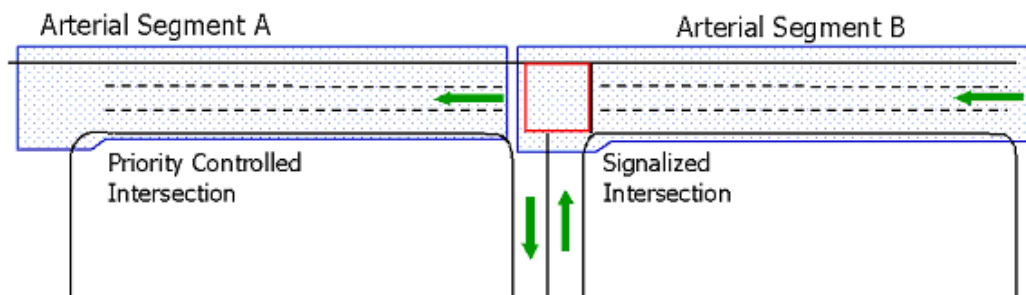


Figure 4.14: Urban street unit of analysis

#### 4.2.2 Transit Vehicle Travel Time Estimation

Transit vehicle tracking data, particularly travel times, have some correlation with roadway congestion and this has been proven by earlier research on transit probe vehicles (Hall et al., 1999; Hall & Vyas, 2000). However, transit vehicles do have characteristic behaviours that are clearly different from the behaviour of most other vehicles on the road. These differences arise from two aspects associated with transit vehicles and their operation, namely the vehicle characteristics and the transit stops. Transit vehicles and

similar large vehicles have different acceleration / deceleration behaviour compared to other more dominant vehicle categories in normal roadway traffic such as cars, mainly due their size, weight, inertia, drag and the limited maneuverability. Hence, they have relatively longer travel times, particularly in urban streets where frequent stops due to traffic controls are more likely. Furthermore, designated stops add dwelling time and a certain amount of lost time in approaching the stop, rejoining the traffic flow and reaching cruising speeds.

#### 4.2.2.1 Transit Data Characteristics

The difference in vehicle characteristics between transit vehicles and other dedicated probe vehicles used in this research were illustrated using a set of vehicle speed-acceleration characteristic curves. These curves illustrate the maximum acceleration of each vehicle type at different speeds. Although these curves define a maximum value for the acceleration at a particular speed, the actual acceleration may be influenced by a host of other factors such as interaction with other vehicles, traffic controls and driver behaviour, thus any value below the maximum could be observed. Furthermore, speed-acceleration may also reflect the driving conditions in a particular facility. For instance, the speed and acceleration choice may differ considerably between suburban uncongested streets and downtown streets where higher levels of interaction between vehicles exist. Therefore, two sets of curves are presented, namely for suburban uncongested and urban congested conditions.

Figure 4.15 A, B and C show speed-acceleration curves from three vehicles in suburban uncongested driving conditions. Figure 4.15A and 4.15B were generated from data collected using a Dodge Caravan and a 1997 Hyundai Elantra while Figure 4.15C was generated from data collected using a transit vehicle. The data points in these three illustrations represent actual accelerations observed at different speeds. The curves represent the maximum acceleration observed at a particular speed, established using the maximum values of data points. Such a curve was used as the characteristic maximum

speed-acceleration curve for the respective vehicle type. The same set of curves for urban driving conditions are given in Figure 4.16.

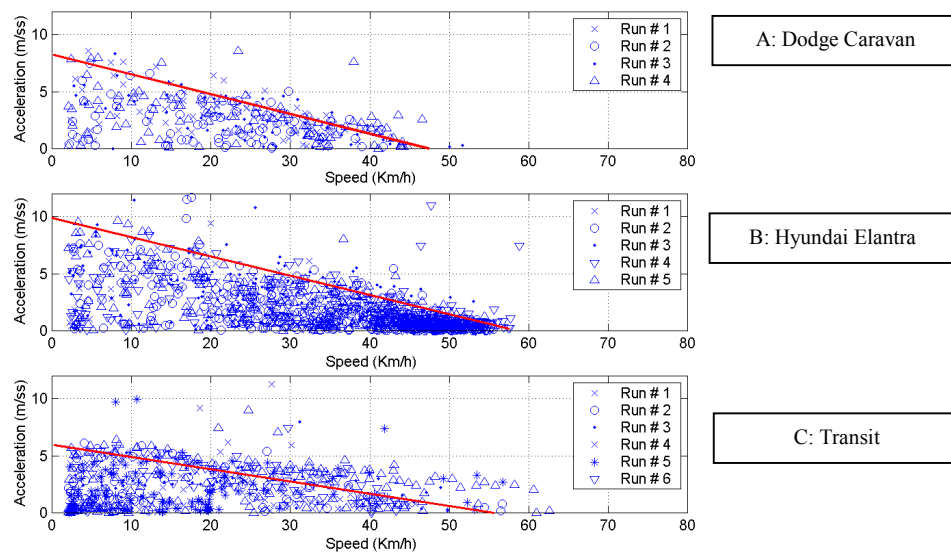


Figure 4.15: Speed-acceleration characteristics curves (urban-congested)

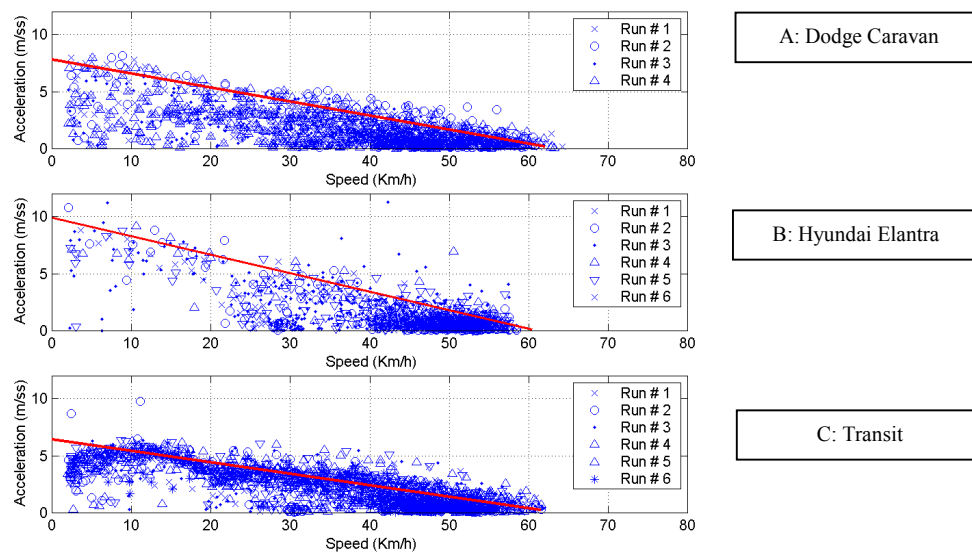


Figure 4.16: Speed-acceleration characteristics curves (suburban-uncongested)

Based on these empirical results, two conclusions can be reached about the vehicle characteristic differences between transit vehicles and the rest of the vehicles that dominate the normal traffic vehicle mix.

- Transit vehicles have significantly lower maximum acceleration capability and therefore take longer to reach cruising speeds after a complete stop compared to other lighter vehicle types that dominate the roadway vehicle mix.
- Transit vehicles have lower operating speeds, thus longer travel times

The transit travel time modification algorithms developed in this research focus on minimizing the bias introduced by the first of these differences. This was considered important as the removal of dwelling time alone cannot account for the total time lost due to transit vehicle stops at designated locations, especially with frequent stops. The second difference was not addressed in the modifications, as there were limited comparisons between transit and non-transit travel times, and the quality of the travel times in relation to travel times observed by other vehicles was not a concern for the incident detection application.

#### 4.2.2.2 Measurements and Dwelling Time Estimation

Time sequenced transit probe position and velocity data is first segmented into streetwise blocks corresponding to street segments and for each street segment, the number of stops at designated transit stops and dwelling time at each stop is stored as an attribute of the street segment record of a particular vehicle trajectory. Therefore, each transit vehicle trajectory provides a series of attribute vectors, each referring to a street attribute set given by

$$TData_{i,j} = [t_0, MTT_{i,j}, DT_{j,1}, \dots, DT_{j,S}] \quad (4.10)$$

where

$TpData_{i,j}$	transit probe street attribute vector for $j^{\text{th}}$ street in $i^{\text{th}}$ trajectory
$t_0$	time of entry to the $j^{\text{th}}$ street
$MTT_{i,j}$	measured transit travel time for $j^{\text{th}}$ street in $i^{\text{th}}$ trajectory
$S$	number of designated transit stops in $j^{\text{th}}$ street
$DT_{j,k}$	dwelling time at $k^{\text{th}}$ designated stop in $j^{\text{th}}$ street.

Dwelling time estimation requires the identification of a vehicle reaching a transit stop zone while reducing its speed and eventually maintaining a stop during the dwelling time. These two conditions were implemented using vehicle along-track position and speed observations with the models given in equations (4.6) and (4.7). The duration through which all vehicle position and velocity estimates satisfy the above conditions was taken as the estimated dwelling time of the vehicle.

#### 4.2.2.3 Modification Algorithm

The modification algorithm eliminates the estimated dwelling times at all transit stops and modifies the time lost due to acceleration and deceleration approaching and leaving the transit stop zone. Using the same notation as above and the travel time data vector for a street segment, the modified travel time is estimated using the equation

$$\text{Travel Time}(t_0, i, j) = MTT_{i,j} - \sum_{k=1}^S DT_{j,k} - \sum_{k=1}^S LT_{j,k} \quad (4.11)$$

where

$\text{Travel Time}(t_0, i, j)$  estimate travel time for probe  $i$  in segment  $j$  entering at time  $t_0$

$\sum_{k=1}^S DT_{j,k}$  total dwelling time in the street segment  $j$

$\sum_{k=1}^S LT_{j,k}$  total lost time associated with  $k$  stops in segment  $j$ .

The lost time for each stop ( $LT_{j,k}$ ) was estimated assuming that the vehicle would continue to travel at the average speed of the segment if it was not required to stop at a designated stop. Furthermore, it is assumed to accelerate up to the cruising speed according to the empirical speed-acceleration curves depicted in Figures 4.15 and 4.16. Hence, the lost time model is given by

$$LT_{j,k} = \int_{v_{cru}}^0 f(v)dt + \int_0^{v_{cru}} f(v)dt \quad (4.12)$$

where

$v_{cru}$  cruising speed in segment  $j$ .

#### 4.2.2.4 Modification Algorithm Testing with Field Data

The above modification algorithm was applied to several transit vehicle data sets collected in the field tests outlined in Chapter 6. Furthermore, Section 6.3.2 provides a comprehensive analysis of the modification algorithm calibration process and the results.

### 4.2.3 Travel Time Modeling Framework

The simulations and the following analysis presented in this thesis were entirely based on fixed traffic demands levels that correspond to the typical workday morning peak period traffic demand in the modeled part of Calgary. However, traffic demand varies over the time of day and may vary from day to day. Therefore, it is possible to identify unique traffic patterns for different days of the week (i.e. weekday and weekend) and times of the day, for instance at the morning peak, off-peak, evening peak and the evening off-

peak (HCM2000, 2000). Usually, traffic demand is expressed as the number of vehicles observed in an interval (i.e. 15-minute intervals). See (HCM2000) for further discussions on traffic demand variations and quantifying such variations according to the time of day and the day of the week.

The objective of the travel time modeling framework was to provide the incident detection algorithm with historical data for several purposes. The primary use of historical travel time was to establish the statistical properties of street segment travel times thus make more information available to the incident detection system in addition to real-time travel time records provided by transit probe vehicles. Furthermore, historical data was also used for detecting outliers in the reported travel times. Figure 4.17 provides a process block diagram for the travel time modeling framework.

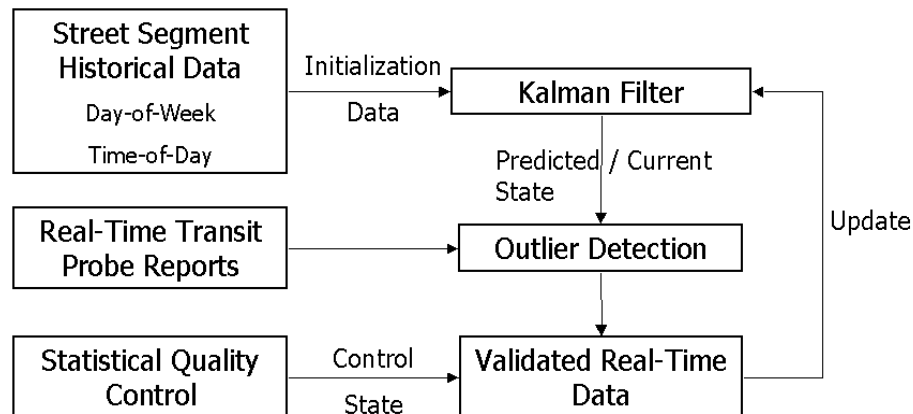


Figure 4.17: Travel time modeling framework

A travel time statistical model was established for each individual street segment in the incident monitoring network. Each street segment travel time model combined the historical knowledge for daily travel time trends and the near real-time probe travel times to estimate an optimal real-time travel time for the street segment. The model estimates also provided the basis for detecting likely outliers in probe vehicle travel time reports. In summary, a street segment travel time model fulfills the following tasks:

- Integrate near real-time probe vehicle travel times and historical travel time trends for a particular street segment for a known period of time (i.e. for a 15 minute interval)
- Segment the hourly, daily and weekly traffic demand variations into intervals for incident algorithms to work on a time interval basis
- Provide a basis for identifying probe travel time reports that are outliers and provide further knowledge to identify clusters of outliers that could indicate longer travel times due to traffic incidents
- Estimate a travel time covariance that reflects the reliability of the travel time estimate.

The variation of travel time in a street segment for a given period of time was modeled as a result of a random process. Over several such periods, the process also follows a variation that was estimated with historical travel time data and is known with a certain level confidence. These requirements can be optimally achieved with a single state Kalman filter with the street segment travel time as the state variable. With the state space notation, the filter state vector is given as

$$X = [\text{Travel Time}] \quad (4.13)$$

Following the same notation used in Section 3.4.2 for Kalman filtering, the state is predicted in time using the process model

$$\bar{X}_i = AX_{i-1} + Bu_{i-1} \quad (4.14)$$

where

- $\bar{X}_i$  predicted travel time for epoch  $i$
- $X_{i-1}$  travel time estimate for epoch  $(i-1)$
- $A$  process model between time epochs  $i$  and  $(i-1)$
- $u_{i-1}$  control signal introduced to the system at time epoch  $(i-1)$ .

The control signal for a full day of operation is estimated prior to real-time operation using all travel time observations available for the street segment. Ideally, the time resolution for the daily travel time variation should be of the order of minutes, especially in intervals where variations are expected, such as transitions between off-peak to peak conditions. Up to 15 minute time intervals could be considered when steady operating conditions are observed. Under the condition of no travel time observations from real-time probe vehicles, the filter follows the estimated historical travel time profiles. Each probe vehicle travel time observation is integrated into the process by using an observation model given by

$$Z_i = HX_i \quad \text{for all } Z_i : \bar{X}_i - n\sigma_{\bar{X}_i} \leq Z_i \leq \bar{X}_i + n\sigma_{\bar{X}_i} \quad (4.15)$$

where

- $Y_i$  probe reported travel time
- $H$  observation model
- $\sigma_{\bar{X}_i}$  estimated standard deviation for predicted travel time for epoch  $i$
- $n$  confidence parameter for outlier detection.

The model was updated with travel time records that are not outliers with the Kalman filter update given as

$$K = \bar{P}_i H^T (H \bar{P}_i H^T + R)^{-1} \quad (4.16a)$$

$$X_i = \bar{X}_i + K(Z_i - H\bar{X}_i) \quad (4.16b)$$

$$P_i = (I - KH)\bar{P}_i \quad (4.16c)$$

The travel time and the associated covariance were then predicted for the next time epoch using the following equations:

$$\bar{X}_{i+1} = AX_i \quad (4.17)$$

$$\bar{P}_{i+1} = AP_i A^T + Q \quad (4.18)$$

#### 4.2.4 Outlier Detection

Detection of outliers in travel time observations is of great importance to maintain the reliability of the system. Under low levels of probe vehicle penetration, it is important to have the capability to reject observations that are contaminated by either measurement errors or factors other than traffic incidents (Dion & Rakha, 2004). The challenge is to distinguish between outliers and sudden changes in observed travel time due to incidents, as both could result longer observed travel times. In order to improve the reliability in detection, outliers were detected by monitoring both average and the range of the travel time observations. These two quantities were calculated using

$$\bar{X} = \frac{\sum_i^{i-n} t_i}{n} \quad (4.19)$$

and

$$\bar{R} = \max(t_i, t_{i-1}, \dots, t_{i-n}) - \min(t_i, t_{i-1}, \dots, t_{i-n}) \quad (4.20)$$

where

- $\bar{X}$  mean travel time
- $\bar{R}$  range of travel times
- $t_i$  travel time reported by vehicle  $i$
- $n$  sample size.

Both  $\bar{X}$  and  $\bar{R}$  indicators respond in a similar manner to either an outlier or a travel time increase due to an incident. This is illustrated in Figure 4.18 using street segment travel times reported by probe vehicles in a simulated street network. A travel time record that was around 30 seconds longer than the observed normal travel time was inserted into the  $\bar{X}$  chart just before 40 minutes into the simulation. As depicted in Figure 4.18, this created increased  $\bar{X}$  and  $\bar{R}$  states. The impact of the incident induced longer travel times

is shown in Figure 4.18 after around 60 minutes into the simulation. Although Figure 4.18 offers no difference between these two influences, their time-differenced version, depicted as Figure 4.19 illustrates the features used for distinguishing incidents and outliers.

In the event of an outlier, Figure 4.19 shows a large positive spike followed by a negative spike of similar magnitude,  $n$  travel time records apart. This characteristic was incorporated into the algorithm for outlier detection. One of the drawbacks is the actual time lag between detecting the first spike and declaring it an outlier. A spike observed in control charts can only be classified either as an outlier or incident induced only after receiving  $n$  subsequent travel time reports, a major factor taken into account in designing the sample size of the control charts.

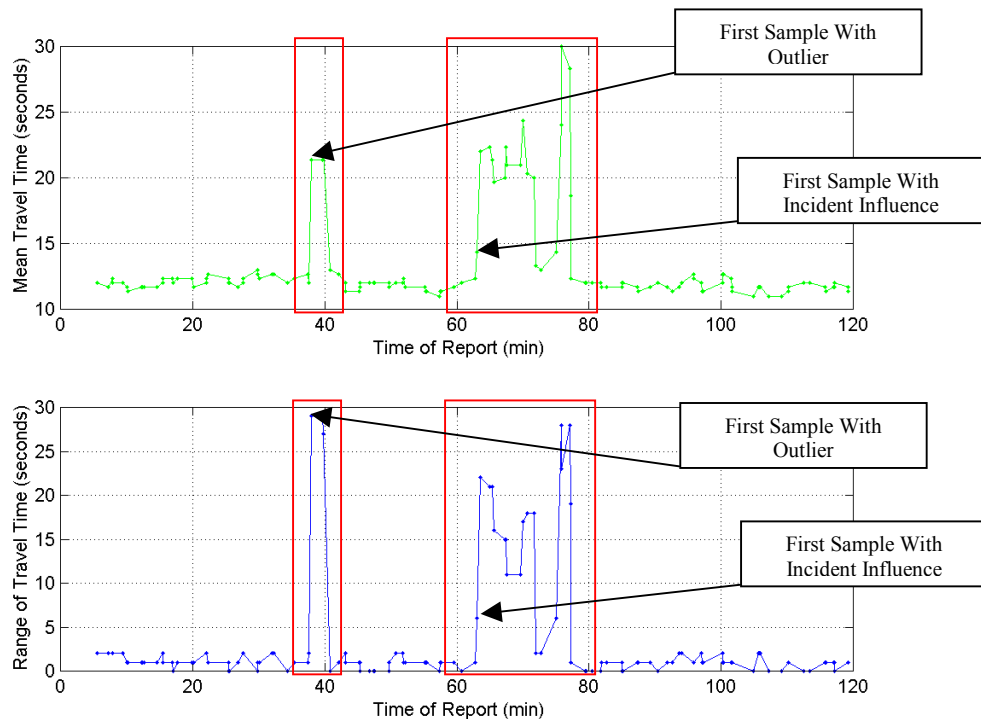


Figure 4.18: Outlier (Left) and incident (Right) influenced  $\bar{X}$  and  $\bar{R}$

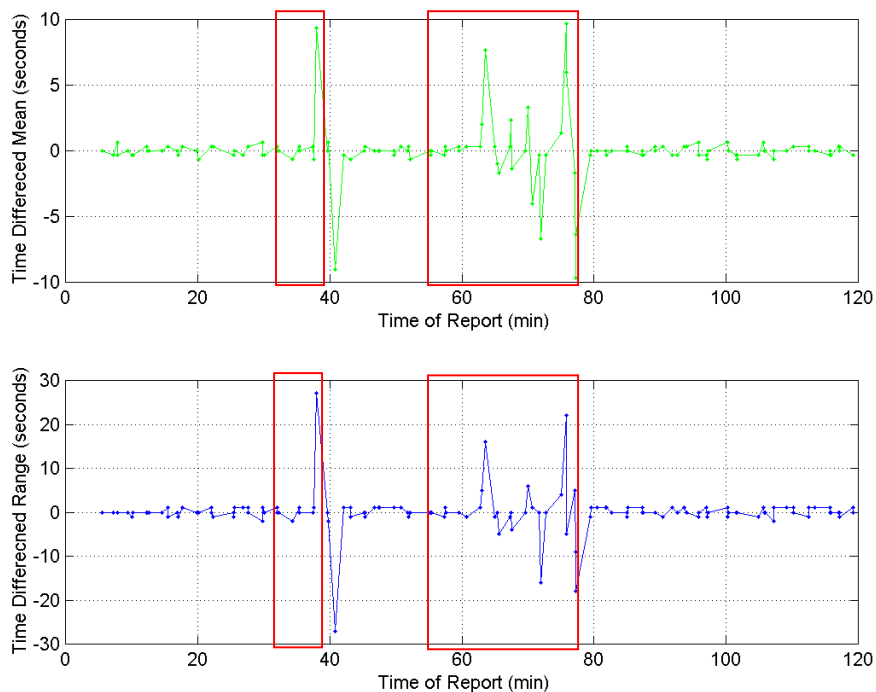


Figure 4.19: Time differenced  $\bar{X}$  and  $\bar{R}$

### 4.3 Traffic Performance Indicators and Incident Detection Parameters

Traffic performance monitoring involves monitoring transportation facility activity indicators to assess many aspects of the service provided by the facility. This includes the Level of Service (LOS) received by the user and the service provided with respect to facility operator's objectives. In long term planning and management, performance measures are used as tools to monitor and manage transportation facilities according to predefined levels of services (NCHRP, 1998). Traffic performance measures address different aspects of roadway operations and cater to different requirements. For instance, LOS indicators could be used for multiple applications such as for real-time traveler or driver information and archived long-term system management and planning purposes. From a system configuration point of view, traffic incident detection can be regarded as a subset of greater traffic performance monitoring systems.

Performance monitoring addresses both short-term (or real-time) and long-term aspects of operation and management of a transportation facility. These areas could include real-time LOS assessment, congestion and incident impact assessment for traffic control and management, traffic volume measurement, LOS reliability assessment, weather related impact monitoring, and emission monitoring with real-time or short term operation and management objectives. Similar indicators are archived over time for management and planning purposes. A comprehensive discussion on the current state of practice in transportation performance monitoring in the United States is given in NCHRP (2003).

#### **4.3.1 Variables of Interest**

This section addresses the variables of interest for traffic incident monitoring and detection. The impact of traffic incidents is frequently measured in terms of variations in travel times and operating speeds, and a host of other parameters. Table 4.3 provides a summary of incident related performance indicators, frequently used in the current state of practice as reported in NCHRP (2003). Based on such proven practices and the existing knowledge base, the travel time was selected as one of the variables of interest of traffic incident detection.

Although these performance indicators are proven to provide reliable indications on the onset of congestion, especially non-recurring congestion, one of the major limitations of those indicators is that they all use conventional traffic sensor data. Furthermore, probe vehicle-based performance variables are currently used in limited applications, mainly for long-term performance analysis such as travel time surveys to assess the impact of major facility improvements or changes.

However, with advancing technology and affordable probe vehicle technologies, the ability to use individual vehicle tracking data for performance monitoring and incident detection has been investigated further in recent research. Quantifying the increased speed fluctuations and stop-and-go driving conditions after incidents has been one of the

main goals of these research efforts. For instance, the ADVANCE program identified speed noise or the standard deviation of speed and the coefficient of variation of speed as indicators of incident induced congestion in addition to conventional indicators such as running time and running speed (Seti et al., 1995). Furthermore, the standard deviation of acceleration is often used as an indicator for congestion, fuel consumption and emission modeling (Greenwood et al., 1998). Therefore, acceleration noise was considered the second incident detection parameter for this research. The incident detection parameters used for this research, travel time variation, and acceleration noise are described below.

Table 4.3: Traffic incident related performance measures

<b>Performance Measure</b>	<b>Definition</b>
Incident Induced Delay	Increased travel time due to incidents
Duration of congestion	Duration of recurrent or non-recurrent incident induced congestion
Incidents	Traffic interruptions caused by traffic incidents in terms of additional delay, capacity reduction, duration or any other incident characteristic
Percentage of system congested	Percentage of area congested due to incidents
Percentage of travel congested	Percentage of travel congested due to incidents in distance traveled
Recurring delay	Longer travel times resulting from recurring congestion without any incident impact
Speed	Distance traveled per unit time
Travel Time	Time taken to travel from one point to another
Travel rate index	Amount of extra travel time
Travel time reliability	Variability or range of travel times or percentage of travelers arriving at the destination within a predefined travel time

### 4.3.2 Acceleration Noise

Under normal traffic conditions, vehicle acceleration and deceleration can be split into two terms, namely a random component and a control signal. The combined magnitude of these two components is a function of many factors including road geometry, surface conditions, roadside activities and more importantly traffic density and volume (Kuhne & Michalopoulos, 1992). Traffic incidents are likely to force vehicles to undergo more lane changing manoeuvres, travel at lower speeds and force stop-and-go driving

conditions. This result in increased speed fluctuations thus increased accelerations and decelerations.

The acceleration noise is formally defined as the root mean square of the deviation of acceleration of a vehicle driven independently of other vehicles (Hermann, 1959). Subsequently, this measure was adopted for characterizing freeway congestion and later on for highway congestion measurement (Sirinivasan & Jovanis, 1996; Winzer, 1980). Winzer (1980) published acceleration noise measurements made on German highways using one hundred and sixty floating vehicles runs under different traffic conditions and developed an empirical model of acceleration noise at different traffic densities. His model, illustrated in Figure 4.20, forms the basis for detecting incidents using acceleration noise. Acceleration noise generated by vehicles traveling in free flow or near capacity stable traffic flow shows distinctly lower values. However, acceleration noise measurements made in the unstable flow region are much higher, and the sharp increase in the transition region provides an ideal measure of driving characteristics changes from stable to unstable flow conditions.

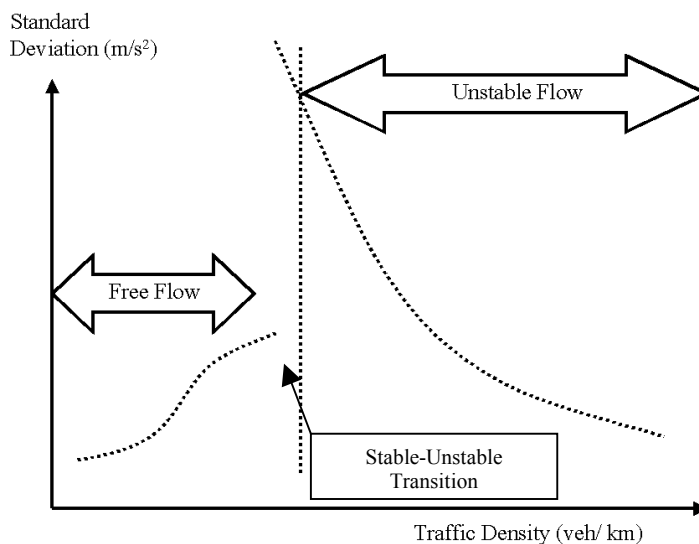


Figure 4.20: Standard deviation of acceleration noise (Winzer, 1980)

Acceleration noise is calculated as the standard deviation of the vehicle acceleration signal for 5-second windows. For comparison purposes, these 5-second acceleration

noise values are aggregated to segment values to derive segment specific total acceleration noise values using the model given by

$$\text{Total Acceleration Noise} = \sum_{\text{Segment}} \sigma_{a,(i-5,i)} \quad (4.21)$$

where

$\sigma_{a,(i-5,i)}$  standard deviation of acceleration for time interval  $(i-5, i)$ .

### 4.3.3 Street Segment Travel Time Variation

The successful use of street segment travel time variations for incident detection depends on archiving travel time data records, identifying the statistical characteristics and using appropriate estimation techniques. Urban street segment travel time analysis is seldom addressed in research primarily due to the cost of collecting data from a large population of vehicles. However, there exists considerable consensus on the most suitable statistical framework for street segment travel time modeling, mostly deduced by the knowledge gained from freeway travel time analysis and urban trip time analysis. For instance, the NCHRP has identified a lognormal distribution as the closest possible theoretical representation for urban street travel time behaviour (NCHRP 20-58, 2002). Although many other researchers have reached the same conclusion, the normal distribution is frequently assumed for practical applications mostly due to technical limitations in measuring a large number of travel times to establish the lognormal distribution (He et al., 2002). Therefore, the first task of the algorithm development is to establish the best possible statistical description of street segment travel times under normal operation.

Travel time measurements from traffic flow unaltered by controlling systems such as traffic signals may be modeled as a lognormal variable as illustrated in Figure 4.21. A

detailed discussion on fitting a lognormal distribution for travel time observations from such a street segment is later presented in Chapter 7 using simulation data.

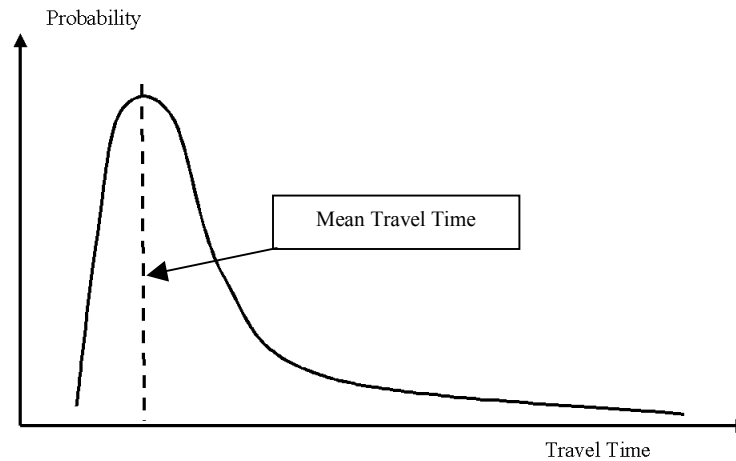


Figure 4.21: Travel time PDF for an unsignalized street segment

However, traffic-controlling devices modify traffic flow properties to a great extent, thus making the lognormal assumption invalid for the analysis of travel times in signalized street segments. Therefore, there exists the need to classify urban street segments into two classes: segments without a traffic signal and segments that have a traffic signal. For the clarity of this thesis, the former category is defined as the Type 1 segment and the latter as the Type 2 urban street segment. The travel time observed from a Type 2 street segment is a combination of two time components, namely running time and the control delay caused by the traffic signal (HCM2000, 2000; Hellinga & Fu, 2002). Although intersection delay models could estimate the delay component added by the signals, such estimates are not capable of establishing the actual running time of a vehicle using its total segment travel time.

The control delay in a Type 2 street travel time is highly correlated with the arrival time of individual vehicles at the beginning of the segment and the traffic volume to capacity ratio of the segment (Graves et al., 1998). Although no clear statistical correlation of travel time and arrival time is apparent in the time domain analysis of Type 2 segment travel times, transformation of vehicle arrival times to a function of traffic signal states

reveal a high degree of correlation with the signal states. A typical street segment travel time vs. vehicle arrival (i.e.: state of the signal at arrival) is shown in Figure 4.22

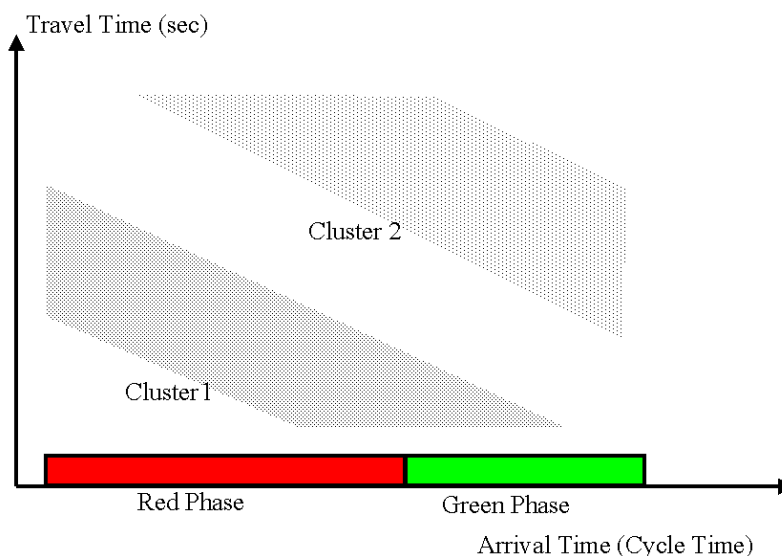


Figure 4.22: Travel time vs. arrival time for a Type 2 Street Segment

Depending on the vehicle volume to capacity ratio in the street, individual vehicle travel times can be clustered into two or more regions in the street entry time relative to the signal state. Vehicles in the first cluster experience minimal delay due to traffic controls. However, the vehicles in the second cluster experience extended periods of delay. The duration could be a single signal cycle or multiple cycles, depending on the saturation of the approach. Therefore, in case of high saturation, there could be more than two clusters in the above classification. Based on empirical findings of this research, each travel time cluster can be represented by a unique lognormal Probability Density Function (PDF). Furthermore, mean travel time of each PDF is highly correlated to the length of the red phase of the signal as illustrated in Figure 4.23. An analysis of statistical properties of travel time of a Type 2 street segment is presented in Chapter 7 using simulated results.

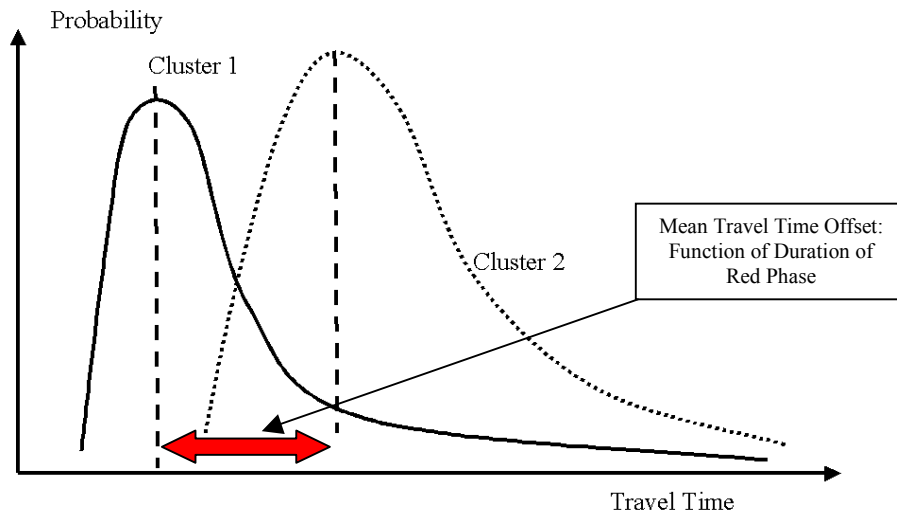


Figure 4.23: Travel time PDF for a Type 2 Street Segment

#### 4.4 Control Charts for Travel Time Monitoring

Based on the statistical properties of street segmental travel time, it is possible to treat travel time as an output of two sub-processes, namely, the statistical process described by the travel time PDF for normal operation and the disturbances created by incidents, which are not represented by the PDF. Hence, the incident detection scheme can be implemented as a Statistical Quality Control (SQC) process on the travel time observations. More specifically, utilizing the historical travel time information provided by the travel time framework and data up to a point of time, current and future process output is monitored for deviations that are not within the average or the range given by its statistical properties. The use of control charts developed using statistical properties of a process to monitor the outcome of industrial processes has its origins in 1924. Walter A. Shewhart first developed this concept in 1924 and the concept was put into wide use and grew rapidly in 1950's and 1960's, see (Walpole et al., 2002).

#### 4.4.1 SQC Variables

The capability of SQC techniques to monitor a process during the operation has made it a very powerful tool in industrial process control, and in the context of this application, this enables the real-time process monitoring, an essential element in automated incident detection. Based on the statistical properties of the travel time distributions, two variables were monitored to detect incidents, namely the mean and the range of observations. The mean monitors the central tendency of the measurements while the range monitors the variability around the mean. For a process at its time epoch  $i$ , these two variables can be calculated as follows using  $n$  observations:

$$\bar{X}_i = \frac{\sum_i^{i-n} t_i}{n} \quad (4.22)$$

and

$$\bar{R}_i = \max(t_i, t_{i-1}, \dots, t_{i-n}) - \min(t_i, t_{i-1}, \dots, t_{i-n}) \quad (4.23)$$

where

- $\bar{X}$  mean travel time
- $\bar{R}$  range of travel times
- $t_i$  travel time reported by vehicle  $i$
- $n$  sample size.

#### 4.4.2 Control Chart Designing

In order to use these two variables in a SQC process, two critical algorithm design aspects have to be addressed. Firstly, the sample size  $n$  must be defined and secondly, the control limits must be established.

As a general rule in sample size selection, frequent sampling of the process with smaller sample sizes is recommended, and sample sizes of  $n = 4, 5$  or  $6$  are often used. Although these sample sizes are considered relatively small for general statistical inference, there are several justifications for using such values for SQC. Firstly, each data point in SQC represents multiple observations, equal to the sample size. Secondly, SQC is a continuous sampling process and the total number of observations in the process is at least several orders of magnitude larger than the sample size. A sample size of 3 was used for this analysis. This sample size yielded the best performance in terms of response to traffic incidents with out-of-control chart indications. However, this performance may vary with higher or lower probe vehicle sampling frequencies, and this is discussed in the concluding remarks.

The second design consideration of establishing control limits is approached as an extension of establishing confidence intervals in the travel time PDFs. The Upper Control Limit (UCL) and the Lower Control Limit (LCL) for  $\bar{X}$  can be written as

$$UCL_{\bar{X}} = \bar{\bar{X}} + K_{\bar{X},UCL} \bar{R} \quad (4.24)$$

$$LCL_{\bar{X}} = \bar{\bar{X}} - K_{\bar{X},LCL} \bar{R} \quad (4.25)$$

where

- $\bar{\bar{X}}$  mean travel time for the street segment
- $K_{\bar{X},UCL}, K_{\bar{X},LCL}$  statistical confidence limits for UCL and LCL
- $\bar{R}$  mean travel time range.

Similarly, UCL and LCL for  $\bar{R}$  can be written as

$$UCL_{\bar{R}} = K_{\bar{R},UCL} \bar{R} \quad (4.26)$$

$$LCL_{\bar{R}} = K_{\bar{R},LCL} \bar{R} \quad (4.27)$$

where

$K_{\bar{R},UCL}, K_{\bar{R},LCL}$  statistical confidence limits for UCL and LCL

$\bar{R}$  mean travel time range.

Using the above control chart design parameters, travel time control charts can be developed for a particular time period of the day as illustrated in Figures 4.24 and 4.25.

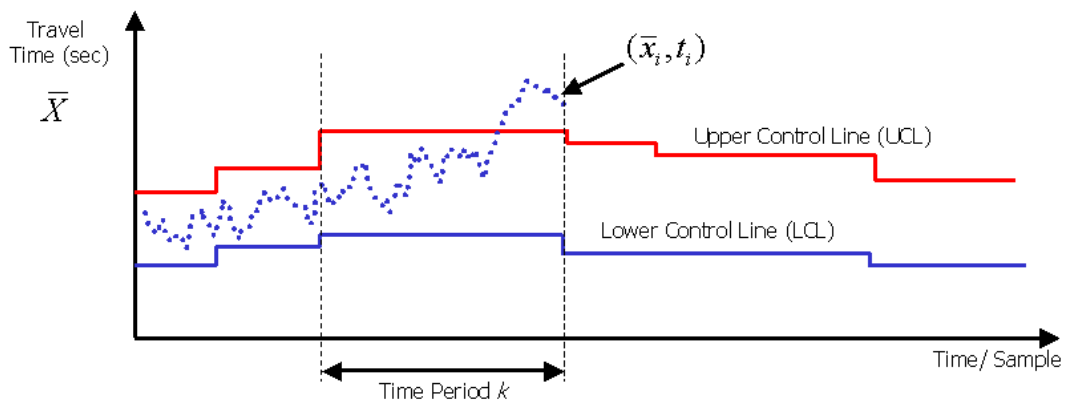


Figure 4.24: Travel time central tendency control chart ( $\bar{X}$  chart)

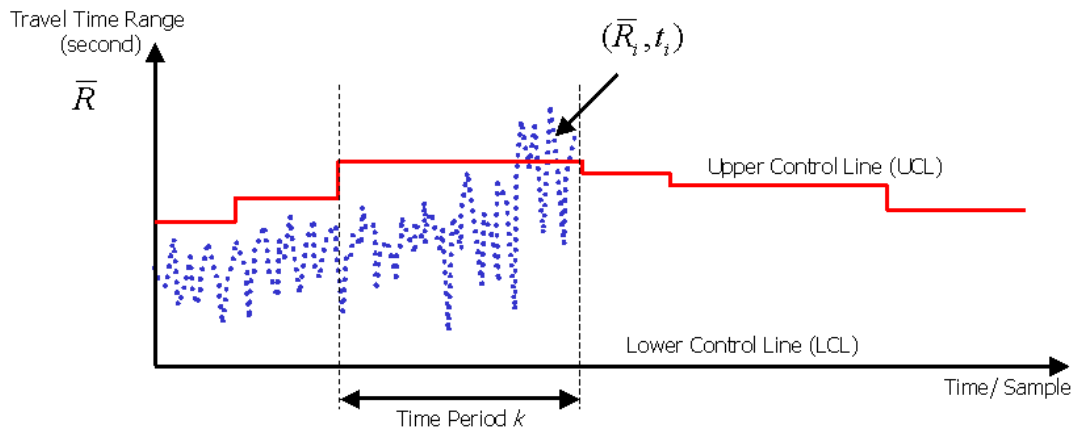


Figure 4.25: Travel time range control chart ( $\bar{R}$  chart)

## 4.5 Incident Detection Algorithm

Incidents are detected by combining the outcome of the travel time control chart and the acceleration noise observations for a particular street segment for a designated time period. A simplified process description of the detection algorithm and the overall system configuration with historical travel time integration is presented in Figure 4.26.

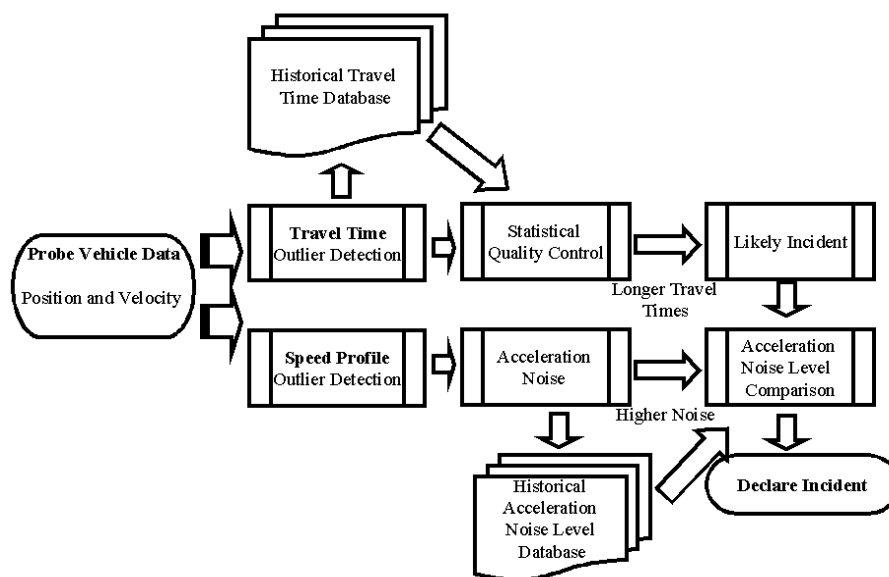


Figure 4.26: Incident detection algorithm

### 4.5.1 Combining Incident Detection Parameters

The incident detection algorithm combines the output states of the travel time monitoring algorithm and the acceleration noise comparison algorithm to declare traffic incidents. This involves three subroutines starting with the travel time variance control chart. Upon detecting an out-of-control state in the variance control, two other subroutines are activated. The first of these analyzes the acceleration noise characteristics of the probes that generated the out-of-control signal, and the second analyzes the central tendency control to detect features typical of incident induced congestion. An incident is declared if the out-of-control signatures of both the central tendency control and the variance control are confirmed by subsequent measurements and the acceleration noise analysis.

The two-variable parameter space used in incident detection and incident declaration process is illustrated in Figure 4.27.

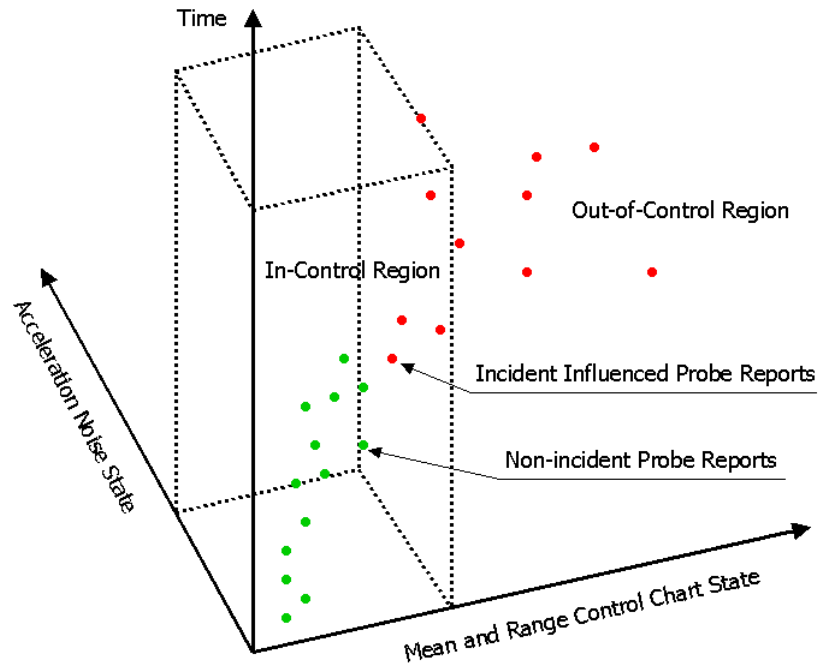


Figure 4.27: Two-variable incident detection parameter space

#### 4.5.2 Combining Indicators from Multiple Streets for Incident Detection

The propagation of incident impact through roadways as shockwaves is a well-known phenomena. However, these shockwaves are considerably altered by traffic signals, and no previous research knowledge exists on shockwave propagation in urban streets. Therefore, no direct correlation was assumed between incident indicator variables of adjacent streets in this research. However, the ability to detect downstream incidents using upstream acceleration noise and travel time variation is investigated using the simulation models. The success rate in detecting downstream incidents and its correlation with incident characteristics are discussed in the results and concluding remarks.

#### **4.6 Algorithm Performance Evaluation**

The performance of incident detection algorithms was evaluated using three performance indicators: Detection Rate (DR), Time to Detect (TTD) and the False Alarm Rate (FAR). DR is defined as the percentage of successfully detected incidents out of all incidents. TTD is expressed as the time lag between the time of the incident and the time of the incident detection. FAR is the percentage of times where incidents were indicated by the algorithm when there was no actual incident. An incident detection algorithm with a higher DR, lower FAR and a faster TTD is capable of functioning as a powerful tool for automated traffic monitoring.

The algorithm performance evaluation included analyzing TTD, FAR and DR parameters under different incident characteristics such as the lateral or the longitudinal location of the incident, extent of the capacity reduction and with varying degrees of GPS degradation. Further analysis was also conducted on the improvements gained by additional dedicated probe vehicles. An analysis is presented in Chapter 7.

## CHAPTER FIVE

### MICROSCOPIC TRAFFIC SIMULATION

Simulation tools are frequently used for planning and optimizing transportation network operations. Their applications range from design optimization prior to system implementation to real-time simulations for traffic control and management. Simulation models mimic real world systems using a collection of sub systems or elements and model their behaviour and interactions using both deterministic and stochastic models. Although a brief introduction is given to a wide array of simulation techniques used in traffic engineering, this chapter focuses on microscopic traffic simulation and its application for the performance evaluation of the incident detection algorithm developed in this thesis. More generalized discussions of simulation applications are given in Lieberman & Rathi (1992) and HCM2000 (2000). Traffic simulation models are categorized using a variety of modeling features. The classification criterion could be the level of detail in the modeling, whether the model is deterministic or stochastic or the modeling approach, such as time-based or event-based simulation. Some of the major simulation model classifications are outlined below.

#### **5.1 Overview of Traffic Simulation**

Traffic simulation models are categorized using a variety of modeling features. The classification, based on model features, is addressed in detail, and other classifications are outlined in brief.

##### **5.1.1 Simulation Model Classification Based on Modeling Details**

The level of modeling details is one of the key features of a simulation model. Simulation models that mimic high levels of microscopic detail in the real system are

known as microscopic simulation models. In a typical traffic microscopic simulation scenario, these models simulate all elements of the system at a high level of detail. For instance, individual vehicles can be simulated, and their interaction with other vehicles and the roadway infrastructure can be influenced through simulation parameters. Therefore, microscopic models can simulate very detailed information of the real-life system, and are very versatile for many applications. At the other end of simulation model classification, macroscopic simulators model systems at a lower level of detail. For instance, the macroscopic approach for simulating traffic flow in a group of connected streets would use models that describe aggregate traffic flow properties such as the volume and the average speed of traffic. Although microscopic simulation appear to be a better tool for simulation based analysis owing to the level of detail that can be controlled by the user, it also has a major disadvantage in that it demands a much more detailed replication of the properties and behaviours of the real life system. Therefore, microscopic models impose stringent validation and calibration needs, which are addressed in detail later on in this chapter.

### **5.1.2 Other Simulation Model Classes**

A number of other simulation model classifications are outlined in this section. Simulations models can be classified according to the types of the simulated variables. Stochastic simulation models use random variables for the simulation, whereas deterministic models are not subjected to randomness. For instance, in a typical scenario of selecting the aggressiveness of a driver, a stochastic model would randomly assign a value for the aggressiveness, whereas a deterministic simulator may have a model comprising of driver's age, experience, driving environment properties and other factors that derives an aggressiveness value, which produces an average value for each type of driver.

Simulation models are usually required to model system behaviour as a function of time. Depending on the type of time increment used, simulation models can be classified as

time-based or event-based models. Time-based simulation models increment time in fixed increments, and the state of all elements in the simulation are updated at each time step, whereas an event-based simulation model would update the simulated element states when specific events occur. For instance, an intersection simulation in an event-based simulation model would only update its state after a change in the signal states, while a time-based simulation model would update its state based on a fixed time step logic throughout the simulation. Although simulation models could be classified based on factors other than those discussed above, emphasis was given to classifications that are considered more relevant for the scope of this thesis. More detailed discussions are given in Lieberman & Rathi (1992) and HCM2000 (2000).

## **5.2 Requirements for Incident Detection Algorithm Performance Evaluation**

The performance evaluation of the traffic incident detection algorithm developed in this thesis required a test bed that fulfills several basic requirements. These requirements are addressed below.

### **5.2.1 Ability to Control Environmental Variables**

The traffic activity in a transportation system is constantly influenced by a host of factors. These factors may include recurring or non-recurring traffic demand fluctuations, traffic incidents, weather, time-of-day or time-of-week variations and the location of the area concerned. A field experiment-based approach for performance evaluation would involve identifying the contributions of all of these factors and isolating the contribution of the factors that are of interest in the exercise. For instance, travel time measurements taken in an area could be highly correlated with daily traffic demand variations and to a lesser extent, although significantly, with the driver population. For instance, drivers who are daily commuters and drivers who are new to the area, such as people driving in for recreational purposes, may observe slightly different travel times. Almost all of the

factors addressed above are beyond the control of the experiment and, the influence of those factors are either hard to model if not impossible.

### **5.2.2 Traffic Incidents and Incident Characteristics**

Traffic incidents are clearly beyond the control of the experimental process. However, it is extremely important to investigate the response of the detection algorithm with varying incident characteristics such as the type of incident, extent of the roadway capacity reduction and lateral and longitudinal location of the incident. Therefore, field experimentation would involve extended periods of data collection; however, this would still not guarantee that certain categories or characteristics of traffic incidents would be observed.

### **5.2.3 Repeatability**

Incident detection algorithm performance evaluation requires repeated experiments, especially to reflect the stochastic nature of traffic flow behaviour. Considering the incident features that need to be correlated with algorithm response and the constantly varying influence factors that are of no importance to the experiment, repeatability would require extended periods of time that may be beyond reach of a study of this nature.

### **5.2.4 Data Collection Requirements and Limitations**

Data collection requirements for a field experiment can be broadly classified into two categories. Firstly, the algorithm itself requires travel time data from transit vehicles as well as dedicated vehicles on a regular basis. This requires installing data collection equipment in a large number of vehicles and leaving them for long periods of time, which was not feasible during this research due to the limitation of the number of sensors available and the level of effort required. Once the data is collected, it needs to be

processed and formatted for the algorithm, an enormous task especially due to the amount of data gathered by vehicle tracking systems and the lack of automated systems for such tasks. Furthermore, based on the experience gained during the limited surveys conducted with Calgary Transit, maintaining data collection equipment in transit vehicles takes a considerable amount of time and disrupts their normal operation, which is not desirable for extended periods of time.

Secondly, a considerable amount of infrastructure-based traffic sensor data is required for gathering basic traffic activity information such as screenline counts, lane usage data, vehicle classification information and traffic control system data. In the context of the test area selected for this research, downtown and suburban Calgary, the infrastructure-based traffic-monitoring network was extremely limited. As depicted in Figure 5.1, the monitoring system was limited to fourteen inductive loop detectors sparsely distributed and only capable of providing screenline counts. Only a few of them were able to gather vehicle speed information and vehicle classification data.

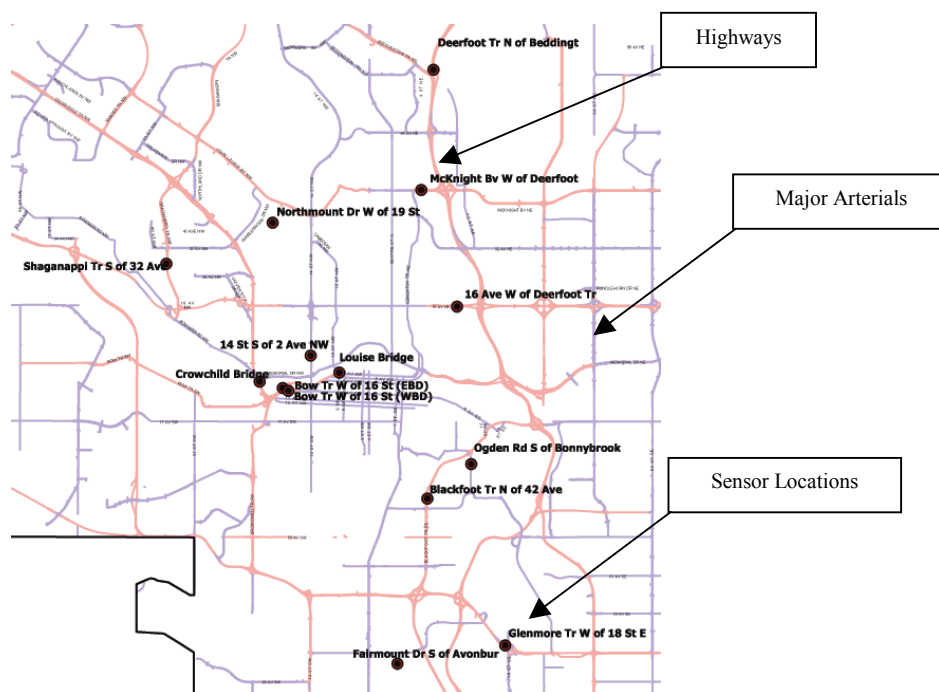


Figure 5.1: Existing traffic sensor network in Calgary

### **5.2.5 Complications Associated with Data Collection**

The above discussion did not include the additional factor of sensor errors and possible human error during data collection and reporting. Even if the sensor errors are assumed to be of less importance and could be modeled easily, incident reporting, which is entirely dependent on human intervention, is liable to introduce biased or even false information. However, incident reporting is of extreme importance as incident characteristics such as the exact time of occurrence, duration, location and the extent of the impact are very important variables for correlating with incident detection algorithm response. Based on previous traffic incident reporting studies, it was noted that incident information is often biased and data from multiple sources do show significant differences (Cambridge Sys Inc et al., 1998).

### **5.3 Microscopic Traffic Simulation for Algorithm Performance Evaluation**

The data requirements addressed above, together with the ability to control environmental variables and repeatability requirements, strongly suggest that a field experiment-based algorithm performance evaluation is beyond the scope of this thesis. Furthermore, microscopic traffic simulation was considered an excellent alternative to a field experiment, as it offers almost all the requirements addressed in Section 5.2. Hence, it was decided to use a test bed built using a microscopic traffic simulator for algorithm development and testing.

Some fundamental aspects of microscopic traffic simulations are addressed here, forming the background for the objectives of the simulation testing and the actual simulation experiments discussed in Section 5.6 and Chapter 6 respectively. Microscopic traffic simulation, as outlined above, models individual elements of the network such as vehicles, street segments, intersections, and traffic controlling devices along with their interaction with each other at a high level of detail. Although it may appear random in real life, traffic activity can be fairly well modeled by a collection of simple rules based

on car-following, gap acceptance and vehicle kinematic theory. However, the closeness of the simulated system to the real-life system always dependent on a variety of factors, with the simulation model capabilities being one of them.

### 5.3.1 Microsimulator Components

Although the implementation may differ from one simulator to another, traffic microsimulators share a set of basic models that govern the behaviour of individual elements in a simulation. These models provide the basic operating logics for simulating the behaviour of system components. Since this thesis addresses microscopic simulation mode calibration that requires the understanding of principles of simulator operation, and for the completeness of this thesis, two simulation model components that govern the lateral and longitudinal movement of vehicles in a traffic microsimulator are briefly discussed in this section.

#### 5.3.1.1 Car-Following Models

The car-following model is one of the fundamental routines in a microscopic traffic simulator. It governs the longitudinal speed and inter-vehicle gap of all vehicles in the simulation. Under free flow conditions, a vehicle could travel at its desired speed, limited only by the speed restrictions imposed by the roadway. However, free flow conditions rarely exist and a vehicle's speed choice is often influenced by the interference from other vehicles, especially the vehicle immediately in front. More specifically, the distance between the host vehicle and the vehicle in front, their relative speed and the speed of the host vehicle are governing factors for controlling the acceleration response of the host vehicle. For instance, the car-following model suggested by Edie (1961) is depicted below:

$$\ddot{x}_{n+1}(t+T) = \frac{\lambda \dot{x}_{n+1}(t+T)}{[x_n(t) - x_{n+1}(t)]^n} [\dot{x}_n(t) - \dot{x}_{n+1}(t)] \quad (5.1)$$

where

$\ddot{x}_{n+1}(t+T)$	acceleration response of the host vehicle at $(t+T)$
$\dot{x}_{n+1}(t+T)$	host vehicle speed at $(t+T)$
$T$	response time (driver perception-reaction time)
$[\dot{x}_n(t) - \dot{x}_{n+1}(t)]$	relative speed between the leader and the follower
$[x_n(t) - x_{n+1}(t)]$	relative distance between the leader and the follower
$\lambda$	modeling parameter.

Equation (5.1) can be rewritten in a more generalized form as:

$$\ddot{x}_{n+1}(t+T) = f((x_{n+1} - x_n), \dot{x}_{n+1}, \dot{x}_n, \ddot{x}_n, T, P) \quad (5.2)$$

where

$P$  modeling parameter.

### 5.3.1.2 Lane Changing Models

Lane changing models govern the lane selection for simulated vehicles. Apart from lane changes that are required to make certain turns, vehicles choose their lane in a multilane roadway based on a model equivalent to the one given below, see Kuhne & Michalopoulos (1992).

$$Q_i(x, t) = \alpha [(k_j - k_i) - (k_{j_0} - k_{i_0})] \quad (5.3)$$

where

$Q_i(x, t)$	lane changing rate in lane $i$
$\alpha$	sensitivity coefficient for intensity of interaction
$(k_j - k_i)$	vehicle density difference between lanes $i$ and $j$
$(k_{j_0} - k_{i_0})$	equilibrium vehicle density difference between lanes $i$ and $j$ .

### 5.3.2 PARAMICS Microsimulator

The traffic microsimulator used in this research, namely PARAMICS (PARAllel MICroscopic Traffic Simulator) had its origins in the early 1990's. It was initially developed by SIAS Ltd in the UK and later further developed at the Edinburgh Parallel Computing Center (EPCC). Druitt & Laird (1999), Druitt (1998a) and Druitt (1998b) have given a detailed insight into the historical development of the PARAMICS traffic microsimulator. Based on the classifications discussed in Section 5.1, PARAMICS is a time-based simulator with both stochastic and deterministic components, some of which will be addressed later in this thesis.

### 5.4 Calibration and Validation of Microscopic Traffic Models

The calibration and validation of a simulation model are two of the most important steps in a simulation process, regardless of the type of simulation model. Both of these processes essentially ensure that the simulation model is a close enough abstraction of the real-world system. The Highway Capacity Manual defines calibration and validation as the process by which the analyst confirms that the model does in fact provide a reasonable approximation of reality (HCM2000, 2000). Although calibration and validation are often used interchangeably, calibration involves evaluating or tuning model parameters to reflect the best agreement with field observed conditions, while validation refers to the process by which key statistical outputs of the model are compared with actual field observed conditions to ensure the correctness of the model. The validation and calibration processes can be written as a mathematical model comparing the simulated outcome with field observations as depicted below:

$$P[|\text{Simulation Output} - \text{Field Observations}| < \delta] > \alpha \quad (5.4)$$

where

- $\delta$       tolerable model error
- $\alpha$       confidence limit for the simulation model.

### 5.4.1 Calibration Parameters

The calibration parameters available for a particular model depend on a variety of factors ranging from the type of the simulation model to the objectives of the simulation. For instance, a microscopic model would require the calibration of driver aggression and awareness, while a macroscopic model would require the calibration of high-level parameters such as free flow speed or the lost time at a signalized intersection. The calibration parameters available with the PARAMICS simulator and the selection of parameters for model calibration are discussed later in Chapter 6.

### 5.4.2 Calibration and Validation Criteria

A calibration and validation criterion is often implemented as an evaluation function similar to the model given in Equation (5.4). The following modified form of Equation (5.4) illustrates a typical evaluation function:

$$|\text{Simulation Output} - \text{Field Observations}| < \delta \quad (5.5)$$

where  $\delta$  is the tolerable model error.

The selection of the proper evaluation function for a model calibration and validation process is crucial, and several practical and theoretical issues need to be addressed in the selection process. First and foremost, the function should be relevant for the purpose of the modeling exercise. For instance, as discussed later in this thesis, travel time was selected as the evaluation function for calibrating and validating the simulation model used in this thesis, as simulated travel time measurements play a crucial role in the incident detection algorithm performance analysis. In addition, the evaluation function variables must be directly measurable or derivatives of the measurable values from both simulations and field observations. See Sacks et al. (2002) for a further discussion on statistical issues on simulation model calibration and validation.

### **5.4.3 Uncertainty of Inputs and Model Variability**

Simulation input variables can be classified into two categories based on their statistical nature. Firstly, some of the simulation model inputs have fully known behaviour such as states of a traffic signal, completely defined by signal timing values and control logics in case of an actuated controlled signal. Secondly, some inputs have statistical properties that cannot be fully captured by a field survey such as the traffic flow or turning movement counts taken at an intersection, which may well not be identical during the same time periods over different days. The second type of inputs requires statistical treatment that agrees with the stochastic nature of the real-life system. However, more often than not, available resources limit the extent of input variable analysis in a simulation exercise. Although not addressed in detail in this thesis for the same reason, the reader is referred to Bayarri et al. (2003) for a discussion on the treatment of stochastic properties of input variables.

## **5.5 Interpretation of Microsimulator Results**

The analysis of simulation results can be regarded as the most important task in a simulation model-based experiment. Although not often addressed, an outcome of a simulation experiment is a result of a statistical experiment, and is not a straightforward solution. Furthermore, simulation outcomes could be highly correlated and non-stationary. Therefore, they violate the basic assumptions in classical statistical techniques, the assumption of independent and identically distributed observations. Thus, special statistical treatments that are beyond conventional statistical techniques are required for simulation result analysis (Lieberman & Rathi, 1992). The simulation results analysis in this thesis focuses on establishing point estimates of incident detection algorithm performance and their confidence intervals and compares performance between different scenarios to minimize the impact from such statistical issues. Furthermore, multiple simulations were combined for each case with independent simulations.

## **5.6 Objectives of Incident Detection Algorithm Performance Evaluation**

The use of the PARAMICS microsimulator for incident detection algorithm performance evaluation provides a multitude of options and excellent capability to control environmental variables and incident repeatability. The objectives of the simulation-based algorithm performance evaluation are summarized below.

### **5.6.1 Validation of Concept Developed in the Thesis**

The primary objective of the simulation-based analysis was to confirm the premise that transit vehicle tracking data can be used as an indicator for traffic incident detection. This was achieved in several stages of the analysis. As the first step, transit vehicle travel time modification algorithms were validated using field observations.

### **5.6.2 Analysis of Statistical Properties of Street Segment Travel Time**

The second objective was to verify the street segment travel time analysis techniques proposed in Section 4.3.3 with simulated transit and dedicated probe vehicle travel times. This included the analysis of statistical distribution of street segment travel times, correlation analysis between travel time and vehicle arrival time for street segments with traffic signals, and establishing threshold values for control chart development.

### **5.6.3 Incident Detection Capability of Individual Incident Detection Parameters**

The performance of the algorithm is dependent on the responsiveness of the two incident detection parameters to traffic flow variations caused by incidents. Hence, the third objective of the analysis was to investigate the responsiveness of travel time variation and acceleration noise levels to traffic incident induced congestion, taken individually and under perfect GPS reception conditions.

#### **5.6.4 Algorithm Development**

As an extension of the third objective, several algorithms were investigated with the objective of developing a robust incident detection.

#### **5.6.5 Traffic Incident Scenarios**

The simulation testing provided total control over the incident characteristics and precise monitoring of the incident impact with simulated traffic sensors. The simulation objectives also included testing a range of scenarios with varying incident characteristics such as the incident location, intensity of the incident and incident duration and to correlate the incident detection system response with incident characteristics.

#### **5.6.6 Performance Improvements with Dedicated Probe Vehicles**

Based on the baseline performance levels established, further improvement that can be made by using a small proportion of dedicated probe vehicles was also investigated. The objective was to analyze the improvements in terms of DR, TTD and FAR parameters compared to transit probe only case and the robustness added to above parameters under degrading GPS performance.

#### **5.6.7 Analysis of Performance Degradation with GPS Errors**

Another critical objective of the simulation-based testing was to conduct an analysis of incident detection capability degradation with different levels of GPS errors. Although PARAMICS does not allow the modeling of measurement errors, different levels of errors were introduced to travel time and vehicle speed data. GPS velocity errors were introduced to acceleration noise-based analysis while GPS position errors translated into

time measurement errors were added for travel time measurements. The magnitudes of these errors were controlled to reflect typical GPS error characteristics.

## CHAPTER SIX

### FIELD TESTING AND SIMULATIONS

This research involved several field data collections. A major part of these involved collecting vehicle tracking data from transit and dedicated probe vehicles. Further field tests were conducted for transit stop zone surveying and for gathering data for simulation model building and calibration. The rest of the simulation model input data was provided by the City of Calgary.

#### **6.1 Transit and Dedicated Probe Vehicle Surveys**

These surveys had two objectives. The first objective was to analyze the vehicle characteristic differences between transit vehicles and other more dominant vehicle types on the road and the contribution of these factors to travel time differences. The ultimate objective was to minimize the influence of vehicle characteristic differences on subsequent transit vehicle tracking data applications developed in this thesis. The field data was also used in calibrating the travel time modification algorithms and subsequent analysis of correlation with congestion and travel times of non-transit vehicles. Travel time data modifications were mainly conducted outside downtown primarily to avoid contamination from GPS error sources, which are addressed separately in the second objective of the field data collection.

The second objective was to gather tracking data for vehicle positioning algorithm development and testing. This required data from urban canyon areas and downtown Calgary provided a perfect setting for such a data collection. Although no exact true vehicle trajectories were available to compare with HSGPS data collected in these surveys, street maps and transit route databases were used as a reference for later analysis.

### 6.1.1 Field Survey Area

The field survey had two objectives, which were outlined above. This required vehicle tracking data in downtown Calgary and its suburban areas. Therefore, two transit routes that run through downtown Calgary and surrounding suburban areas were selected for the survey. These two routes are shown in Figure 6.1. Both routes start from the northern end of the city and had about a 5 km stretch of predominantly open sky areas before entering downtown. Both routes have around 1 to 2 km distances through downtown with varying degrees of urban canyon conditions along the routes. These two routes shared approximately 1 km of the downtown route as shown by Figure 6.1. One route traveled to the southern end of the city (route number 3), while the other had its destination in the western end of the city (route number 2). Transit vehicles traveled in continuous loops in these routes totaling around six loops per day per vehicle, while their crew was changed approximately two to three times a day.

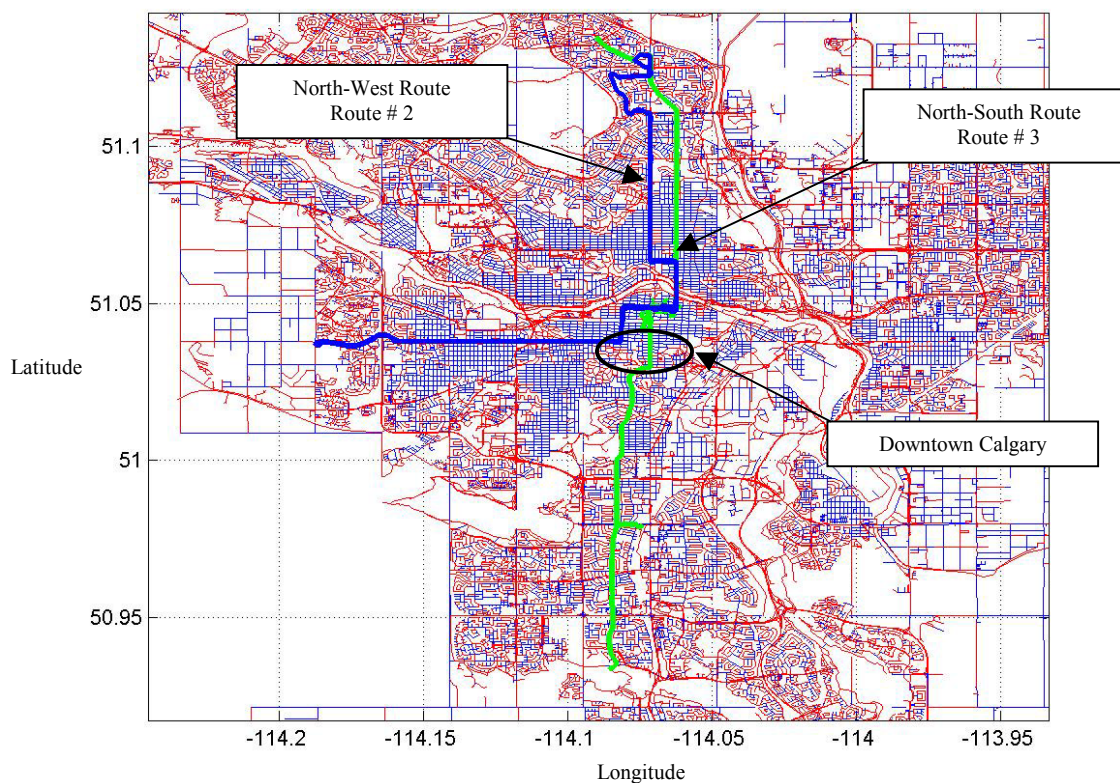


Figure 6.1: Transit routes in vehicle tracking data collection

### 6.1.2 Test Vehicles and Test Setup

Three vehicle types were used for the field data collection. These included five Calgary Transit vehicles similar to the one shown in Figure 6.2a, a Dodge Caravan belonging to the Department of Geomatics Engineering, and a 1997 Hyundai Elantra. These vehicles are shown in Figure 6.2.

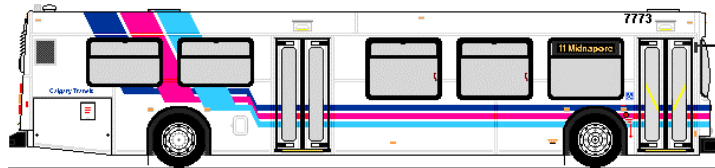


Figure 6.2(a): Calgary Transit test vehicle



Figure 6.2(b): Dedicated test vehicles: Hyundai Elantra & Dodge Caravan

All the test vehicles were equipped with a basic GPS receiver and data logger configuration. This configuration consisted of a SiRF HSGPS receiver, patch GPS antenna, laptop computer for data logging and a power supply unit that converted the vehicle's power supply to the receivers. The SiRF HSGPS receiver is capable of tracking L1 GPS signals and was the main GPS receiver used in this research. Three of the vehicles had additional NovAtel DL4 GPS receivers, which are geodetic grade receivers capable of tracking both L1 and L2 GPS signals. The configuration with both GPS

receivers is shown in Figure 6.3. For the single receiver configuration, only the SiRF HSGPS receiver was included, and the receiver output was directly made to the data logger without an interfacing unit. As the SiRF GPS receiver was the primary source for data collection, the single receiver configuration was considered Setup 1 whereas the two-receiver configuration was considered Setup 2.

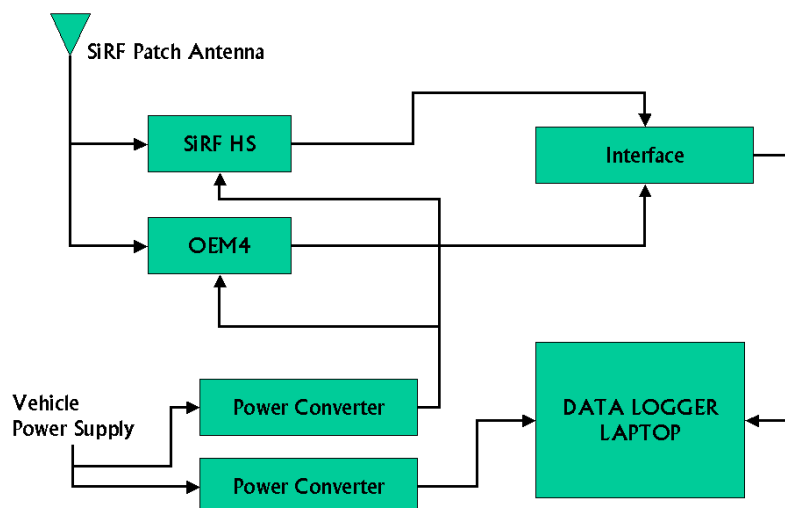
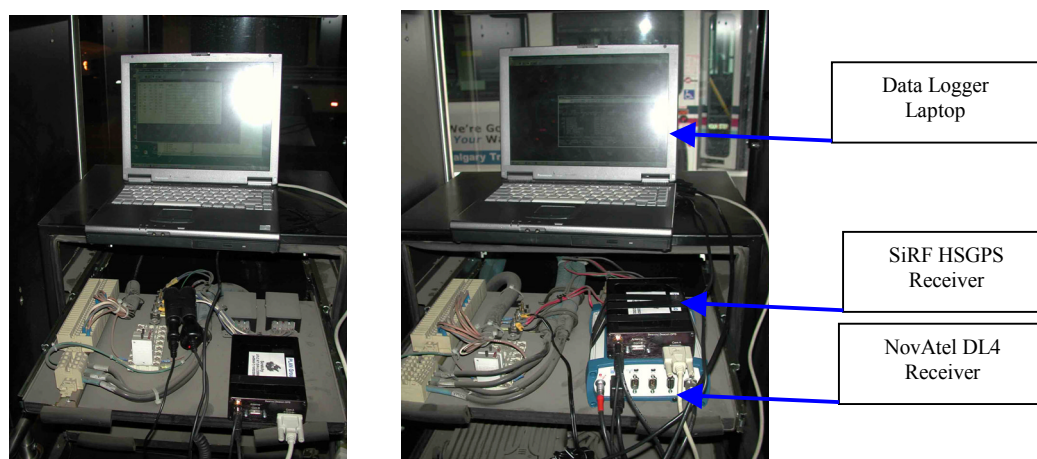


Figure 6.3: GPS receiver/ data logger configuration (Setup 2)

#### 6.1.2.1 Transit Test Vehicles

The transit vehicle data collection was conducted over two days. The first phase of the data collection was conducted with a single transit vehicle and the dedicated probe vehicle Dodge Caravan, referred as the dedicated probe number 1 throughout this thesis. The transit vehicle was restricted to route number 3 throughout the data collection. The second phase of the data collection involved a total of four Calgary Transit vehicles similar to the one used in the first phase of the data collection. These transit vehicles had their own automated passenger counting systems and GPS tracking systems, although they were not considered for the data collection of this research. During the data collection, the GPS receiver/ data logger setup was installed in a protected housing behind the operator as shown in Figure 6.4a. The equipment setup that was included is shown in Figure 6.4b.



### 6.1.2.2 Dedicated Test Vehicles

Both dedicated probe vehicles had Setup 2 with a SiRF HSGPS receiver and a NovAtel OEM4 receiver. The setup in dedicated probe vehicle 1 is shown in Figure 6.5.

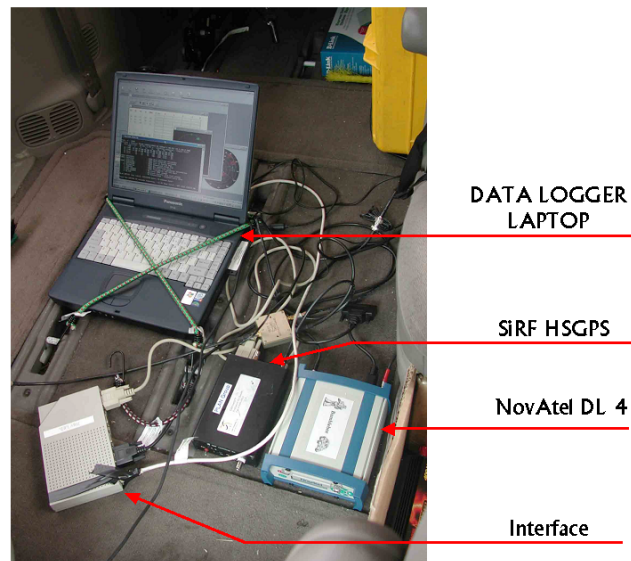


Figure 6.5: Instrument setup for dedicated vehicles (Setup 2)

### 6.1.3 Data Collection Methodology

The data collection equipment in transit vehicles were installed prior to their day operation and were set up to automatically log data for a period of 12 hours on a continuous basis. There was no access available to these setups until the end of the day. The GPS receivers in dedicated vehicles were manually controlled to log data only during the data collection trips.

During the data collection, measuring dedicated and transit vehicle travel times under similar conditions was considered critical to minimize the impact of events and traffic flow fluctuations that could mask the possible correlation of the two measurements. Hence, dedicated test vehicle trips were planned to coincide with transit vehicle trips. Dedicated vehicle drivers were instructed to start their route sufficiently after the transit vehicle and pass it approximately halfway through the trip. Although this does not ensure identical driving conditions due to traffic signals, pedestrian activity and other factors that change in a faster timescale, it minimizes the influence of varying traffic

conditions over relatively longer time durations. Travel time measurement pairs taken in such coincident trips were taken for modification algorithm analysis.

#### 6.1.4 Data Collection Summary

This section contains a summary of all the data collected from transit vehicles and the dedicated probe vehicles. SiRF HSGPS receivers were configured to log vehicle position and velocity data at a 1 Hz rate. In addition to collecting receiver output data, its GPS measurements were also logged for subsequent analysis. These additional data included pseudorange measurements and Doppler measurements at a 1 Hz rate. The NovAtel DL4 receivers were used for two purposes, namely to assess the difference in performance between conventional GPS and HSGPS and to precisely position the transit stops using DL4 data, which is much more accurate in open sky conditions. Table 6.1 provides a summary of all data sets collected during the two phases of the field data collection. In the number of data collection trips, transit and dedicated test vehicle coincident trips are also indicated.

Table 6.1: Data collection summary

	DEDICATED PROBES		TRANSIT PROBES	
PHASE 1				
Number of Vehicles Used	1		1	
Route	3		3	
Northbound Trips	5		5 (4)	
Southbound Trips	5		5 (3)	
Equipment Setup	Setup 1		Setup 1	
Duration	8:00 am – 6:00 pm		6:00 am – 9:00 pm	
PHASE 2				
Number of Vehicles Used	1	1	2	2
Route	2	3	2	3
Northbound Trips	6	5	6 (3)	6 (3)
Southbound Trips	7	6	6 (4)	7 (3)
Equipment Setup	Setup 2	Setup 2	Setup 1 & 2	Setup 1& 2
Duration	8:00 am – 6:00 pm		5:00 am – 10:00 pm	

## **6.2 Locating Designated Transit Stops**

The accurate estimation of dwelling time spent by transit vehicles at designated transit stops and the time lost approaching and departing stops is essential in comparing transit and non-transit travel times. Therefore, the precise location of transit stops along the selected transit routes was essential in estimating time spent at stops and any associated time loss. Although the City of Calgary has a digital street map and the transit routes can be defined as a collection of streets on the digital map, no database exists on the location of transit stops. Therefore, it became necessary to conduct a separate survey to locate all transit stop locations along routes 2 and 3, routes selected for the travel time data collection. However, some of the NovAtel DL4 data collected during the travel time data collection was also used to supplement the stop location data.

### **6.2.1 Equipment Setup and Methodology**

The stop location survey was conducted with differential GPS corrections to achieve improved accuracy. Therefore, the setup included a base station receiver in addition to the rover receiver that was installed in a vehicle. The base station was setup in the Navigation Laboratory maintained by the PLAN (Position, Location and Navigation) research group in the University of Calgary CCIT (Calgary Centre for Innovative Technology) building. The base station setup included a NovAtel DL4 GPS receiver and was logging both GPS L1 and L2 data during the test period. Another NovAtel DL4 receiver was used as the rover and was mounted on the test vehicle (Dodge Caravan). For accuracy comparison purposes, a SiRF HSGPS receiver was also included in the rover receiver configuration, thus the making the rover vehicle setup equivalent to Setup 2 shown in Figure 6.5.

For surveying the exact location of the stops, two practical considerations were taken into account. Firstly, transit vehicles stop in a region around a marked stop location rather

than at a single marked location. Therefore, it was required to mark a region rather than a point. Secondly, it was practically impossible to stop at each of the stops as the total number of stops in the area surveyed was over one hundred. As a solution to these requirements, the DL4 receiver's time mark utility was used to time mark multiple positions within the transit stop zone. As a standard, three points (one at the beginning of the stop zone, a second at the stop marker and the third at the end of the zone) were marked as the vehicle drove by the transit stops. An operator manually marked the time marks by pressing a device that sent a trigger to the GPS receiver's time mark function. These time marks and their corresponding positions were later retrieved in the post-mission data processing.

### **6.2.2 GPS Data Processing**

A carrier smoothed, differentially corrected pseudorange-positioning method was used in the kinematic mode for locating the transit stops. The post-mission data processing was done using the C<sup>3</sup>NAVIG<sup>2</sup>™ (Combined Code and Carrier for NAVigation with GPS and GLONASS) software developed by the University of Calgary PLAN research group. This software first generates a correction file using carrier smoothed GPS pseudorange measurements made at the base station and applies the corrections to the rover data processed using the same carrier phase smoothed pseudorange technique (Petovello et al., 2000). Position accuracy using the above differential software and NovAtel receivers is about 2-3 m (2DRMS).

### **6.2.3 Transit Stop Location**

The position estimates corresponding to manual time marks were retrieved from the carrier smoothed, differentially corrected GPS vehicle trajectory generated by post-mission processing. Using an automated processing algorithm, all of these markers were converted into transit stop zones, assuming the first and the last markers for each stop as

the beginning and the end of the stop zone. The transit stop zones identified for routes 2 and 3 in the northern part of the city are shown in Figure 6.6.

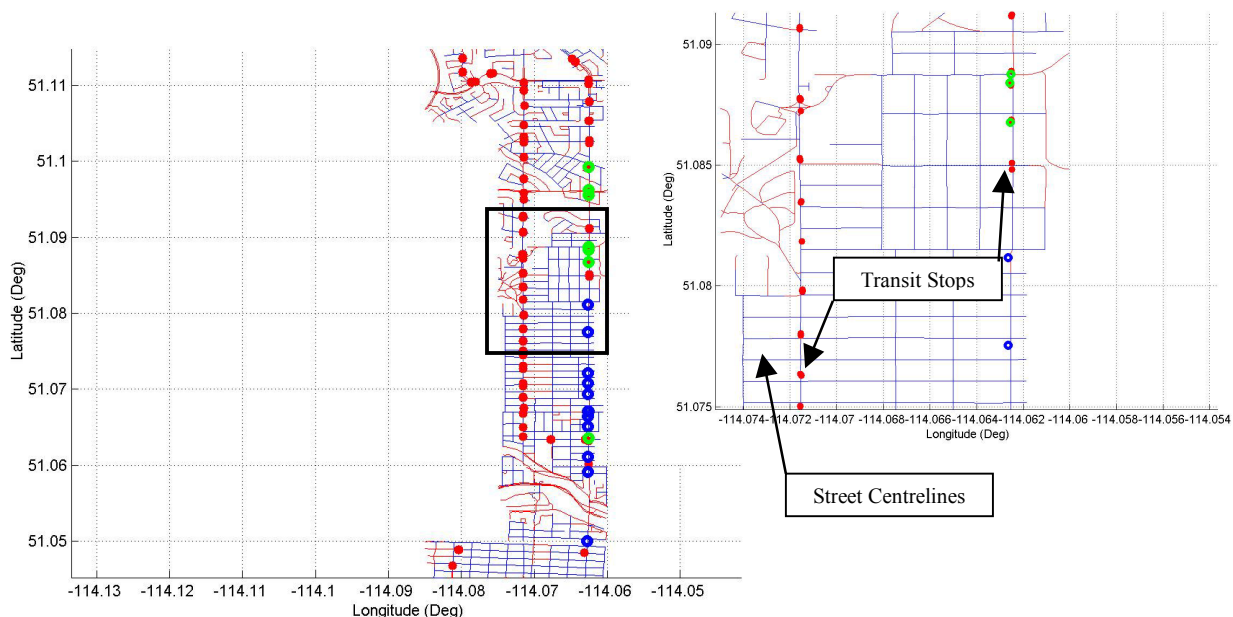


Figure 6.6: Transit stop zones for Routes 2 and 3 (Northern section only)

### 6.3 Data Analysis

This section summarizes the results of the data analysis and outlines the conclusions reached. In addition, the applicability of models developed using this data and the data itself in other parts of the thesis is also addressed.

The primary purpose of the data collection and analysis was to identify the differences in travel time observed by transit vehicles and other vehicles in different parts of the roadway network at approximately the same time and under similar traffic conditions. The differences were attributed to two causes, namely transit vehicle driving patterns with stops and their acceleration/ deceleration lost time approaching and departing transit stops. The latter was considered important, as the lost time was significant for travel time estimation. Based on these empirical results, transit travel time modification algorithms

were developed for transit tracking data modifications. In order to prove the hypothesis that modified transit vehicle travel times do have a correlation with the travel times of other vehicles, and therefore with recurrent or non-recurrent congestion, modified transit travel times had to be compared with corresponding travel times obtained from non-transit vehicles. Although no effort was made to directly compare modified transit travel times with travel times from non-transit vehicles, identifying the correlation between them and calibrating the transit tracking data modification algorithms for travel time estimation were the main goals.

### **6.3.1 Acceleration / Deceleration Characteristic Curves**

Acceleration and deceleration characteristics of transit vehicles vary considerably between transit vehicles and other dominant vehicle types in normal traffic flow. This was addressed in greater depth in Chapter 4. Section 4.2.2 also discusses the Acceleration-Speed curve estimation process for different vehicle types. Data collected in this survey was used to develop the Acceleration-Speed models presented in the above section. Furthermore, these characteristic curves were used for calibrating the PARAMICS simulation model as described in Chapter 5.

### **6.3.2 Calibrating the Transit Travel Time Modification Algorithm**

The travel time modification algorithm development was discussed in detail in Chapter 4. The modification algorithm estimates the dwelling times at each of the transit stop zones using vehicle-tracking data and the locations of transit stop zones established by one of the surveys outlined above. In addition, the modifications include a lost time correction for each transit stop to account for the time lost during the approach to the stop zone and departure. The estimation technique used for this lost time estimation and the underlying assumptions were outlined in Chapter 4. This section presents the results of travel time modification algorithm calibration.

In order to illustrate the travel time modification model calibration, travel time data from three sections of transit routes were selected. These three sections are shown in Figure 6.7. In order to minimize the influence of GPS errors on the calibration process, these sections were selected from areas with open sky conditions for GPS. Of the three sections analyzed, both routes shared section A whereas sections B and C were unique to routes 3 and 2 respectively.

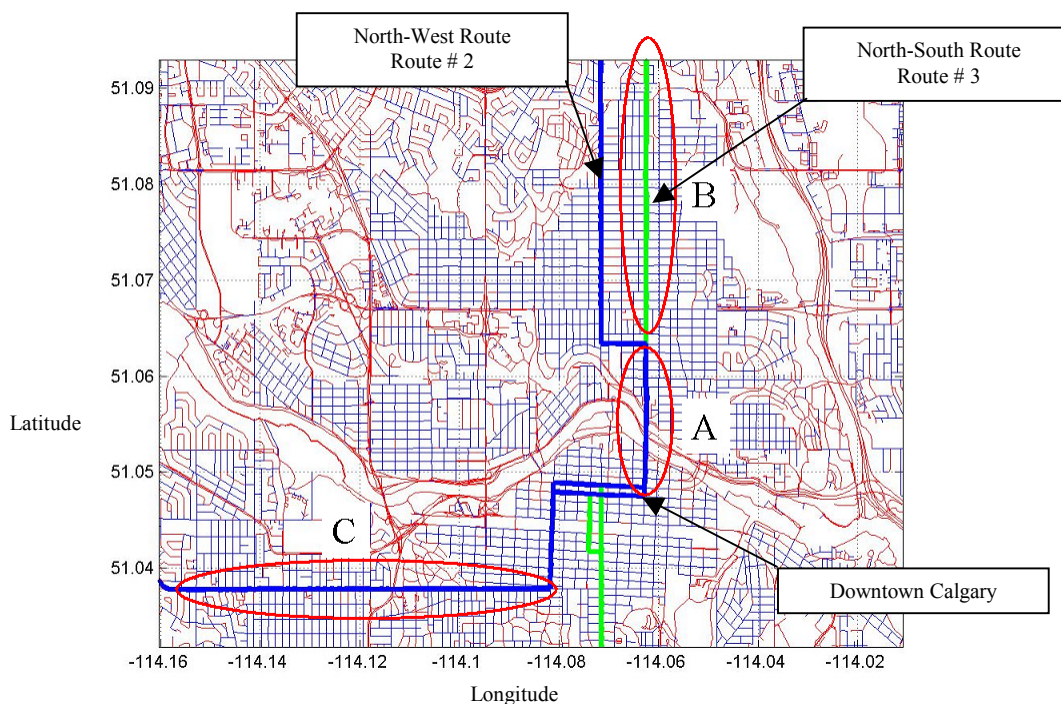


Figure 6.7: Transit route sections selected for travel time analysis

Travel times measured by transit and dedicated test vehicles in sections A, B and C in coincident trips were selected for further analysis in this section. These travel time measurements are shown in Figure 6.8 according to the segment exit time of each vehicle. This figure does not show any correlation of travel time with time-of-day or correlation between transit and dedicated test vehicle travel times. Furthermore, on average, transit vehicle travel times were around twice as long as the coincident dedicated vehicle travel time. The same data set was modified with the calibrated transit travel time modification algorithm, and the result is shown in Figure 6.9. Figure 6.9 shows a considerable reduction of transit vehicle travel times. Their correlation with

corresponding dedicated test vehicle travel times is illustrated with Figure 6.10. Figure 6.10 shows a very high degree of correlation between modified transit vehicle travel times and dedicated test vehicle travel times in all sections selected for the analysis.

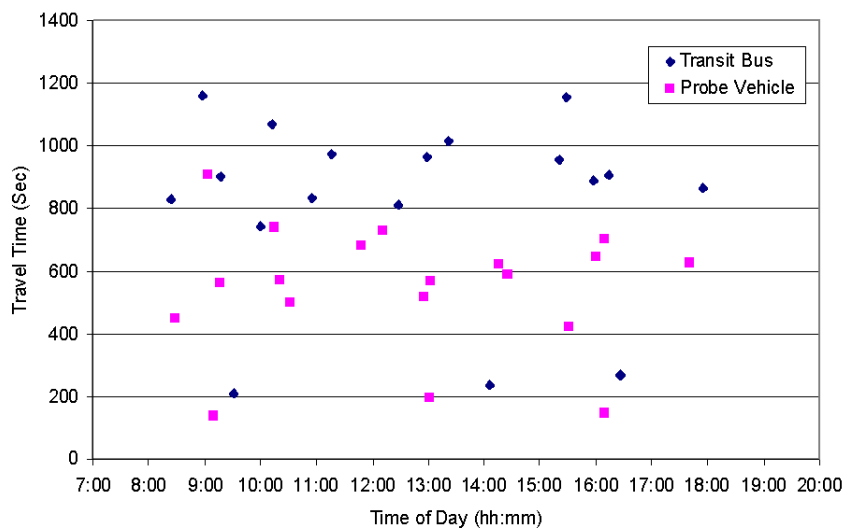


Figure 6.8: Transit and dedicated vehicle travel times (coincident trips)

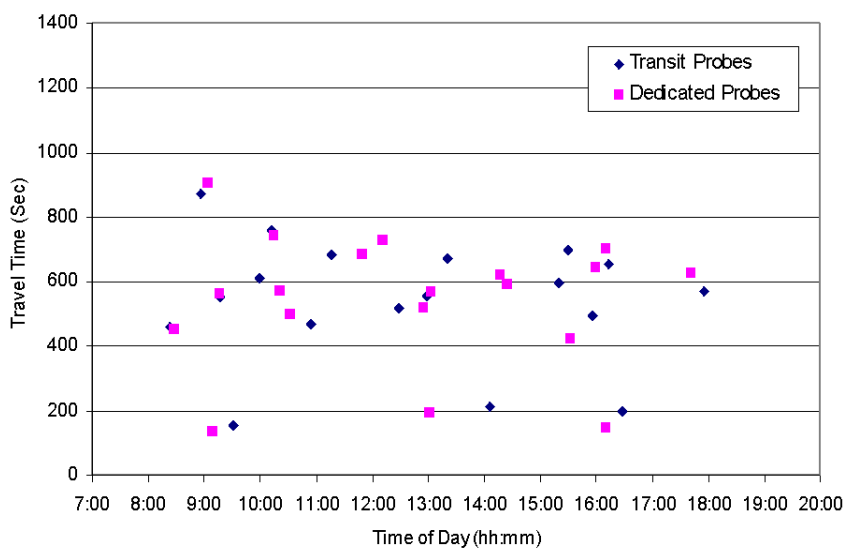


Figure 6.9: Modified transit and dedicated vehicle travel times (coincident trips)

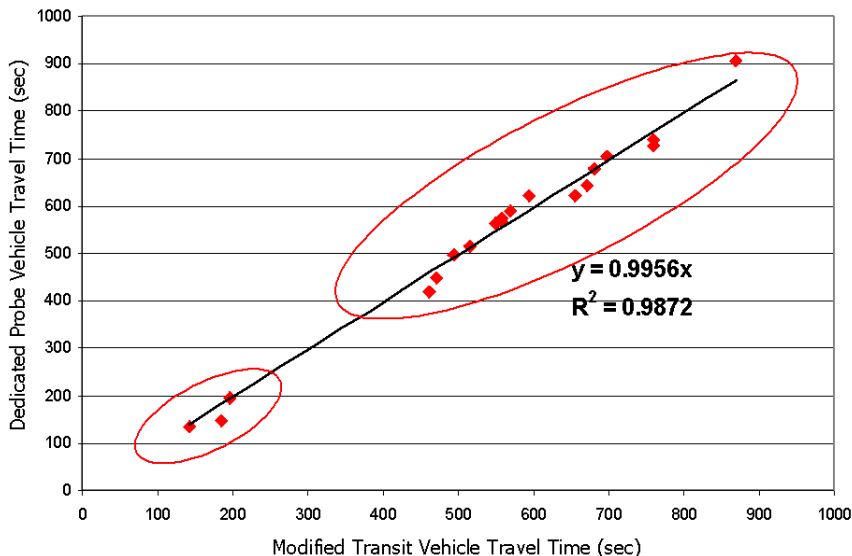


Figure 6.10: Correlation of Modified transit and dedicated vehicle travel times

#### 6.4 Data Collection for Simulation Model building, Calibration and Validation

The data required for simulation model building, calibration and validation accounted for the vast majority of the data collected for this research. This included a variety of data including roadway geometry, traffic control, and traffic activity data and calibration and validation data. These data requirements are described in detail below.

##### 6.4.1 Data for Simulation Model Building

The area chosen for the microsimulation model encompasses a major traffic corridor in and out of downtown Calgary and a part of the downtown core as illustrated in Figure 6.11. This included over 30 street segments. However, the actual traffic incident simulation and their impact analysis were performed in a subset of street segments in downtown area. A larger area was modeled to integrate other parts of this research into an area-wide analysis and to facilitate the inclusion of additional field data into the model validation and calibration process. All adjacent parts of the street network were modeled

with traffic origin-destination zones. Figure 6.11 also depicts the street sections, defined as validation zones, used for model validation by means of comparing field observed and simulated travel times. The validation results are outlined later in the chapter.

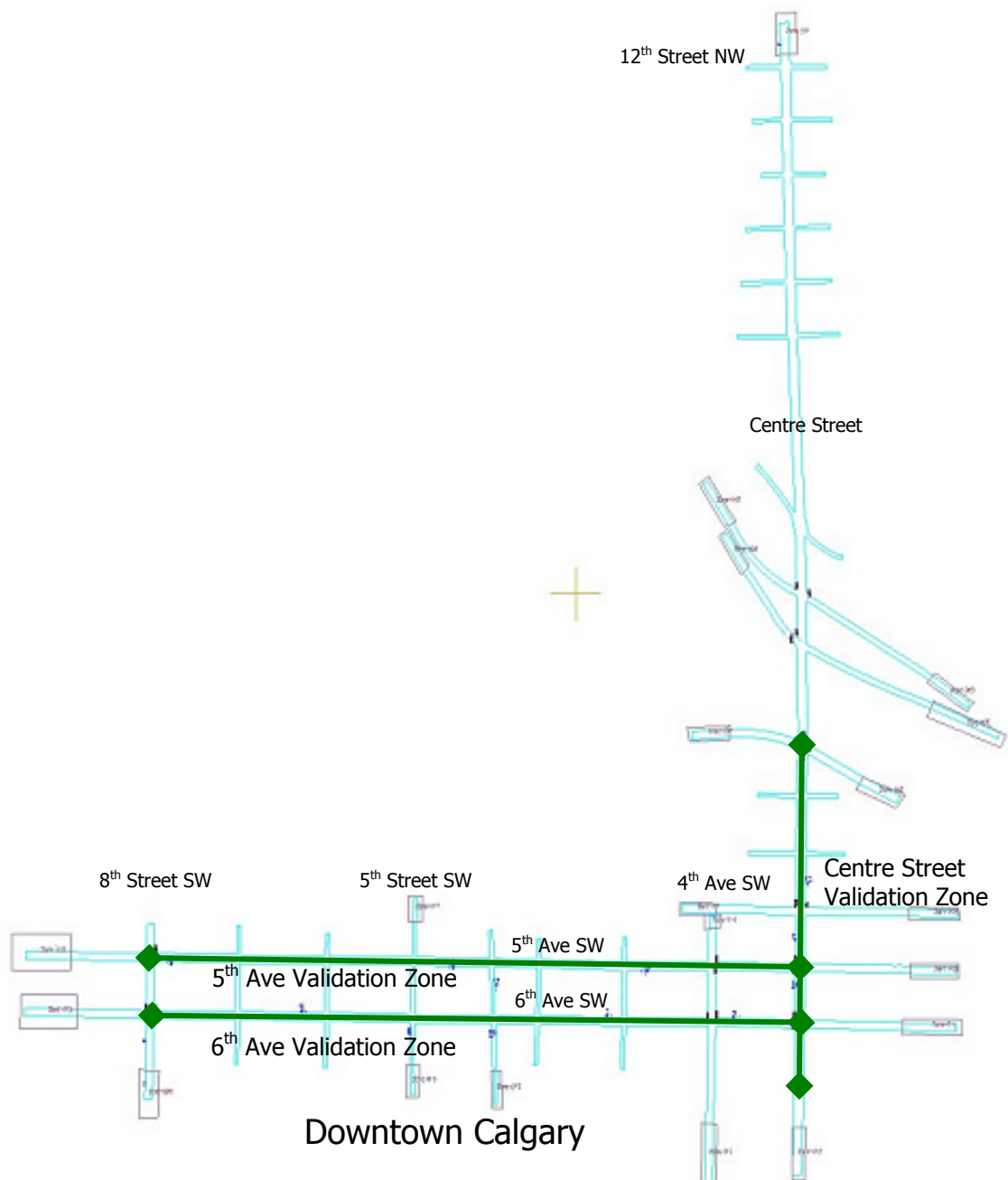


Figure 6.11: PARAMICS simulation model of Calgary

Three major categories of data were collected for model building: geometrical data such as street, lane and intersection arrangements, traffic activity data with vehicle demand and vehicle mix information and traffic control data with traffic signal arrangements and their timing. The City of Calgary, the authority responsible for maintaining and operating all the streets in and around Calgary, archives some of this information on a regular basis as a part of their routine operation. These three data categories and the sources of information are outlined below.

#### 6.4.1.1 Geometrical Data

The simulation model building involves replicating all lanes, streets, intersection and their features in the modeled area with a high level of detail. This requires detailed information such as lane widths, intersection arrangements including turn bans and pedestrian activity and exact lengths of all roadways. A street centerline map was taken as the basis for establishing street layouts along with aerial photographs and construction drawings provided by the City of Calgary as supplementary data. Figure 6.12 shows an aerial photograph showing the area just north of downtown core. See Appendix A for an outline of all the data used for model building.



Figure 6.12: Aerial view of simulated area: North of downtown

#### 6.4.1.2 Traffic Activity Data

The modeled traffic activity in terms of the number of vehicles generated and attracted by each zone in the simulated area was probably the most complex set of information used in this simulation. Traffic counts taken at different points of the network and intersection turn counts for most of the intersections in the modeled area were gathered from the City of Calgary archived data. In addition, 24 hour automatic traffic counts taken in the modeled area were used to estimate the daily variation of traffic activity, identifying features of the morning off-peak, morning peak, off-peak, evening peak and evening off-peak. However, the temporal variation of the traffic demand was not considered for the simulation and was constant at the typical morning peak traffic demand levels. More specifically, traffic counts and intersection counts observed for the period 8:00 am to 8:15 am were used for model building.

Appendix A provides a summary of all traffic demand data collected for traffic demand modeling. Although vehicle counts and turn counts provide point data for traffic demand modeling, the simulator requires the number of vehicles originating and ending at all zones in the simulated area, which is often referred to as an Origin-Destination (OD) matrix or table. The OD estimation process is addressed later on in this chapter. A total of 23 OD zones were simulated in the model, representing sinks and sources for vehicles generated and attracted by locations outside of the simulated area.

#### 6.4.1.3 Traffic Control System Data

The simulation model includes over 20 intersections controlled by traffic signals and several more intersections controlled by priority rule. Traffic signal timings for all of these intersections, namely the cycle times and the green time for the main phase were obtained from the City of Calgary Traffic Operations Division. Almost all of the traffic signals operate on a timing scheme that varies over the day based on estimated traffic demand for different directions. Furthermore, some signals, mostly outside the

downtown core, had vehicle-actuated systems. All traffic signals in the simulator were coded with signals settings in the selected time period 8:00 am to 8:15 am. See Appendix A for signal timing plans and timing details.

#### **6.4.2 Transit Operation Data**

The modeled area of downtown Calgary served multiple transit routes and therefore had a high degree of transit service compared to the suburban areas. This was part of the reason for selecting this part of the city as the test area since transit probe coverage and frequency of probe reports are important factors. Although there were more than two routes serving this area, routes 2 and 3, selected for the data collections discussed above, were the focus of the simulation.

Simulation model data requirements for transit operation modeling included the streets served by the route, route stop locations, average stop times, frequency of operation and number of transit vehicles serving the route. For these data requirements, Calgary Transit, the transit authority of the City of Calgary, provided data on streets served by the route, average stop times and other operational data. Transit stop location data was incorporated from the surveys results discussed above for all transit stops outside of the downtown area. For downtown stop locations, maps generated by conventional surveying techniques were used to locate the transit stops to avoid additional GPS related errors

#### **6.4.3 Data for Model Validation and Calibration**

A generalized discussion of microscopic simulation mode validation and calibration was presented in Chapter 5 and PARAMICS microsimulator specific issues are further discussed later in this chapter. Although the simulation model's ability to replicate the real system in every respect is important, its ability to replicate the travel times observed

in the real system was considered especially important, as travel time was used as the primary output for almost all the analysis throughout this thesis. Therefore, travel time was considered to be the main calibration and validation criterion. Hence, a large number of travel time observations were required for the calibration and validation process.

Travel time data for simulation model validation and calibration was collected through multiple sources. Firstly, travel time observations from the transit and dedicated test vehicle survey, discussed earlier in this chapter were formatted into segment travel times. Secondly, the City of Calgary provided travel time records from two probe vehicle surveys conducted before and after a traffic signal plan change. Although travel times observed prior to signal plan change was not applicable, observed travel times after the implementation were used for model calibration. A set of travel times used in this research is given in Appendix A. For travel times recorded outside the simulated time interval, observations were scaled to the required time period using historical records of daily travel time variation and traffic flow from Grey (2002).

## **6.5 Microsimulation Model Building**

This section and the rest of this chapter address specific simulation model building, validation and calibration issues related to the PARAMICS simulator. PARAMICS allows the use of a map of the simulated area as a template in the model building process. Therefore, a map of the street centerlines in the intended model area was used as a template, and streets, intersection and OD zones were assembled on the template. Details of the model building process discussed here are limited to traffic demand estimation. See the PARAMICS user manual for additional information on simulation model building (SIAS Limited, 2002).

### 6.5.1 Traffic Demand Modeling

The objective of traffic demand estimation was to generate an Origin-Destination (OD) matrix that describes the traffic flow patterns observed in the simulated network. Under ideal conditions, the origin and the destination of all vehicles in the network are required to generate a complete OD matrix. This would require collecting OD information from every single vehicle through interviews or recording vehicle identification information such as license plates at all entry and exit points of the simulated network and post-mission data matching to construct the OD matrix. However, the use of this approach was considered impossible with the resources available.

Alternatively, OD estimation is often conducted using statistical techniques and abstract information that can be collected more easily and at a lower cost, such as screenline counts and intersection turn counts, see SIAS Limited (2002). The PARAMICS simulator provides a built-in estimator tool that can simplify the OD estimation process using data that is relatively easy to collect. Figure 6.13 illustrates the process of the matrix estimator tool. The estimation requires prior OD information, an approximate OD usually estimated based on a limited interview based survey. It also requires constraint data on the network and additional screenline and turn movement counts. The matrix estimator combines this data using an iterative process, estimates the best fitting OD matrix to the screenline and turn movement counts provided.

Turn counts and screenline counts obtained from the field data collections were used with the PARAMICS OD estimator to develop traffic flow OD matrix for the simulations. Representative traffic turn count and screenline counts used for this purpose are illustrated in Appendix A. Some field data was scaled based on daily and monthly traffic trends from Grey (2002) to suit the modeled day and time interval.

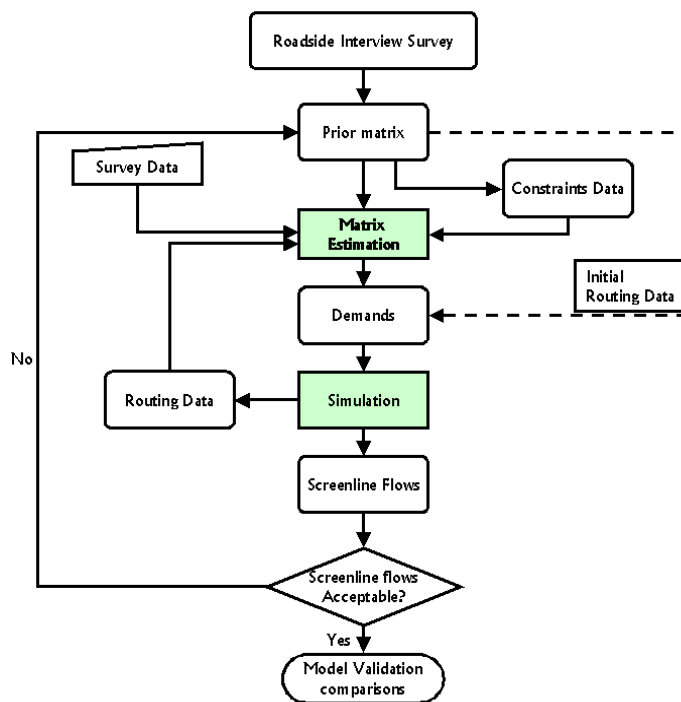


Figure 6.13: Traffic demand estimation using survey data

## 6.6 Model Calibration and Validation

Model calibration and validation was entirely based on observed and simulated vehicle travel times between control points in the simulation and the real roadway network. The calibration and validation data requirements were discussed earlier on in this chapter, and this section focuses on the actual calibration and the validation of the simulation model.

### 6.6.1 PARAMICS Model Calibration

The PARAMICS microsimulator provides a range of calibration parameters that influence several layers of entities in the simulation. The main calibration parameters available include two aggression and awareness distributions modeling the driver behaviour, speed-acceleration characteristic curves for each vehicle type, and a headway factor for streets that influence the traffic flow characteristics through vehicle headways

(SIAS Limited, 2002). The speed-acceleration curve for each vehicle type represents the driver implemented acceleration at different speeds under different driving conditions. The maximum acceleration at a particular speed represents the theoretical maximum acceleration that could be achieved by vehicles of that type under constraints imposed by other vehicles.

Since this thesis involved a considerable number of probe vehicle based data collections, and thus gathered a considerable amount of individual vehicle data, vehicle speed-acceleration curves were used as a calibration parameter. Furthermore, no effort was made to recalibrate the default driver awareness and aggression models and the default headway parameters due to practical limitations. PARAMICS provides default speed-acceleration curves for all vehicle types and allows modifications through the selection of values for weight, maximum speed, maximum acceleration, maximum deceleration, drag and inertia for the vehicle type. However, no explicit model is given in the simulator, and only a graphical representation of the resulting speed-acceleration curve is given. Not all of these values were measured during testing (i.e. weight), and their correlation was not known, as the model is not available to the user. Therefore, PARAMICS speed-acceleration curves for transit vehicles and other vehicle types were visually matched using the curves established by field data.

The entire field data collection involved five transit vehicles and two dedicated probe vehicles. Data from both dedicated probe vehicles were used for establishing speed-acceleration curves as they represented two vehicle types, namely cars and vans. Only one transit vehicle data set was used, as they were very similar in operating characteristics. Separate curves were developed for downtown and suburban areas, as driving conditions could differ significantly due to increased interaction between vehicles in downtown along with lower operating speeds. The data sets are illustrated in Figures 6.14 to 6.16.

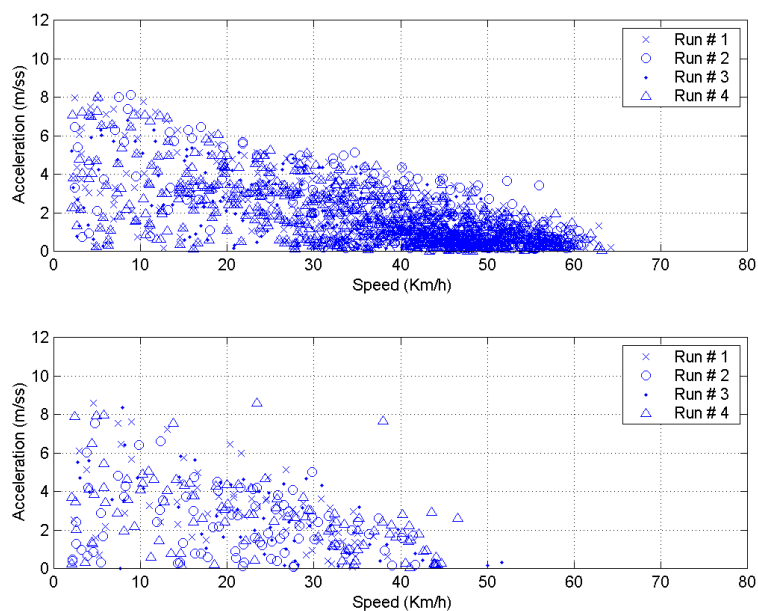


Figure 6.14: Speed-acceleration data for Driver 1/ Vehicle 1 suburban area (top) / downtown (bottom)

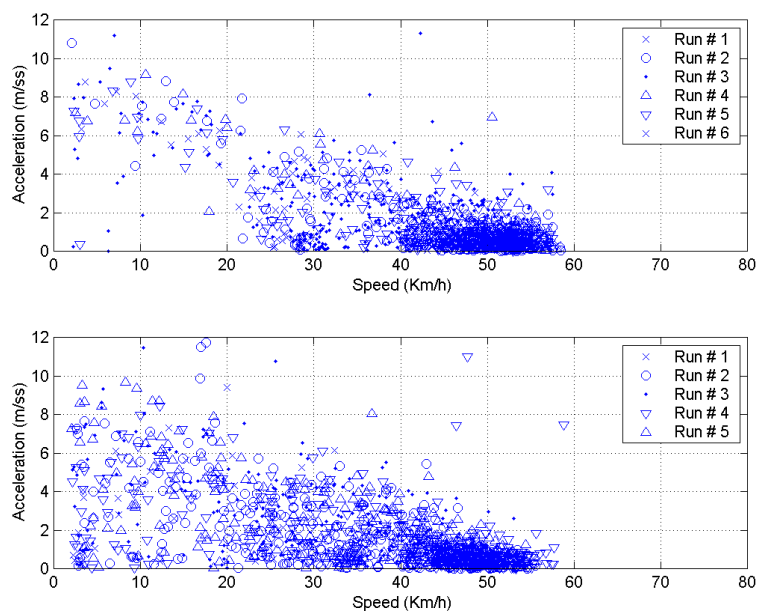


Figure 6.15: Speed-acceleration data for Driver 2/ Vehicle 2 suburban area (top) / downtown (bottom)

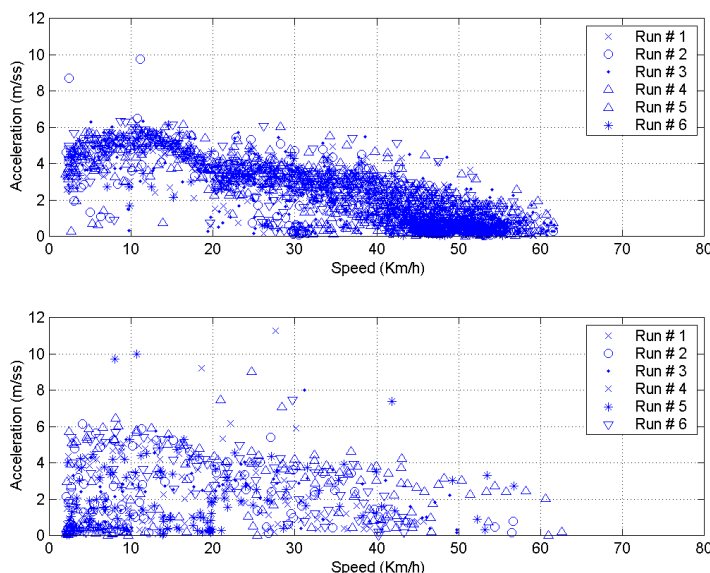


Figure 6.16: Speed-acceleration data for Driver 3 & 4/ Transit Vehicle 1 suburban area (top) / downtown (bottom)

## 6.6.2 Simulation Model Validation

The simulation model was validated using the travel times observed by field test vehicles and simulated vehicle travel times. Travel times from street sections were used for the validation process and three such street sections were used in this model. These comprised of two East-West street sections or validation zones (5<sup>th</sup> and 6<sup>th</sup> Avenue) and one North-South street section (Centre Street) as illustrated in Figure 6.11. The distribution of simulated vehicle travel times were compared with mean travel time observed by the test vehicles. Figure 6.17 depicts the comparison of simulated travel time distribution and the mean test vehicle travel time for 5<sup>th</sup> and 6<sup>th</sup> Street validation zones. Figure 6.18 shows the same comparison for Centre Street Northbound and Southbound validation zones.

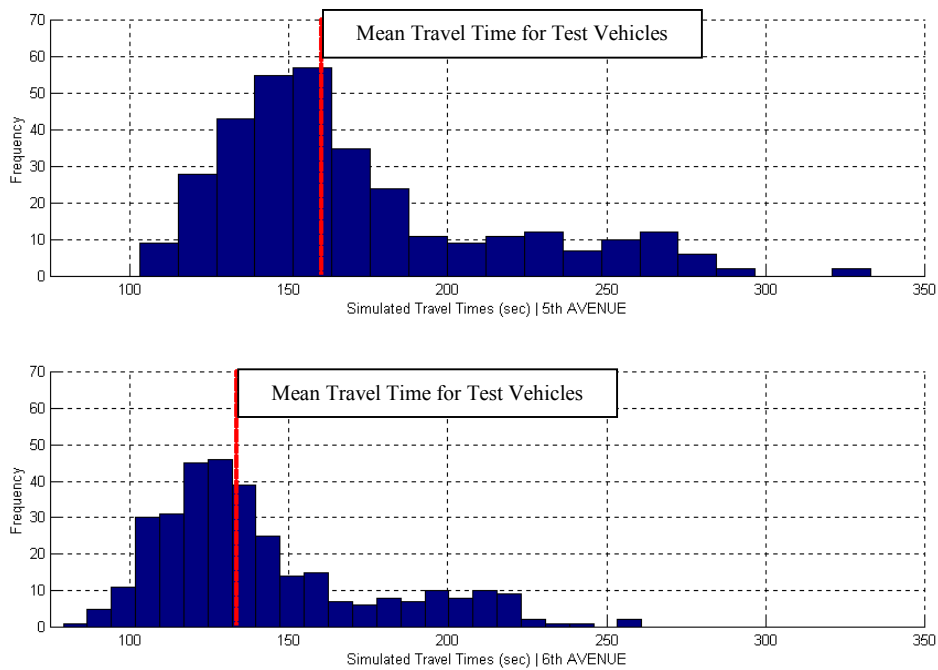


Figure 6.17: Simulated travel time distribution and observed mean travel times in 5<sup>th</sup> and 6<sup>th</sup> Avenues

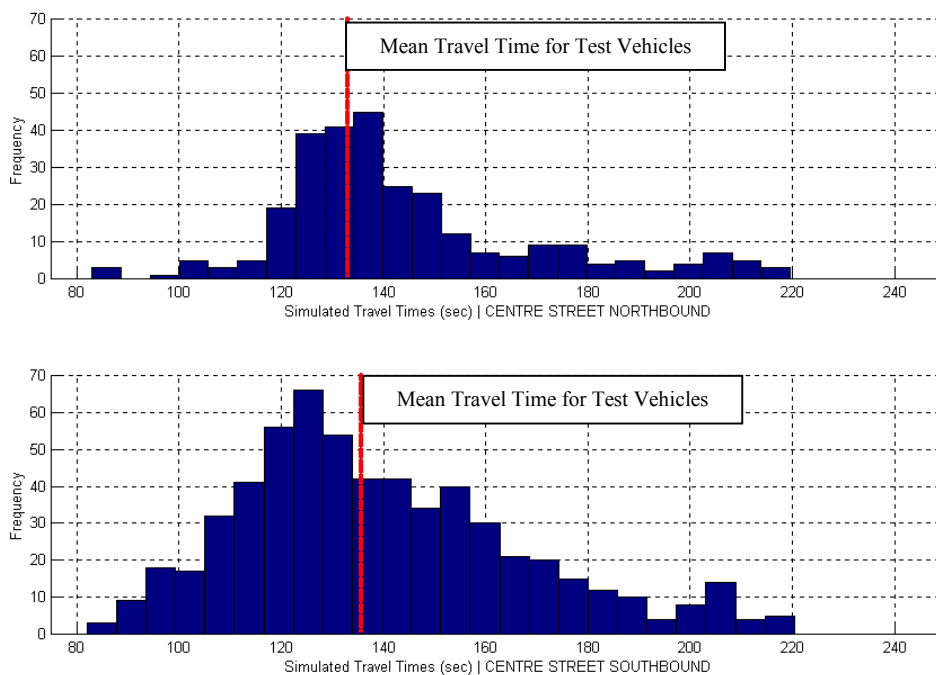


Figure 6.18: Simulated travel time distribution and observed mean travel times in Centre Street

## 6.7 Traffic Incident Simulation

Traffic incidents were simulated with the objective of creating incident scenarios that address all objectives identified in Section 5.6. This included analyzing the incident detection parameters, travel time and acceleration noise, and the combined algorithm performance under different scenarios. Three variables were included in creating simulation scenarios: incident location, GPS performance degradation and the probe vehicle fleet. Incident location was varied to mid-block and intersection incidents, and for the former, single lane and multi-lane capacity reductions were simulated. For the probe vehicle fleet variation, two categories were simulated with transit probes only and transit probes with dedicated probes. A summary of the simulation scenarios and the variables are given in Table 6.2.

Table 6.2: Simulation scenarios

<b>Transit Probe Based Incident Detection Data</b>		
<b>No Simulated GPS Errors</b>	<b>Incident Location / Capacity Reduction</b>	
	<b>Mid-Segment</b>	<b>Intersection</b>
Travel Time	X	X
Acceleration Noise	X	X
<b>Simulated GPS Errors</b>	<b>Incident Location / Capacity Reduction</b>	
	<b>Mid-Segment</b>	<b>Intersection</b>
Travel Time	X	X
Acceleration Noise	X	X
<b>Transit Probe &amp; Dedicated Probe Based Incident Detection Data</b>		
<b>No Simulated GPS Errors</b>	<b>Incident Location / Capacity Reduction</b>	
	<b>Mid-Segment</b>	<b>Intersection</b>
Travel Time	X	X
Acceleration Noise	X	X
<b>Simulated GPS Errors</b>	<b>Incident Location / Capacity Reduction</b>	
	<b>Mid-Segment</b>	<b>Intersection</b>
Travel Time	X	X
Acceleration Noise	X	X

## CHAPTER SEVEN

INCIDENT DETECTION ALGORITHM AND PERFORMANCE  
ANALYSIS

## 7.1 Analysis Scenarios

The performance analysis was conducted using incidents simulated in a two-street segment section of a westbound street as shown in Figure 7.1. However, for the clarity of presentation and to illustrate the incident impact on both segments, the beginning of Segment B was always considered the start of the analysis segments in subsequent illustrations in this chapter. The distance axis established based on the above definition is also shown in Figure 7.1. Two incident locations, varying incident-induced capacity reductions and controlled GPS errors were simulated for analyzing a range of performance issues. These issues are summarized below and presented in Table 7.1.

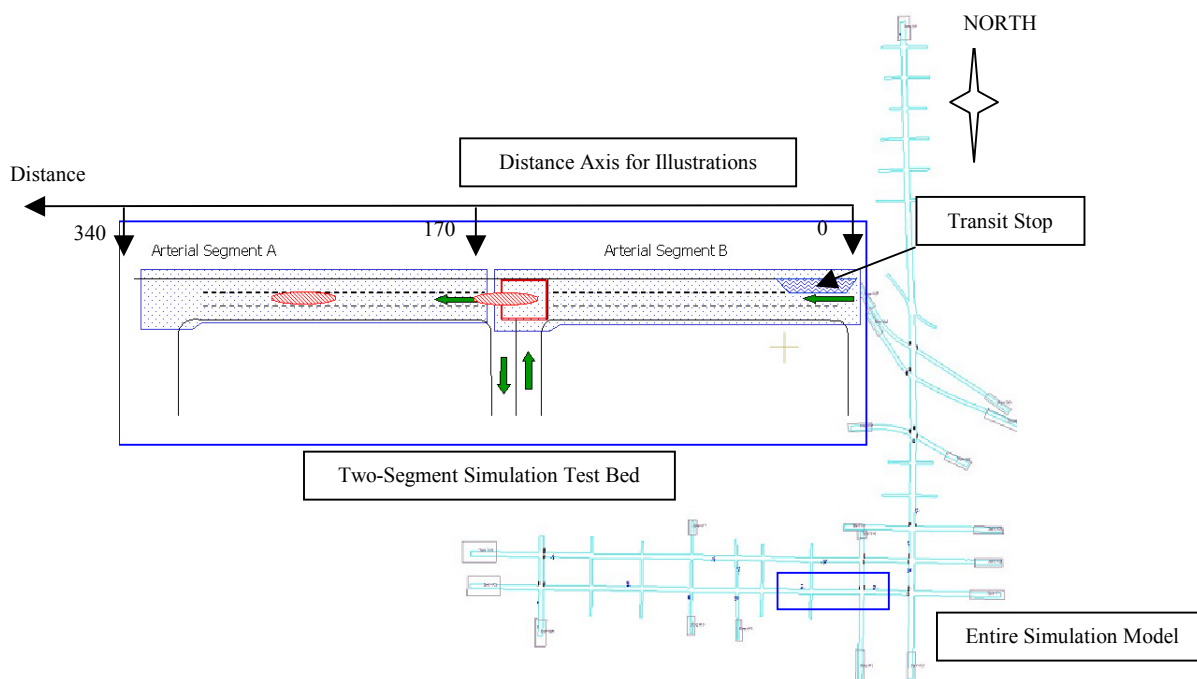


Figure 7.1: Simulation test bed

### **7.1.1 Performance of Individual Incident Indicator Parameters**

The performance of the algorithm was dependent on the responsiveness of the two incident detection parameters to traffic flow variations caused by incidents. Hence, the first phase of the analysis investigated the responsiveness of travel time variation and acceleration noise levels to traffic incident induced congestion, taken individually and under perfect GPS reception conditions.

### **7.1.2 Performance Degradation with GPS Errors**

The second phase illustrates the degradation of incident detection capability with different levels of GPS errors. Although PARAMICS does not allow for the modeling of measurement errors, different levels of normally distributed errors were introduced to simulate travel time and vehicle speed data. GPS velocity errors were introduced to acceleration noise-based analysis, while GPS position errors translated into time measurement errors were added for travel time measurements. The magnitudes of these errors were controlled to reflect typical GPS error characteristics.

### **7.1.3 Incident Location**

The lateral and longitudinal location of the incident in a street segment may have an impact on the ability to detect incidents. This is especially true when using transit vehicles for incident detection. For instance, it is logical to assume that a single lane incident in a lane that is not often used by transit vehicles may take longer to detect using transit travel times. The analysis includes two incident locations, namely mid-block and intersection, along with varying capacity reductions. These features are correlated with the incident detection capability later in this chapter.

#### **7.1.4 Impact of Downstream Incidents**

The impact from incidents propagates through streets; hence, different street segments upstream of the incident may experience varying degrees of impact. However, the characteristics of such propagated shockwaves are highly distorted by upstream traffic signals, due to the platooning effect from traffic signals. This analysis investigated ability to detect downstream incidents from upstream observations.

#### **7.1.5 Performance of the Incident Detection Parameters and Algorithm**

The purpose of analyzing incident detection parameters individually was to assess the correlation of their individual performance with incident features. This enables the combination of those parameters in a complementary manner to obtain the best performance from the incident detection algorithm. Individual parameters and the algorithm performance is evaluated in terms of DR, TTD and FAR.

#### **7.1.6 Performance Improvement with Additional Dedicated Probe Vehicles**

Based on the baseline performance levels established from previous analysis scenarios, further improvement that can be made by using a small proportion of dedicated probe vehicles was also assessed. This was analyzed in terms of the improvement to DR, TTD and FAR parameters in the baseline case as well as the robustness added to the above parameters under degrading GPS performance.

### **7.2 Selection of Incident Scenarios**

The simulation-based analysis involved multiple incident scenarios, with varying incident location and intensity conditions. For each simulation scenario, further cases of GPS performance degradation were simulated. Furthermore, multiple simulations were

conducted for each scenario to account for the stochastic nature traffic flow. The collection of data from each simulation and subsequent processing and analysis involved considerable amount of data formatting and computations. Thus, the number of simulation scenarios had to be limited to a minimum while addressing the conditions that are highly likely in an actual implementation of the system. Two major factors were considered in selecting the scenarios.

### **7.2.1 Incident Intensity**

The intensity conditions that can be simulated ranged from a total closure of the street to a single lane incident. It was assumed that if single-lane and two-lane incidents can be successfully detected, incidents that cause total closure could be detected much faster with better reliability. Therefore, single-lane and two-lane incidents were simulated and no incidents that caused total closure were simulated.

### **7.2.3 Incident Lane Selection**

The street segments selected to simulate incidents consisted of three lanes as depicted in Figure 7.1. The curbside lane always accommodated transit stops and Segment B included a transit stop. Therefore, the right lane was the preferred lane for transit vehicles in order to access the transit stops. Transit vehicles rarely used the middle lane and none used the left lane. Based on this observation and the requirement to limit the number of possibilities analyzed, no incidents were simulated in the right lane. It was assumed that if incidents in lanes that are rarely used by the probe vehicles can be detected successfully, incidents in lanes that are mostly used can be detected even faster with much better reliability.

Table 7.1: Analysis scenarios

<b>Transit Probe-Based Incident Detection Data</b>		
No Simulated GPS Errors	Incident Location / Capacity Reduction	
	Mid-Segment	Intersection
Travel Time	TTD / FAR / DR	TTD / FAR / DR
Acceleration Noise	TTD / FAR / DR	TTD / FAR / DR
Simulated GPS Errors	Incident Location / Capacity Reduction	
	Mid-Segment	Intersection
Travel Time	TTD, FAR, DR Degradation	TTD, FAR, DR Degradation
Acceleration Noise	TTD, FAR, DR Degradation	TTD, FAR, DR Degradation
<b>Transit Probe &amp; Dedicated Probe-Based Incident Detection Data</b>		
No Simulated GPS Errors	Incident Location / Capacity Reduction	
	Mid-Segment	Intersection
Travel Time	TTD / FAR / DR	TTD / FAR / DR
Acceleration Noise	TTD / FAR / DR	TTD / FAR / DR
Simulated GPS Errors	Incident Location / Capacity Reduction	
	Mid-Segment	Intersection
Travel Time	TTD, FAR, DR Degradation	TTD, FAR, DR Degradation
Acceleration Noise	TTD, FAR, DR Degradation	TTD, FAR, DR Degradation

### 7.3 Analysis of Incident Detection Variables With No GPS Errors

For this analysis, no additional errors were simulated, thus open sky GPS reception conditions were assumed. A total of ten simulations were conducted for two incident scenarios, namely with a mid-block incident and an incident in the intersection. These two cases were labeled as Incident Scenario 1 and Incident Scenario 2 for the mid-block incident and incident in the intersection, respectively. This is also illustrated in Figure 7.2. Out of all ten simulations, five simulated Scenario 1 and the rest of the simulations simulated Scenario 2. Transit vehicle speed profiles, travel times and additional dedicated vehicle travel times were collected over the length of the test area. Only one of the transit vehicle routes used the transit stop zone in Segment B out of four transit routes operating through the test area.

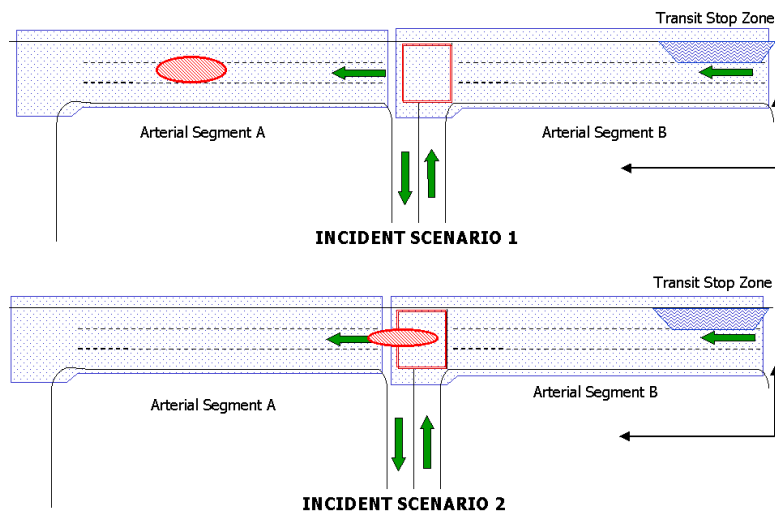


Figure 7.2: Incident Scenarios 1 and 2

### 7.3.1 Incident Detection Variable: Acceleration Noise

The GPS speed profiles of the transit vehicles were the basic measurements made for deriving the acceleration noise. Speed measurements taken at 1 Hz were differentiated to derive the acceleration signal for the vehicle. This discussion presents only the analysis of a single simulation from each scenario and summary statistics for all ten simulations.

#### 7.3.1.1 Incident Scenario 1

The analysis of the 4<sup>th</sup> simulation run of Scenario 1 is presented in this section. See Appendix C for complete data for all five simulation runs in Scenario 1. Speed profiles for 21 transit vehicles and travel times for each street segment were collected during the two-hour simulation period. Six of these vehicles traveled through street Segment A while the incident was in effect, which was a single lane incident starting at 60 minutes to the simulation run with a duration of 15 minutes. However, the exact time of entry for each vehicle to either segment A or B was not recorded, as the simulator was not able to record the entry times for probe vehicle data collection. Figure 7.3 shows a contour plot

of the transit vehicle speed profiles through Segments A and B. According to the earlier definition of segment length measurement, street length axis starts from the beginning of Segment B and the intersection is located 170 m from the beginning of Segment B, which is indicated by a separator at 170 m street length. Transit probe vehicles with numbers 6 to 11 traveled through Segment A while the incident was in progress.

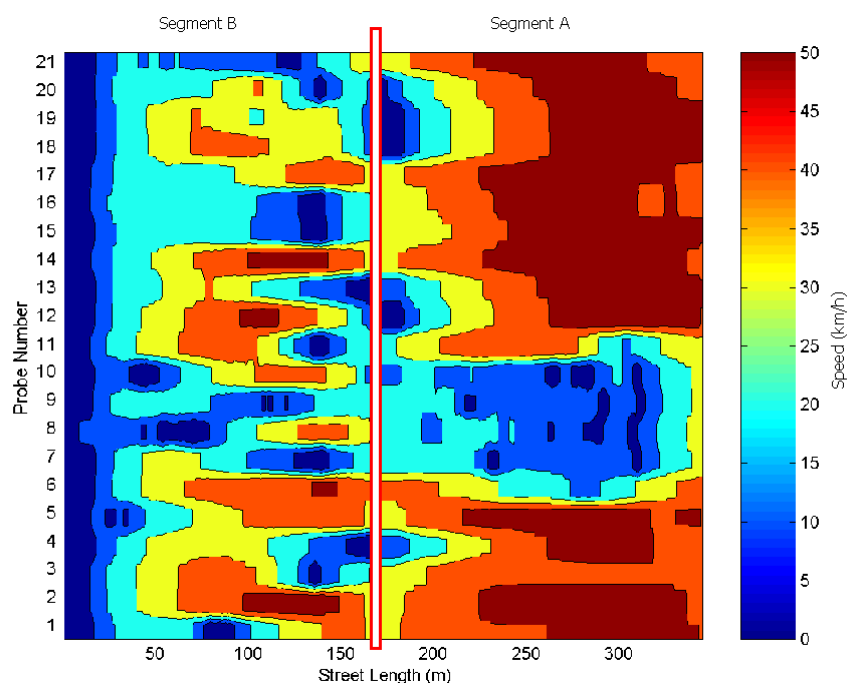


Figure 7.3: Speed contour: incident Scenario 1: Test Run 4

The speed profiles of transit probes 6 to 11 in Figure 7.3 shows clear speed reductions compared to other speed profiles, particularly along Segment A. Furthermore, these speed profiles show relatively low speeds and increased speed fluctuations in the upstream Segment B, although these reductions are not as evident as in Segment A due to the presence of the intersection which, adds control delays and forced stops to travel patterns in Segment B. Only two probes used the transit stop zone, namely probe number 5 and 10, and these are indicated by zero or close to zero speeds before the 50 m mark in Segment B.

Acceleration noise was estimated using the acceleration signal derived by differentiating the speed profiles. An acceleration noise estimation window size of 5 seconds was used for this analysis based on the optimum response to incidents. Following the same layout as in the case of Figure 7.3 above, Figure 7.4 illustrates the resulting acceleration noise contour plot. Acceleration noise above  $2 \text{ ms}^{-2}$  was indicated as  $2 \text{ ms}^{-2}$  to avoid the loss of information presented in Figure 7.4 at lower noise levels.

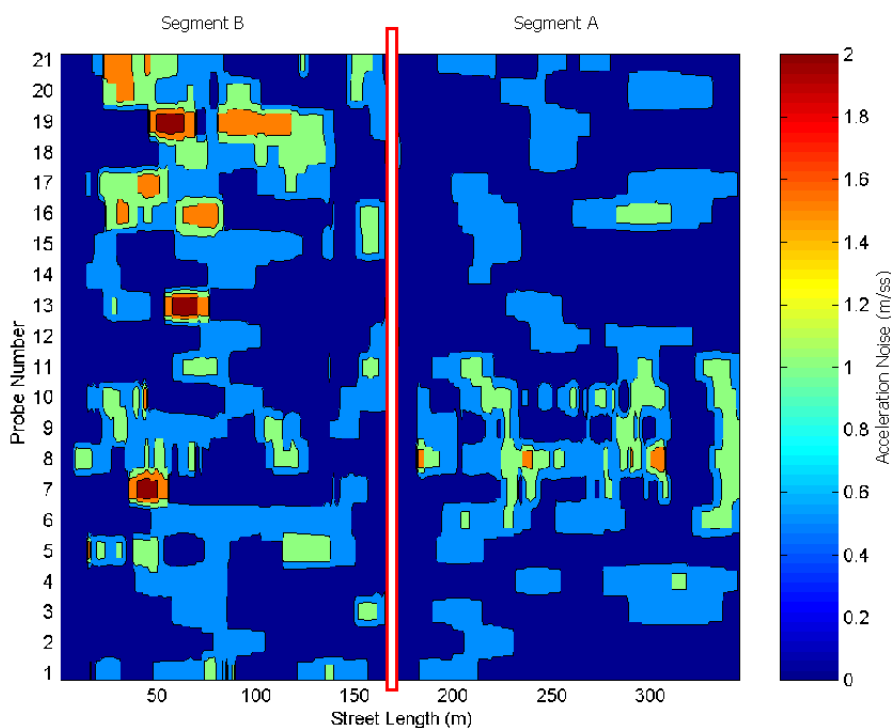


Figure 7.4: Acceleration noise contour: incident Scenario 1: Test Run 4

As indicated by Figure 7.4, acceleration noise values of vehicles in Segment A show a clear increase during the incident and this is partially continued into Segment B. However, a clear increase is not evident and thus requires a parameter to differentiate acceleration noise under normal traffic conditions for each segment from the increased levels of noise under incidents. The segment summation of probe acceleration noise was used for this purpose. Illustrated in Figure 7.5 below are the acceleration noise summations for all transit probe vehicles for both Segments A and B.

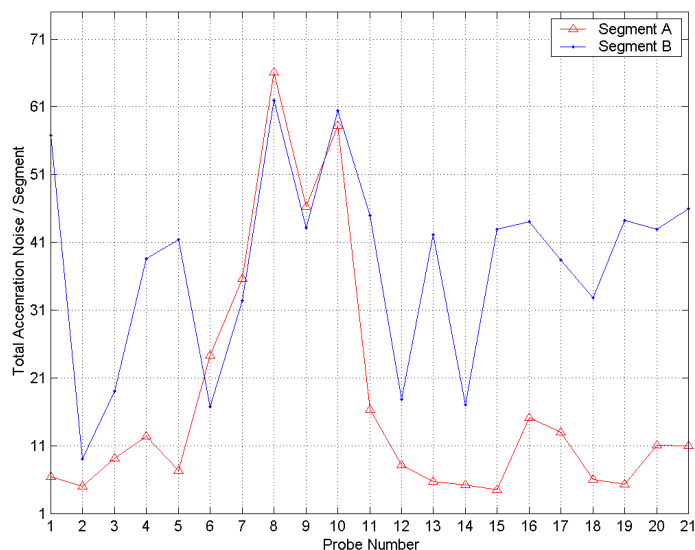


Figure 7.5: Acceleration noise street segment summations: Scenario 1: Test Run 4

The acceleration noise summations for Segment A, shown in Figure 7.5 indicate considerably high values for transit probes that traveled during the incident. All five probes that traveled in the incident influenced traffic flow have acceleration noise summations significantly higher than those of the vehicles that traveled under the normal traffic flow. However, to classify these increases as statistically significant indications of a traffic incident, a threshold was established. In order to establish the threshold of total acceleration noise for both Segments A and B, all transit probe speed profiles collected during non-incident periods, a total of 122 probe speed profiles, were combined together, and their statistics are presented in Table 7.2. The established thresholds and percentage of observations below the thresholds under normal operation are also presented in Table 7.2.

Based on Table 7.2 thresholds, the 4<sup>th</sup> simulation run has a 100 % DR and 0 % FAR with acceleration noise based incident detection. Although the statistical properties of the total acceleration noise under normal operation were not associated with any standard statistical distributions, the fact that 95 % and 100 % of the observations fell below the

established threshold indicates high level of success in discriminating incident and non-incident conditions based on the acceleration noise.

Table 7.2: Total acceleration noise statistics for normal operation

	Segment A	Segment B
Mean	7.5	34.1
Standard Deviation	6.0	14.5
Threshold	15	70
% Below Threshold	95	100

Probe vehicle acceleration noise measurements taken from all simulations were then categorized as incident influenced probe speed profiles and speed profiles measured under normal operation. Presented in Table 7.3 are the mean and standard deviations of the total acceleration noise for both Segment A and Segment B, under normal operation and under the influence of incidents, recorded from all 5 simulations in Scenario 1. This analysis included 28 transit vehicles, which traveled along these segments while the incident was in progress, and 63 more transit vehicles, which traveled under normal operation conditions. The statistics for normal operation for both Segments A and B show similar values in Table 7.2 and Table 7.3 showing the consistency of total acceleration noise performance in all ten simulations in Scenarios 1 and 2. In addition, the mean total acceleration noise for Segment A shows a marked increase over normal operations. Furthermore, Segment B acceleration noise totals show a significant increase with incidents in the downstream street, Segment A.

Table 7.3: Total acceleration noise statistics for Scenario 1

NORMAL OPERATION		
	Segment A	Segment B
Mean (seconds)	7.6	34.3
Standard Deviation (seconds)	6.0	14.5
INCIDENT SCENARIO 1		
Mean (seconds)	56.5	60.0
Standard Deviation (seconds)	31.1	40.4

Using the thresholds established in Table 7.2 and the simulation data for Scenario 1, the DR and FAR values for detecting incidents in Segment A were calculated based only on the acceleration noise. The DR and FAR for Segment A for individual simulations and the overall DR and FAR are given in Table 7.4 below.

Table 7.4: Acceleration noise-based detection on Segment A: summary for Scenario 1

Simulation No	Total Transit Probes		Incident Detection		DR	FAR
	Incident	Non-incident	Detected	False Alarms		
1	6	11	5	0	83	0
2	6	11	6	0	100	0
3	6	15	6	0	100	0
4	4	11	4	2	100	50
5	6	15	6	1	100	17
Total	28	63	27	3	96	11

It shows an impressive 96 % DR and a very low 11 % FAR under conditions similar to open sky GPS performance. However, no TTD was evaluated, as the PARAMICS simulator was not able to record street segment entry and exit times while recording speed profile data for probe vehicles. In addition, not all transit probes were recording their speed profiles, as the simulator was only able to record up to a maximum of three profiles at a time. Furthermore, 5 of the probe vehicles enabled the detection of the downstream incident from Segment B acceleration noise, giving only a 17 % DR for downstream incident detection. However, there were no false alarms in the downstream incident detection, yielding a 0 % FAR.

### 7.3.1.2 Incident Scenario 2

This section analyses the 2<sup>nd</sup> simulation run of Scenario 2 as the representative simulation for Scenario 2. It also presents summary statistics for Scenario 2 as in the case of section 7.3.1.1 above. See Appendix C for complete data for all five simulation runs in Scenario 2. During the simulation analyzed in this section, speed profiles of 20 transit vehicles

were collected during the two-hour simulation period. Six of these vehicles traveled through street Segment B while the incident was in progress. The simulated incident was a single lane incident starting at 60 minutes into the simulation run with duration of 15 minutes. Figure 7.6 shows a contour plot of the transit vehicle speed profiles through Segments A and B.

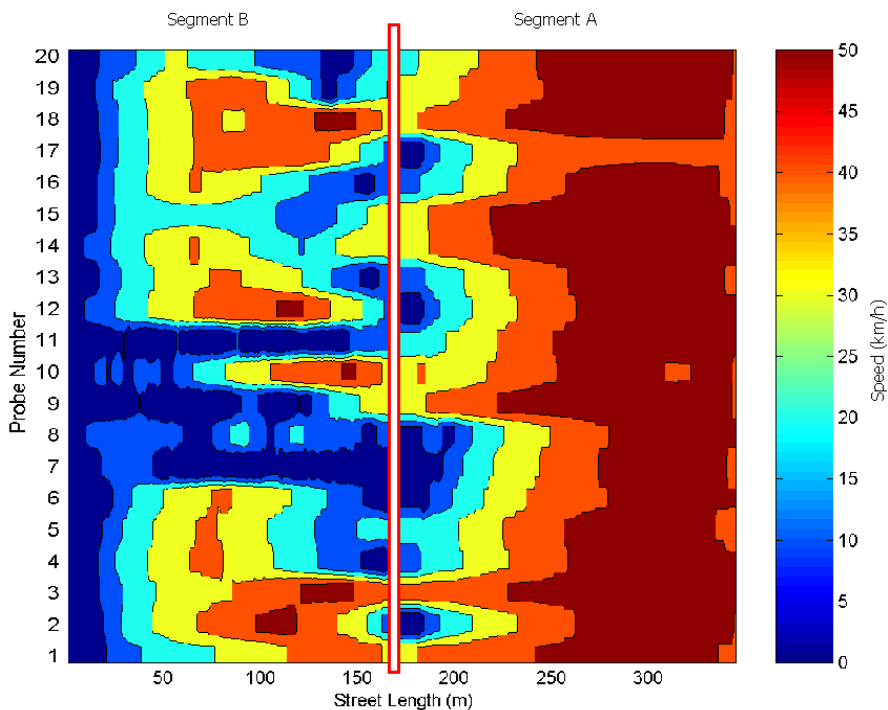


Figure 7.6: Speed contour plot for incident Scenario 2: Test Run 2

The transit probe vehicles 6 to 11 in Figure 7.7 were traveling through Segment B while the incident was in progress. Although probes 7 to 9 and 11 show noticeable speed reduction, probes 6 and 10 show no visible reduction of the speed. This is explained by the fact that most of the transit vehicles used the curbside lane (right) while the incident was blocking the left lane: therefore, some transit vehicles were able to partially avoid the incident induced congestion. The fluctuation of speed is not as noticeable in the Figure 7.6 as in the case of Scenario 1 analysis due to the reduced speeds resulting from the incident. The acceleration noise values for the same set of probes are presented in Figure 7.7 below and values above  $2 \text{ ms}^{-2}$  were indicated as  $2 \text{ ms}^{-2}$  to avoid the loss of information presented in at lower noise levels.

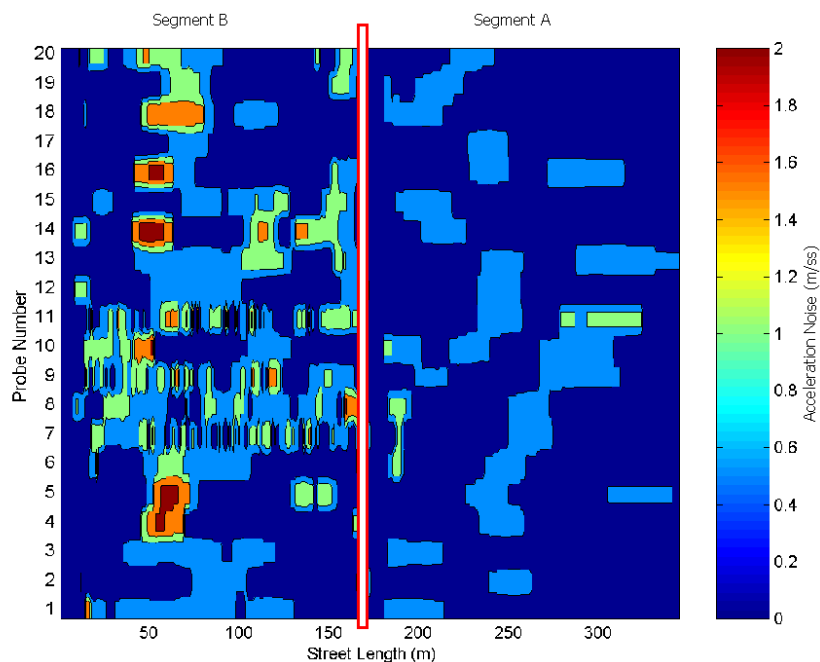


Figure 7.7: Acceleration noise contour: incident Scenario 2: Test Run 2

As indicated by Figure 7.7, acceleration noise values of vehicles in Segment B shows distinguishably high levels of acceleration noise, which is also highly variable for probes 6 to 11. The segment summation of probe acceleration noise is illustrated in Figure 7.8 below for all transit probe vehicles for both Segments A and B.

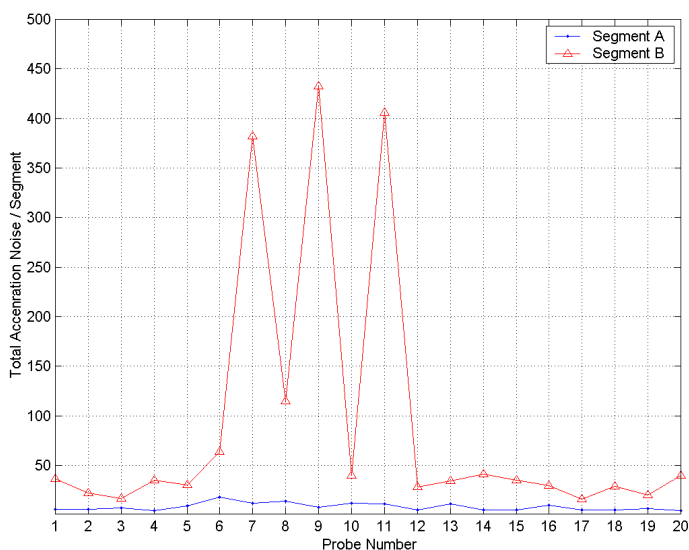


Figure 7.8: Acceleration noise street segment summations: Scenario 2: Test Run 2

The acceleration noise summations for Segment B, shown in Figure 7.8, indicate considerably high values for transit probes that traveled during the incident. These summations show considerably higher normal operation values compared to Segment A, and this is explained by the impact of the traffic signals at the end of Segment B.

Based on the threshold values set for Segment B, 5 out of 6 probes that traveled during the incident recorded acceleration noise levels above the minimum, thus yielding an 83 % DR for Scenario 2 Simulation 2. There were no false alarms thus yielding a 0 % FAR. Using the thresholds established in Table 7.2 and simulation data from scenario 2, DR and FAR values for Segment B were calculated based only on the acceleration noise. DR and FAR for Segment B for individual simulations and the overall DR and FAR are given in Table 7.5 below.

Table 7.5: Acceleration noise-based detection on Segment B: summary for Scenario 2

Simulation No	Total Transit Probes		Incident Detection		DR	FAR
	Incident	Non-incident	Detected	False Alarms		
1	3	15	3	1	100	33
2	6	14	4	0	67	0
3	7	11	6	0	86	0
4	5	11	2	0	40	0
5	4	11	3	1	75	25
Total	25	62	18	2	72	8

Table 7.5 provides a summary of the simulation results in Scenario 2 and it shows 72 % DR and an 8 % FAR under conditions similar to open sky performance of GPS. Although not as convincing as in the case of Scenario 1, these values reflect the capability to measure congestion based only on acceleration noise. This analysis only included 13 % of the transit vehicles due to data collection limitations imposed by PARAMICS.

### **7.3.2 Incident Detection Variable: Travel Time Variation**

This section presents an analysis of travel time statistics for both types of street segments defined in this thesis with no additional GPS errors simulated on measured travel times. Travel time statistics for Segment Types 1 and 2 are analyzed based on observations made in multiple simulations. The objective of the statistical analysis of travel time data is to confirm the premise that lognormal PDF is the best statistical representation of street segment travel time for both Types 1 and 2 streets under normal operating conditions. This is followed by two illustrations of incident detection and summary statistics for all ten simulations.

#### **7.3.2.1 Street Segment Travel Time Analysis: Type 1**

This section illustrates the statistical model building process for the travel time of a Type 1 street segment. Travel time records from three independent simulations were used for the analysis, totaling 1115 simulated travel time records. The techniques outlined in Section 4.3.3 of this thesis were used as the basis for the statistical curve fitting and the histogram of observed travel times is depicted in Figure 7.9. The data set was then fitted with a curve using the Generalized Lambda Distribution (GLD) using the method of moments technique. See Karian & Dudewicz (2000) for more details on the GLD technique. The fitted curve is also depicted in Figure 7.9.

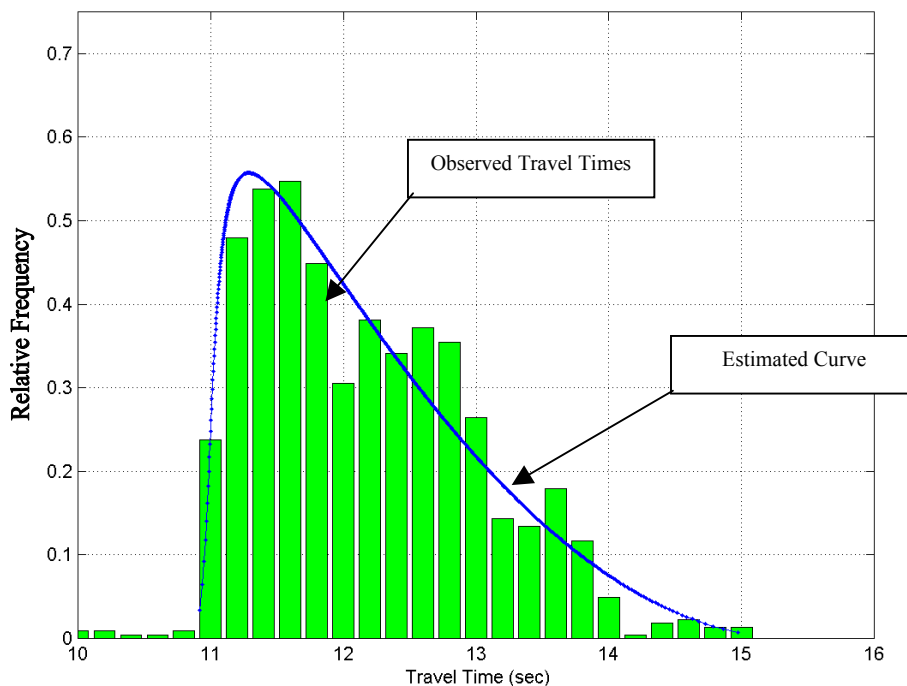


Figure 7.9: Street segment travel time histogram: Type 1

### 7.3.2.2 Street Segment Travel Time Analysis: Type 2

The statistical properties of vehicle travel times observed from a Type 2 street segment differ significantly from that of a Type 1 segment due to the platooning effect of traffic signals. Segment B travel time records corresponding to all vehicles used in Section 7.3.2.1 analysis were used for the analysis in this section. Since there was a high degree of correlation between travel times and arrival time of vehicles with respect to the traffic signal state, travel times were first analyzed against the signal stage at the arrival time. Figure 7.10 shows the travel time vs. vehicle arrival time plot for all observations taken from Segment B (from three simulation runs).

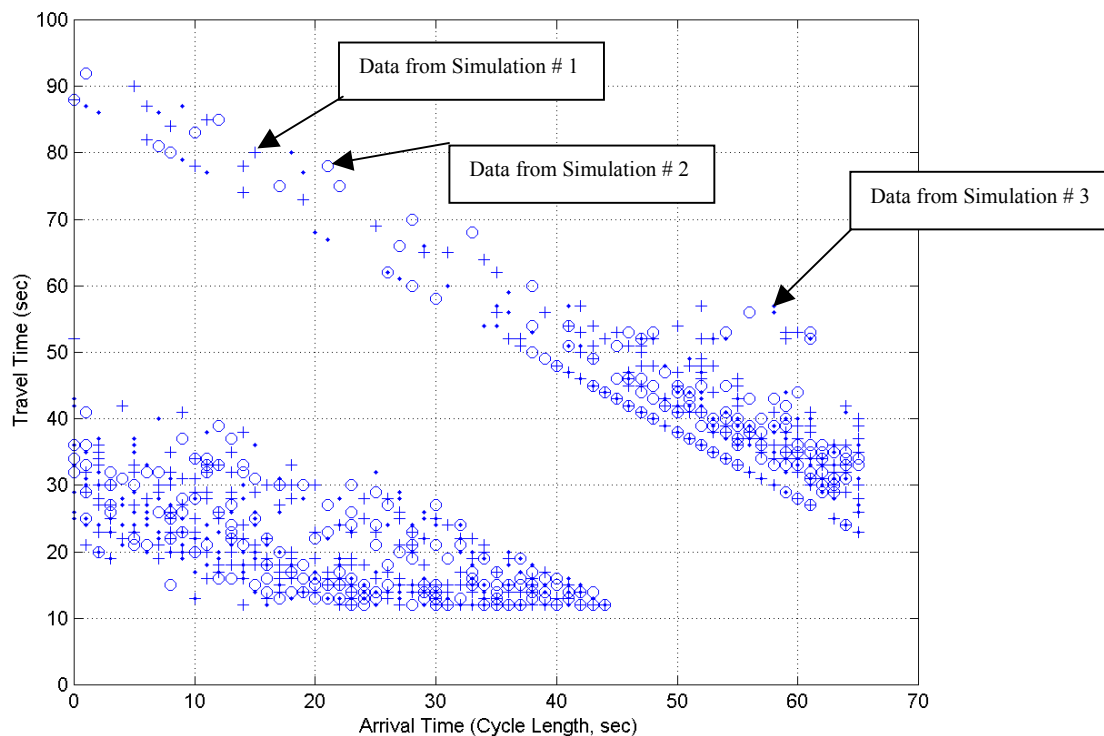


Figure 7.10: Vehicle travel times vs. signal stage at arrival time

Based on the classification technique discussed in Section 4.3.3 and data depicted in Figure 7.10, close to 500 travel time records from a total of over 1000 records were assigned to a second cluster. Travel time records from both clusters were then plotted in histograms in a similar manner to Figure 7.9 for Type 1 segments. The resulting histograms are depicted in Figure 7.11.

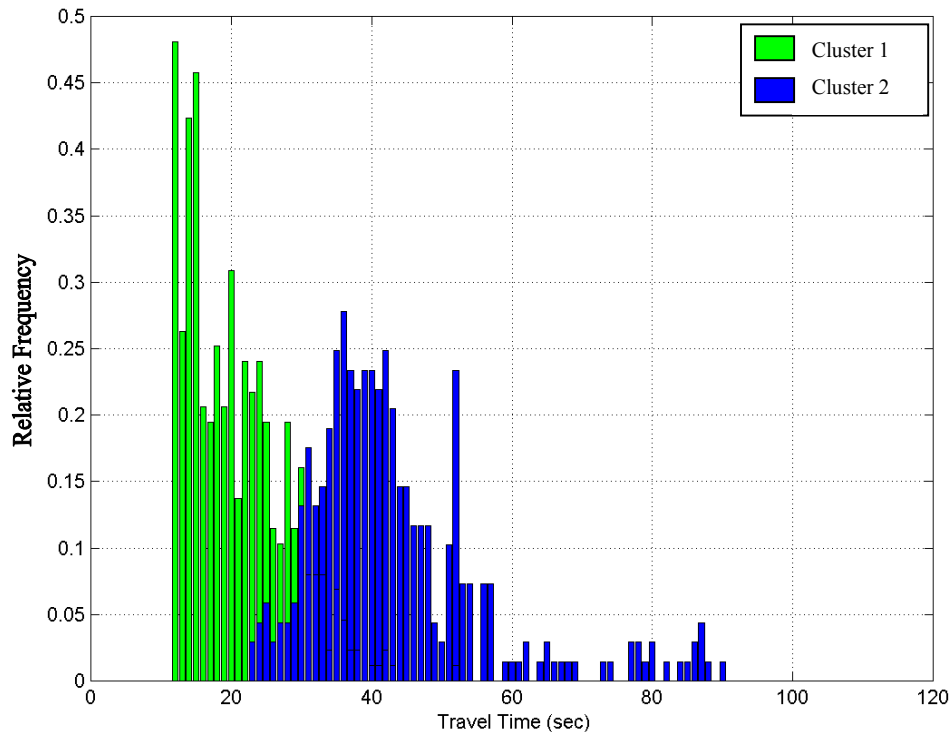


Figure 7.11: Travel time PDF for Cluster 1 and 2 observations

The histogram of travel time records in Cluster 1 shows almost identical characteristics to a Type 1 street segment travel time distribution. Compared to the distribution shown in Figure 7.9, Cluster 1 has a longer mean travel time and a slightly larger variance. The Cluster 2 was approximated by a normal distribution.

### 7.3.2.3 Travel Time Based Incident Detection: Type 1

The travel time probability distribution developed in Section 7.3.2.1 was implemented as a set of control charts for central tendency control and range control. This section presents the results of the control chart based analysis of the recorded travel times. The Upper Control Limits (UCL) were established as the 95-percentile value of the travel time distribution established in Section 7.3.2.1, and the corresponding range threshold was derived using the travel time threshold, thus completely defining the control charts. In order to illustrate the mechanism of out-of-control signal generation using the control

charts, the travel time records from the 4<sup>th</sup> simulation of Scenario 1 was selected. Shown in Figure 7.12 are the travel time records from all probe vehicles, both transit and non-transit, for the two-hour simulation. A total of 330 travel time records were reported for the 2-hour period, of which 132 were transit vehicles. The time axis shows the time of exit of the last vehicle in the three-vehicle travel time record group (a sample size of 3 was used for this analysis). The transit vehicle population constituted around 5% of the total vehicle flow, thus with dedicated probe vehicles, the total probe penetration was around 10 %. Transit vehicle and dedicated probe vehicle travel times are depicted separately in Figure 7.12.

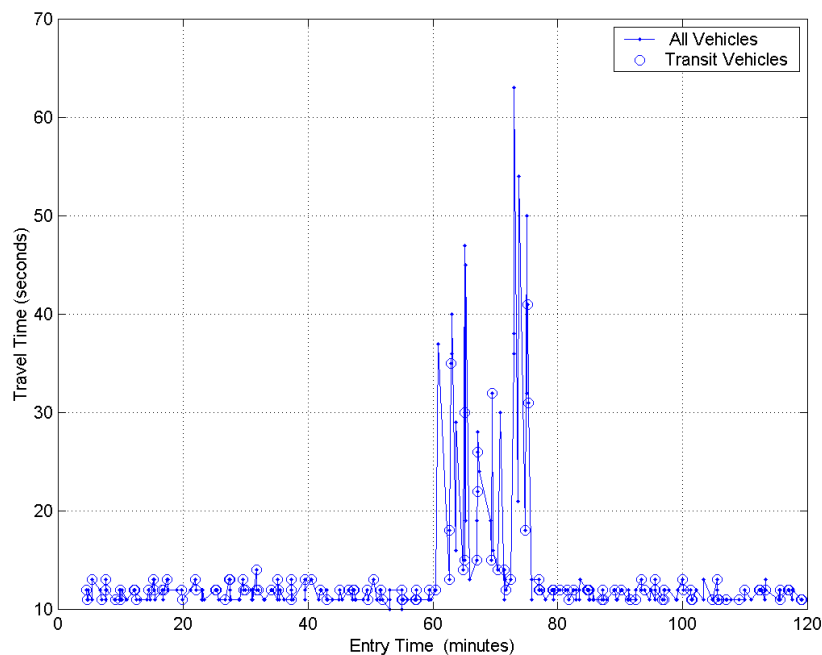


Figure 7.12: Transit and dedicated probe vehicle travel time observations

The travel time records shown in Figure 7.12 were then analyzed using the control charts. For comparison purposes, the central tendency control charts of transit vehicle travel times and transit and dedicated vehicles travel times are illustrated in the same figure in the following illustration. The same presentation method was adopted for a range control chart as well. The central tendency control charts for the simulated data are illustrated in Figure 7.13.

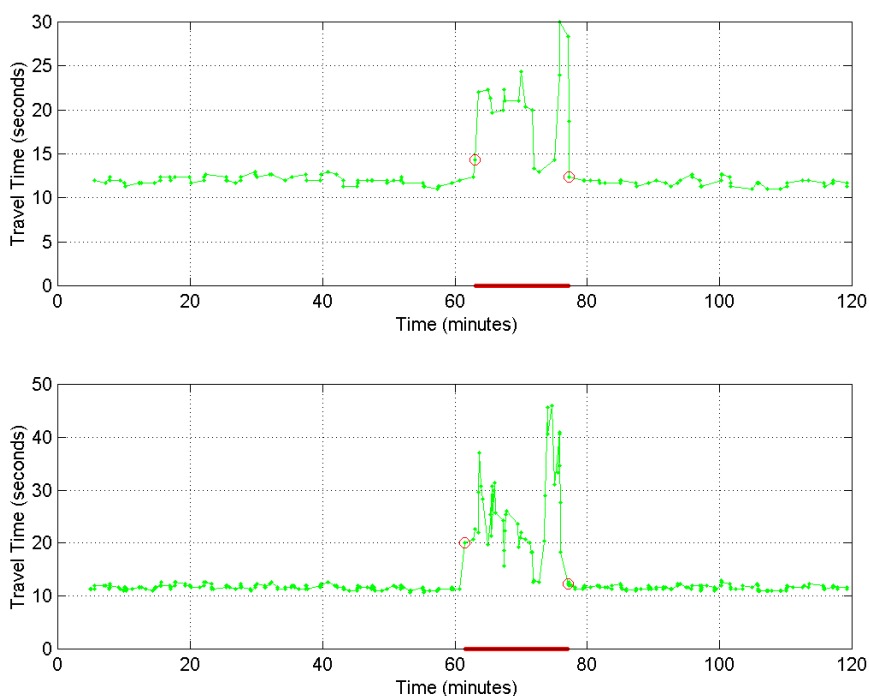


Figure 7.13: Transit probe (top) and transit & dedicated probe (bottom) central tendency control charts

Each data point in Figure 7.13 represents the mean of three travel time records. A highlighted data point indicates the starting point of the out-of-control signal and the subsequent highlighted point indicates the end of the out-of-control declaration. The time axis of the control chart also indicates the status of the process. For instance, in Figure 7.13, markings on the time axis indicates the out-of-control status. Although not clearly visible due to the larger time scale, all-vehicle out-of-control signal was declared at least 2 minutes prior to the transit only case. A TTD, DR and FAR comparison between these two cases is presented later on for all simulations in Scenario 1. Comparing the top and the bottom plots of Figure 7.13, the bottom figure (transit and dedicated vehicle) shows a higher resolution with frequent travel time records and the transit control chart (top) shows considerably longer periods without a new travel time being reported, the longest being close to 4 minutes.

The comparison of the transit and all probe vehicle charts also illustrates one of the drawbacks of using only the transit vehicles for incident detection. The incident simulated for this scenario was only obstructing the left lane of the three-lane street. The transit vehicles were mostly using the curbside lane, as they frequently had to approach transit stops located in the curbside lane. Therefore, transit vehicles suffered less delay compared to some dedicated vehicles, which were using the middle lane. Furthermore, the delay observed in transit vehicles can be partially explained by the impact from other vehicles that changed lanes from incident lane to middle and right lanes. The longest delays observed by probe vehicles are indicated by the highest point reached by either of the plots in Figure 7.13. The transit-only mean reached only a maximum of 30 seconds whereas the corresponding all-vehicle chart reached a value of 46 seconds. Therefore, some dedicated vehicles clearly experienced delays that are much larger than the delays experienced by the transit vehicles. This bias is discussed later and correlated with TTD and the DR. The range control charts for the same data set are presented in Figure 7.14 and they show characteristics similar to the central tendency controls charts in Figure 7.13.

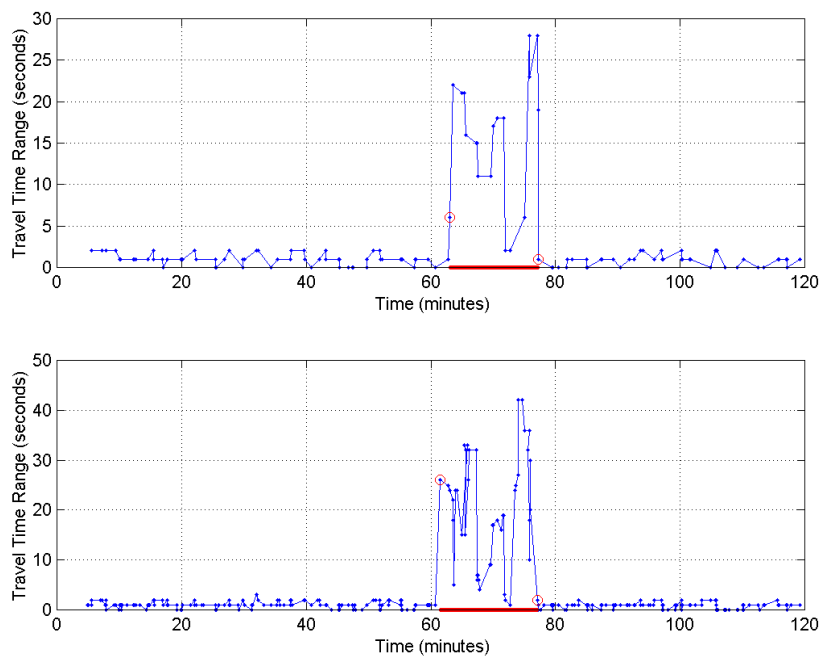


Figure 7.14: Transit probe (top) and transit with dedicated probe (bottom) range control chart

A total of 18 simulations were conducted for analyzing the control chart based incident detection approach. This included the five simulations that provided simulated data for acceleration noise performance analysis. In the majority of the simulations, a single incident was simulated obstructing the middle lane only. However, three simulations had simulated incidents in the left lane, and 3 simulations had simulated incidents that caused the temporary total closure of the middle and the left lane. The summary DR, TTD and FAR statistics for all 18 simulations is presented in Table 7.6 below, for both the transit probe only scenario and the transit and dedicated probe scenario.

Table 7.6: Average DR, TTD and FAR for all simulations: in-segment

Single Lane Incident (Middle Lane)		
	Transit Only	Transit and Dedicated
Simulations	12	12
TTD	91	64
DR	100	100
FAR	0	0
Single Lane Incident (Left Lane)		
	Transit Only	Transit and Dedicated
Simulations	3	3
TTD	342	146
DR	100	100
FAR	0	0
Two Lane Incident (Left and Middle Lane)		
	Transit Only	Transit and Dedicated
Simulations	3	3
TTD	38	29
DR	100	100
FAR	0	0

Table 7.6 as a whole indicates that at least a 30 % reduction of TTD could be achieved with additional dedicated probe vehicles. However, the DR and FAR were the same for both probe populations, a confirmation of the validity of using transit vehicles as probes for incident detection.

Since TTD was observed to be the most sensitive parameter with varying incident characteristics and probe population selection, Figure 7.15 provides a comparison of TTD for all 18 simulations. The simulations were arranged in ascending order of combined probe vehicle TTD in Figure 7.15 for clarity of presentation. The first three simulations contained the simulated incident that occupied two lanes whereas the last three simulated incidents were in the left lane. The rest of the simulations had incidents in the middle lane.

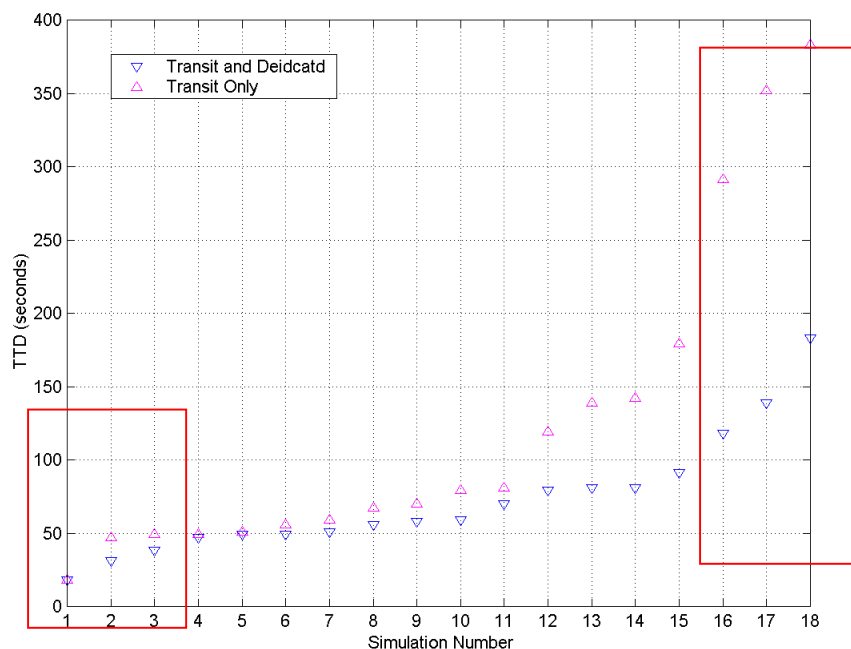


Figure 7.15: TTD for all simulations in Scenario 1

According to Figure 7.15, the two lane incidents were detected in under 50 seconds on average by both probe populations. As given in Table 7.6, these TTDs were 38 seconds and 29 seconds for transit only and transit and dedicated vehicle cases respectively. For the incidents in the left lane, TTD values were considerably longer even for the combined probe population, indicated by an average TTD of 146 seconds for left lane incidents, whereas incidents in the middle lane were detected at an average 64 seconds with the same probe system. This is explained by the lower lane usage for the left lane for all

vehicles. Furthermore, transit vehicles were not using this lane as they were mostly traveling towards the curbside lane to facilitate the easy approach to transit stop zones.

Apart from detecting a traffic incident that occurred in a particular street segment using its own travel time observations, the possibility of detecting downstream incidents using upstream street segment travel times was also investigated using the simulations. Summarized in Table 7.7 are the incident detection statistics from street Segment B (upstream) travel time observations while the incidents took place in the downstream Segment A.

The travel time analysis of the upstream Segment B for detecting downstream incidents in Segment A revealed that none of the incidents simulated in the left lane of Segment A could be detected using upstream data. Furthermore, the analysis only detected one incident, out of a total of 12 simulations, in which the incident took place in the middle lane. Therefore, only the two-lane incidents in Segment A are presented in Table 7.7.

Table 7.7: Summary of DR, TTD and FAR for all simulations: downstream segment

Downstream Two Lane Incident (Left and Middle Lane)		
	Transit Only	Transit and Dedicated
Simulations	3	3
TTD	331	249
DR	100	100
FAR	0	0

As indicated by Table 7.7, only the incidents causing major capacity reduction in downstream street segment can be detected using upstream travel time data. However, such incidents can be detected equally well by using either transit vehicles alone or transit and dedicated probe vehicles. The introduction of dedicated probes provides an average TTD reduction of close to 75 %.

### 7.3.2.4 Travel Time Based Incident Detection: Type 2

The 2<sup>nd</sup> simulation of Scenario 2 was used for the analysis in this section, and the analysis is presented in a similar manner to Section 7.3.2.3 for Type 1 segments. Depicted in Figure 7.16 are the travel times for all probe vehicles. The same notation was used distinguishing transit and non-transit vehicles.

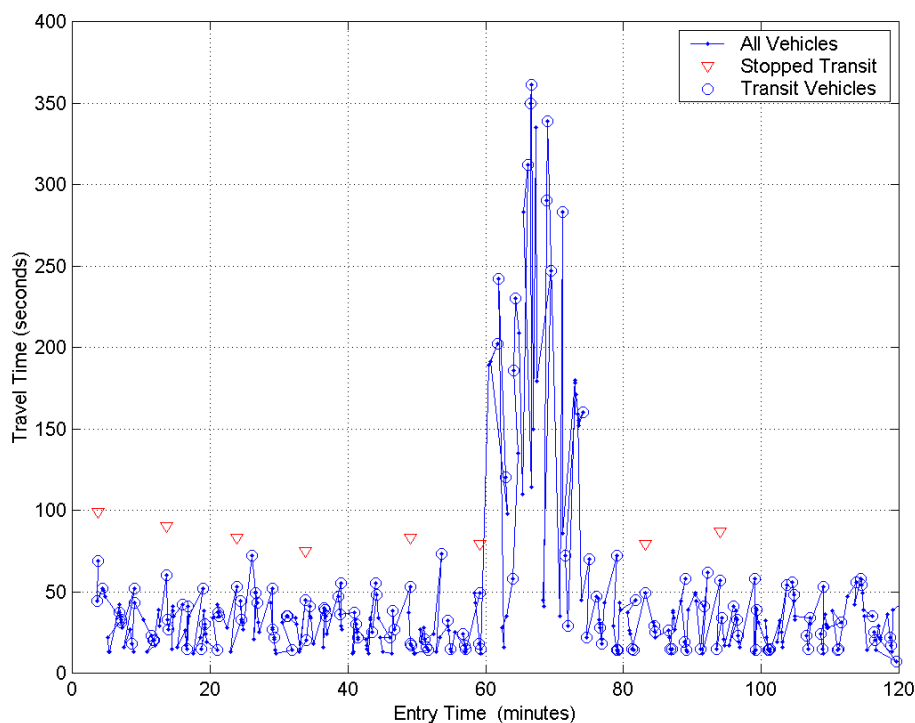


Figure 7.16: Transit and dedicated probe vehicle travel time observations

The street segment analyzed, Segment B, has two distinctive characteristics. Firstly, it includes a signalized intersection as depicted in Figure 7.1. Secondly, a transit stop zone was located at the beginning of the segment. The former adds delays to a majority of the vehicles, thus Segment B has a relatively higher average travel time compared to Segment A. More specifically, these travel times actually belong to two observation clusters as illustrated in Figure 7.11, with the majority belonging to the second cluster, where travel times include a control delay. The latter characteristic, the transit stop zone, may have had two impacts on the segment travel times. Firstly, transit vehicles that

stopped for passenger activity recorded a travel time that reflects a dwelling time and secondly, the transit vehicle activity in the stop zone may have influenced other vehicles, which may have caused longer travel times. The travel times of transit vehicles that stopped in the stop zone were modified using the travel time modification algorithm developed in Chapter 4. The unmodified travel times that were subsequently modified by the above algorithm are highlighted in Figure 7.16, and only the modified travel times were used for the rest of the analysis.

Figure 7.17 illustrates the central tendency control chart for the above travel time records. Although a single control chart was presented, there were two actual upper control limits corresponding to Clusters 1 and 2, which were applied to travel times in either cluster separately. The observed travel times were associated with either Cluster 1 or 2 based on the recorded vehicle arrival time with respect to the intersection signal state. The corresponding range control chart is illustrated in Figure 7.18.

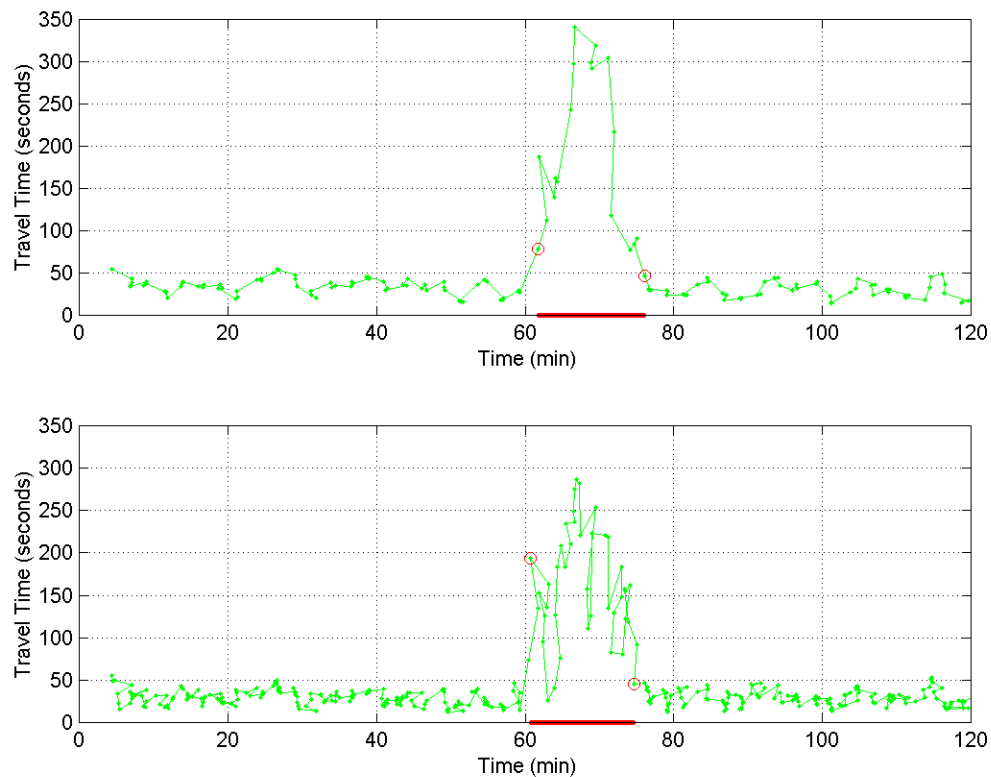


Figure 7.17: Transit probe (top) and transit with dedicated probe (bottom) central tendency control chart

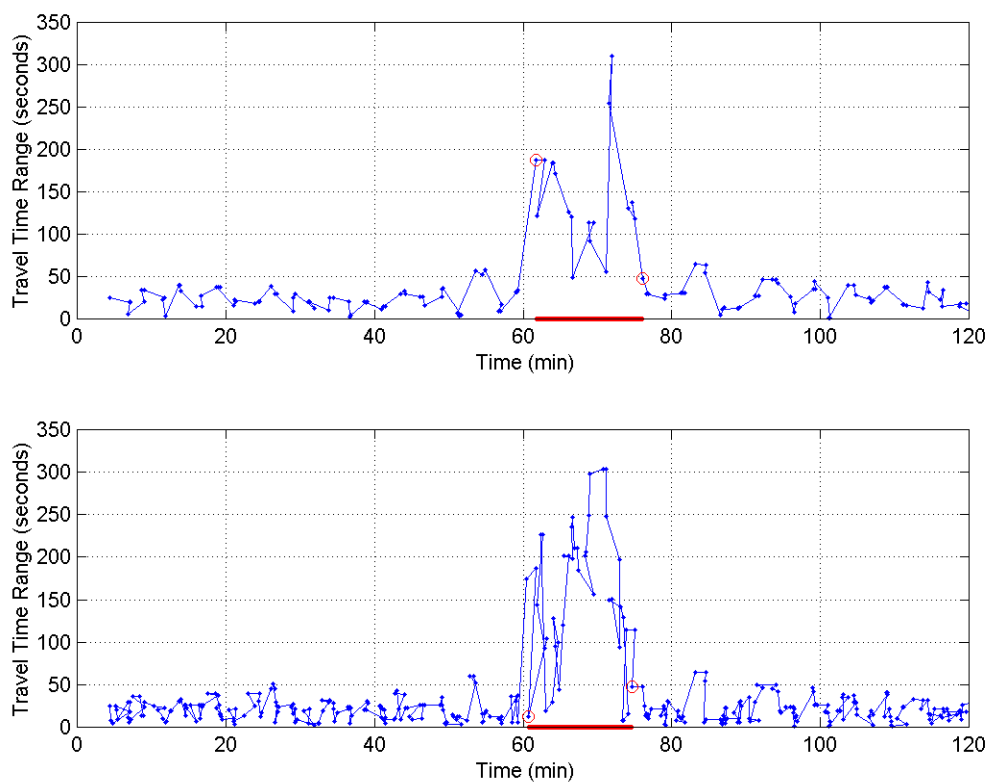


Figure 7.18: Transit probe (top) and transit with dedicated probe (bottom) range control chart

The above analysis presents only one simulation out of a total of six simulations conducted under Scenario 2. Five of these simulations were used for the acceleration noise based analysis in Section 7.3.1.2. Table 7.8 summarizes the DR, TTD and FAR statistics for all six simulations.

Table 7.8: Summary of DR, TTD and FAR for all simulations

Single Lane Incident (Middle Lane)		
	Transit Only	Transit and Dedicated
Simulations	6	6
TTD	227	148
DR	100	100
FAR	0	0

Table 7.8 shows that incident impact can be equally well detected in Type 2 street segments using the control chart approach. However, the TTD was much longer compared to Segment Type 1 streets. Furthermore, the time lag between transit only and combined probe scenarios was wider in Type 2 street segments.

#### **7.4 Analysis of Incident Detection Variables With Simulated GPS Errors**

The impact of GPS performance degradation was one of the major concerns investigated in this thesis. This section provides an impact analysis of the incident detection parameters with additional GPS errors. However, only a single error magnitude was investigated, corresponding to the largest error observed with the proposed vehicle-positioning algorithm in either the position or the velocity domain under urban canyon conditions. The analysis was limited to a comparison of TTD, DR and FAR parameters and figures indicating increased noise levels in the measurements. The following results are presented in an identical format to that of Section 7.3.

##### **7.4.1 Incident Detection Variable: Acceleration Noise**

Under degrading GPS performance, the probe vehicle acceleration noise is influenced through degrading velocity measurement quality. Therefore, simulated errors were included in the velocity measurements to mimic the impact of degrading GPS performance on vehicle acceleration noise. The magnitude of error was selected based on experimental results, and normally distributed random errors with a magnitude of up to  $1 \text{ ms}^{-1}$  were introduced in to velocity measurements.

###### **7.4.1.1 Incident Scenario 1**

Figure 7.19 depicts a comparison of speed contour plot for the 4<sup>th</sup> simulation of scenario 1 with open sky GPS conditions and with simulated GPS degradation. The top plot

shows the speed contours with open sky GPS conditions (depicted earlier in Figure 7.3), reproduced for the ease of comparison with the simulated GPS errors. The bottom plot of Figure 7.19 depicts the speed contours with additional GPS errors.

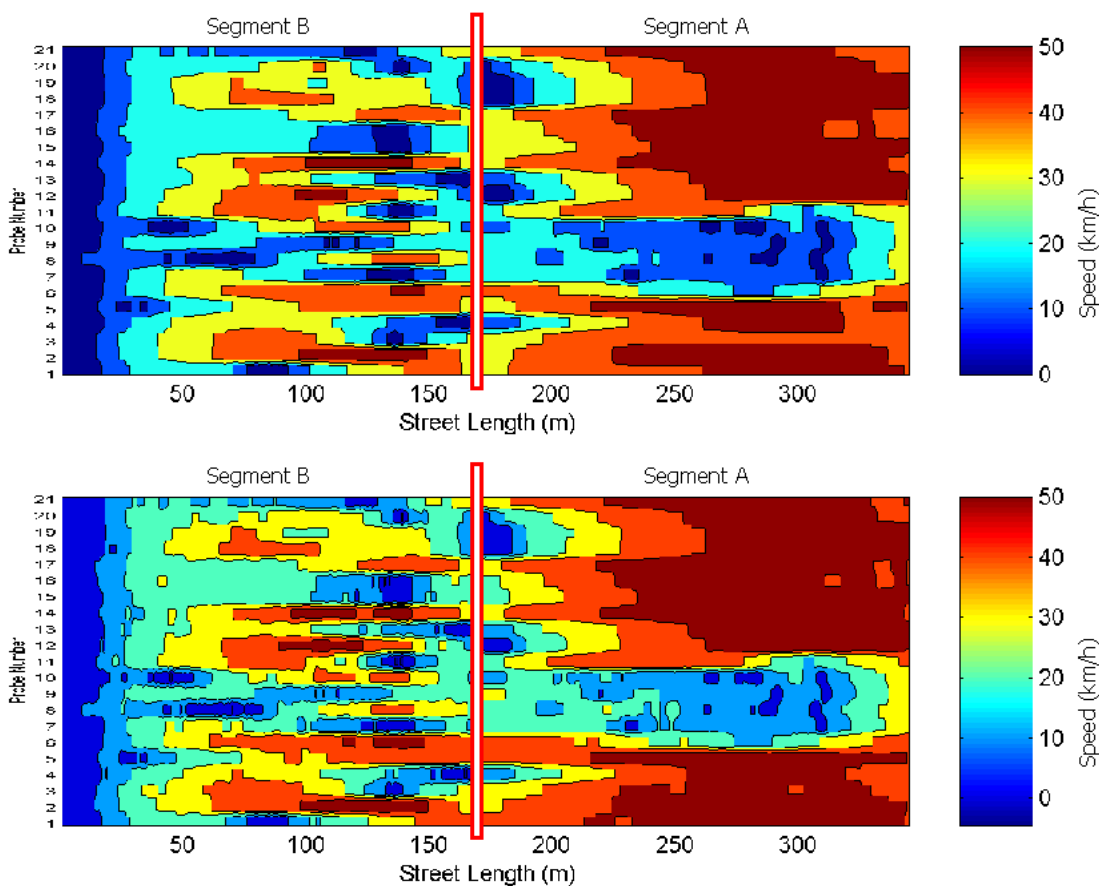


Figure 7.19: Speed contour plots for Simulation 4 of Scenario 1  
open Sky GPS (top) and with GPS errors (bottom)

The corresponding acceleration noise contour plot is depicted in Figure 7.20. Similar to the case in Figure 7.19, the top plot was reproduced from Figure 7.4, in which open sky GPS performance was assumed. The bottom plot shows increased acceleration noise due to increased GPS velocity measurement errors.

The total acceleration noise for all 21 transit probe vehicles is depicted in Figure 7.21. Although the majority of vehicles influenced by the incident (probes 6 to 11) show

increased total acceleration noise, the overall noise level under normal operation has increased by several magnitudes due to noisy velocity measurements.

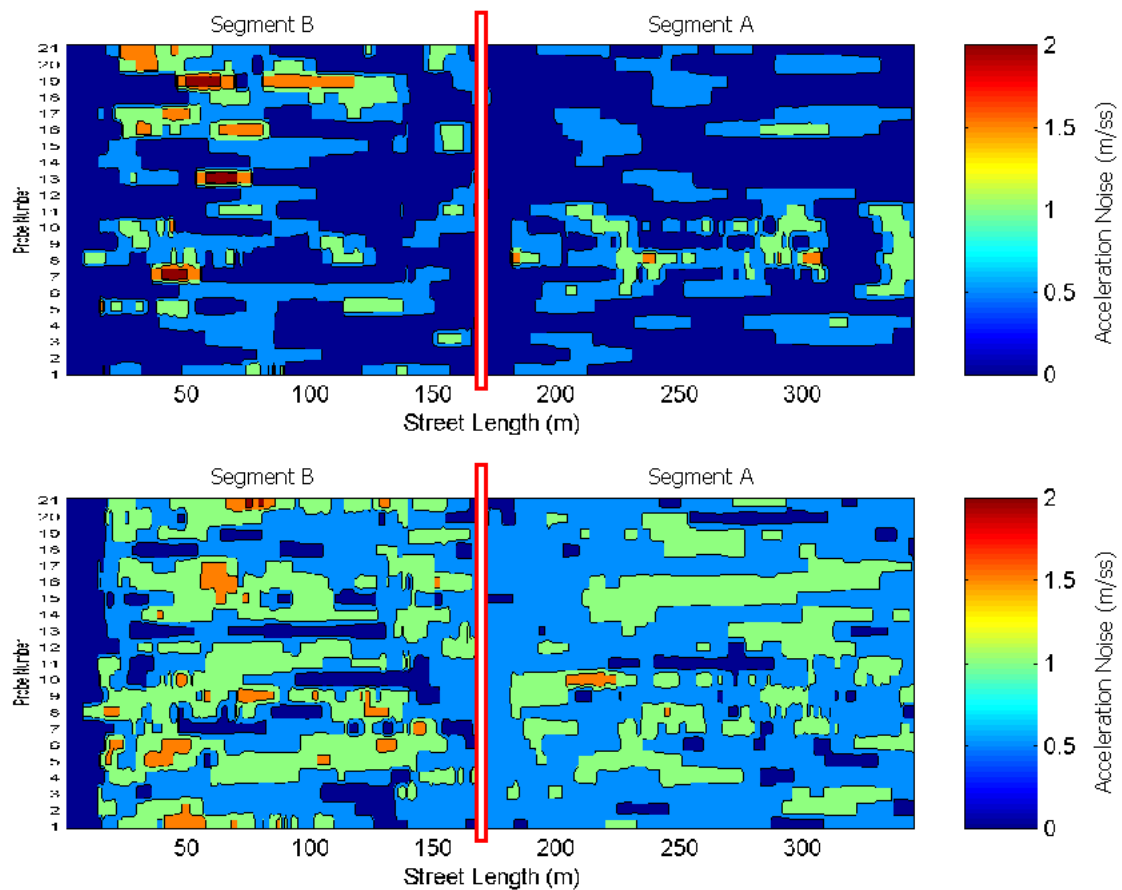


Figure 7.20: Acceleration noise contour plots for Simulation 4 of Scenario 1  
open sky GPS (top) and with GPS errors (bottom)

In order to estimate the acceleration noise thresholds for Segments 1 and 2, all probe vehicle speed profiles generated during normal operation were analyzed and the estimated thresholds are given in Table 7.9.

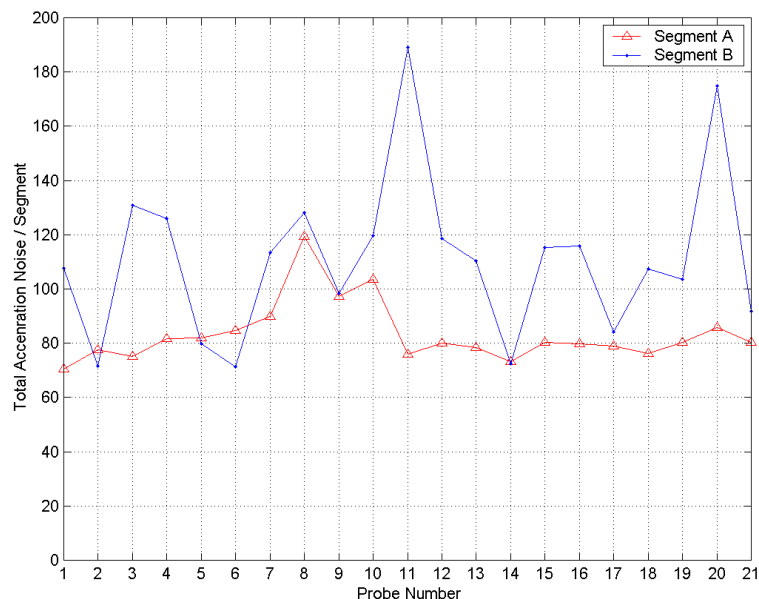


Figure 7.21: Acceleration noise street segment summations for Scenario 1: Test Run 4

Table 7.9: Acceleration noise statistics for normal operation: with simulated GPS errors

	Segment A	Segment B
Mean	93	115
Standard Deviation	26	33
Threshold	95	220
% Below Threshold	86	84

The values given in Table 7.9 and the corresponding set of values with open sky GPS, given as Table 7.2, show marked differences. For instance, thresholds established for the scenario with simulated GPS error were at least three times the values under open sky conditions. Furthermore, the confidence on the threshold was lower compared to the no GPS error scenario. The summary of TTD, DR and FAR parameters for individual simulations and for all simulations are given in Table 7.10.

Table 7.10: Acceleration noise-based detection in Segment A: summary for Scenario 1

Simulation No	Total Transit Probes		Incident Detection		DR	FAR
	Incident	Non-incident	Detected	False Alarms		
1	6	11	4	0	67	0
2	6	11	3	0	50	0
3	6	15	6	3	100	50
4	4	11	3	0	75	0
5	6	15	3	3	50	50
Total	28	63	19	6	68	21

Table 7.10 shows degrading DR and FAR parameters compared to the open sky GPS scenario. However, the results are still comparable to or better than existing arterial incident detection capabilities. These results are further discussed later in this chapter.

#### 7.4.1.2 Incident Scenario 2

For Scenario 2 simulations, only the summary TTD, DR and FAR values are presented and are given in Table 7.11.

Table 7.11: Acceleration noise-based detection on Segment B: summary for Scenario 2

Simulation No	Total Transit Probes		Incident Detection		DR	FAR
	Incident	Non-incident	Detected	False Alarms		
1	3	15	3	2	100	67
2	6	14	5	2	83	33
3	7	11	5	2	71	29
4	5	11	4	2	70	40
5	4	11	4	2	100	50
Total	25	62	21	10	84	40

## 7.4.2 Incident Detection Variable: Travel Time Variation

This section discusses the possibility of GPS performance degradation and the subsequent impact on measured travel times. Since the PARAMICS simulator does not allow intrinsic modeling of such errors, simulated travel time errors were introduced based on several assumptions. Two magnitudes of travel time error were considered, and the incident detection analysis was conducted for the worst-case scenario. Normally distributed travel time errors of magnitudes 2.5 seconds and 5 seconds were simulated for this analysis.

### 7.4.2.1 Street Segment Travel Time Analysis: Type 1

Depicted in Figure 7.22 are the estimated travel time distributions for street Segment A with open sky conditions (reproduced from Figure 7.9), normally distributed errors with a magnitude of 2.5 seconds and normally distributed errors with a magnitude of 5 seconds.

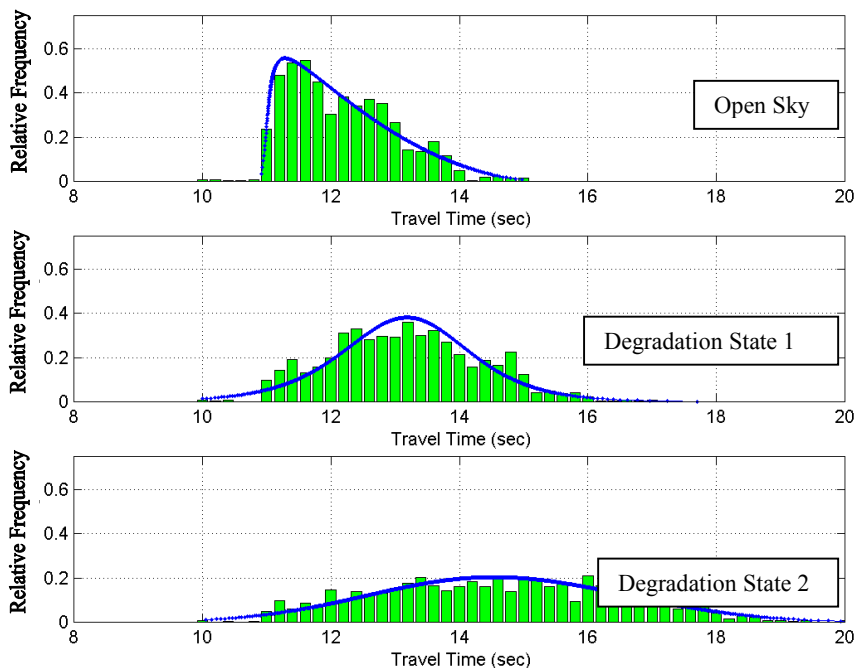


Figure 7.22: Travel time distribution in Street Segment A

Figure 7.22 shows the clear deformation of the initial travel time PDF fitted for the open sky conditions with degrading measurement capability. In the Degradation State 2, where travel time measurements up to 5 seconds were considered, the PDF has lost the shape of a lognormal function and has approached the shape of a normal distribution. Based on the techniques discussed in Chapter 4, the appropriate 95-percentile travel time was used as the Upper Control Limit (UCL) of the control chart for each degradation state.

#### 7.4.2.2 Street Segment Travel Time Analysis: Type 2

Figure 7.23 depicts the results of a similar analysis on travel time measurement error and its impact on the travel time PDF of Segment B travel times. The top plot illustrates the PDFs of two travel time clusters under open sky conditions (reproduced Figure 7.11). The rest of the plots show the impact of travel time measurement errors on these PDFs.

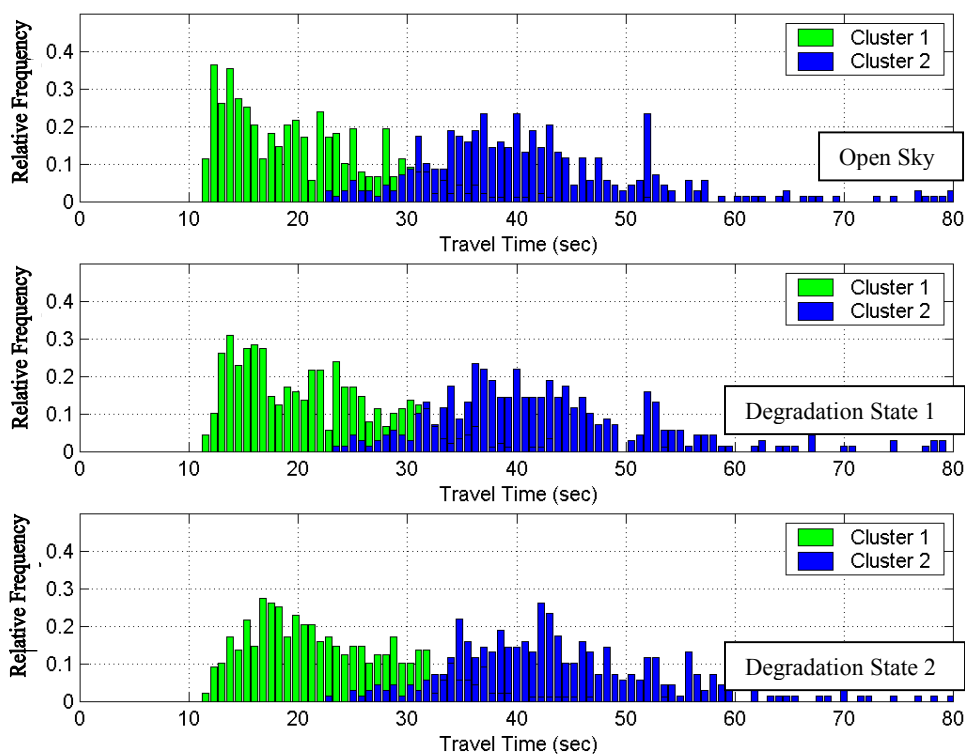


Figure 7.23: Travel time distribution with GPS errors

Travel time behaviour in a Type 2 street segment was discussed in detail earlier and under open sky conditions (top plot of Figure 7.23), the Cluster 1 travel times were successfully approximated using a lognormal distribution. The second cluster was approximated with a normal distribution. As illustrated by the second and the third plots in Figure 7.23, the Cluster 1 PDF deforms to a normal distribution while Cluster 2 retains its shape with increasing travel time errors.

#### 7.4.2.3 Travel Time Based Incident Detection: Type 1

Table 7.12 summarizes the TTD, DR and FAR parameters with simulated errors on travel time measurements in a Type 1 street segment. From the two error states considered in Sections 7.4.2.1 and 7.4.2.2, only the worst-case scenario was considered in this analysis.

Table 7.12: Average DR, TTD and FAR for all simulations: in-segment

Single Lane Incident (Middle Lane)		
	Transit Only	Transit and Dedicated
Simulations	12	12
TTD	171	88
DR	84	100
FAR	33	17
Single Lane Incident (Left Lane)		
	Transit Only	Transit and Dedicated
Simulations	3	3
TTD	363	207
DR	67	100
FAR	0	0
Two Lane Incident (Left and Middle Lane)		
	Transit Only	Transit and Dedicated
Simulations	3	3
TTD	71	40
DR	100	100
FAR	0	0

The first category of incidents in Table 7.12 (single lane incident in the middle lane) clearly shows the impact of additional errors with longer TTD and comparably poor DR and FAR values compared to the performance under open sky conditions, given as Table 7.6. The combined TTD has increased from 64 to 88 seconds and corresponding transit only value has increased from 91 to 171 seconds. The transit only detection rate has decreased to 84 % along with an increased FAR of 33 %. Whereas the combined DR has remained at 100 % with a lowered FAR of 17 %, thus indicating the robustness added by additional dedicated probes under degrading measuring capability. The incidents in the left lane were detected far later than the open sky scenario by transit only probes. Furthermore, one of the three incidents went undetected by the system, resulting in a DR of 67 %.

However, the two lane incidents were detected comparably faster than the first category of incidents. For instance, the TTD for open sky conditions with combined probe population was 29 seconds, which has only increased to 40 seconds and the corresponding transit only case has increased from 38 seconds to 71 seconds. Furthermore, both probe scenarios resulted in a DR of 100 % and a FAR of 0 %, indicating less performance degradation with increasing errors.

The TTD values for all simulations presented in Table 7.12 are graphically illustrated in Figure 7.24. The simulations are numbered in the same order as in Figure 7.15, using the same performance criteria under open sky conditions. The first three simulations correspond to the third incident category in Table 7.12 (two-lane incidents) while the last three simulations had the second incident category in Table 7.12 (single-lane incident in left lane). The rest of the TTD values depicted in Figure 7.24 correspond to single-lane incidents in the middle lane. The TTD for undetected incidents are shown as zero TTD.

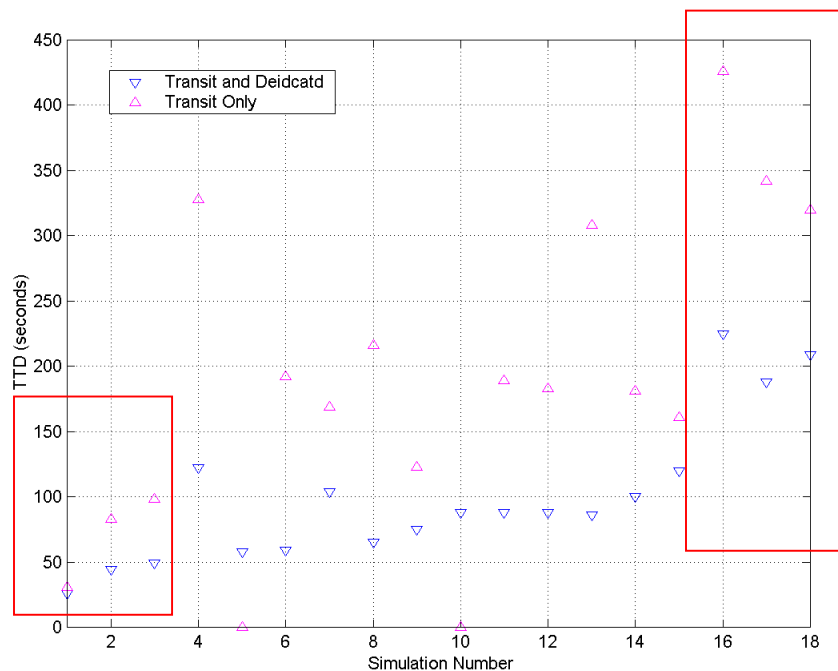


Figure 7.24: TTD for all simulations in Scenario 1

Table 7.13 shows the TTD, DR and FAR parameters for detecting the downstream incident using upstream data from Segment B. These values show considerable performance degradation compared to the performance under open sky condition given in Table 7.7. For instance, The TTD for transit only scenario has increased from 331 to 403 seconds and in the corresponding combined probe scenario from 249 to 322 seconds. Furthermore, the transit only DR has decreased and the FAR had increased to 33 % for combined probe approach.

Table 7.13: Summary of DR, TTD and FAR for all simulations: downstream segment

Two Lane Incident (Left and Middle Lane)		
	Transit Only	Transit and Dedicated
Simulations	3	3
TTD	403	322
DR	67	100
FAR	0	33

#### 7.4.2.4 Travel Time Based Incident Detection: Type 2

Table 7.14 summarizes the results from all simulations with simulated incident in Segment B and with simulated GPS errors.

Table 7.14: Average DR, TTD and FAR for all simulations: in-segment

Single Lane Incident (Middle Lane)		
	Transit Only	Transit and Dedicated
Simulations	6	6
TTD	275	187
DR	84	100
FAR	0	33

Compared to the results presented in Table 7.8 under open sky conditions, simulated travel time errors have resulted in longer TTDs, lower DR and higher FAR. For instance, the TTD had increased by almost a minute for the transit only case, whereas the increase for the combined probe approach was around 40 seconds. Furthermore, the transit-only DR has declined to 84 % and combined case FAR has increased to 33 %.

### 7.5 Incident Detection With Travel Time and Acceleration Noise

The combined incident detection approach involves monitoring the travel time variation and acceleration noise increase for all probe vehicles as a time series analysis. In order to illustrate the concept involved, travel time records and acceleration noise measurements of all probe vehicles recorded for acceleration noise based analyses were combined in the following illustration. A total of 70 transit probe vehicles with both travel time, acceleration noise measurements were used for this analysis, and 30 of those probes were influenced by simulated incidents. The central tendency control chart values and the

acceleration noise value of all those probes were plotted as a function of time in Figure 7.25. The vertical time axis shows the recorded exit time of each transit probe from street Segment A.

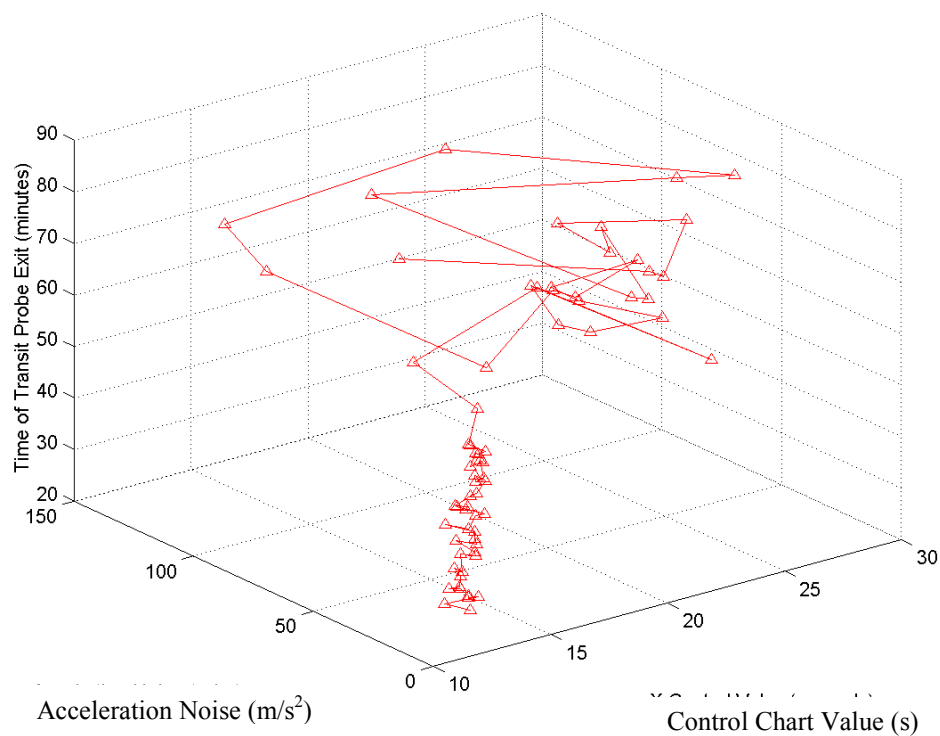


Figure 7.25: Time evolution of central tendency control and acceleration noise

Figure 7.25 shows a series of clustered points up to around 60 minute exit time, and the following values show large variations, indicating large acceleration noise or central tendency control chart values. Figure 7.26 shows the two variable plots of Figure 7.25 and further illustrates the creation of an out-of-control region in Figure 7.25.

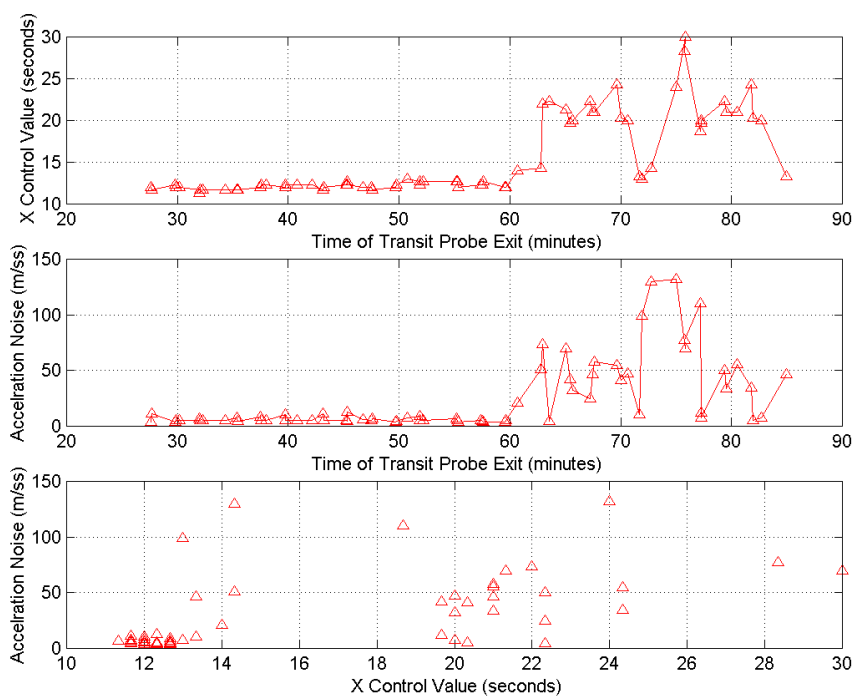


Figure 7.26: Central tendency control and acceleration noise

The in-control region has distinctively smaller variation in time, thus the transition can be clearly identified. Illustrated in Figures 7.27 and 7.28 is the time evolution of the  $\bar{X}$  - Acceleration noise time series in the in-control region, up to the 60 minute exit time.

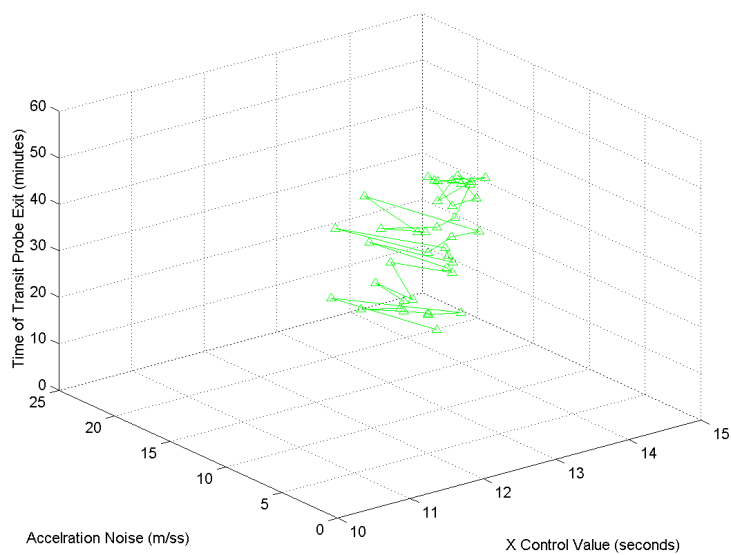


Figure 7.27: Time evolution of central tendency control and acceleration noise during normal operation

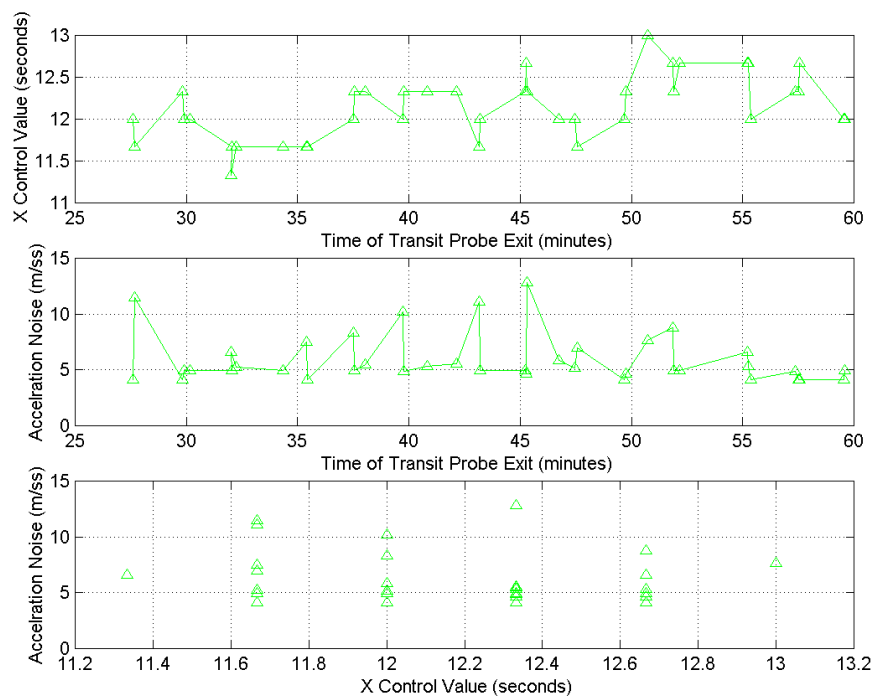


Figure 7.28: Central tendency control and acceleration noise during normal operation

Based on the analysis presented in Figures 7.27 and 7.28, a control region can be defined using the central tendency control limits and acceleration noise. A deviation from the in-control region was declared as an incident, effectively combining the performance of individual incident detection parameters.

## CHAPTER EIGHT

### CONCLUSIONS AND FUTURE DIRECTIONS

#### 8.1 CONCLUSIONS

As two major research areas were addressed, namely vehicular navigation systems in the context of Intelligent Transportation Systems applications and automated traffic incident detection using transit vehicle tracking data, the conclusions are also presented classified into two categories. The concluding remarks relate to the objectives discussed in Section 1.3.

##### 8.1.1 Vehicular Navigation Systems for ITS

###### **Uninterrupted Vehicle Tracking Using GPS and HSGPS**

An analysis of GPS and HSGPS receiver technology performance for vehicle navigation was presented for different operation environments. Emphasis was given to urban environments where standard GPS performance degrades considerably. The advantages offered by HSGPS and the augmentations that could improve its performance were discussed. A range of augmentation techniques was tested with HSGPS for urban vehicular navigation.

As illustrated by numerous field experiments in this thesis, HSGPS provides far better availability over conventional GPS. However, the compromise in accuracy in gaining improved availability was addressed. This thesis presents an analysis of typical HSGPS accuracy degradation scenarios in urban vehicular navigation. Several approaches were presented to improve the accuracy of HSGPS especially in urban vehicular navigation and the improvements gained were illustrated using field-testing. Furthermore, future

research needs for building HSGPS-based high availability and high-accuracy vehicle navigation systems were also identified.

### **Map-Matching as an Augmentation to HSGPS**

Map-matching was considered the primary augmentation technique for HSGPS in the context of the application in this thesis. Extending beyond the conventional across-track error minimization approach in map-matching, a technique was developed for minimizing the along-track errors in urban vehicle navigation. Furthermore, the prior knowledge of vehicle route was also utilized for improved vehicle navigation performance, particularly applicable for transit vehicle navigation and positioning. Finally, the performance of these augmented HSGPS/ map-matching systems were illustrated with extensive field-testing involving both transit vehicles and non-transit probe vehicles.

#### **8.1.2 Automated Traffic Incident Detection**

##### **Vehicle Tracking Information Processing for Traffic Engineering Application**

A vehicle tracking information framework was developed and data archiving and integration techniques were developed for combining historical and real-time information. The framework was implemented using a Kalman filter, and it also enables the detection of outliers in travel time data reports. The analysis presented in this thesis was limited to a single time period with uniform traffic demand. However, varying demand can be accommodated by segmenting the daily or hourly demand variation into time intervals with approximately constant demand (for instance into 15 minute intervals) and applying the algorithm for individual intervals.

### **Probe-Based Traffic Incident Detection Parameters**

Two traffic incident detection parameters were investigated using probe vehicle tracking data, namely street segment travel time variations and acceleration noise. These two parameters were extensively analyzed with varying accident characteristics and varying degree of GPS degradation, which could result in degrading detection capability in urban environments. The analysis shows the robustness of the parameters and the advantage of combining the parameters in a complementary manner.

### **Traffic Incident Detection Algorithm**

The incident detection algorithm developed in this thesis represents an optimum combination of incident detection parameters with respect to fast and accurate incident detection capability and lowest likelihood for false alarms. As illustrated by the simulation results, the algorithm provides a very high incident Detection Rate and a fast Time To Detect while maintaining a low False Alarm Rate. Although a slight degradation was noted with GPS performance degradation, the algorithm still provides better performance with good GPS availability and better or at least comparable performance with existing arterial incident detection algorithms even under degraded GPS performance.

### **Passive Probe Vehicles for Traffic Monitoring and Incident Detection**

This thesis contributes significantly to the current state of knowledge in the use of passive probe vehicles for traffic monitoring and incident detection. Techniques were developed to minimize biases in passive probe vehicle tracking data, and the degree of success in doing so was illustrated through field experiments and simulated data. The limitations in using passive probe vehicles alone as the probe vehicle fleet was also identified, and

remedial measures such as the use of additional dedicated probe vehicles were investigated. Although traffic monitoring in general was not specifically addressed, the improvements observed with additional dedicated probe vehicles suggest the potential for using this system as a traffic performance monitoring system.

### **Performance Evaluation of Incident Detection Algorithms**

The incident detection algorithm developed herein was extensively tested using simulation techniques. Although testing with a working prototype would add more practical sense to it, simulation based testing provided highly controllable test environment for investigating detailed performance issues of the algorithm. The results illustrate the effectiveness of individual incident detection parameters and the robustness of the combined algorithm, especially with degrading GPS performance typical of urban environments.

### **Quantifying GPS Performance Levels**

The analysis conducted in this thesis has revealed that probability density functions established for travel time variations in street segments are equally influenced by two factors, namely travel time measurement errors and fluctuating traffic congestion levels. Therefore, any algorithm that monitors street segment travel time variation as a measure of incident induced congestion must have a mechanism that can distinguish between incident induced longer travel times and longer travel times resulting from travel time measurement errors, often arising from poor vehicle positioning system performance. This research proposes a vehicular navigation system that can provide timely system accuracy information for the incident detection process, providing this critical requirement.

### **Transit Only vs. Dedicated Probes**

The results show that incidents that have a major impact on the traffic circulation could be equally well detected by using only transit vehicles and the performance gained is marginal. For instance, incidents that reduced the roadway capacity by over 50 percent were equally well detected by using only the transit probes and transit and dedicated probes, although marginal performance gains do exist with additional dedicated vehicle data. Furthermore, transit only probe systems perform relatively well even with degrading GPS performance in detecting incidents with a large impact, whereas incidents with lesser impact may go undetected under such conditions.

### **Downstream Incident Detection Using Upstream Data**

Detecting downstream incidents using upstream data was only feasible with incidents that cause major disruptions to the roadway traffic. Based on the simulation results, the capability to detect single-street incidents using upstream data was almost negligible, however, two-street segments that reduced the roadway capacity below 50 percent were detected successfully even with transit only probe systems. However, with the influence of GPS errors, transit only system performance degrades considerably, and the use of additional dedicated probes provides considerable increase in system reliability.

## **8.2 Future Directions**

Although effort was made to gain complete insight into several research areas where little or no previous knowledge existed, some assumptions and simplifications were made to limit the scope of this thesis, and thus to make it achievable within the time and resources available. Some key issues are identified that need to be investigated further to bridge the gap between the knowledge base gained from this research and the ultimate objective of

developing a system that works based on those principles. These future directions are also addressed as two areas, automated traffic incident detection using transit vehicle tracking data and vehicle navigation in urban environments, two research areas that formed the foundation of this thesis.

### **8.2.1 Vehicular Navigation Systems in ITS**

#### **HSGPS and Filtering Techniques**

The availability advantage of HSGPS, especially in urban vehicular navigation applications, is clearly illustrated through the field experiments described in this thesis. However, of the two measurement options available with the HSGPS receivers used in this thesis as discussed in Section 4.1.4, this research used receiver-generated filtered measurements, due to the advantages it offers from the application point of view. Furthermore, augmentation techniques were used to ensure that any biases resulting from receiver internal filtering had minimal impact on the final GPS measurement. Based on the empirical findings of this research, it is identified as a requirement and is considered feasible to develop a filtering technique that uses HSGPS pseudorange measurements to achieve similar results to internally filtered HSGPS.

### **8.2.2 Automated Traffic Incident Detection**

#### **Field Proof-of-Concept Studies**

The incident detection parameter analysis and incident detection algorithm performance evaluation presented in this thesis were based on simulated results. Although the microscopic traffic simulation approach provides the best alternative over field experiment oriented proof-of-concept study, it may not represent a perfect match for the real system. For instance, these simulations did not consider factors such as drivers using

alternative routes to bypass incident induced congestion or impact of ITS strategies such route guidance information systems. A field proof-of-concept study with conventional and ITS sensors, conducted over long period of time to record sufficient number of incidents, would provide the necessary practical dimension to the work presented in this thesis.

### **Incident Detection Variables and Traffic Flow Variation**

The analysis presented in this thesis was conducted with the typical traffic flow demands observed in the morning peak period in downtown Calgary along with the typical vehicle mix observed in the same period of operation. The response of incident detection parameters may vary with changing traffic volume capacity ratio and vehicle mix. For instance, acceleration noise may have considerably higher normal operation values with increased congestion or with larger heavy vehicle proportion that would result in reduced roadway capacity, thus generating similar effects, although not as intensely as in the case of larger traffic volumes. Therefore, it is not possible to generalize the success rate observed in this work to traffic conditions outside of the range investigated in this thesis. Hence, further work is needed to study the characteristics of both travel time variation and acceleration noise under varying conditions.

### **Combining Fixed Sensor Data With Probe Vehicle Data**

Even though new ITS traffic monitoring techniques, including the system proposed in this thesis are emerging rapidly and have proven their effectiveness, many cities around the world still use conventional traffic monitoring techniques such as inductive loop detectors. Considering the infrastructure built around such legacy systems, new generation techniques are likely to appear as add-on systems rather than total replacements. Therefore, the ability to seamlessly integrate with existing systems and

share conventional sensor data will greatly improve the attractiveness of ITS incident detection systems. Hence, more work is needed on building sensor integration strategies for ITS incident detection systems, especially for integrating conventional traffic sensor data.

## REFERENCES

- Bar-Shalom, Y. and T. Fortmann (1988) Tracking and Data Association. Mathematics in Science and Engineering, 179, Academic Press.
- Basnayake, C. and G. Lachapelle (2003) Accuracy and Reliability Improvement of Standalone High Sensitivity GPS Using Map Matching Techniques. Proceedings of ION AM 2003, Albuquerque, NM, pp. 209-216. The Institute of Navigation.
- Basnayake, C., O. Mezentsev, G. Lachapelle and M. E. Cannon (2004) A Portable Vehicular Navigation System Using High Sensitivity GPS Augmented with Inertial Sensors and Map-Matching. SAE 2004 World Congress, Detroit, MI. Society of Automotive Engineers.
- Bayarri, M. J., J. O. Berger, N. M. Rouphail and J. Sacks (2003) Assessing Uncertainties in Traffic Simulation: A Key Component in Model Calibration and Validation. Report No. 137. National Institute of Statistical Sciences (NISS).
- Bhandari, N., F. S. Koppelman , J. L. Schofer, V. Seti V, and J. N. Ivan (1995) Arterial Incident Detection: Integrating Data from Multiple Sources. Transportation Research Record, 1510, pp. 60-69.
- Biacs, Z., G. Marshall, M. Moeglein and W. Riley (2002) The Qualcomm/ SnapTrack Wireless Assisted GPS Hybrid Positioning System and Results from Initial Commercial Deployments. Proceedings of GPS ION 2002. The Institute of Navigation.
- Booz, Allen & Hamilton (1998) Incident Management: Detection, Verification and Traffic Management: A Cross-Cutting Study. Report No. FHWA-RD-JPO-034. Federal Highways Administration, U. S. Department of Transportation, Washington, DC.

Brackstone, M., M. McDonald, B. Sultan, and B. Mould (2000) Five Years of the Instrumented Vehicle: What Have We Learned? Traffic Engineering and Control. June 2000.

Cambridge Sys Inc., H. Cohen and Science Applications International Corporation (1998) Sketch Methods for Estimating Incident Related Impacts. Report No. DTFH61-95-00060: 21. Office of Environment and Planning, Federal Highway Administration, Washington, D. C.

Cannon, M. E., C. Basnayake, S. Syed and S. Crawford (2003) A Precise GPS Sensor Subsystem for Vehicle Platoon Control. Proceedings of GPS ION 2003. Portland, OR. The Institute of Navigation.

Chansarkar, M. and L. Garin (2000) Acquisition of GPS Signals at Very Low Signal to Noise Ratio. Proceedings of GPS National Technical Meeting 2000. The Institute of Navigation.

Collin, J., J. Kappi, J. Saarinen (2001) Unaided MEMS-based INS Application in a Vehicular Environment. Proceedings of ION GPS 2001. pp. 1343-1348. The Institute of Navigation.

Corby, M. J. and F. F. Saccomanno (1997) Analysis of Freeway Accident Detection. Transportation Research Record, 1603, pp.80-89.

Dion, F. and H. Rakha (2004) Estimating Spatial Travel Times Using Automatic Vehicle Identification Data. National Transportation Library, US Department of Transportation. [www.ntl.bts.gov](http://www.ntl.bts.gov)

Druitt, S. (1998a) An Introduction to Microsimulation. Traffic Engineering and Control, September 1988.

Druitt, S. (1998b) Some Real Applications of Microsimulation. Traffic Engineering and Control, November 1998.

Druitt, S. and J. Laird (1999) Edinburgh City Centre: A Microsimulation Case Study. Traffic Engineering and Control, February 1999.

Eddie, L. C. (1961) Car-following and Steady State Theory for Non-Congested Traffic. Operation Research, 9(1), pp. 66-76.

Gallagher, J. (1996) Travel Time Data Collection Using GPS. National Traffic Data Acquisition Conference (NATDAC '96), New Mexico. pp. 147-161.

Gelb, A. (1974) Applied Optimal Estimation. M. I. T. Press, Cambridge, Massachusetts.

Graves, T. L., A. F. Karr and P. Thakuriah (1998) Variability of Travel Times on Arterial Links: Effects of Signals and Volume. National Institute of Statistical Sciences (NISS).

Greenfeld, J. (2002) Matching GPS Observations to Locations on a Digital Map. Proceedings of 81st Annual Meeting of the Transportation Research Board, Washington, DC.

Greenwood, I. D., R. C. M. Dunn and R. R. Raine (1998) Modeling Non-Steady Speed Driving. ARRB Transport Research, Sydney, Australia.

Grey, E (2002) Peak Traffic Trends in Calgary Between 1991 and 2001 Based on Permanent Count Station Data. Transportation Data Division, Planning and Transportation Policy, The City of Calgary

Hall, R. W. and N. Vyas (2000) Buses as a Traffic Probe: Demonstration Project. Transportation Research Record, 1731, pp. 96-103.

Hall, R. W., N. Vyas, C. Shyani, V. Sabnani and S. Khetani S (1999) Evaluation of the OCTA Transit Probe System. Report No. UCB-ITS-PRR-99-39. California Partners for Advanced Transit and Highways (PATH).

Han, L. D. and A. D. May (1988) Artificial Intelligence Approaches for Signalized Network Control. Working Paper USB-ITS-WP-88-4. Institute of Transportation Studies, University of California, Berkeley, CA.

Han, L. D. and A. D. May (1989) Automatic Detection of Traffic Operational Problems on Urban Arterials. Working Paper UCB-ITS-RR-89-15. Institute of Transportation Studies, University of California, Berkeley, CA.

HCM2000 (2000). Highway Capacity Manual 2000. Transportation Research Board (TRB).

He, R. R., H. X. Liu, A. L. Kornhauser and B. Ran (2002) Temporal and Spatial Variability of Travel Time. Report No. UCI-ITS-WP-02-10. Institute of Transportation Studies, University of California, Irvine, CA.

Hellinga, B. R. and L. Fu (2002) Reducing Bias in Probe-Based Arterial Link Travel Time Estimates for ITS Applications. Transportation Research Part C: Emerging Technologies, 10(4), pp. 257-273.

Hellinga, B. R. and G. Knapp (2000) Automatic Vehicle Identification Technology-Based Freeway Incident Detection. Transportation Research Record, 1727, pp. 142-153.

Hermann, R. (1959) Traffic Dynamics: Analysis of Stability in Car Following. *Operational Research*, 7, pp. 86-106.

Hounsell, N. B., M. McDonald and C. F. S. Wong (1988) Traffic Incidents and Route Guidance in a SCOOT Network. PTRC Transport and Planning Summer Annual Meeting. University of Bath, England

Ibrahim, D. (2000) Improving Accuracy for GPS Vehicle Navigation Systems in London. *Traffic Engineering and Control*, June 2000, pp. 228-232.

ITS America (1992) Strategic Plan for Intelligent Vehicle Highway Systems in The United States. ITS America, Washington D.C.

ITS Canada (2000) ITS Architecture for Canada. Intelligent Transportation Systems, Transport Canada.

ITS US DOT (2000) Incident Management Successful Practices: A Cross-Cutting Study. US Department of Transportation.

Karian, Z. A. and E. J. Dudewicz (2000) Fitting Statistical Distributions: The Generalized Lambda Distribution and Generalized Bootstrap Methods. CRC Press, Washington, D.C.

Koppelman, F. S., C. Wen, W. Lin and T. Peng (1996) ADVANCE: Evaluation of Arterial Probe Vehicle, Fixed Detector and Expressway Fixed Detector Incident Detection Algorithms. Final Report. Transportation Centre, North Central University, Evanston, Illinois.

Kuhne, R. and P. Michalopoulos (1992) Continuum Flow Models. *Traffic Flow Theory: A State of the Art Report*, N. Gartner, C. J. Messer and A. K. Rathi, eds., Turner-

Fairbank Highway Research Center, Federal Highway Administration, U.S. Department of Transportation.

Kuusniemi, H. and G. Lachapelle (2004) GNSS Signal Reliability Testing in Urban and Indoor Environments. Proceedings of NTM 2004 (San Diego, January 24-28), pp. 210-224. The Institute of Navigation.

Laird, D. (1996) Emerging Issues in the Use of GPS for Travel Time Data Collection. National Traffic Data Acquisition Conference (NATDAC '96), New Mexico. pp. 117-123.

Lieberman, E. and A. K. Rathi (1992) Traffic Simulation. Traffic Flow Theory: A State of the Art Report. N. Gartner, C. J. Messer and A. K. Rathi, eds., Turner-Fairbank Highway Research Center, Federal Highway Administration, U.S. Department of Transportation.

MacGougan, G., G. Lachapelle, R. Klukas, K. Siu, L. Garin, J. Shewfelt, and G. Cox (2002) Performance Analysis of A Stand-Alone High Sensitivity Receiver. GPS Solutions, 6(3), pp. 179-195. Springer Verlag.

McDonald, M. and M. Brackstone (1997) The Role of the Instrumented Vehicles in the Collection of Data on Driver Behaviour. Monitoring of Driver and Vehicle Performance Colloquium. Institute of Electrical Engineers.

McDonald, M., M. Brackstone, B. Sultan and C. Roach (1997) Close Following on the Motorway: Initial Findings of an Instrumented Vehicle Study. Proceedings of 7<sup>th</sup> Vision in Vehicles Conference, Marseille, France.

Metropolitan Transportation Commission: San Francisco (2001) 511 Case Studies, San Francisco Bay Area. U. S. Department of Transportation.

Mezentsev, O., G. Lachapelle, Y. Lu and R. Klukas (2002) Vehicular Navigation in Urban Canyons Using a High Sensitive Receiver Augmented With Low Cost Sensors. Proceedings of GPS 2002, Portland, Oregon. The Institute of Navigation.

Misra, P. and P. Enge (2001) Global Positioning System: Signals, Measurements, and Performance. Ganga- Jamuna Press, Lincoln.

Moore, M. and J. Wang (2003) An Extended Dynamic Model for Kinematic Positioning. Journal of Navigation, 56, pp. 79-88.

Moore, J., S. Cho, A. Basu and D. Mezger (2001) Use of Los Angeles Freeway Service Patrol Vehicles as Probe Vehicles. Report No. UCB-ITS-PRR-2001-5, California PATH Program.

NAVCEN (2004) US Coast Guard Navigation Center. [www.navcen.uscg.gov](http://www.navcen.uscg.gov)

NCHRP (1998) Multimodal Transportation: Performance Based Planning Process. Report No. NCHRP 8-32(02). National Cooperative Highway Research Program (NCHRP), Transportation Research Board (TRB), Washington, DC.

NCHRP (2003) Performance Measures of Operational Effectiveness for Highway Segments and Systems. Report No. NCHRP Synthesis 311. Transportation Research Board, Washington, D. C.

NCHRP 20-58 (2002) Interim Planning Activities for a Future Strategic Highway Research: Reliability. Report No. NCHRP 20-58. National Cooperative Highway Research Program (NCHRP), Transportation Research Board (TRB), Washington DC.

Parkany, A. E. and D. Bernstine (1993) Using VRC Data for Incident Detection. Pacific Rim TransTech Conference, ASCE 3rd International Conference on Application of Advanced Technologies in Transportation Engineering, Seattle, WA.

Parkinson, B. W., J. J. Spilker and P. Axelard (1996) Global Positioning System: Theory and Applications. American Institute of Aeronautics and Astronautics.

PBS&J (2001) Innovative Traffic Data Collection: An Analysis of Potential Uses in Florida. Technical Memorandum No.1. PBS&J, Tallahassee, Florida.

Peeta, A. and D. Das (1998) Continuous Learning Framework for Freeway Incident Detection. Transportation Research Record, 1644, pp. 124-131.

Petovello, M. G., M. E. Cannon, G. Lachapelle (2000) Operating Manual, Combined Code and Carrier for Navigation with GPS and GLONASS (C<sup>3</sup>NAVIG<sup>2</sup>™). Position, Location and Navigation (PLAN) Group, Department of Geomatics Engineering, University of Calgary.

Petovello, M. G. (2003) Real-Time Integration of a Tactical-Grade IMU and GPS for High-Accuracy Positioning and Navigation, PhD Thesis, Department of Geomatics Engineering, University of Calgary

URL <http://www.geomatics.ucalgary.ca/links/GradTheses.html>

Raud, R. A. and J. L. Schofer (1997) Managing Incidents on Urban Arterial Roadways. Transportation Research Record, 1603, pp. 12-19.

Roden, D. (1996) Travel Time Data Collection Using GPS Technologies. Proceedings of National Traffic Data Acquisition Conference (NATDAC '96), New Mexico, pp. 163-182.

Roden, D. (1997) GPS-Based Travel Time Data Collection. 76th Annual Meeting of the Transportation Research Board, Washington, DC.

Sacks, J., N. M. Rouphail, B. Park and P. Thakuriah P (2002) Statistically-Based Validation of Computer Simulation Models in Traffic Operations and Management. *Journal of Transportation and Statistics*, 5(1), pp. 1-15.

Sanwal, K. and J. Walrand (1995) Vehicles as Probes. Report No. UCB-ITS-PWP-95-11. California PATH Program.

Scott, C. and C. Drane (1994) Increased Accuracy of Motor Vehicle Position Estimate By Utilizing Map Data, Vehicle Dynamics, and Other Information Sources. *Proceedings of Vehicle Navigation and Systems Conference*, pp. 585-590. IEEE.

Sermons, M. W. and F. S. Koppelman (1996) Use of Vehicle Positioning Data for Arterial Incident Detection. *Transportation Research Part C: Emerging Technologies*, 4(2), pp. 87-96.

Seti, V, N. Bhandari, F. S. Koppelman and J. L. Schofer (1995) Arterial Incident Detection Using Fixed Detector and Probe Vehicle Data. *Transportation Research Part C: Emerging Technologies*, 3(2), pp. 99-112.

SIAS Limited (2002) PARAMICS 2002 Reference Manual. SIAS Limited, Manor Place Edinburg

SIRF Technologies (2004) [www.sirf.com](http://www.sirf.com)

Sirinivasan, K. and P. Jovanis (1996) Determination of Number of Probe Vehicles Required for Reliable Travel Time Measurements in Urban Network. *Transportation Research Record*, 1537, pp. 15-22.

Stephanedes, Y. J., A. P. Chassiakos and P. Michalopoulos (1992) Comparative Performance Evaluation of Incident Detection Algorithms. Transportation Research Record, 1360, pp. 50-57.

Stephen, J. (2000) Operation of an Integrated Vehicle Navigation System in a Simulated Urban Canyon. Proceedings of ION GPS 2000, 19-22 September 2000, Salt Lake City, UT, The US Institute of Navigation.

Stephen, J., Development of a Multi-Sensor GNSS Based Vehicle Navigation System, M.Sc. Thesis, Department of Geomatics Engineering, University of Calgary. UCGE Report No. 20140.

URL <http://www.geomatics.ucalgary.ca/links/GradTheses.html>

Thancanamootoo, S. and M. G. H. Bell (1988) Automatic Detection of Traffic Incidents on a Signal Controlled Network. Transport Operations Research Group No. 76. University of Newcastle-upon-Tyne, Newcastle-upon-Tyne, U. K.

TrafficMaster (2004) [www.trafficmaster.co.uk](http://www.trafficmaster.co.uk).

Transport Canada (2004) Intelligent Transportation Systems, Getting There Together: Smart Transport and Safe Travel. Transport Canada: [www.its-sti.gc.ca](http://www.its-sti.gc.ca)

TRB (2004) Collecting, Processing, and Integrating GPS Data into GIS: A Synthesis of Highway Practice. Report No. NCHRP 301. National Cooperative Highway Research Program. Transportation Research Board.

U. S. Coast Guard Navigation Center (NAVCEN) [www.navcen.uscg.mil](http://www.navcen.uscg.mil)

Walpole, R. E., R. H. Myers, S. L. Myers and K. Ye (2002) Probability and Statistics for Engineers and Scientists. Prentice Hall, New Jersey.

Wells, D E., N. Beck, D. Delikaraoglou, A. Kleusberg, E. J. Krakiwsky, G. Lachapelle, R. B. Langley, M. Nakiboglou, K. P. Schwarz, J. M. Tranquilla and P. Vanicek P (1986) Guide to GPS Positioning. Canadian GPS Associates

[http://plan.geomatics.ucalgary.ca/special\\_publications.html](http://plan.geomatics.ucalgary.ca/special_publications.html)

White, C. B., D. Bernstine, A. L. Kornhauser (2000) Some Map-Matching Algorithms for Personal Navigation Assistants. Transportation Research C, 8, pp. 91-108.

Winzer, T. (1980) Measurement of Acceleration Distributions. Research on Road Construction and Traffic Engineering. Research on Road Construction and Traffic Engineering, 319. Bonn, Germany.

Wolshon, B. and Y. Hatipkarasulu (2000) Results of Car-Following Analyses Using Global Positioning System. Journal of Transportation Engineering, July/ August, pp. 324-331.

Woo, M. and J. Choi (2001) Carrier Phase GPS/ Millimeter-Wave Radar for Vehicle Platooning. Proceedings of International Symposium on Industrial Electronics. Pusan, Korea. pp. 1548-1552. IEEE.

Yim, Y. and R. Cayford (2001) Investigation of Vehicles as Probes Using Global Positioning System and Cellular Phone Tracking: Field Operational Test. Report No. UCB-ITS-PWP-2001-9, California PATH Program.

## APPENDIX A

### SIMULATION MODEL BUILDING AND DATA

#### A1. Aerial Photographs of Modeled Area

Shown below are some of the aerial photographs of the modeled area. These were used to verify the PARAMICS microsimulator model features of downtown and suburban Calgary (Provided by The Transportation Data Division, The City of Calgary).



Figure A1: Centre Street/ North of 2<sup>nd</sup> Avenue (1)



Figure A2: Centre Street/ North of 2<sup>nd</sup> Avenue (2)



Figure A3: Centre Street/ South of 2<sup>nd</sup> Avenue



Figure A4: Centre Street/ 3<sup>rd</sup> and 4<sup>th</sup> Avenues

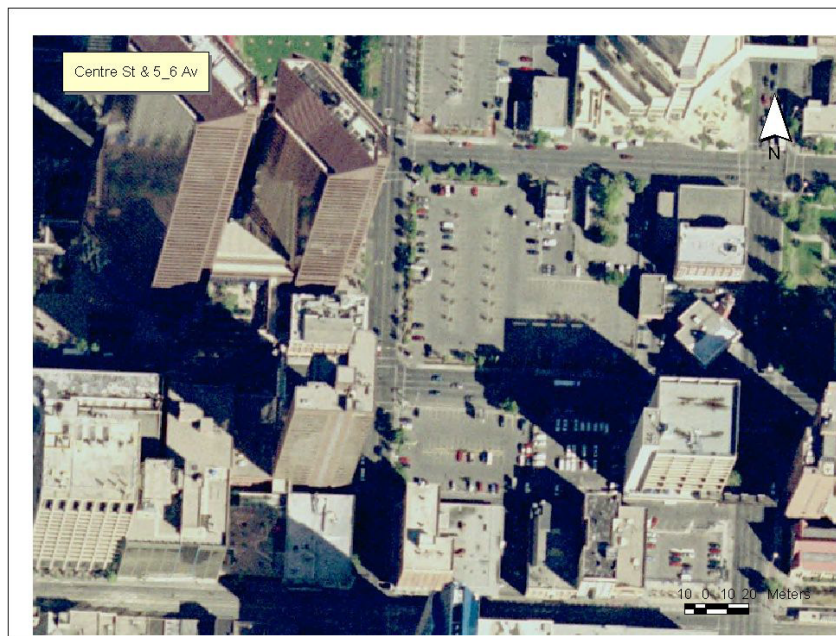


Figure A5: Centre Street/ 5<sup>th</sup> and 6<sup>th</sup> Avenues



Figure A6: Centre Street/ North of 8<sup>th</sup> Avenue

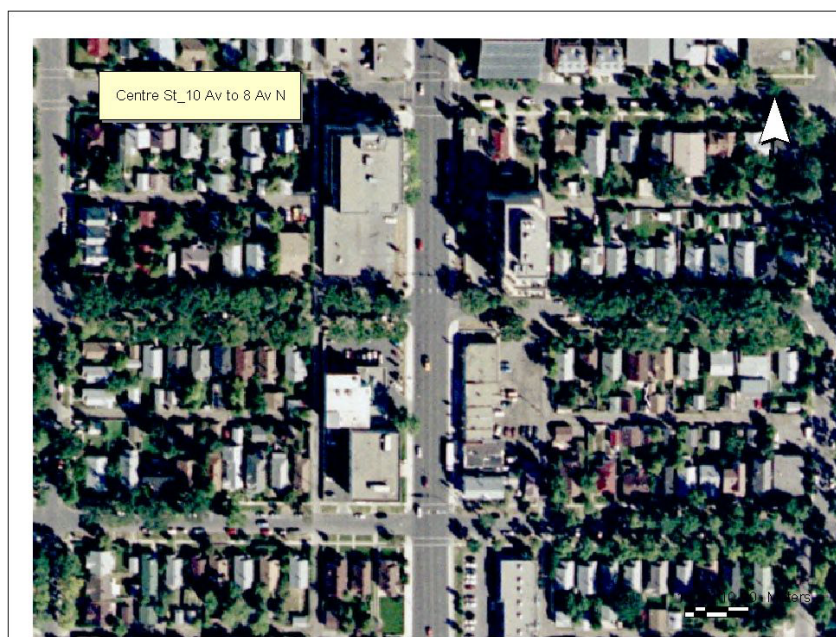


Figure A7: Centre Street/ 8<sup>th</sup> to 10<sup>th</sup> Avenues



Figure A8: Centre Street/ 10<sup>th</sup> to 12<sup>th</sup> Avenues

## A2. Traffic Demand Data

Two traffic demand related data sets were used for constructing the OD demand matrices and calibrating the PARAMICS model. This included turn counts from most of the intersections in the modeled area and screenline traffic counts from most of the streets. Representative data sets from specific intersections and streets, identified using Figure A9 are presented below. Figure A9 depicts the PARAMICS model of Calgary and the selected test area within the model.

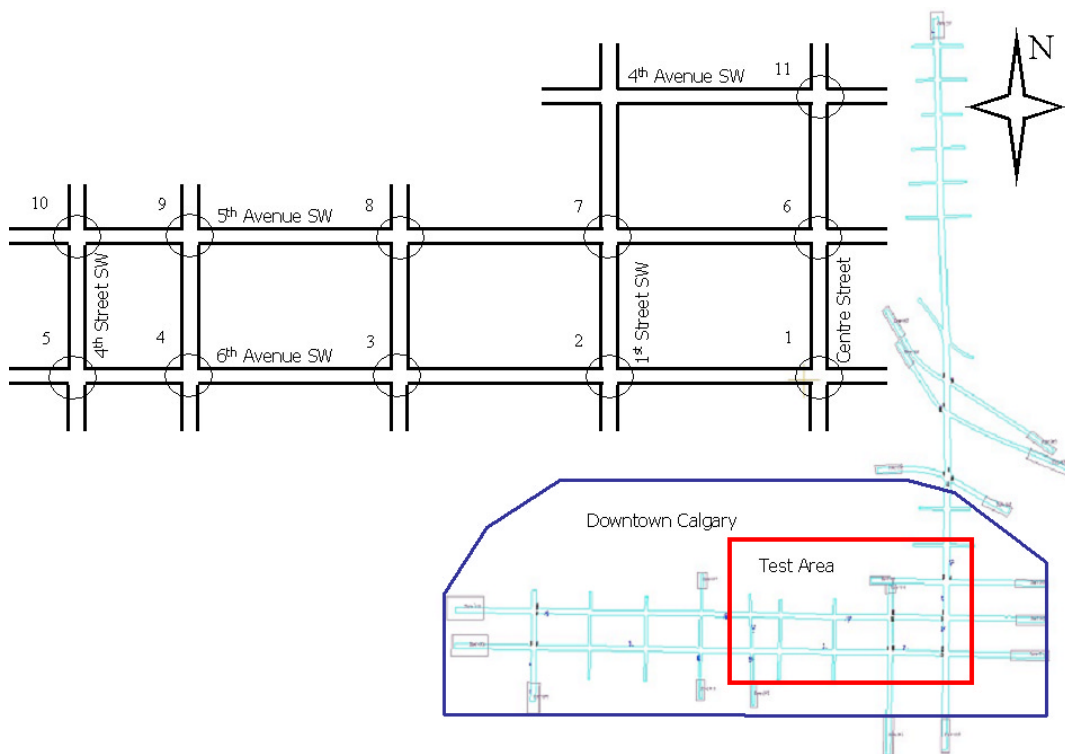


Figure A9: Simulation Model of Calgary and Test Area. The top left insert illustrates the intersection and lane arrangement in the test area within modeled downtown and suburban Calgary

Tables A1 and A2 depicts the turn counts observed from intersections 6<sup>th</sup> Avenue / 1<sup>st</sup> Street and 6<sup>th</sup> Avenue / 4<sup>th</sup> Street, respectively. These correspond to intersections 2 and 5 in Figure A9.

Table A1: Turn Counts from 6<sup>th</sup> AV 1<sup>st</sup> ST Intersection

Period Beginning	North			South			East			West			Vehicle Totals
	North Left	North Straight	North Right	South Left	South Straight	South Right	East Left	East Straight	East Right	West Left	West Straight	West Right	
7:00:00	0	34	58	32	64	0	17	325	26	0	0	0	556
7:15:00	0	61	50	31	91	0	22	391	26	0	0	0	672
7:30:00	0	56	72	34	83	0	23	365	27	0	0	0	660
7:45:00	0	65	59	37	85	0	35	462	42	0	0	0	785
8:00:00	0	67	67	36	98	0	26	467	38	0	0	0	799
8:15:00	0	67	59	38	79	0	17	414	42	0	0	0	716
8:30:00	0	61	67	45	64	0	24	389	38	0	0	0	688
8:45:00	0	63	47	30	62	0	26	366	29	0	0	0	623
TOTAL	0	474	479	283	626	0	190	3179	268	0	0	0	5499
PEAK	0	260	252	156	326	0	102	1732	160	0	0	0	2988
11:00:00	0	50	32	31	55	0	20	240	11	0	0	0	439
11:15:00	0	61	41	20	59	0	26	274	16	0	0	0	497
11:30:00	0	80	41	31	45	0	21	265	23	0	0	0	506
11:45:00	0	86	50	28	68	0	25	289	20	0	0	0	566
12:00:00	0	56	42	26	47	0	36	270	19	0	0	0	496
12:15:00	0	67	36	34	54	0	23	238	17	0	0	0	469
12:30:00	0	61	35	29	55	0	27	244	7	0	0	0	458
12:45:00	0	43	31	35	46	0	18	279	22	0	0	0	474
TOTAL	0	504	308	234	429	0	196	2099	135	0	0	0	3905
PEAK	0	283	174	105	219	0	108	1098	78	0	0	0	2065
16:00:00	0	54	53	18	25	0	16	267	24	0	0	0	457
16:15:00	0	50	44	29	55	0	13	310	35	0	0	0	536
16:30:00	0	75	48	36	75	0	12	339	30	0	0	0	615
16:45:00	0	63	38	36	64	0	19	257	23	0	0	0	500
17:00:00	0	86	34	33	82	0	14	244	24	0	0	0	517
17:15:00	0	65	48	36	83	0	24	235	23	0	0	0	514
17:30:00	0	81	33	26	58	0	23	243	20	0	0	0	484
17:45:00	0	63	48	32	75	0	42	230	11	0	0	0	501
TOTAL	0	537	346	246	517	0	163	2125	190	0	0	0	4124
PEAK	0	274	164	134	276	0	58	1150	112	0	0	0	2168

Table A2: Turn Counts from 6<sup>th</sup> AV 4<sup>th</sup> ST Intersection

Period Beginning	North			South			East			West			Vehicle Totals
	North Left	North Straight	North Right	South Left	South Straight	South Right	East Left	East Straight	East Right	West Left	West Straight	West Right	
7:00:00	0	0	0	36	156	0	1	276	23	0	0	0	492
7:15:00	0	0	0	35	204	0	0	322	25	0	0	0	586
7:30:00	0	0	0	49	231	0	0	342	30	0	0	0	652
7:45:00	0	0	0	63	298	0	0	351	34	0	0	0	746
8:00:00	0	0	0	64	292	0	0	367	41	0	0	0	764
8:15:00	0	0	0	51	223	0	0	370	26	0	0	0	670
8:30:00	0	0	0	47	201	0	0	416	39	0	0	0	703
8:45:00	0	0	0	36	190	0	0	363	38	0	0	0	627
TOTAL	0	0	0	381	1795	0	1	2807	256	0	0	0	5240
PEAK	0	0	0	225	1014	0	0	1504	140	0	0	0	2883
11:00:00	0	0	0	29	160	0	0	280	28	0	0	0	497
11:15:00	0	0	0	38	158	0	0	354	33	0	0	0	583
11:30:00	0	0	0	41	167	0	0	328	31	0	0	0	567
11:45:00	0	0	0	64	167	0	0	391	34	0	0	0	656
12:00:00	0	0	0	57	138	0	0	340	35	0	0	0	570
12:15:00	0	0	0	42	138	0	0	344	26	0	0	0	550
12:30:00	0	0	0	50	109	0	0	271	16	0	0	0	446
12:45:00	0	0	0	44	144	0	0	305	29	0	0	0	522
TOTAL	0	0	0	365	1181	0	0	2613	232	0	0	0	4391
PEAK	0	0	0	200	630	0	0	1413	133	0	0	0	2376
16:00:00	0	0	0	55	181	0	1	421	45	0	0	0	703
16:15:00	0	0	0	62	182	0	1	512	35	0	0	0	792
16:30:00	0	0	0	44	221	0	1	514	33	0	0	0	813
16:45:00	0	0	0	63	236	1	0	452	28	0	0	0	780
17:00:00	0	0	0	58	223	0	0	448	33	0	0	0	762
17:15:00	0	0	0	50	243	0	0	405	32	0	0	0	730
17:30:00	0	0	0	41	181	0	0	427	24	0	0	0	673
17:45:00	0	0	0	55	151	0	0	410	15	0	0	0	631
TOTAL	0	0	0	428	1618	1	3	3589	245	0	0	0	5884
PEAK	0	0	0	227	862	1	2	1926	129	0	0	0	3147

Tables A3 and A4 depicts the screenline traffic counts observed from streets leading to the above intersections.

Table A3: Screenline Traffic Counts Taken West of 6<sup>th</sup> AV 1<sup>st</sup> ST Intersection

HOURS	Minutes				TOTAL	% TOTAL FLOW
	0	15	30	45		
00:00:00 - 00:45:00	75	70	50	40	235	1.1
01:00:00 - 01:45:00	43	38	34	39	154	0.7
02:00:00 - 02:45:00	28	29	30	41	128	0.6
03:00:00 - 03:45:00	25	21	16	19	81	0.4
04:00:00 - 04:45:00	19	21	15	28	83	0.4
05:00:00 - 05:45:00	4	41	62	93	200	0.9
06:00:00 - 06:45:00	105	168	218	305	796	3.7
07:00:00 - 07:45:00	316	373	408	491	1588	7.4
08:00:00 - 08:45:00	416	409	363	319	1507	7
09:00:00 - 09:45:00	277	319	306	288	1190	5.5
10:00:00 - 10:45:00	296	301	324	335	1256	5.8
11:00:00 - 11:45:00	348	350	353	334	1385	6.4
12:00:00 - 12:45:00	341	307	313	355	1316	6.1
13:00:00 - 13:45:00	361	364	384	377	1486	6.9
14:00:00 - 14:45:00	386	356	324	365	1431	6.6
15:00:00 - 15:45:00	341	359	366	385	1451	6.7
16:00:00 - 16:45:00	406	422	460	383	1671	7.8
17:00:00 - 17:45:00	415	351	366	312	1444	6.7
18:00:00 - 18:45:00	318	269	270	228	1085	5
19:00:00 - 19:45:00	226	185	194	162	767	3.6
20:00:00 - 20:45:00	174	156	189	149	668	3.1
21:00:00 - 21:45:00	195	205	155	160	715	3.3
22:00:00 - 22:45:00	170	138	117	113	538	2.5
23:00:00 - 23:45:00	116	108	77	75	376	1.7
A.M. Peak Hour	7:30:00 AM - 8:30:00 AM	Flow	1724	8%		
P.M. Peak Hour	4:15:00 PM - 5:15:00 PM	Flow	1680	7.80%		
TOTAL 24 Hour		Flow	21551			
12 Hour Summary (7 AM to 7 PM)		Flow	16810			
16 Hour Summary (7 AM to 11 PM)		Flow	19498			
6 Hour Summary (7-9, 11-1, 4-6)		Flow	8911			

Table A4: Screenline Traffic Counts Taken West of 6<sup>th</sup> AV 4<sup>th</sup> ST Intersection

Minutes						
HOURS	0	15	30	45	TOTAL	% TOTAL FLOW
00:00:00 - 00:45:00	87	85	83	59	314	1.4
01:00:00 - 01:45:00	69	54	61	78	262	1.1
02:00:00 - 02:45:00	47	47	60	53	207	0.9
03:00:00 - 03:45:00	32	28	18	25	103	0.4
04:00:00 - 04:45:00	20	22	19	26	87	0.4
05:00:00 - 05:45:00	29	20	66	76	191	0.8
06:00:00 - 06:45:00	94	145	192	251	682	3
07:00:00 - 07:45:00	279	335	381	416	1411	6.1
08:00:00 - 08:45:00	368	352	307	290	1317	5.7
09:00:00 - 09:45:00	281	287	296	275	1139	4.9
10:00:00 - 10:45:00	278	282	297	337	1194	5.2
11:00:00 - 11:45:00	313	351	357	349	1370	6
12:00:00 - 12:45:00	346	327	319	341	1333	5.8
13:00:00 - 13:45:00	375	347	369	384	1475	6.4
14:00:00 - 14:45:00	388	395	366	381	1530	6.6
15:00:00 - 15:45:00	366	388	414	443	1611	7
16:00:00 - 16:45:00	486	520	524	501	2031	8.8
17:00:00 - 17:45:00	519	494	443	390	1846	8
18:00:00 - 18:45:00	406	344	305	280	1335	5.8
19:00:00 - 19:45:00	286	221	202	200	909	3.9
20:00:00 - 20:45:00	207	184	207	182	780	3.4
21:00:00 - 21:45:00	238	200	203	168	809	3.5
22:00:00 - 22:45:00	179	163	148	131	621	2.7
23:00:00 - 23:45:00	141	138	97	87	463	2
A.M. Peak Hour	7:30:00AM - 8:30:00 AM	Flow	1517	6.59%		
P.M. Peak Hour	4:15:00PM - 5:15:00 PM	Flow	2064	8.97%		
TOTAL 24 Hour		Flow	23020			
12 Hour Summary (7 AM to 7 PM)		Flow	17592			
16 Hour Summary (7 AM to 11 PM)		Flow	20711			
6 Hour Summary (7-9, 11-1, 4-6)		Flow	9308			

### A3. Traffic Circulation, Signal Arrangements and Timings

The traffic circulation within the downtown core was controlled through one-way streets and time dependent turn bans. Figure A10 depicts the traffic circulation pattern within the downtown test area.

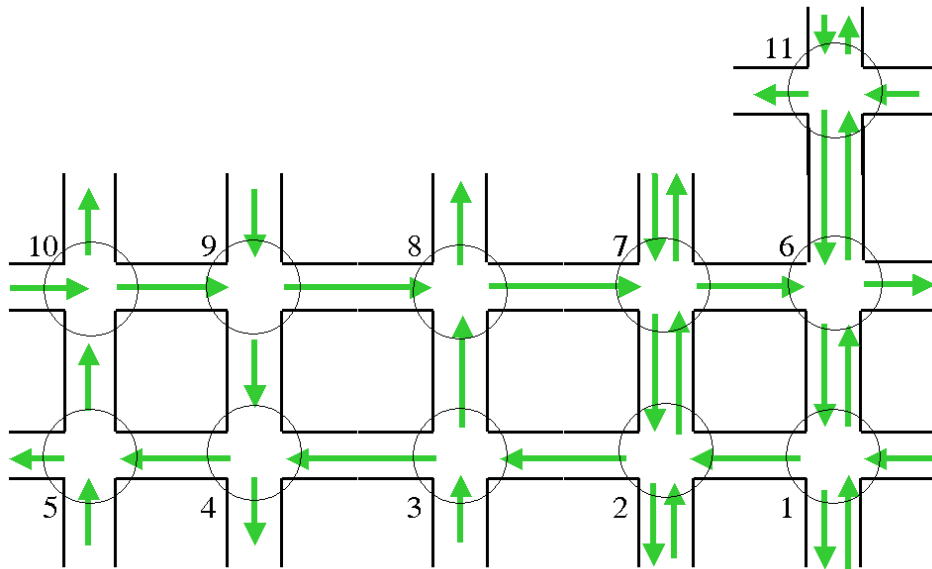


Figure A10: Traffic Circulation Pattern Within Downtown Calgary

One-way street and turn bans were implemented through a series of intersection control measures. The area illustrated in Figure A10 contained 11 intersections controlled according to one of eight traffic signal phasing schemes. These schemes are depicted in Figure A11.

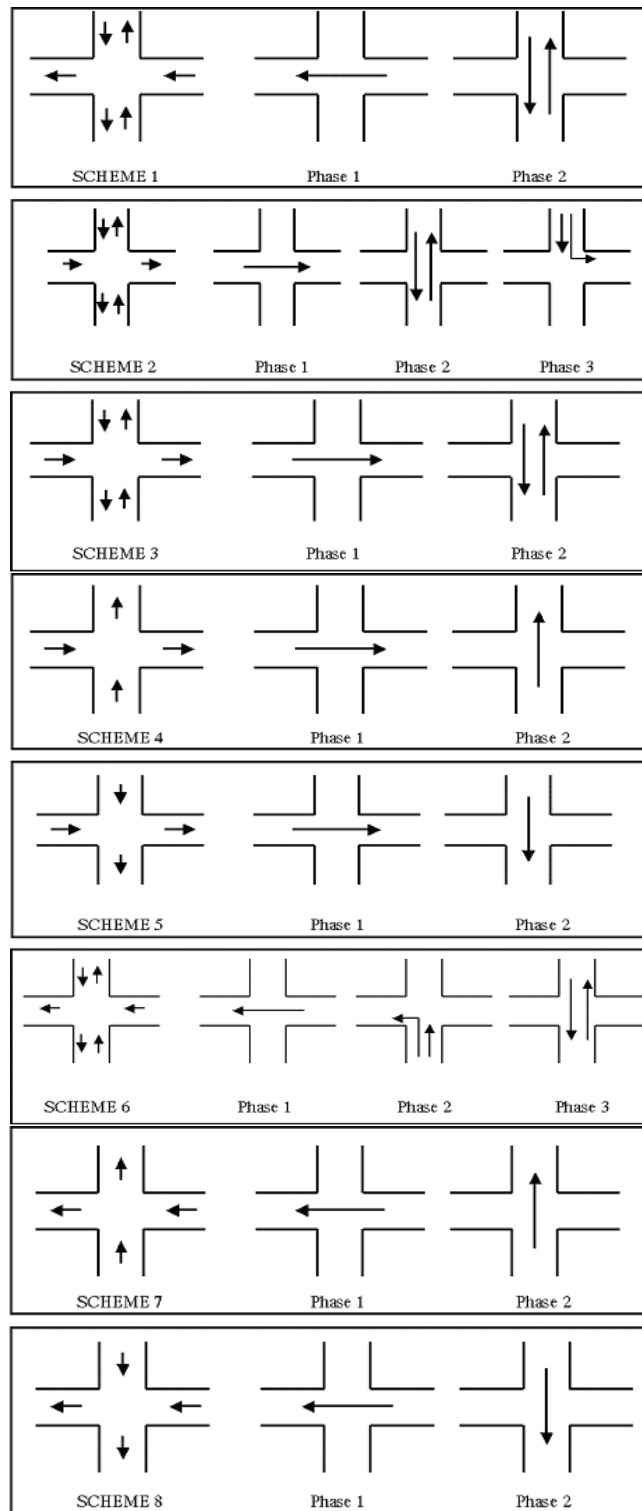


Figure A11: Traffic signal phasing schemes in the test area

The signal timings for all traffic signals are given in Table A5 for the morning peak period operation. The intersection numbers given in Table A5 correspond to the numbering illustrated in Figures A9 and A10. Furthermore, the phasing scheme numbers correspond to phasing schemes given in Figure A11.

Table A5: Signal Timings for Simulated Intersections

Intersection	Signal Scheme	Cycle Length (sec)	Offset (sec)	Green Time Split (seconds)		
				Phase 1	Phase 2	Phase 3
1	1	90	10	38.0	42.0	
2	6	90	20	41.5	10.5	24.0
3	7	90	30	52.5	26.5	
4	8	90	39	54.5	25.0	
5	7	90	43	43.5	36.0	
6	2	90	5	41.0	24.0	10.0
7	3	90	80	49.5	29.5	
8	4	90	65	52.0	28.0	
9	5	90	48	55.5	23.5	
10	4	90	44	50.0	30.0	
11	1	90	86	49.5	29.5	

#### **A4. Calibration and Validation Travel Times**

Shown in Table 6 are a fraction of dedicated probe vehicle travel times used for the calibration and validation of the traffic simulation model (data collected by the City of Calgary).

Table A6: Probe Vehicle Travel Times

Record	DATE	TIME	Location	Travel Time (sec)	Dist. (m)	Average	Speed
5104	1/25/2003	13:01:05	1 St South of Riverfront Av	189.00	1475		7.80 m/s
5475	1/25/2003	13:08:50	1 St South of Riverfront Av	150.00	1475		9.83 m/s
5870	1/25/2003	13:16:55	1 St South of Riverfront Av	138.00	1475		10.69 m/s
6212	1/25/2003	13:23:45	1 St South of Riverfront Av	193.00	1475		7.64 m/s
6597	1/25/2003	13:31:56	1 St South of Riverfront Av	199.00	1475		7.41 m/s
6981	1/25/2003	13:39:47	1 St South of Riverfront Av	151.00	1475		9.77 m/s
7354	1/25/2003	13:46:49	1 St South of Riverfront Av	200.00	1475		7.38 m/s
7763	1/25/2003	13:55:49	1 St South of Riverfront Av	144.00	1475		10.24 m/s
8143	1/25/2003	14:02:55	1 St South of Riverfront Av	143.00	1475		10.31 m/s
8527	1/25/2003	14:10:45	1 St South of Riverfront Av	203.00	1475		7.27 m/s
8919	1/25/2003	14:19:51	1 St South of Riverfront Av	264.00	1475		5.59 m/s
9308	1/25/2003	14:28:51	1 St South of Riverfront Av	148.00	1475		9.97 m/s
9713	1/25/2003	14:36:50	1 St South of Riverfront Av	148.00	1475		9.97 m/s
10092	1/25/2003	14:43:56	1 St South of Riverfront Av	136.00	1475		10.85 m/s
10464	1/25/2003	14:50:51	1 St South of Riverfront Av	195.00	1475		7.56 m/s
10855	1/25/2003	14:59:50	1 St South of Riverfront Av	144.00	1475		10.24 m/s
11249	1/25/2003	15:06:50	1 St South of Riverfront Av	150.00	1475		9.83 m/s
11618	1/25/2003	15:13:45	1 St South of Riverfront Av	152.00	1475		9.70 m/s
11972	1/25/2003	15:20:43	1 St South of Riverfront Av	152.00	1475		9.70 m/s
12345	1/25/2003	15:28:00	1 St South of Riverfront Av	138.00	1475		10.69 m/s
12724	1/25/2003	15:36:22	1 St South of Riverfront Av	165.00	1475		8.94 m/s
13055	1/25/2003	15:44:39	1 St South of Riverfront Av	150.00	1475		9.83 m/s
13421	1/25/2003	15:51:42	1 St South of Riverfront Av	155.00	1475		9.52 m/s
			Average	165.52			9.16 m/s
			Average	2.76			32.99 km/h
			Standard Deviation	31.21			1.42 m/s
			Standard Deviation	0.52			5.11 km/h

## APPENDIX B

### ANALYSIS OF INCIDENT DETECTION PARAMETERS

#### B1. Time Series of Corrections to HSGPS Measurements

This section illustrates the time series of across-track corrections made to HSGPS and HSGPS single point (HSGPS-SP) positions and velocities. Results from four test runs are presented and the statistics are presented and discussed in Chapter 4.

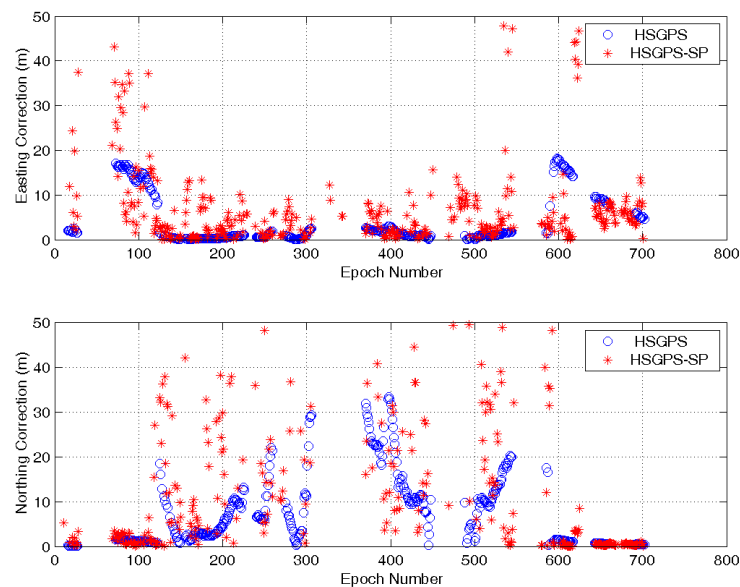


Figure B1: Position Corrections for Test Run 2

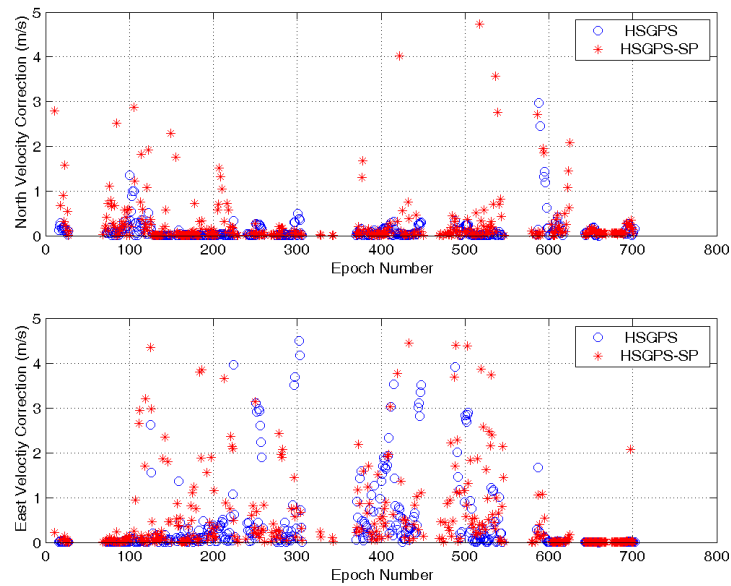


Figure B2: Velocity Corrections for Test Run 2

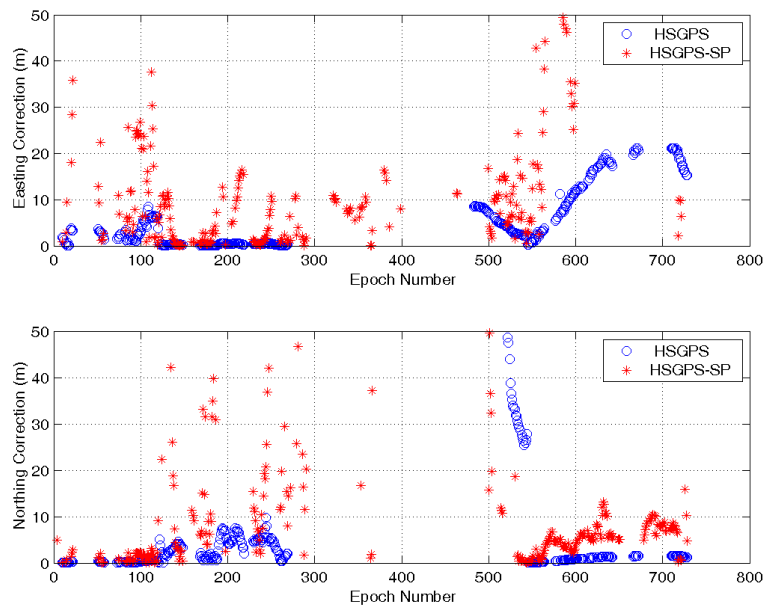


Figure B3: Position Corrections for Test Run 3

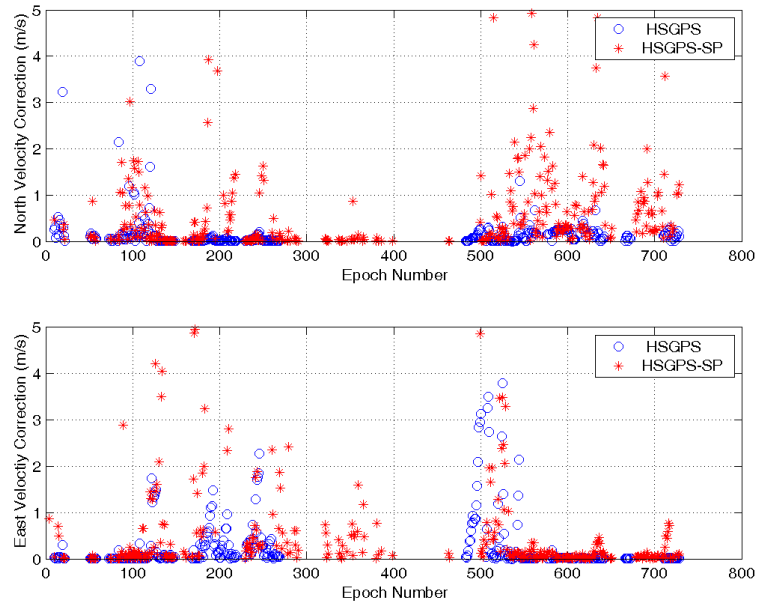


Figure B4: Velocity Corrections for Test Run 3

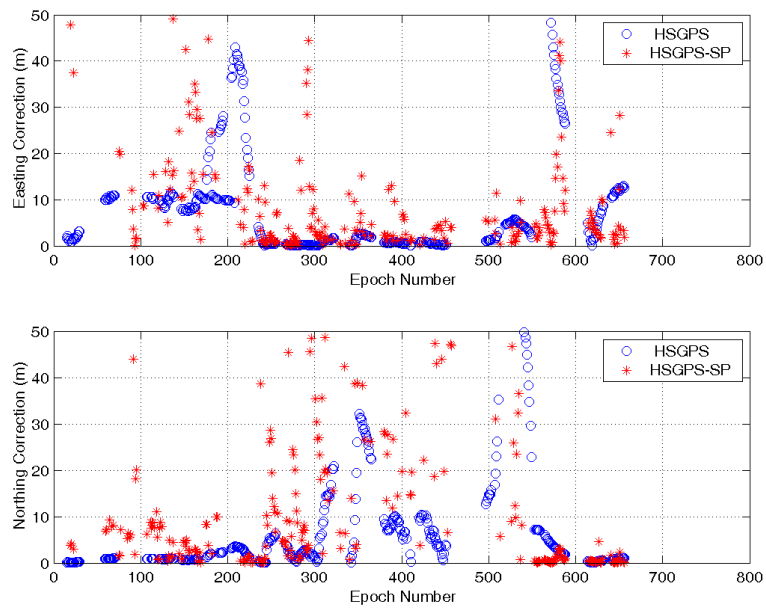


Figure B5: Position Corrections for Test Run 5

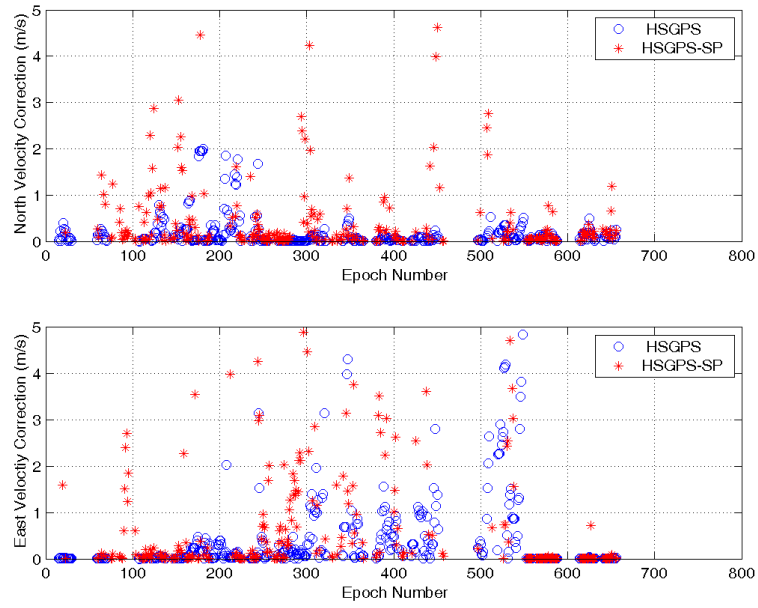


Figure B6: Velocity Corrections for Test Run 5

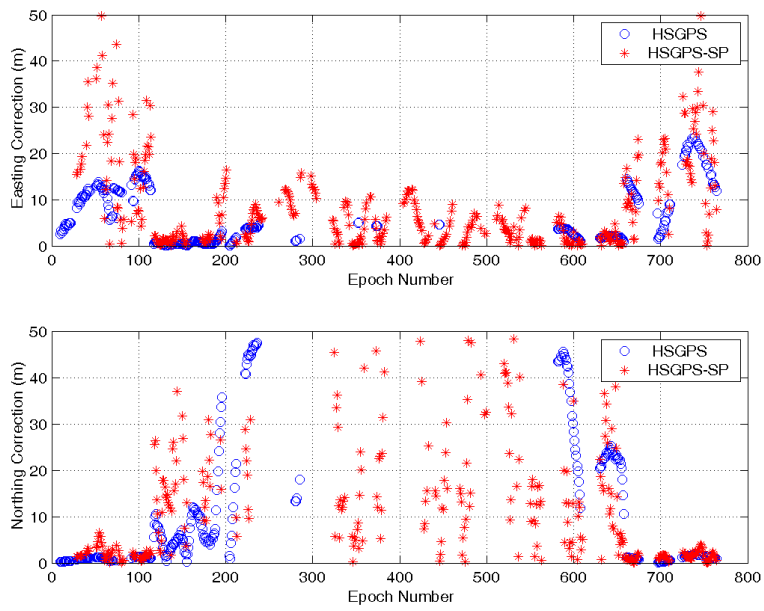


Figure B7: Position Corrections for Test Run 6

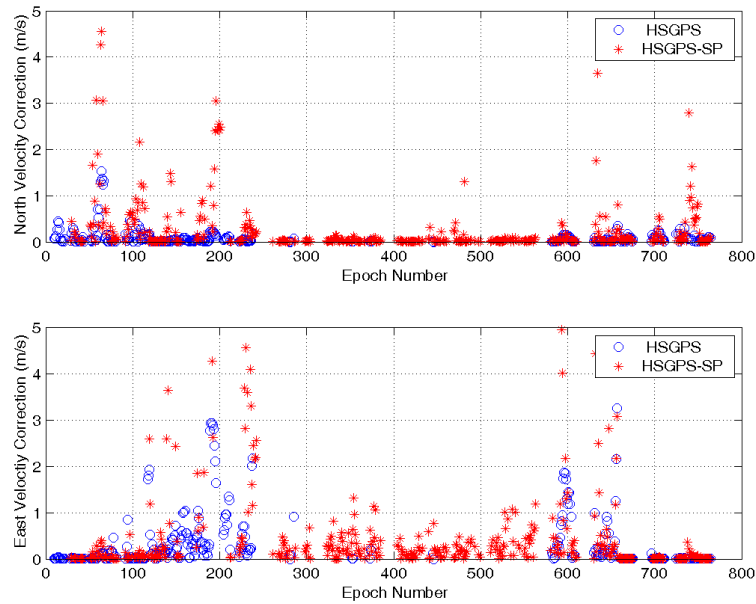


Figure B8: Velocity Corrections for Test Run 6

## B2. Transit Vehicle Positioning Field Test Results

This section illustrates the results of the modified transit vehicle-positioning algorithm presented in Chapter 4. Results from three downtown tests are presented and the results of a 4<sup>th</sup> test are discussed in Chapter 4.

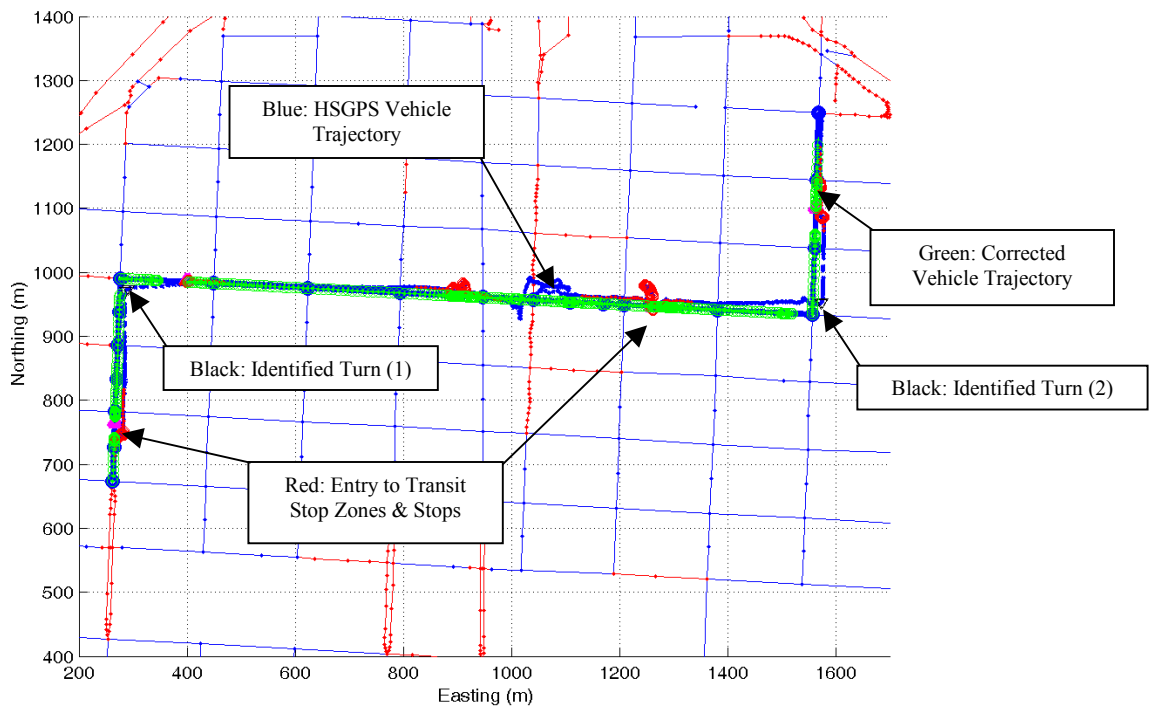


Figure B9: Route Constrained Map-Matched Solution: Test Run 2

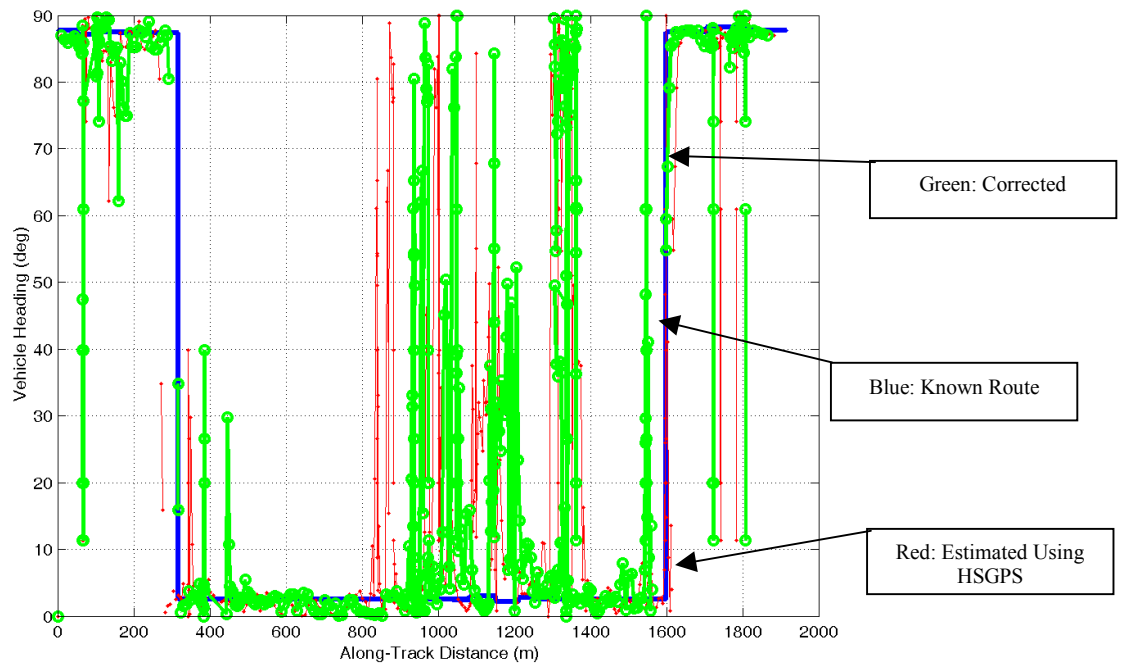


Figure B10: Corrected Vehicle Heading: Test Run 2

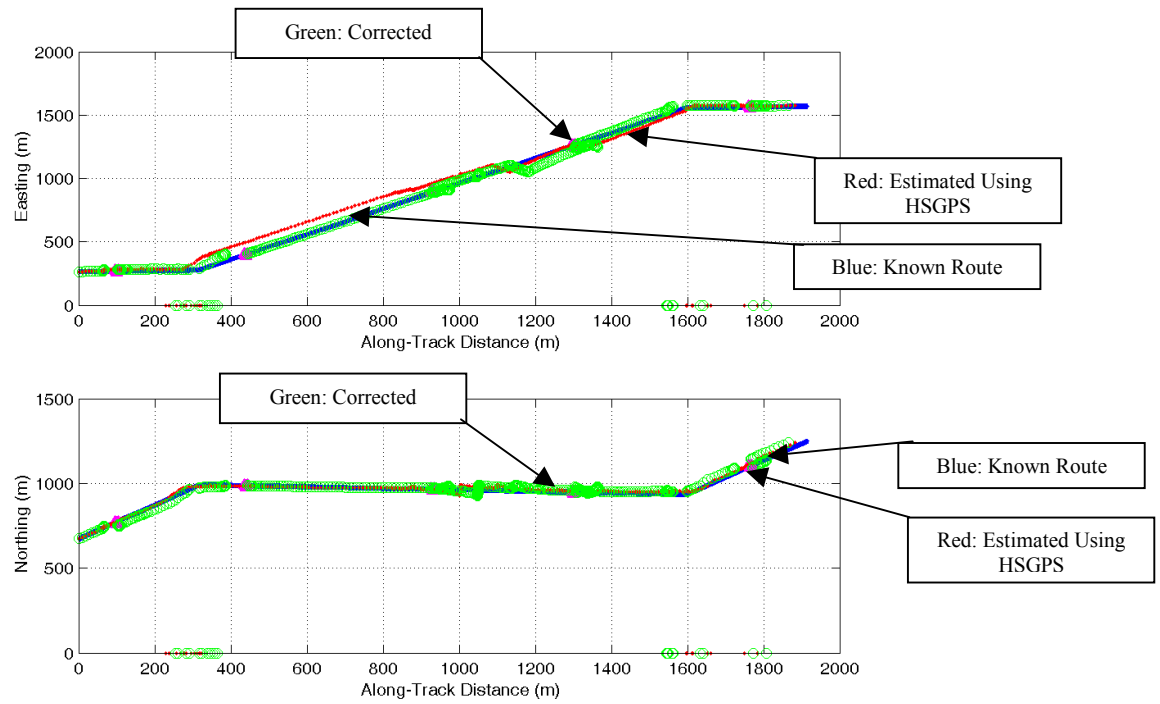


Figure B11: Northing and Easting Results: Test Run 2

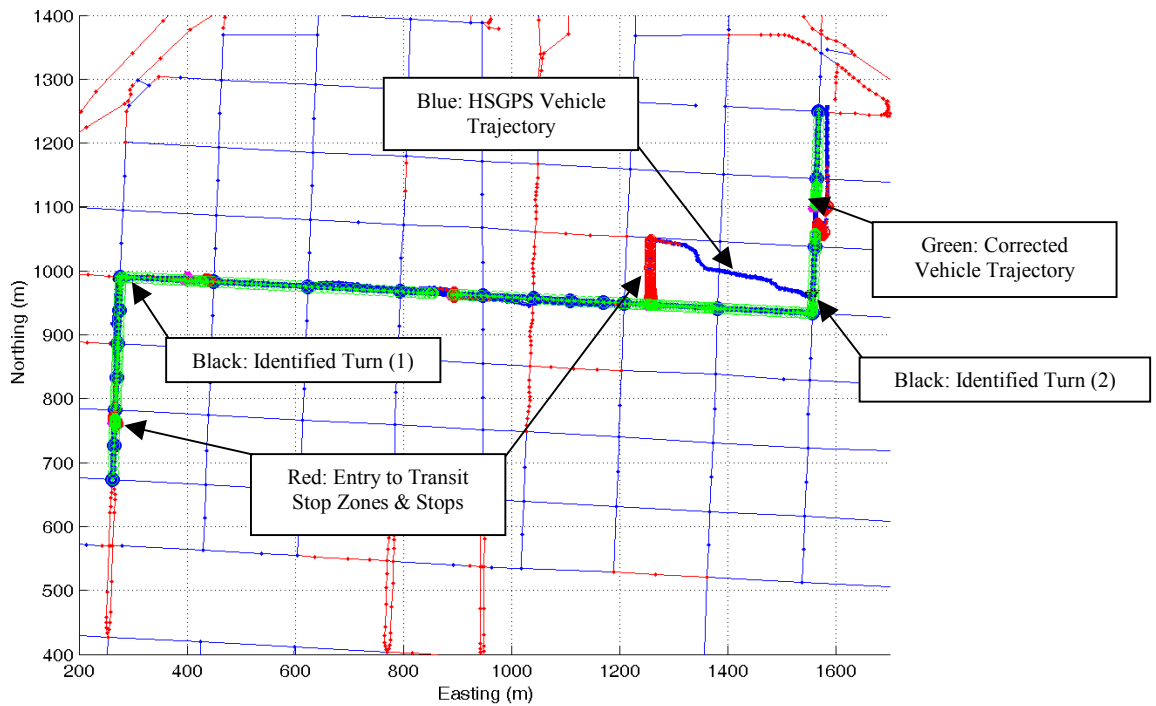


Figure B12: Route Constrained Map-Matched Solution: Test Run 3

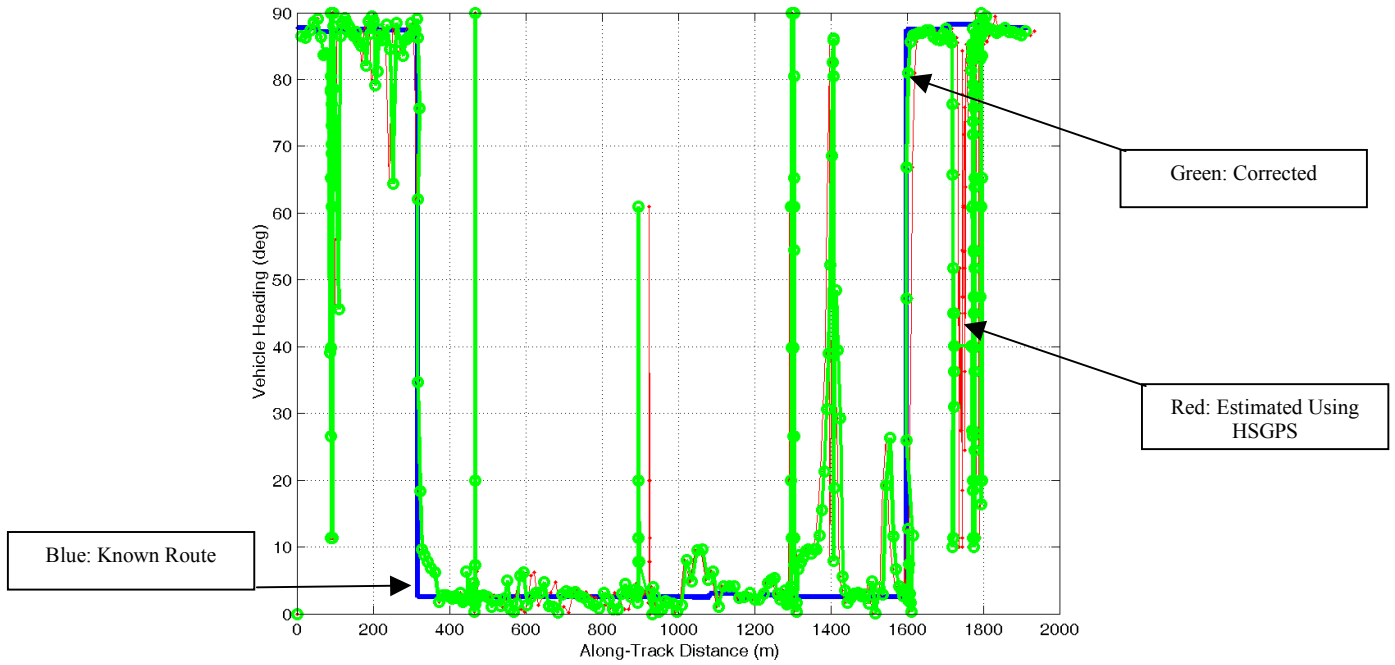


Figure B13: Corrected Vehicle Heading: Test Run 3

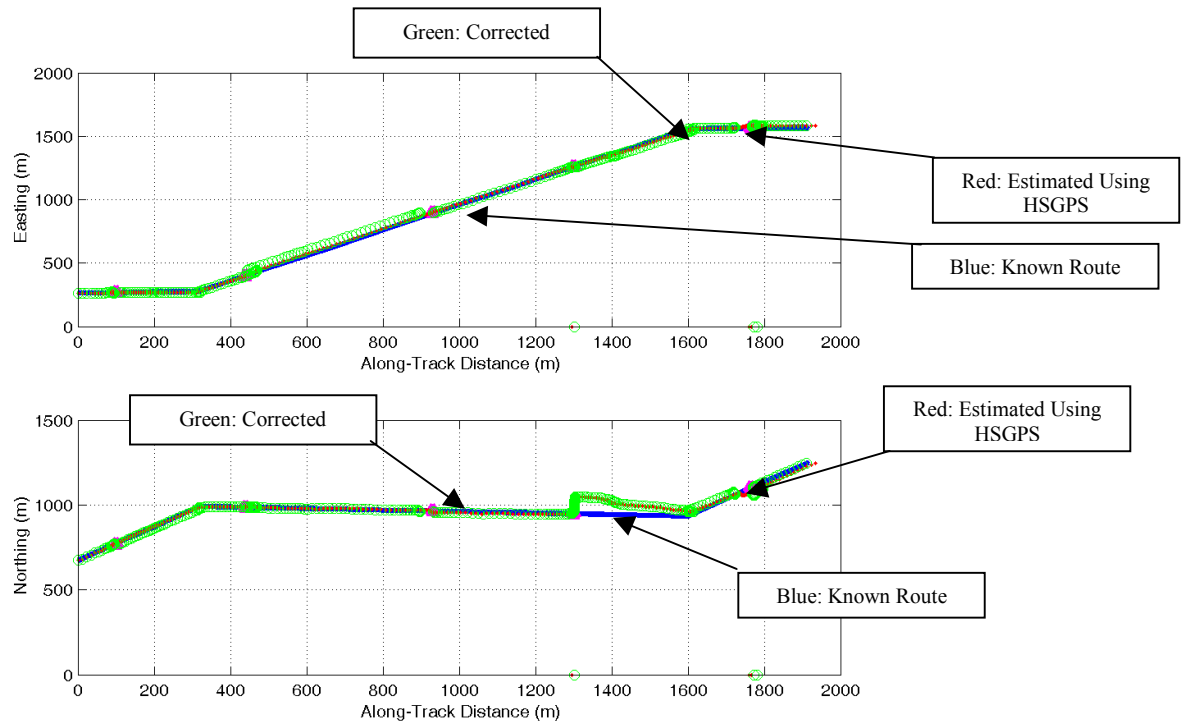


Figure B14: Northing and Easting Results: Test Run 3

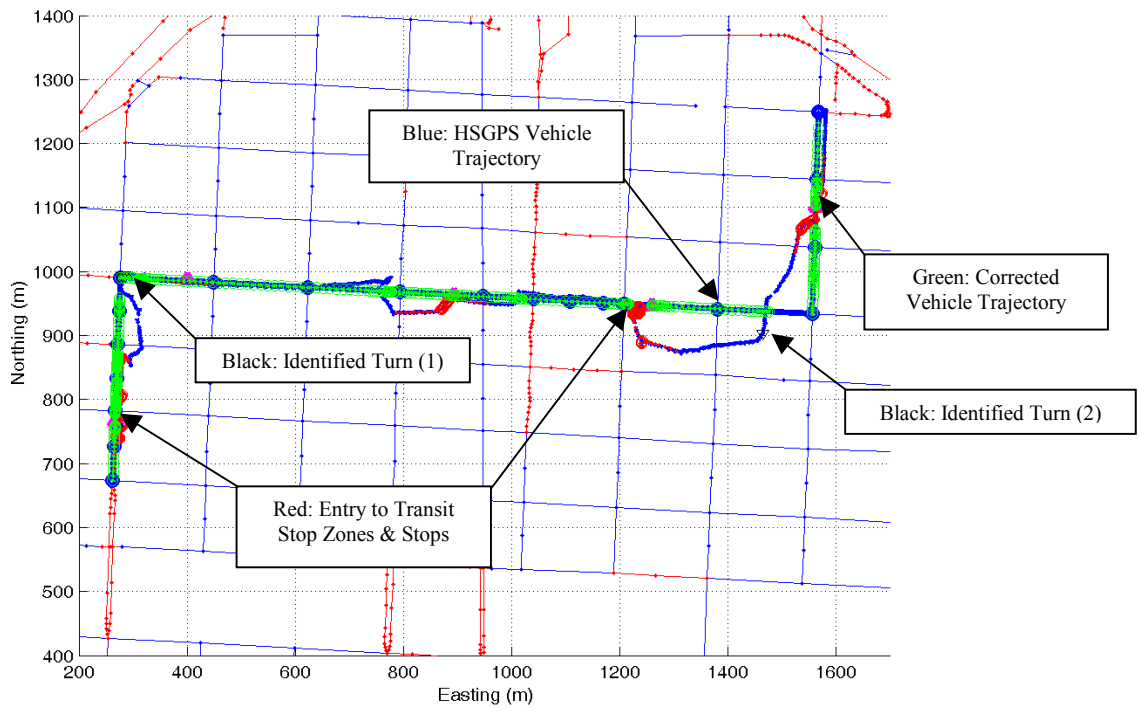


Figure B15: Route Constrained Map-Matched Solution: Test Run 5

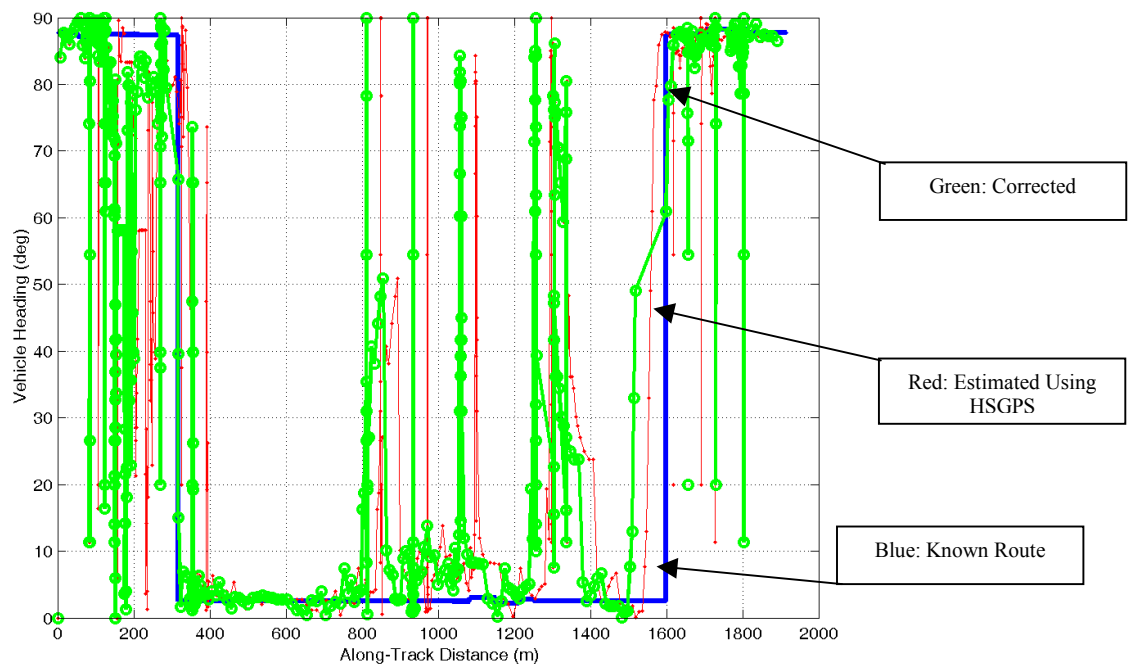


Figure B16: Corrected Vehicle Heading: Test Run 5

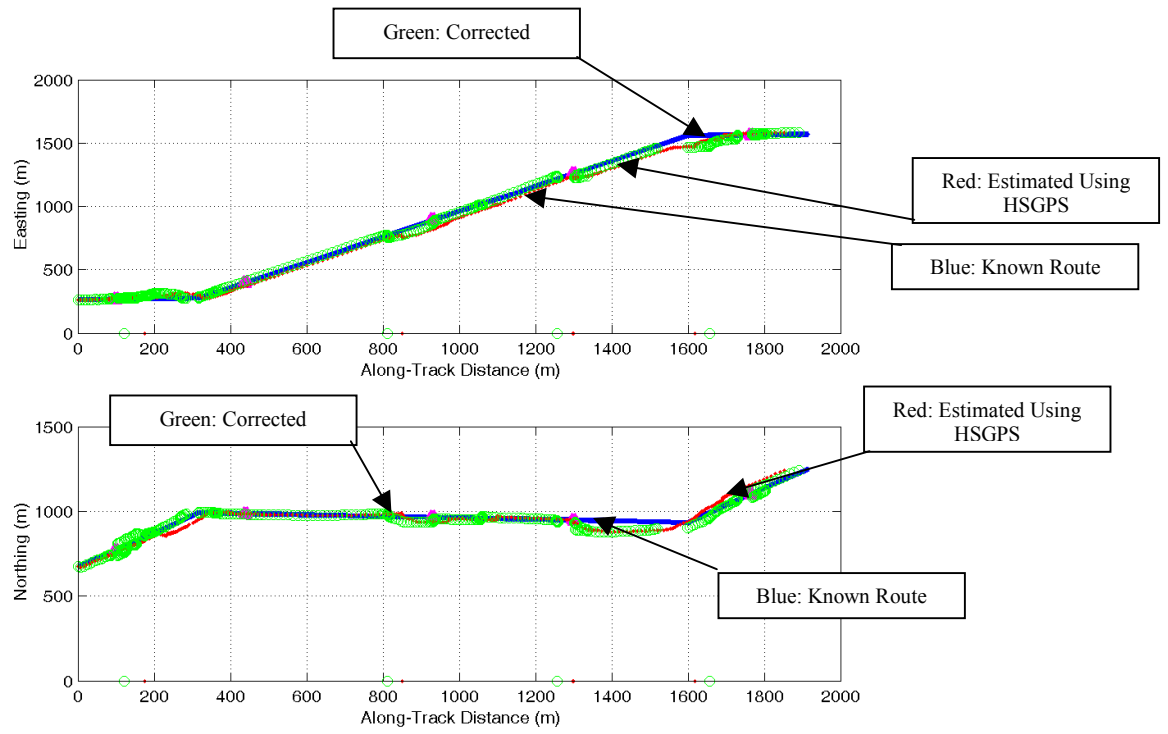


Figure B17: Northing and Easting Results: Test Run 5

## **APPENDIX C**

### **SIMULATED SPEED PROFILES AND ACCELERATION NOISE**

#### **C1. Scenario 1 Simulations**

The simulated transit vehicle speed contours and corresponding acceleration noise contours for simulation Scenario 1 (simulated incident in Street A) are presented in this section. Speed and acceleration noise observed from vehicles, which traveled while the incident was in progress, are highlighted. The upstream street segment (Segment B) is also highlighted in order to illustrate the impact on the upstream street segment. The results of one of the simulations are discussed in detail in Chapter 7.

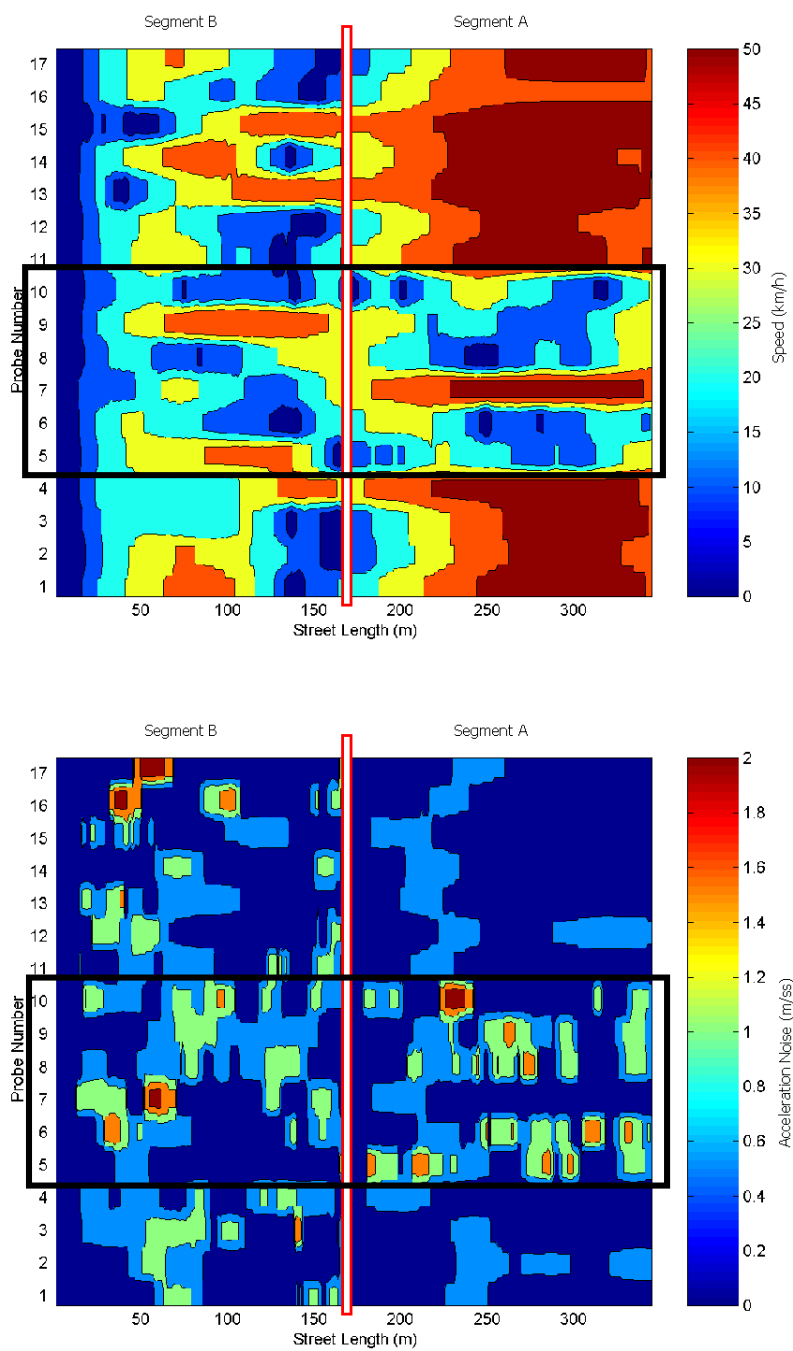


Figure C1: Speed Profiles (Top) and Acceleration Noise (Bottom): Simulation 1

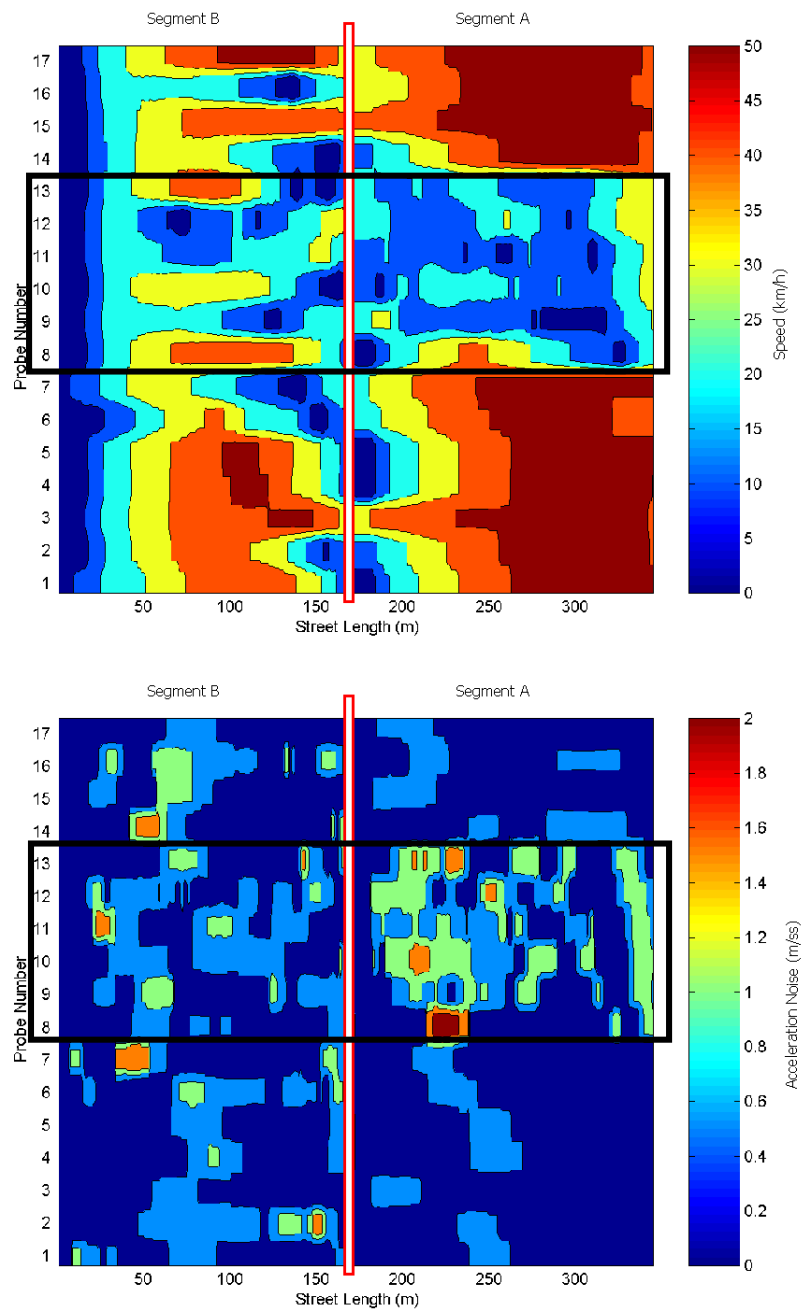


Figure C2: Speed Profiles (Top) and Acceleration Noise (Bottom): Simulation 2

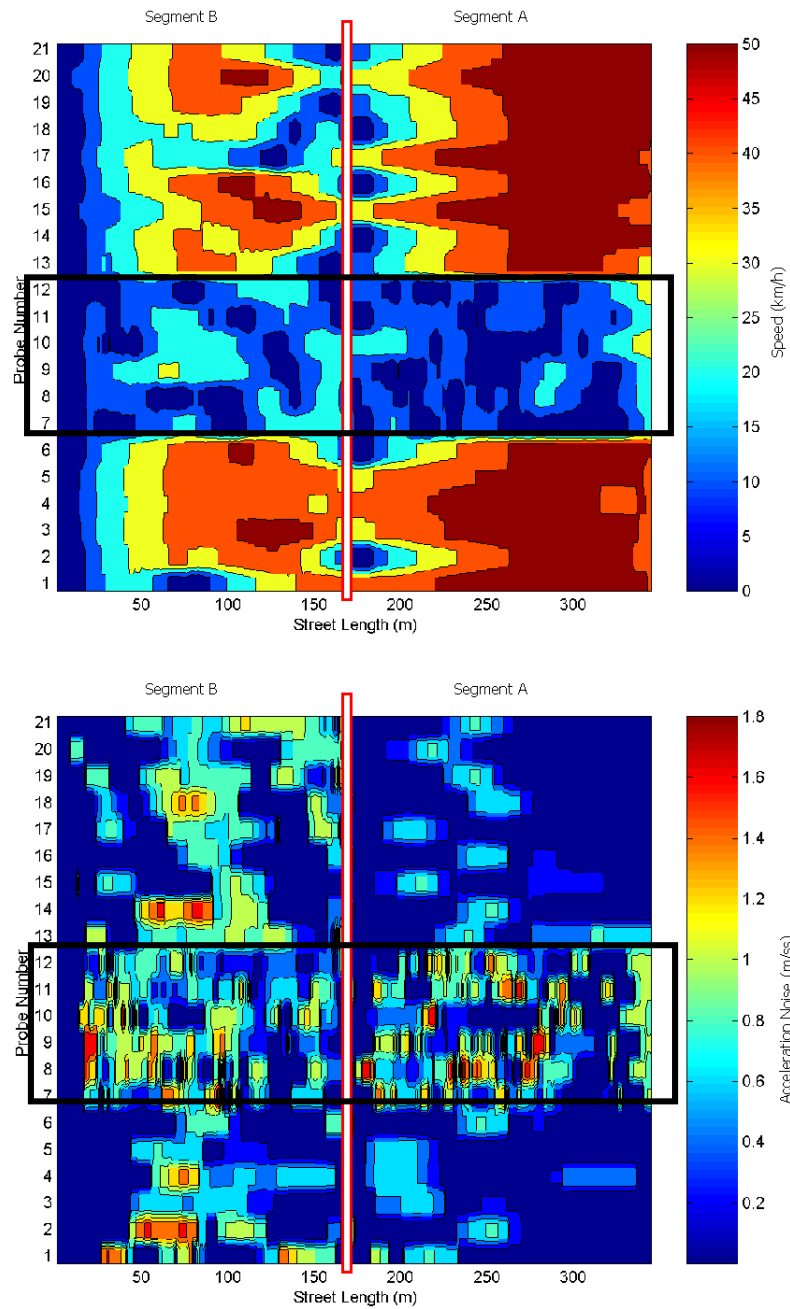


Figure C3: Speed Profiles (Top) and Acceleration Noise (Bottom): Simulation 3

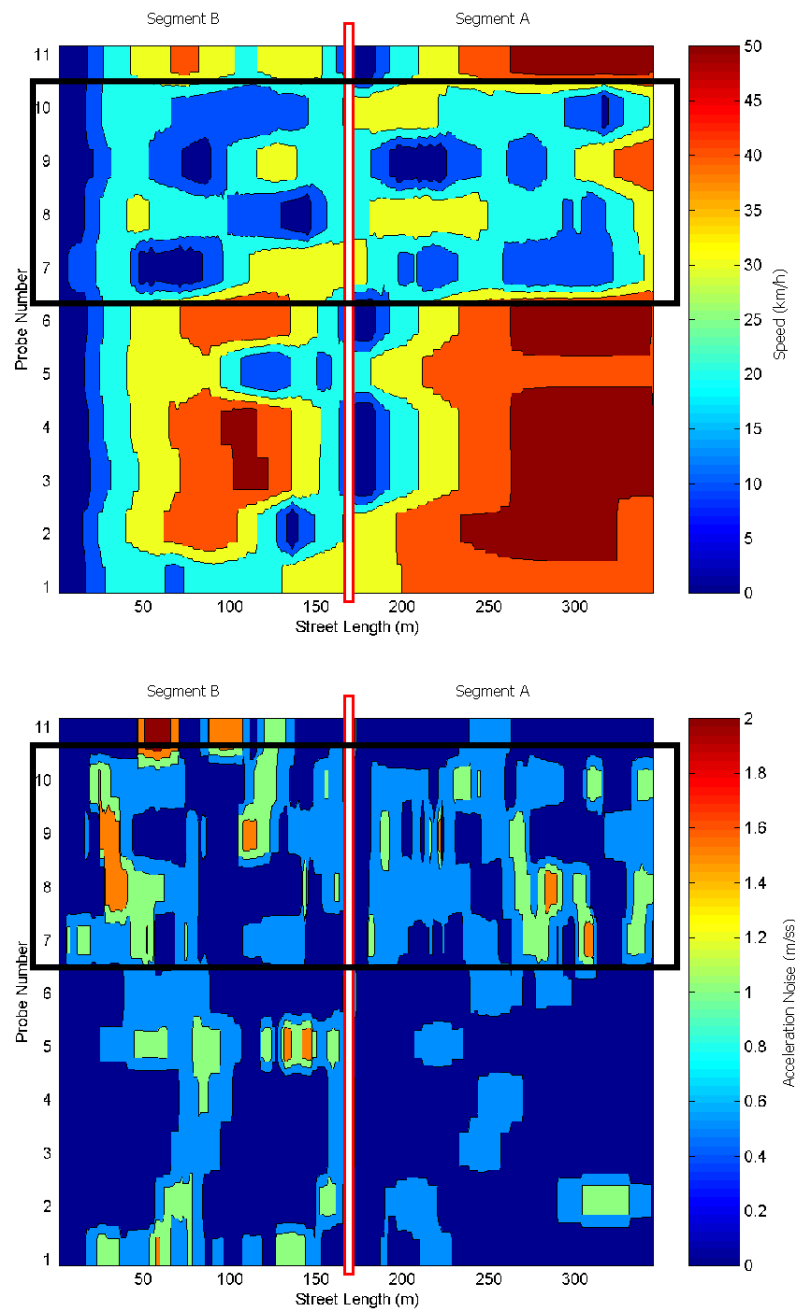


Figure C4: Speed Profiles (Top) and Acceleration Noise (Bottom): Simulation 4

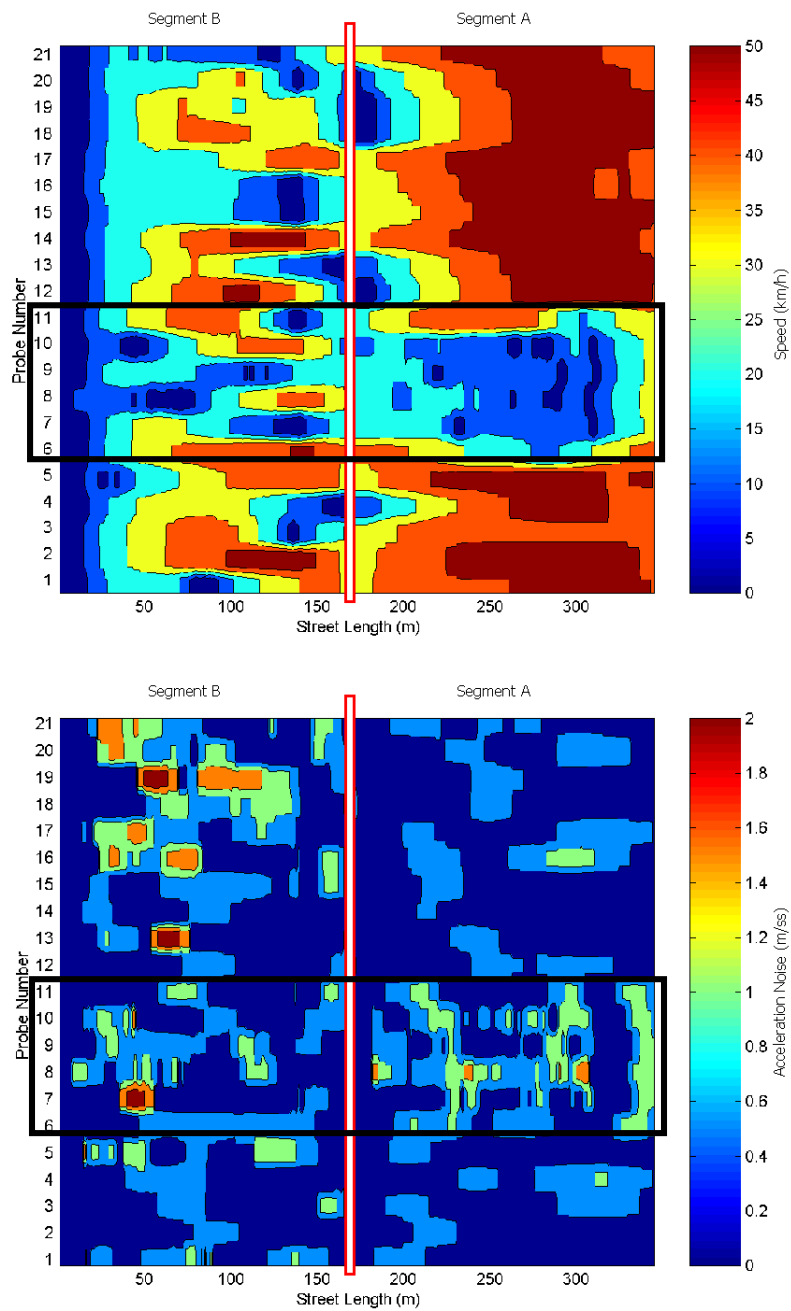


Figure C5: Speed Profiles (Top) and Acceleration Noise (Bottom): Simulation 5

## **C2. Scenario 2 Simulations**

The simulated transit vehicle speed contours and corresponding acceleration noise contours for simulation Scenario 2 (simulated incident in Street B) are presented in this section. Similar to Scenario 1 illustrations, speed and acceleration noise observed from vehicles, which traveled while the incident was in progress, are highlighted. The results of one of the simulations are discussed in detail in Chapter 7.

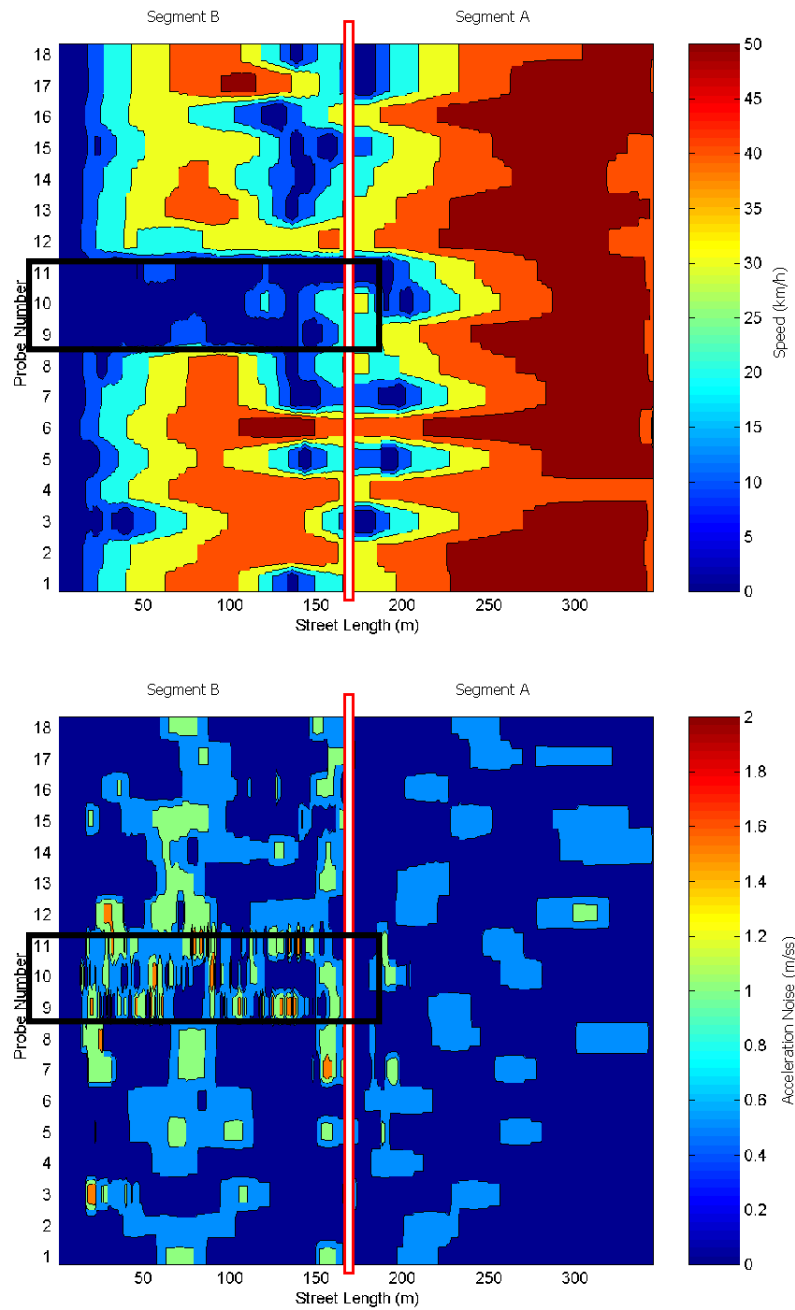


Figure C6: Speed Profiles (Top) and Acceleration Noise (Bottom): Simulation 1

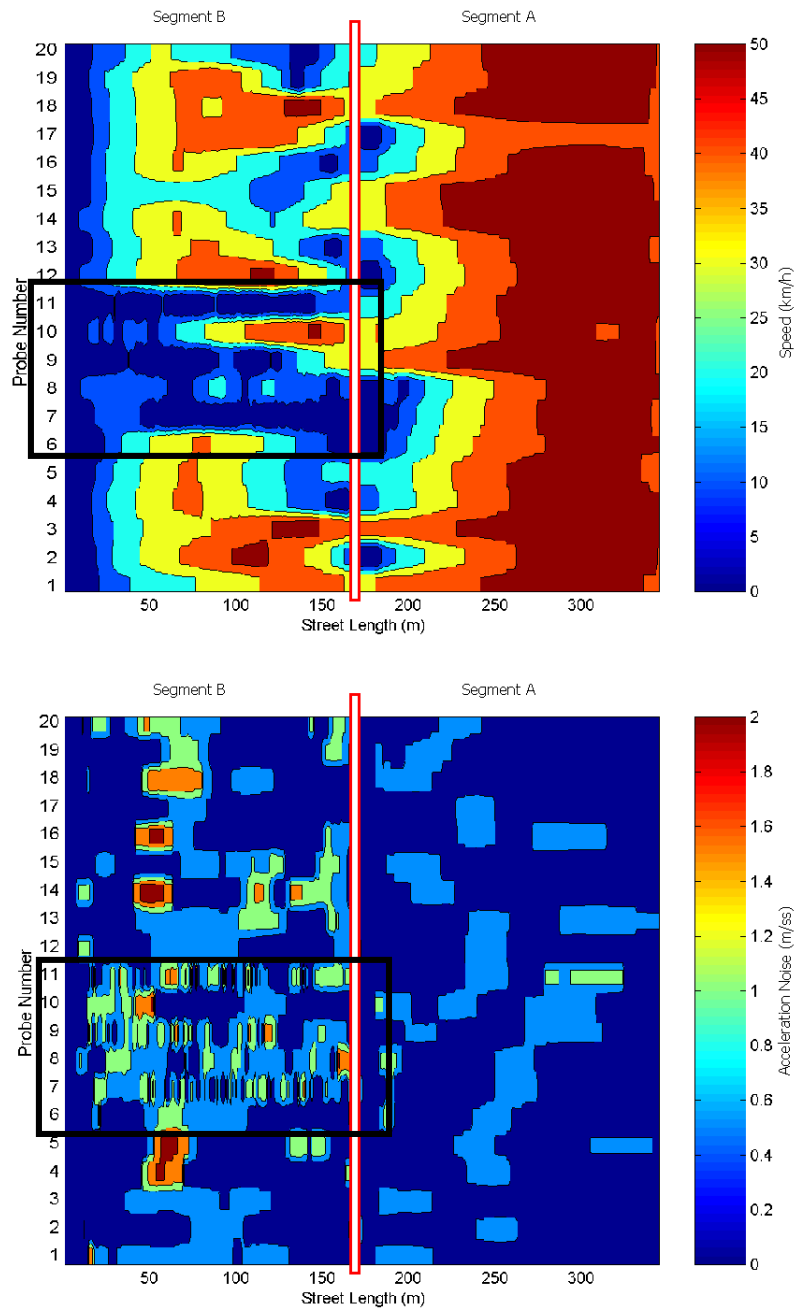


Figure C7: Speed Profiles (Top) and Acceleration Noise (Bottom): Simulation 2

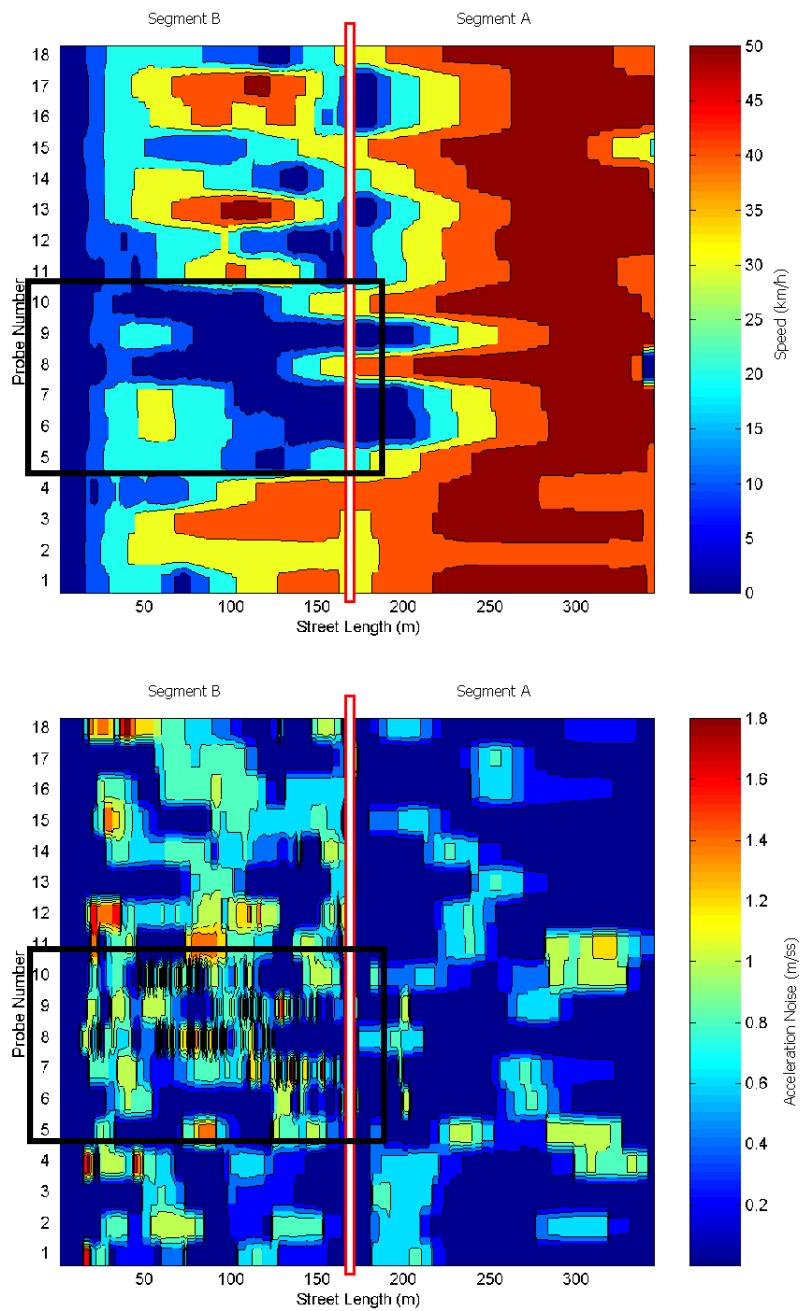


Figure C8: Speed Profiles (Top) and Acceleration Noise (Bottom): Simulation 3

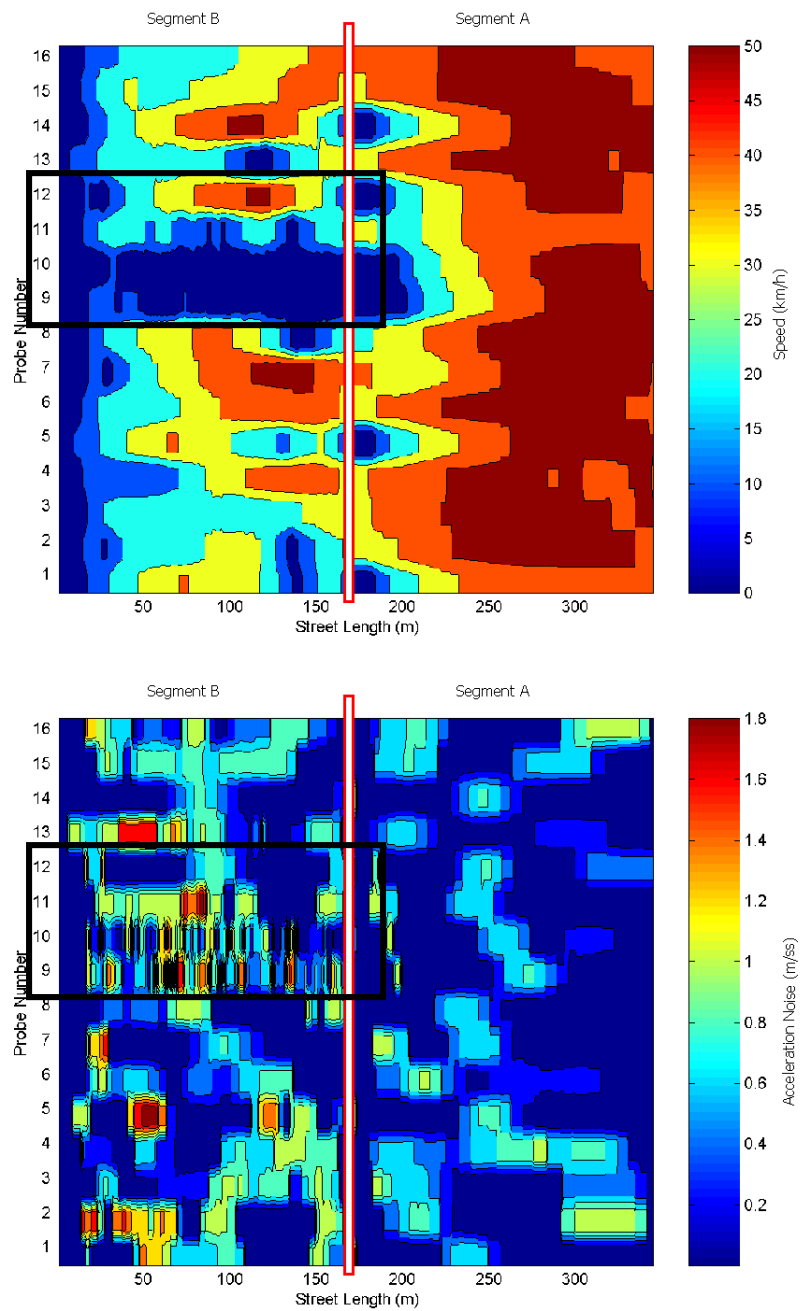


Figure C9: Speed Profiles (Top) and Acceleration Noise (Bottom): Simulation 4

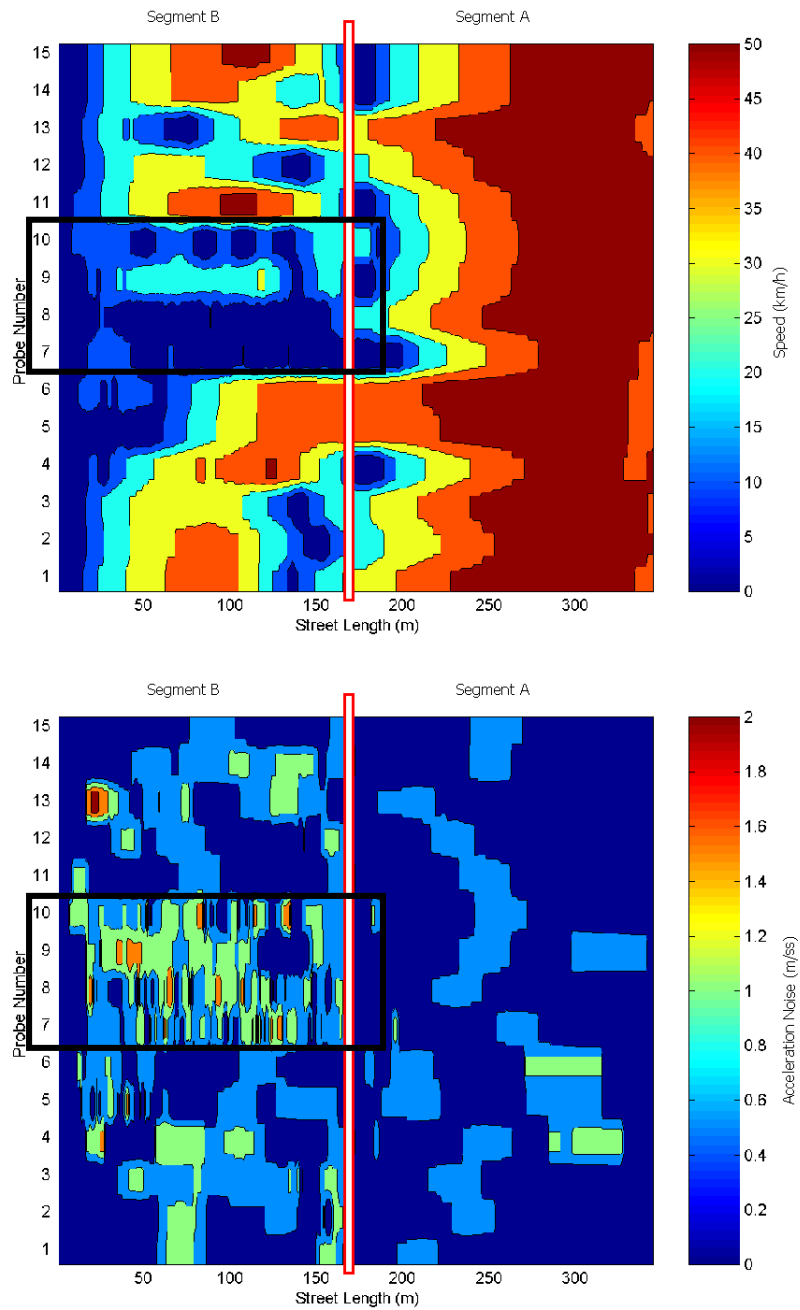


Figure C10: Speed Profiles (Top) and Acceleration Noise (Bottom): Simulation 5

## APPENDIX D

### PREVIOUSLY PUBLISHED MATERIAL

This thesis includes some material that was fully or partially published previously in journals, conference proceedings, posters and oral presentations. The citations for all journal publications and conference proceedings are provided below.

Basnayake, C., O. Mezentsev, G. Lachapelle and M. E. Cannon (2004) A Portable Vehicular Navigation System Using High Sensitivity GPS Augmented with Inertial Sensors and Map-Matching. SAE 2004 World Congress, Detroit, MI. Society of Automotive Engineers.

Basnayake, C., O. Mezentsev, G. Lachapelle and M. E. Cannon (2004) An HSGPS, Inertial and Map-matching Integrated Portable Vehicle Navigation System for Uninterrupted Real-Time Vehicle Navigation. International Journal of Vehicle Information and Communication Systems (IJVICS). (In Press)

Basnayake, C. and G. Lachapelle (2003) Accuracy and Reliability Improvement of Standalone High Sensitivity GPS Using Map Matching Techniques, Proceedings of ION AM 2003, Albuquerque, NM, pp. 209-216. The Institute of Navigation.

Basnayake, C., A. MacIver and G. Lachapelle (2003) A GPS-Based Calibration Tool for Microscopic Traffic Simulation Models, Proceedings of Smart Moving 2003. National Exhibition Center, Birmingham, England. April 2003. ITS UK.

Cannon, M. E., C. Basnayake, S. Syed and S. Crawford (2003) A Precise GPS Sensor Subsystem for Vehicle Platoon Control. Proceedings of GPS ION 2003. Portland, OR. The Institute of Navigation.